Enamel Amino Acid Racemisation Dating and its Application to Building Proboscidean Geochronologies

---

Marc R Dickinson

PhD

University of York

Chemistry

July 2018

Abstract

Analysis of the predictable breakdown of proteins and amino acids in ancient biominerals enables age estimation over the Quaternary, but to date, its application to mammalian remains has been challenging. It has been postulated that enamel is a suitable biomineral for the long-term survival of endogenous amino acids and thus, it can be used for age estimation. Directly dating mammalian remains is integral to understanding mammalian evolution and for understanding palaeoecology and palaeoclimatology.

Analysis of multiple amino acids for geochronological studies is typically achieved using a RP-HPLC method. However, the low concentrations of amino acids coupled with high concentrations of inorganic species makes accurate determination of amino concentrations challenging. The initial focus of this thesis covers the development of a novel method for the separation of amino acids from inorganic species. This was initially attempted via a HILIC SPE, but was later superseded by a biphasic separation method, which was shown to greatly improve the RP-HPLC analysis of amino acids in enamel.

Bleaching experiments have shown that the amino acids isolated from enamel through prolonged exposure to a strong oxidant, exhibit effectively closed system behaviour, signifying a potentially stable environment over geological time-scales. Elevated temperature experiments investigating the processes of intra-crystalline protein degradation do not appear to match the fossil patterns, reinforcing the need for a comprehensive understanding of the underlying mechanisms of protein degradation.

The methods developed in this thesis have been used to build an enamel amino acid racemisation geochronology based on Proboscidean teeth from UK sites with independent evidence of age. This model has shown good adherence to the UK stratigraphical framework, signifying enamel is a suitable biomineral for AAR age estimation.

Finally, enamel AAR has been used in a pilot study to begin to build a chronology for elephants from the isle of Sicily. This framework has been constructed to aid in understanding the process behind island dwarfing of insular elephant species on Sicily.

Table of Contents

List of Tables

List of Figures

Acknowledgements

I would appreciatively like to acknowledge the help and support of the people that have supported me though this journey. Firstly, I would like to thank my supervisors Kirsty Penkman and Adrian Lister for your guidance and patience in developing me into the scientist am today. I would also like to thank Jane Thomas-Oates as my internal panel member for your invaluable support and discussions during the TAP meetings. I would like to thank the staff at the BGS for trusting me to take a drill to some of their specimens and Katharine Scott for your time and expertise at Stanton Harcourt.

I have had the privilege of working/sharing an office with a wonderful group of people and would like to thank you all. I particularly I would like to thank Kirsty High for making to time to read through and offer comments on the various stages of writing this thesis, not to mention brightening the day with pictures of Darwin. I would also like to thank Adam Pinder for all advice and pet related chat along the way, and Scott Hicks for breaking up the days with inane chat. I would also like to thank Sheila Taylor for all your support in keeping the lab running smoothly and more importantly for keeping everyone sane(ish) with the morning tea breaks.

I would like to thank my friends for ensuring that I still have a social life outside work; especially Cob for organising my life and for living with me for basically the duration of my university education. Lastly, I would like to thank my family for all of your love and support over the years.

Declaration

I declare that this thesis is a presentation of original work and I am the sole author. This work has not previously been presented for an award at this, or any other, University. All sources are acknowledged as references.

Signed:

Date:

Chapter 1: An introduction to amino acid geochronology

The Quaternary is the most recent period in the geological record, spanning the last ~2.5 Ma (Gibbard *et al*., 2010). It is characterised by climatic fluctuations between cold and warm periods (known as glacials, stadials, interglacials, and interstadials), which has resulted in a complex record of landforms, sedimentary and biological remains, and assemblages of human artefacts (e.g. Pettitt & White, 2012). The geological and biological evidence from Quaternary sites has facilitated the reconstruction of the environmental conditions and faunal habitats associated with these particular periods of time (e.g. Jackson *et al*., 2000; Lowe & Walker, 2014).

Reconstruction of these climatic oscillations and the resulting shifting habitats during the Quaternary is essential to predicting how future climates and ecosystems will react in a world dominated by anthropogenic alterations. Climate studies rely on understanding feedback models and how cosmological processes affect the Earth's numerous systems (e.g. Bony *et al*., 2006; Andrews *et al*., 2012; Lord *et al*., 2017; Skeie *et al.*, 2018); the key to these is the study of past responses. Additionally, conservation efforts protecting vulnerable species on the brink of extinction can be aided by understanding the driving forces and key factors involved in the extinction and evolution of past fauna (Owen-Smith, 1989). Despite the significance of the Quaternary for developing our comprehension of the earth's ecological and climatic systems, there is still a great deal that we do not yet know, with one of the main challenges being dating of the material found. Establishing robust chronologies for deposits is essential to understanding their context, their relationship to the regional and global climate signal, and thus their interpretation. However, dating over the Quaternary time period is complex. A number of different techniques work well on certain substrates, but directly dating mammalian remains is exceptionally challenging (Walker, 2005; Grün *et al*., 2010).

The primary aim of this thesis was to investigate the potential for the use of enamel as a material for intra-crystalline protein degradation (IcPD) dating of mammals. This first chapter introduces the geological background to the Quaternary and the geochronological methods that can be used to place mammalian remains in a temporal context. It then

outlines the potential for amino acid dating, detailing the chemistry and some of the assumptions employed by this method, as well as how they are addressed. Finally, the chapter concludes with a brief outline of the aims of the project and the topics covered in the rest of this thesis.

1.1. Understanding the Quaternary

Geological time scales are used to describe the timings and relationships of events over the Earth's history. The Cenozoic Era is the most recent era. It began 66 Ma ago after the K-T extinction event and is an era that is dominated by birds and mammalian fauna (e.g. Feduccia, 1995). The Cenozoic Era is subdivided into three periods: the Paleogene, Neogene and Quaternary (Figure 1.1). The Quaternary is the most recent period in the Cenozoic Era, dating from 2.58 Ma (Gibbard *et al.*, 2010) and includes the present day. Currently, the Quaternary is further sub-divided into two epochs: the Pleistocene and the Holocene, the distinction between which occurred 11,700 cal years ago (during the Late Glacial Maximum at the end of the Younger Dryas; Lisiecki & Raymo, 2005).

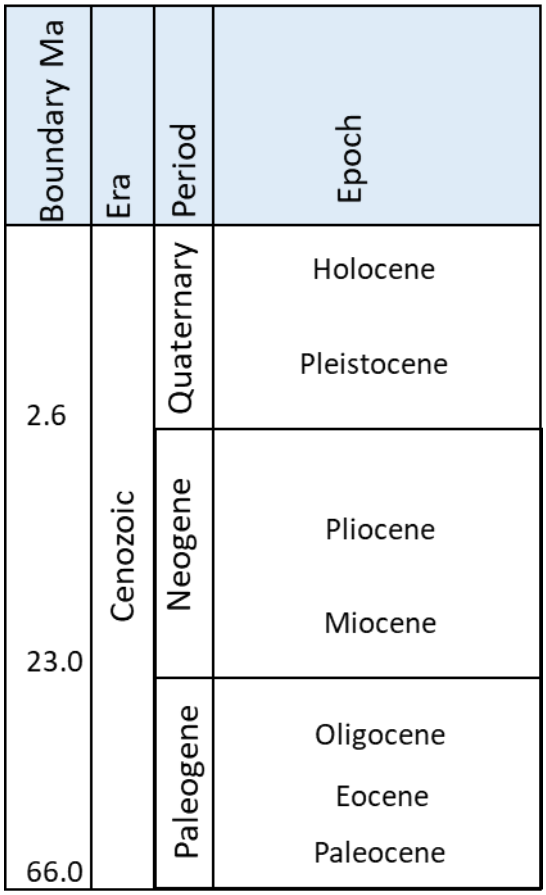

Figure 1.1. Cenozoic time scales (reproduced from Gibbard et al., 2010)

The Quaternary is characterised by its fluctuating climate, which has led to the expansion and contraction of glaciers, primarily at the Earth's poles (Denton & Hughes, 1981; Anderson *et al*., 2002). These periods of cooling and warming have had a profound effect on the Earth's ecology, driving the evolutionary adaptation of species and often leading to extinctions.

1.1.1. Drivers of long term climate change over the Quaternary

The forces driving the fluctuating climate during the Quaternary are complex and not fully understood; however, astronomical cycles have been revealed to be strongly influential (Hays *et al*., 1976; Bol'shakov, 2014). For example, the shape of the Earth's orbit around the Sun transitions from a near perfect circle to an oval. This change in orbit, termed eccentricity, happens on a roughly 100,000-year cycle and has an impact on the radiative forcing experienced by the Earth. The Milankovitch theory is used to explain the collective effect of the changes in the Earth's movements, e.g. precession, axial tilt and eccentricity on the radiative forcing experienced by the Earth (the energy input from the Sun; Kostadinov & Gilb, 2014). These processes are believed to drive large-scale climate changes on Earth over long-time periods (Hays *et al*., 1976; Imbrie *et al*., 1984).

At present, low-altitude glaciers are predominantly confined to the Earth's poles, but during the Quaternary, cooler climates allowed for the expansion of the Fennoscandian and Laurentide ice sheets as far south as Southern UK (51.5°N) engulfing much of North America (Clark *et al*., 2008; Denton & Hughes, 1981), as well as expansion of the Antarctic ice sheet (Anderson *et al*., 2002). Periods of cold climate where glaciers generally advance are known as glacials and warmer period between glacials are known as interglacials; these periods occur over the tens and hundreds of thousands of year's timescales. Stadials and interstadials also describe periods of colder and warmer climate (respectively) however, these terms define phases over shorter time periods and are used to further sub-divide glacials and interglacials (Lisiecki & Raymo, 2005).

The expansion and contraction of glaciers has had an extensive impact on the geological processes and environments occurring during the Quaternary, which has resulted in the formation of a complex record of deposits. Study of these formations and deposits has led to the reconstruction of past climates and ecosystems, but correlation of different deposits both regionally and globally remains challenging. The deposits remaining today are not a complete representation of all the material that has entered the depositional environment,

as only a fraction of the total material is preserved. Most material is recycled in the bio/geosphere and any biological soft tissues quickly degraded and are lost.

There are several different mechanisms for material to enter the palaeontological record. For example, faunal remains are frequently found in cave systems, but the taphonomy of the material is often difficult to interpret and is often biased. Some of the faunal material may have been transported into the cave by streamflow, or where caves have been used by predators such as *Crocuta crocuta*, faunal remains are often actively brought into the cave, as evidenced by bite marks on the bones (Lister 2001b). Lake sediments often contain more complete faunal skeletons. Large mammalian remains found in lake sediments probably represent the remains of animals that fell through the ice during colder periods or after becoming trapped in mud whist drinking (Lister, 2009).

The formation of river and shallow marine deposits are influenced by the geology of the surrounding environment and the climate, which over the course of interglacial and glacial climates can cycle through periods of deposition and erosion. These cycles of deposition can alter the taphonomy of deposits, e.g. interglacial river deposits are much more likely to contain faunal material that was spatially proximal to the river channel than glacial river deposits (Lowe & Walker, 2014). However, fluvial deposits are frequently biased by hydraulic sorting, which results in the selective fragmentation or removal of material based on size (Lowe & Walker, 2009).

A significant breakthrough in the understanding of the Quaternary climate system occurred when patterns in the Earth's movements were shown to correlate to changes in the oxygen isotopes preserved in marine microfossils (Emiliani & Geiss, 1959).

1.1.2. Marine oxygen isotope stages (MIS)

Oxygen naturally occurs in three stable isotopic forms: ^{16}O, ^{17}O and ^{18}O, but the oxygen isotopes used in most palaeo-reconstruction studies are ^{16}O and ^{18}O, which constitute 99.6 and 0.2 % of oxygen on Earth respectively (Faure, 1986). Foraminifera are amoeboid protists that live in both planktonic (floating in a body of water) and benthic (lowest level of a body of water which includes the sediment surface) marine environments. Some foraminifera construct their skeletons from calcium carbonate ($CaCO_3$). The seawater temperature in which the shells of foraminifera calcify alters the thermodynamic isotopic equilibrium between seawater and calcite (Emiliani, 1954), with the lighter oxygen isotope favoured in colder temperatures.

It was proposed that the alternating temperature of the oceans through periods of glacial and interglacial cycles would alter the stable isotopic composition of the calcium carbonate skeletons of foraminifera, which when preserved in sediments can be retrieved though coring (Emiliani, 1955). This effect is compounded by the bioavailability of the different isotopes in the seawater (Vincent & Berger, 1981). The selective uptake of the lighter oxygen isotope (^{16}O) from marine waters during evaporation of H_2O, combined with the preferential precipitation of the heavier oxygen isotope (^{18}O), ultimately results in a disproportionate amount of ^{16}O in the composition of glaciers compared to the oceans. During periods of glacial (colder) climate, this results in isotopically heavier ocean water (Emiliani, 1955). It is this relationship between the temperature of the oceanic waters and the amount of water isolated in ice-sheets/glaciers that results in an alteration of the isotopic composition available for use in construction of the foraminifera shells (Ravelo & Hillaire-Marcel, 2007).

The ratio of oxygen isotopes ^{18}O and ^{16}O is expressed as a $\delta^{18}O$ value (Equation 1) where the standard isotopic composition is sourced from a known isotopic composition, such as the Vienna Standard Mean Ocean water (Kendall & Caldwell, 1998).

$$\delta^{18}O = \left(\frac{\left(\frac{^{18}O}{^{16}O}\right)_{sample}}{\left(\frac{^{18}O}{^{16}O}\right)_{standard}} - 1 \right) \times 1000\ ‰$$

Equation 1

The carbonate of foraminifera microfossils preserved in the sediments can therefore be analysed by isotope ratio mass spectrometry (IRMS) and the ratios used as proxies for palaeoclimate. Comparable studies have analysed oxygen isotope values in corals and used these to extrapolate mean ocean temperatures, with most of the work conducted on the Laurentide ice sheet (Erez, 1978).

Isotopic analysis of the oxygen in these foraminifera illuminated the effect the radiative cycles had on the global climate (Emiliani & Geiss, 1959). The record of alternating warm and cool climates has led to individual marine oxygen isotope stages (MIS) being defined based on the distinct peaks and troughs observed in the oxygen isotope values when plotted against age (Figure 1.2). Some of the stages have been further subdivided, as there can be significant climatic fluctuation within a defined stage.

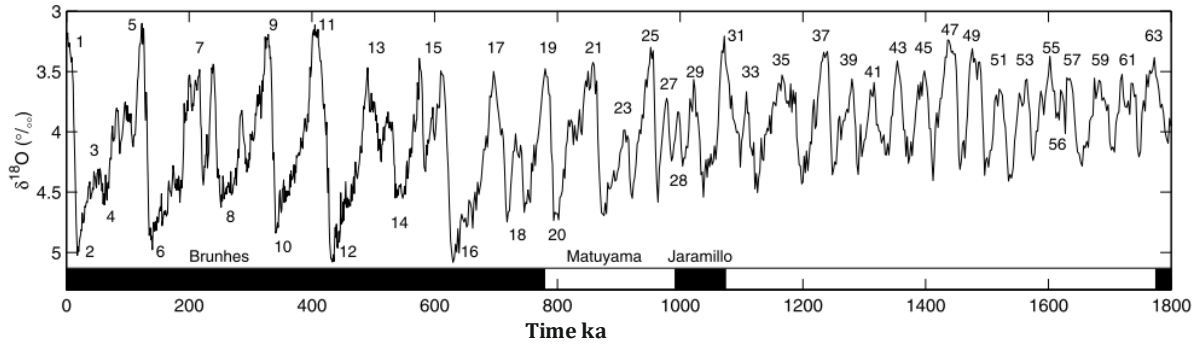

Figure 1.2. The benthic $\delta^{18}O$ stack constructed from 57 globally distributed records, displaying the positions of the marine oxygen isotope stages (Lisiecki & Raymo, 2005).

For samples younger than 50 ka old, radiocarbon dating can be used to estimate the age of the carbonate of foraminifera shells in tandem with establishing their oxygen isotopic composition (Heier-Nielsen *et al*, 1995). Beyond 50 ka, dating the δ^{18} O signal in cores can be more challenging. Several techniques can be used to correlate marine oxygen isotope trends. Magnetostratigraphy measures the natural remnant magnetisation of iron-containing sediments, the orientation of which is binary. The signal changes through the course of the Quaternary and can be used to date key points in the $\delta^{18}O$ signal. Sediment accumulation rates can also be used to estimate the age of sections in marine cores, but accumulation rates can vary significantly, and deep-water currents can remove sediment leading to apparent hiatuses in sediment accumulation. Dating by orbital tuning has also been used to establish chronologies in the $\delta^{18}O$ record (Imbrie *et al*., 1984; Ruddiman *et al*., 1986). The principle of orbital tuning is to adjust the orbitally-derived $\delta^{18}O$ signal to develop greater accordance with the known orbital forcing through correlation with major climate or environmental events. However, caution is advised when applying this method, especially over shorter time-scales due to the circularity of this assumption (Blaauw, 2012).

In 2005, a global synthesis of the average marine benthic $\delta^{18}O$ values was achieved by consolidating data from 57 marine oxygen isotope cores distributed around the world (; Lisiecki & Raymo, 2005). This work provided a reference for a variety of diverse studies and a common time scale for fluctuations in climate during the Quaternary. $\delta^{18}O$ signals from ice cores and corals have also supported the model developed from the marine record, with the added advantage in ice cores of a direct record of the past atmospheric composition recorded in tandem (Fairbanks & Matthews, 1978; Petit *et al*., 1999).

A key assumption made when extrapolating temperatures from the oxygen isotope values is that the skeletal $CaCO_3$ is incorporated at, or close to, the isotopic equilibrium of the

surrounding sea water (Erez & Luz, 1983). However, studies have shown that this may not be the case; selective uptake of a certain isotope or the influence of symbiotic algae may impact the composition of the skeletal $CaCO_3$, thus increasing the variability of data (Erez, 1978). In addition, bioturbation is a major source of error in oxygen isotope stratigraphy. Reworking of the top 1–20 cm of sediment by benthic organisms can cause mixing and homogenisation, resulting in a time-averaged effect and blurring the isotope signal (Bouchet *et al*., 2009). Despite this, the marine record remains the best dated global picture of Quaternary climate

Detailed reconstructions of terrestrial events can be constructed using pollen signals in undisturbed sedimentary sequences (Tinner & Lotter, 2001). Pollen stratigraphy is frequently used to define regional zones, with characteristic pollen signals being used to infer the prevailing climate at the time of deposition. These sequences have been shown to correlate with the marine oxygen isotope signal, thus potentially linking the marine and terrestrial signals (Tzedakis et al., 1997). However, linking these palaeoceanographic signals to the terrestrial record can be challenging, often requiring multiple techniques/approaches to be used in tandem.

1.1.2.1.River terrace stratigraphy

There are several different ways in which terraces can form: fluvial, kame, marine, lacustrine and travertine. Fluvial terraces or river terraces form when a river cuts through a valley floor, abandoning material on the former floodplain to produce a step-like sequence of material on either side of the river bed (Figure 1.3; Bridgland, 2006). Incision of the valley floor occurs in response to a variety of complex variables (Maddy, 1997). However, it is often triggered by the influx of large volumes of water, for example potentially caused by the melting of permafrost during the transition between glacial and interglacial cycles (Bridgland, 2006).

In the six-phase formation model proposed by Bridgland (2000), incision of the valley floor occurs during warming in glacial-interglacial conditions because of fluvial discharge from melting permafrost; this is then followed by aggradation of material during the same climate conditions. Fine-grained sedimentation occurs during the subsequent interglacial climate, but it is suggested that this material is rarely preserved. A second incision of the valley floor occurs during the interglacial-glacial transition followed again by aggradation of sediments. During the cold, glacial climates, little activity occurs. The cycle can then return to phase one. Periods of uplift are integral in the formation of river terraces (Bridgland,

2000). Without significant uplift, sediment is often completely recycled and thus it can be difficult to assign material to specific terraces and hence time periods (Hey, 1991).

Palaeontological sites such as those found within the Thames and Trent River terraces (UK) are abundant sources of evidence for the impact of Quaternary climate on the terrestrial environment. River terraces often yield material of comparable age in well-defined beds and thus provide a means for establishing palaeo-reconstructions (Bridgland *et al*., 1999). For example, the preserved flora and fauna can indicate the type of ecosystems that existed during the time period in which the deposits were laid down (Bennett, 1987; Schreve, 2001). In addition, the chronological constraints hypothesised in the terrace formation model allow distinct terraces to be directly linked to the glacial/interglacial cycles and therefore the global climate record (Engels *et al*., 2008; White *et al*., 2017). Dating methods such as radiocarbon dating, OSL and biostratigraphy are often used to estimate the ages of the deposits within terrace sequences, providing a variety of mechanisms for dating terrestrial deposits and the associated mammalian fauna (e.g. Gibbard & Stuart, 1975).

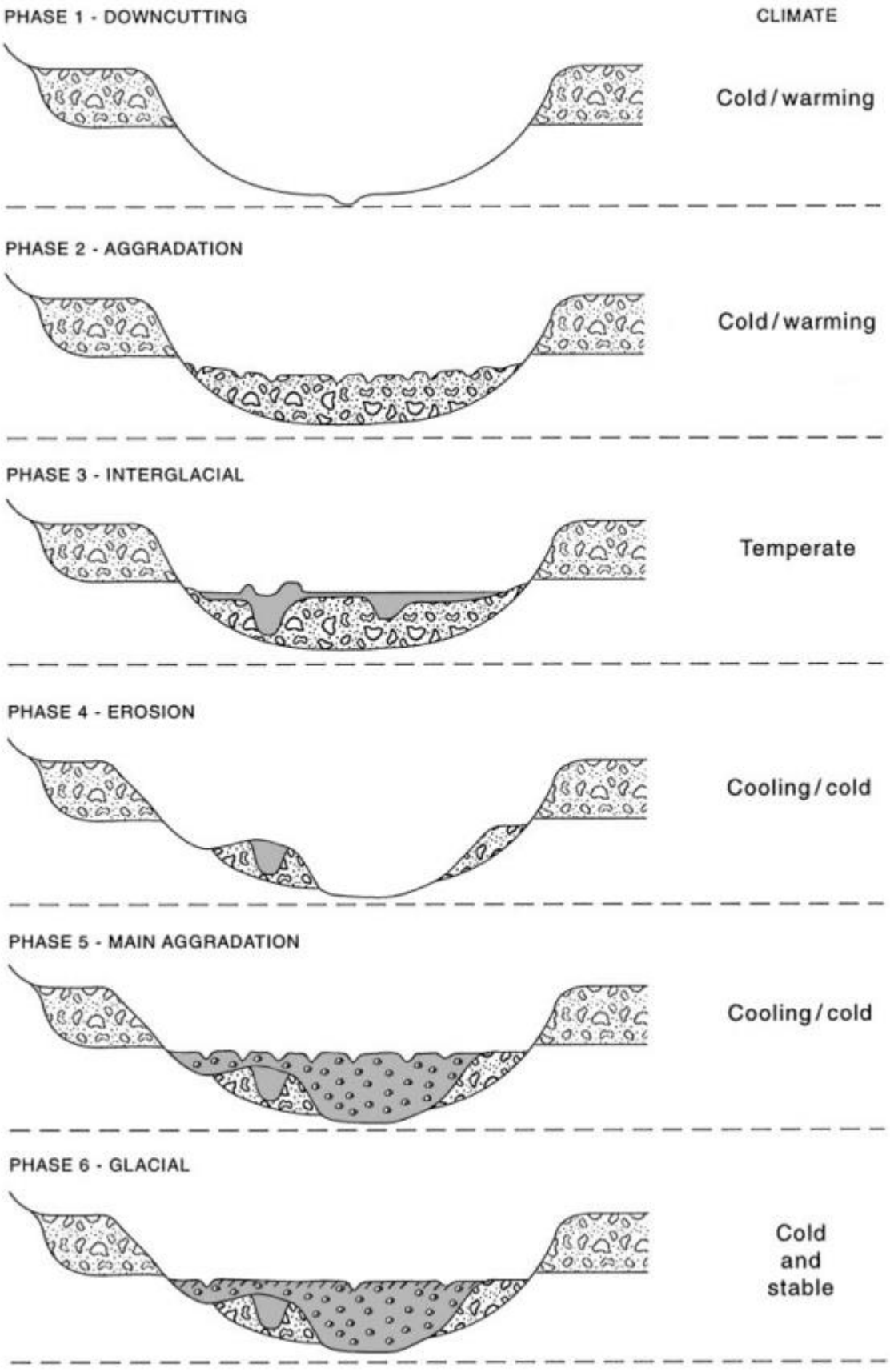

Figure 1.3. Six-phase model for terrace formation driven by the climate oscillations occurring during the Quaternary. Figure taken from Bridgland (2000).

1.1.3. Quaternary Geochronology

There are many ways to date the various pieces of evidence that can be found in the geological record and each has its own set of strengths and limitations (Walker, 2005). The methods employed to date Quaternary remains can broadly be categorised into a few basic principles: relative dating methods put multiple pieces of evidence in chronological order, direct numerical dating provides specific dates, and correlative methods establish correlations between two or more records and infer dates/conclusions based on these comparisons. Many of the techniques have a specific time range for which they are applicable, for example most of the direct dating methods are limited by a process reaching equilibrium or becoming so small as to be beyond the limits of detection. It is typically through the combination of multiple techniques that robust chronostratigraphical interpretation can be achieved (Antoine *et al*., 2007; Rixhon *et al*., 2017). Some of the key methods for dating terrestrial deposits, focusing on those most applicable to mammalian remains, are reviewed in the subsequent sections.

1.1.3.1. Faunal Stratigraphy

Biological remains are preserved in sediments of both terrestrial and aquatic settings, making them ideal targets for both biostratigraphical and palaeo-reconstruction studies (e.g. Serdyuk, 2006). A survey of the faunal remains in a single sedimentary horizon, such as those formed in the beds within river terraces, can be used to correlate to other horizons with a similar faunal composition (Schreve, 2001). Once a record of fauna present in a particular time period has been established, the presence or absence of characteristic species can also help date sites. For example, the presence of *Hippopotamus amphibus* (Hippopotamus) is known to occur in the British fossil assemblages of the last interglacial (MIS 5e) and thus has assisted in constraining the age of Late Middle Pleistocene sites containing this species (Schreve, 2001). The absence of a species can also be informative. The bivalve *Corbicula fluminalis* is thought to have been absent from the British Isles during the last interglacial and thus its absence has aided in biostratigraphical correlations (Keen, 2001; Schreve, 2001).

In addition to the absence or presence of a species, distinct evolutionary changes in response to changes in environment can also aid in correlative studies. For example, the appearance of the metapodials and first phalanges of horses during the late Middle Pleistocene in the British Isles show discrete quantifiable changes, making them appropriate for biostratigraphic analysis (van Asperen, 2011).

When evaluating the age of particular sites, it is important to routinely date sites using other independent methods (Vanderlaan & Ebach, 2014). The circular argument of dating faunal remains using the biostratigraphical correlations or markers can lead to inaccuracies in dating. Reworking can also be particularly problematic, especially in fluvial contexts when reworking is commonplace (Meijer & Preece, 2000).

The dynamic climates present throughout the Quaternary have induced recurrent changes in the demography of many species (e.g. Lister & Sher, 2001; Hoffmann & Sgro, 2011). Using uniformitarian principles, it is possible to make assumptions about past climates based on the contemporary understanding of organisms and ecosystems. The population patterns of certain dominant species can therefore indicate the type of environmental conditions present at the time.

1.1.3.2. Luminescence dating

Luminescence refers to the spontaneous emission of light by certain materials in response to some external stimulus, such as electromagnetic radiation (radioluminescence), ionising radiation (photoluminescence) or heat (resulting in thermoluminescence). When photoluminescence (stimulation) is by visible light, the process is referred to as optically stimulated luminescence (OSL), and when it is by near-infrared radiation it is referred to as infrared stimulated luminescence (IRSL; Walker 2005). Luminescence dating is conducted on natural crystals, usually feldspar and/or quartz sediments.

Ionising radiation (alpha and beta particles, and gamma radiation), emitted by the decay of radioactive elements within the minerals and immediate external environment, and from cosmic rays, can excite electrons to the conduction band which creates a corresponding hole in the valence band (Walker, 2005). Some of the electrons in the conduction band may become trapped in structural defects or chemical impurities in the crystalline lattice. The length of time electrons remain trapped at ambient temperatures depends on the properties of the trap site; some sites can hold electrons for millions of years whilst others only a few days. Stimulation of the trapped electrons excites them back to the conduction band where they either return to the ground state, become trapped in a similar site or encounter a recombination centre. At recombination centre, excess energy is emitted as either heat or as luminescence (Walker, 2005).

The emitted photons can be detected, and the signal used to calculate the dose the material has absorbed. Once further irradiation does not result in luminescence the mineral/sediment is referred to as saturated. The response of the mineral grains to an

increasing radiation source can be used with the natural signal (calculated using a specific heat for TL or wavelength photon for OSL) to estimate the dose the mineral sediment has absorbed since burial. This measurement is referred to as the equivalent dose. A subsample of the sediment used to calculate the equivalent dose is analysed for radioactive elements such as U, Th, and K and used to calculate the rate at which ionising energy is absorbed (Aitken, 1998). By dividing the equivalent dose by the dose rate, an estimate of age is calculated.

Luminescence dating requires the average water content of the entire sample burial period (or since last heated for TL) to be estimated because water attenuates radiation. It also needs to be established if the U-series decay chain has been in a state of disequilibrium, as both effects will affect the average dose rate (Stokes *et al*., 2003).

1.1.3.3. Direct dating of mammalian remains

Indirect dating of faunal remains assumes that the age of the material in question is the same age as the matrix from which it was recovered. This assumes that: the fossils are found *in situ* and the fossils haven't been reworked during their depositional history. The issue of reworking/intrusion of material can confound interpretation and have serious repercussions in palaeo-reconstruction studies (Westaway 2011; Coughlan *et al*., 2018). Direct dating through independent means mitigates these issues and can provide a more robust approach to dating faunal remains. There are three main ways of directly dating mammalian fauna: radiocarbon, electron spin resonance (ESR), and U-series. Radiocarbon dating is the most commonly used technique but yields either infinite results or age underestimations beyond ~50-60 ka (Jacobi *et al*., 2006). In ideal circumstances, U-series and ESR dating of bones and teeth are capable of age estimation up to several millions of years, but due to the open system nature of these biogenic minerals this is rarely possible (Grün *et al*., 2010).

1.1.3.3.1. Radiocarbon Dating

Radiocarbon dating was one of the first numerical dating methods to be developed and it can be used to date a range of different materials, including: wood, peat, organic sediment, plant, bone, teeth and shell remains, and charcoal (Walker, 2005). The method works by measuring the residual radiocarbon (^{14}C) content. ^{14}C is formed in the upper atmosphere when neutrons in ^{14}N are converted into protons by the action of high energy cosmic rays (Kromer & Münnich, 1992). Once formed, ^{14}C can oxidise through the process of photosynthesis, forming CO_2 where it becomes incorporated into living matter (Zazzo &

Saliege, 2011). Upon death, organisms cease to interact with the atmosphere. The amount of ^{13}C remains constant (assuming there are no external factors affecting this process) whilst the radioactive nature of ^{14}C means it decays back to ^{14}N, with an estimated half-life of 5,568 years (note that this is the half-life used by convention to enable comparisons between laboratories; it may not be an accurate half-life; Mook, 1986). Accelerator mass spectrometry is used to detect and quantify the different C isotopes and allows their ratios to be determined, revealing the age of the sample. However, within approximately nine half-lives, the amount of ^{14}C becomes too small for reliable dates to be acquired, limiting the technique to dating organic material less than 50,000 years old (Pigati *et al*., 2007: Zazzo & Saliege, 2011; Briant *et al.,* 2018).

The initial ^{14}C content assumes that radiocarbon in the atmosphere can be accurately estimated (through calibration; Reimer *et al*., 2013) and that living organisms are in equilibrium with the atmosphere. Calibration of radiocarbon dates is required because the $^{14}C/^{12}C$ ratio in the atmosphere has not been constant (Taylor 1987). Whilst these assumptions appear to hold true for many cases, some organisms have been shown to incorporate carbon from the surrounding water: the 'hard water' effect which effectively adds 200 – 1200 years to the perceived age of the sample (Peglar *et al*., 1989). Trace quantities of ^{14}C have also been found in coal leading to speculation that microbial and fungal activity may introduce ^{14}C in to samples, leading to potential underestimations of age (Lowe, 1989).

Radiocarbon dating of skeletal remains can be conducted on the carbon content of the organic and inorganic matrix of bone or enamel. Radiocarbon dating of the inorganic carbon from *Mammuthus primigenius* enamel has helped elucidate the possible causes of the extinction by establishing an accurate timeline for the last presence of this species on different continents (Vartanyan *et al*, 1993; Graham *et al*., 2016). However, this reservoir of carbon is susceptible to secondary calcite infiltration and diagenetic alterations. Bone mineral is less dense than enamel and is therefore thought to be more prone to diagenetic alterations. Acetic acid and hydrochloric acid have been proven effective in removal of some of the secondary calcite (Haynes, 1968). However, this is not the only source of contamination and variability in the ^{14}C dating of apatites, isotopic exchange of bicarbonate ions from the burial environment (Berger *et al*., 1964) has led to the underestimation of the age of bone material (Zazzo *et al*., 2011).

Analysis of collagen for ^{14}C dating of bones has proven to be more reliable than dating of the mineral apatite. However, due to the low concentration of proteins this is not applicable to dating enamel. Some bone samples do not contain sufficient material to extract the collagen, especially in arid or semi-arid regions where rates of collagen hydrolysis are faster (Dunseth *et al*., 2017). Sample preparation improvements for ^{14}C dating (including the use of ultrafiltration; Higham *et al*., 2006) has enabled more accurate ^{14}C ages to be determined on bone collagen through the purification of endogenous collagen proteins.

1.1.3.3.2. Electron Spin Resonance (ESR) and U-series dating

Electron spin resonance (ESR) dating was initially used to estimate the absolute age of speleothem calcite (Ikeya, 1975) but since then has been used on a range of minerals, including tooth enamel (Rink, 1997). It has been postulated that ESR dating is theoretically applicable to material as old as 5 Ma, but the reliability of this dating method (especially past 0.8 Ma) is greatly limited by a range of factors, and thus is not presently considered applicable to fossil enamel beyond 0.5 - 0.8 Ma (Duval & Grün, 2016).

ESR dating is based on the principle that the electrons in the valence band of crystalline minerals, such as found in tooth enamel, can be promoted to an excited state by natural sources of ionising radiation, e.g. X-rays and cosmic radiation and promoted into a conduction band (Figure 1.4, Walker, 2006). In most cases, excited electrons recombine with positive charge sites and return to the valence band, but some recombine at charge deficit sites and become trapped. These charge deficit sites are associated with defects and impurities in the crystalline structure. Trapped electrons form paramagnetic centres, the signal of which can be measured and therefore the density of paramagnetic sites can be calculated (Ikeya, 1993). The crystals are therefore acting like natural dosimeters, recording the cumulative charge post-deposition.

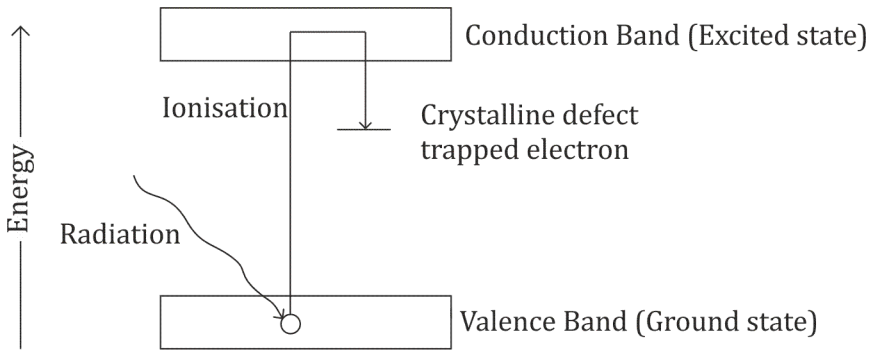

Figure 1.4. The basic principles of ESR (adapted from Walker, 2006).

The paramagnetic signal from the trapped electrons and radicals may be measured using an ESR spectrometer and combined with an understanding of the sample's depositional (and particularly its radiation) history, the age of the sample can be calculated (Equation 2).

$$I_t = t \times D \times S \qquad \textit{Equation 2}$$

Where I_t is the intensity of the natural ESR signal, t is the time since the ESR signal was zero, D is the average radiation flux or dose rate at the sample site and S is the sample sensitivity (change in ESR signal intensity per unit radiation). For age estimation the ESR signal must first be zeroed so that at t = 0, I_t = 0.

The average radiation flux experienced by the sample is a combination of the internal (D_{int}) and external (D_{ext}) dose rates. To calculate these average dose rates, the sample and surrounding sediments would ideally form a geochemically stable environment. The internal dose rate is produced by the presence of radioactive isotopes, such as uranium (U), potassium (K) and thorium (Th). *In vivo,* hydroxyapatite-based biominerals (such as teeth and bone) do not naturally contain high concentrations of these radioactive isotopes (e.g. U < 1-50 ng g^{-1}; Tandon *et al*., 1998), but post-mortem they can uptake U-isotopes from the surrounding environment, giving rise to the internal dose rate (Th is not water soluble and thus is assumed to not diffuse into the mineral). Several mathematical models have been proposed for the modelling of U-uptake. The early up-take model assumes that U is quickly incorporated into the mineral hydroxyapatite (Bischoff & Rosenbauer, 1981), whilst the linear uptake model proposes a steady uptake of U over time (Ikeya, 1982). However, leaching of the U can occur and thus enamel and bone are described as open system with respect to U (Grün *et al*., 2010). This dynamic system makes the average internal dose challenging to establish accurately. Consequently, ESR dating is confronted by a series of assumptions that cannot be accounted for in error calculations. The open system nature of bones and teeth with respect to U would normally preclude the use of these materials for purposes of dating but in the absence of other suitable techniques, numerous attempts have been made to apply this dating technique to bones and teeth (Sambridge *et al*., 2012).

To improve the robustness of ESR dating, U-series dating is often used in combination to obtain a more reliable model for U-uptake (Grün, 2006). U-series dating can estimate the age of a fossil based on the degree to which secular equilibrium (where production rate is equal to decay rate) has been reached between ^{230}Th and ^{234}U (Schwarcz, 1989). U-series dating has an upper age limit of ~500 ka after which further radiometric measurements can be made (Th/U-Pa/U) to extend the range to ~ 750 ka, but this is limited by the demand for

sample sizes in the order of 1 g (Grün *et al*., 2010). Understanding the U-isotope history of the enamel and bone samples informs the U-uptake model for ESR dating and thus yields a more precise estimation of age.

Combined ESR and U-series dating of mammoth tooth from a Thames site in Oxfordshire (Stanton Harcourt) suggested that even when combined with U-series analysis, ESR could systematically underestimate the age of tooth samples (Zhou *et al*., 1997). The age estimated using these techniques places the site between MIS 3 and 4, contradicting the biostratigraphical, lithostratigraphical evidence and the dates calculated using amino acid racemisation ratios (White *et al*., 2006; Penkman *et al*., 2013). Variations in hydrology (and hence the uranium composition of the groundwater) may have been responsible for the inaccuracies seen using ESR and U-series (Zhou *et al*., 1997). Cases like this highlight the need for a multi-faceted approach to dating remains.

ESR dating can also be conducted on quartz sediments. The main difficulty for ESR dating of this kind is the resetting phenomenon for the quartz signals. Incomplete bleaching (linked to the environment and conditions of transport/deposition) results in a residual dose which is added to the post-depositional dose accumulated since deposition, thus leading to an overestimation of the age (Voinchet *et al*., 2016).

1.1.3.3.3. Amino acid dating in biominerals

All biominerals contain protein, as it is fundamental to the biomineralisation process (e.g. Zeichner-David, 2001; Weber *et al*., 2014). Organic matter is often used as an instrument to nucleate and regulate mineral growth, and incorporation of organic matter is also thought to modulate the structural properties of biominerals (Boyde & Martin, 1984). Amino acids were first isolated from fossil shells in 1954 (Abelson, 1954). However, it wasn't until Hare and Mitterer (1967) documented the correlation between the age and relative concentration of the D-isomer through kinetic simulation reactions that the potential for them to be used as a dating tool was realised. Since 1967, a wide range of subfossil material (including biominerals such as shells and teeth) have been analysed for their amino acid composition, with mixed results (e.g. Bada *et al*., 1973; Bada 1981; 1985; Miller *et al*., 1979; Taylor 1983; Blackwell *et al*., 1990; Torres *et al*., 1997). However, recent innovations in isolating proteins that exhibit closed system behaviour in calcium carbonate biominerals have been successful in estimating age from their breakdown (Brooks *et al*., 1990, Penkman *et al*., 2010; 2011; 2013).

1.2. Amino acid racemisation

1.2.1. The general structure of amino acids

Proteins are ubiquitous in nature, required in almost every aspect of biological function. Amino acids are the constituent units of proteins, the sequence of which forms its primary structure. DNA utilises a triplet base-pairing system to encode the primary sequence of amino acids, which subsequently controls the 3D formation and function of the protein. All 22 proteinogenic amino acids have an amine, carboxylic acid and hydrogen atom attached to an α-carbon or less commonly a β-carbon.

Free amino acids in solution at neutral pH are largely in zwitterionic form, in which the amine group is protonated and positively charged and the carboxyl group is deprotonated with a negative formal charge, resulting in a neutral net charge (Figure 1.5). Changing the pH of the solution alters the relative proportion of the ionic states. Some amino acids have additional acidic or basic groups (e.g. aspartic acid) and thus can become doubly charged in certain pH environments.

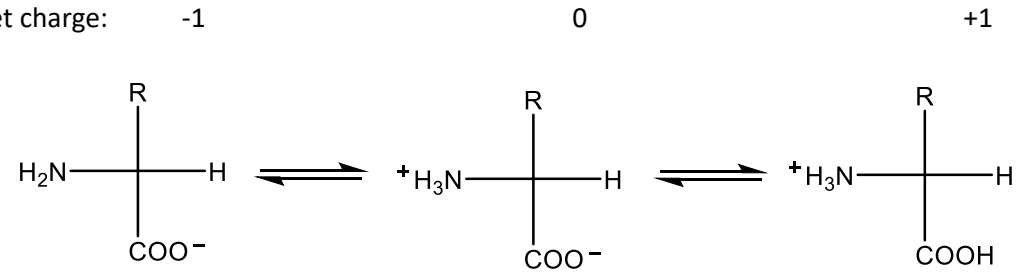

Figure 1.5. Ionic forms of a generic amino acid. The R group represents a variable group, the identity of which depends on the amino acid.

Except for glycine (R = hydrogen atom), all the naturally-occurring amino acids have four different group attached to the α-carbon or β-carbon, yielding a stereogenic centre. The interchanging of any two of these groups leads to the formation of an enantiomeric isomer, which is non-superimposable on the original isomer. Two of the proteinogenic amino acids have a second stereogenic site centred on their β-carbon: isoleucine and threonine (Figure 1.6). These amino acids can form four different stereoisomers. When the groups attached to both stereogenic centres are arranged differently, diasteroisomers are formed, which unlike enantiomers are chemically different isomers.

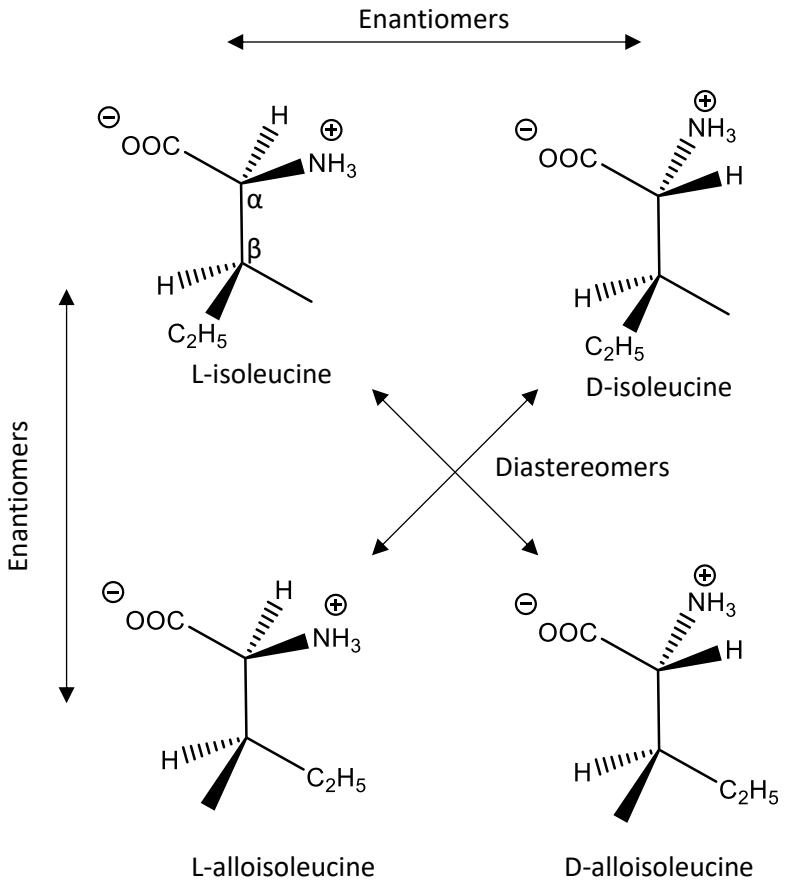

Figure 1.6. Enantimeric and diastereomeric structures of (allo) isoleucine

1.3. Survival of peptides and amino acids in the fossil record

Deamination and/or decarboxylation of amino acids results in the formation of carboxylic acids and amines and eventually hydrocarbons. In most depositional environments this process occurs slowly, and thus amino acids can be found deep into time (Miller *et al*., 1979). The maximum length of time amino acids and proteins can survive for in the context of the fossil record is not yet known although some studies have demonstrated their presence in biominerals as old as several million years (Penkman *et al*., 2013). For example, highly sensitive tandem mass spectrometric (MS/MS) techniques have been used to sequence peptides from ostrich eggshell from sites such as Laetoli (Tanzania), dating back to 4.3–2.6 Ma (Demarchi *et al*., 2016). Intact peptides persisting that far back in time are rare and require optimum conditions for survival. Demarchi *et al*. (2016) argued that peptides were preserved in egg shell due to the stabilization effects of the calcite biomineral and low water diffusion rates.

Amino acids exhibiting closed system behaviour have been recovered from molluscan opercula dating back to the Late Eocene (~33 Ma; Penkman *et al*., 2013). Amino acid signatures from these samples were heavily degraded, with unstable amino acids such as aspartic acid, serine and phenylalanine present only at very low concentrations and the more stable alanine at higher concentrations. Most of the amino acids present in these opercula were free amino acids rather than present bound as part of a peptide.

Organic matter in well preserved sauropod dinosaur eggshells from the Late Cretaceous (100–66 Ma) was reported to potentially contain heavily altered amino acids and peptides a few amino acids in length, identified through immunological studies (Schweitzer *et al*., 2005). However, these types of studies have been known to yield false positives, indicating the presence of specific peptide sequences when none are present (Lendaro *et al*., 1991). Schweitzer *et al*. (2013) have also reported that detailed microstructures structures can survive in dinosaur bone dating back to 68 Ma and that the protein subunits in them can be sequenced, but this work is highly controversial and is not widely accepted due to concerns primarily regarding contamination (Bern *et al*., 2009; Grellet-Tinner *et al*., 2010; Buckley *et al*., 2017).

The stability of peptides and amino acids in fossils enables these biomolecules to be used as potential targets for palaeontological studies deep into geological time. The stability of proteins and amino acids in enamel is unknown, but it is likely that their survival will be comparable to that of other biominerals, and this was assessed during the work described in this thesis. Proteins and amino acids degrade via a multitude of pathways, but the key mechanisms most relevant for degradation over geological time scales are hydrolysis, racemisation and deamidation, all of which are discussed in the following sections.

1.4. Hydrolysis

Peptides and proteins are made from units of amino acids that are connected by amide bonds (peptide bonds). Peptides are distinguished from proteins based on the length of the amino acid chain, with proteins generally considered to be at least 50 amino acid residues in length (Jones, 1992). An amide bond is formed by the condensation reaction of the carboxylic acid and the amine moieties attached to the α-carbon or β-carbon of two amino acid residues. Forming peptide bonds requires energy and thus in living organisms, adenosine triphosphate (ATP) is required as an intracellular source of energy for bond formation. The reverse process (hydrolysis) requires the addition of water. However, despite the thermodynamic instability of peptide bonds, cleavage is extremely slow (von

Endt, 1980). It is thought that peptide bond hydrolysis occurs via the nucleophilic attack of the carbonyl bond by water (Figure 1.7). This forms a zwitterionic intermediate which subsequently dissociates, cleaving the bond (Pan *et al*., 2011). The rate determining step, involving the nucleophilic attack, has a barrier to activation caused by resonance stabilisation which decreases the electrophilicity, and stabilises the carbonyl and thus hinders the spontaneous cleavage of the peptide bond, giving it kinetic stability.

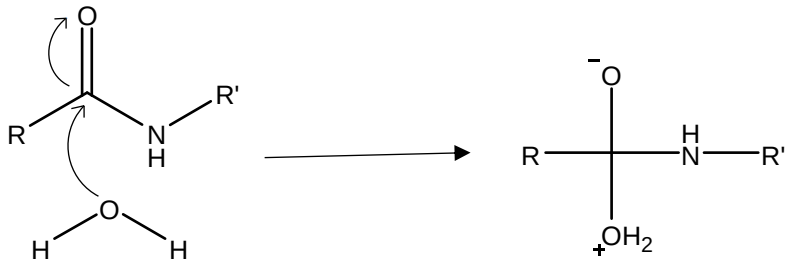

Figure 1.7. Mechanistic peptide bond hydrolysis via the nucleophilic attack of a carbonyl bond by water, forming zwitterionic intermediates at neutral pH.

The stability of a peptide bond is dependent on the structure of the two bound amino acids, their position in the peptide chain (Radzicka & Wolfenden, 1996) and their external chemical environment (Demarchi *et al*., 2016). Some amino acid residues (e.g. Asp) are significantly more liable to cleavage than others and therefore cleavage occurs more readily at those bonds (Inglis, 1950). Continual iterations of peptide-bond hydrolysis via internal cleavage eventually results in free amino acids (Riley & Collins, 1994).

The time taken for the complete breakdown of proteins and peptides into free amino acids in the context of the palaeontological record is highly variable. Many factors including temperature, pH, redox potential, and geochemistry of the surrounding sediment can all greatly influence the degradation of proteins, especially if the organic material is in a system vulnerable to external processes (Hofreiter *et al*., 2012).

1.5. Racemisation

Racemisation is the conversion of a group of molecules all the same stereoisomer to a mixture of stereoisomers. Most amino acids have one stereogenic centre and thus undergo racemisation, but Ile and Thr have two stereogenic centres and the conversion between

their isomeric forms is more properly termed epimerization. The term racemisation in this thesis will generally encompass both terms.

The 3D structure of proteins is fundamental to their role in biological systems. As such, in order to appropriately function, biological systems almost exclusively incorporate one chiral form of amino acids (L) into proteins. The exact origin of the preferential, almost exclusive, use of L-amino acids is still unknown (Kojo, 2010), although it has been potentially linked to the stabilisation of polypeptides (Mason, 1984). Studies have shown that D-amino acids fulfil specific biological functions in animals and have been linked to certain diseases; however, their concentrations are comparatively low (Fuchs *et al*., 2005; Fujii *et al*., 2011). Many species of bacteria also utilise D-amino acids to form part of the peptidoglycan, a key component in bacterial cell walls (Corrigan 1969; Lam *et al*., 2009).

Racemisation is a spontaneous process and therefore occurs naturally in organisms during and after their lifetimes. In live biological systems, most proteins have short life-times and modifications such as racemisation can be repaired or lead to replacement of the protein. D-amino acid oxidase is an enzyme that catalyses the oxidative deamination of D-amino acids and thus selectively eliminates D-amino acids (Genchi, 2017). However, in long-lived extracellular proteins D-amino acids can accumulate and have been linked to some degenerative diseases (Ritz-Timme & Collins 2002; Fujii, 2005; McCudden & Kraus, 2006). Tissue turnover ends upon death and the interconversion of amino acids from their L- to D-forms is no longer biased by the biological system, meaning that formation of the D-isomer is favoured initially through thermodynamics (Hare & Alelson, 1967). Eventually over time equilibrium between the two isomers is reached (for most amino acids this is when D/L ≈ 1).

It is generally understood that racemisation of free amino acids occurs predominantly by the base-catalysed abstraction of the α-proton to form a planar sp^2 hybridised carbanion intermediate (Figure 1.8; Neuberger, 1948). The subsequent re-addition of a proton can attack from either plane of the carbanion, reforming the amino acid either in the same configuration, or as a stereoisomer of the initial molecule (Figure 1.8). The activation barrier for the forward and back reactions are theoretically equal for amino acids with a single stereocentre, and thus equilibrium should form equal concentrations of both isomers (D/L = 1).

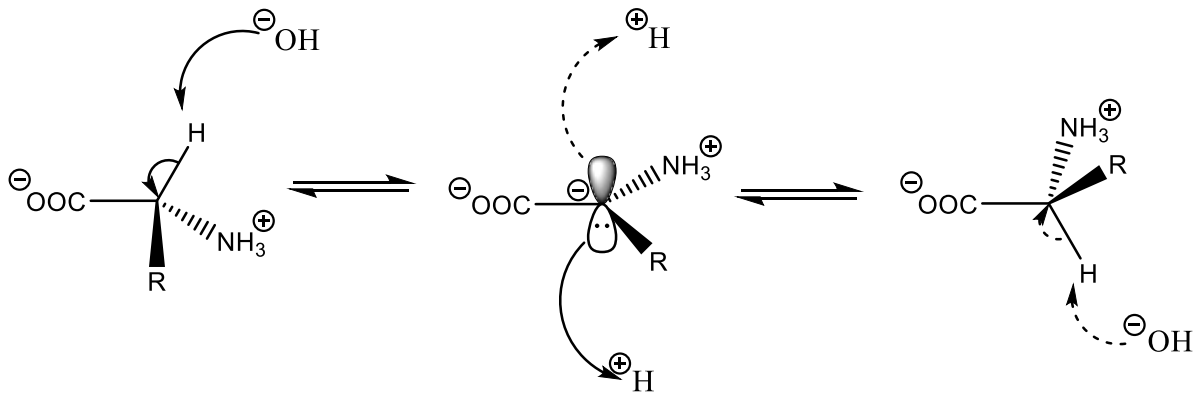

Figure 1.8. Arrhenius base-catalysed mechanism for amino acid racemisation. Forward direction is represented by a continuous line and backwards by a dashed line (Neuberger, 1948).

The carbanion is stabilised by a resonance structure with the carboxylic acid group, and by the electron withdrawing inductive positive charge centred on the amine group (Figure 1.9). The R group (which defines the amino acid), also influences the stability of the intermediate, and thus alters the thermodynamic barrier for racemisation (Neuberger, 1948). Electron-withdrawing groups generally stabilise the carbanion intermediate, lowering the barrier of activation and thus increasing its rate of racemisation. The reverse is generally true for electron donating groups. These trends have been observed in the kinetic studies of a range of biominerals, supporting the carbanion mechanism (Canoira *et al*., 2003; Tomiak *et al*., 2010; Wehmiller *et al*., 2012; Crisp *et al*., 2013).

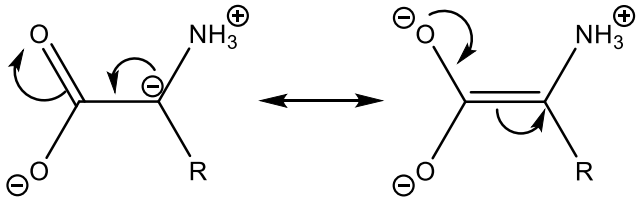

Figure 1.9. Stabilising resonance structures for a carbanion intermediate in the racemisation of free amino acids (Neuberger, 1948)

In addition to base-catalysed racemisation, Neuberger (1948) also proposed an acid-catalysed mechanism, whereby the carboxylic acid acts as a proton accepter, promoting the loss of a proton on the α-carbon/β-carbon. However, it is believed that this mechanism is not favoured in a paleontological context due to its slower rate of reaction (Schroeder & Bada, 1976).

It was originally thought that racemisation of amino acids is likely to occur irrespective of whether they are free in solution, bound internally within peptide chains or on the terminus (Wehmiller, 1982). However, the rate of racemisation has been found to be highly dependent on their position (e.g. free, bound or terminal). Mitterer and Kriausakul (1984) postulated that N-terminal racemisation was the most likely pathway for bound amino acids and the mechanism for within-chain racemisation was not prevalent for most amino acids. It has been reported in high temperature kinetic experiments that terminally bound amino acids in a range of proteins (bovine ribonuclease, lysozyme and cytochrome C) racemise 4-6 times faster than the respective free amino acids under the same conditions (Csapó *et al,* 1997).

When an amino acid is internally bound within a peptide, most amino acids are conformationally restricted from readily racemising (Kriausakul & Mitterer, 1980; Mitterer & Kriausakul, 1984). It is likely that the steric barrier for in-chain racemisation is great enough that appreciable levels of racemisation for most amino acids is unlikely. However, aspartic acid and serine have been observed to racemise whilst internally bound within a peptide chain (Stephenson & Clarke, 1989; Demarchi *et al*., 2013a).

1.5.1. Deamidation and the succinimide intermediate

Deamidation is thought to facilitate the in-chain racemisation of aspartic acid (Stephenson & Clarke, 1989). Deamidation refers to the conversion of an amide group in the side chain of an amino acid to another group, usually a carboxylic acid. Glutamine and asparagine are the only proteinogenic occurring amino acids that can undergo deamidation, forming glutamic and aspartic acids respectively. Studying the degradation pathway using the composite signal of these amino acids is complex, and the racemisation of the individual amino acids in the fossil record is thus less well understood. The initial ratio of the two amino acids that form the composite signal (e.g. aspartic acid/asparagine) in a biomineral can therefore potentially influence the observed rates of racemisation over time. Consequently, it is potentially important to consider the impact of deamidation when comparing the kinetics of racemisation or changes in amino acid composition over time (Crisp *et al*., 2013).

Deamidation occurs via a succinimide intermediate (Figure 1.10) of either a five- (asparagine) or six- (glutamine) membered ring (Stephenson & Clarke, 1989). Deamidation during preparation of samples, in particular protocols that require hydrolysis of peptide bonds, make the analysis of asparagine/glutamine and aspartic/glutamic acid as separate

amino acids challenging. Therefore, the single terms Asx and Glx have been used to group together asparagine and aspartic acid, and glutamine and glutamic acid respectively.

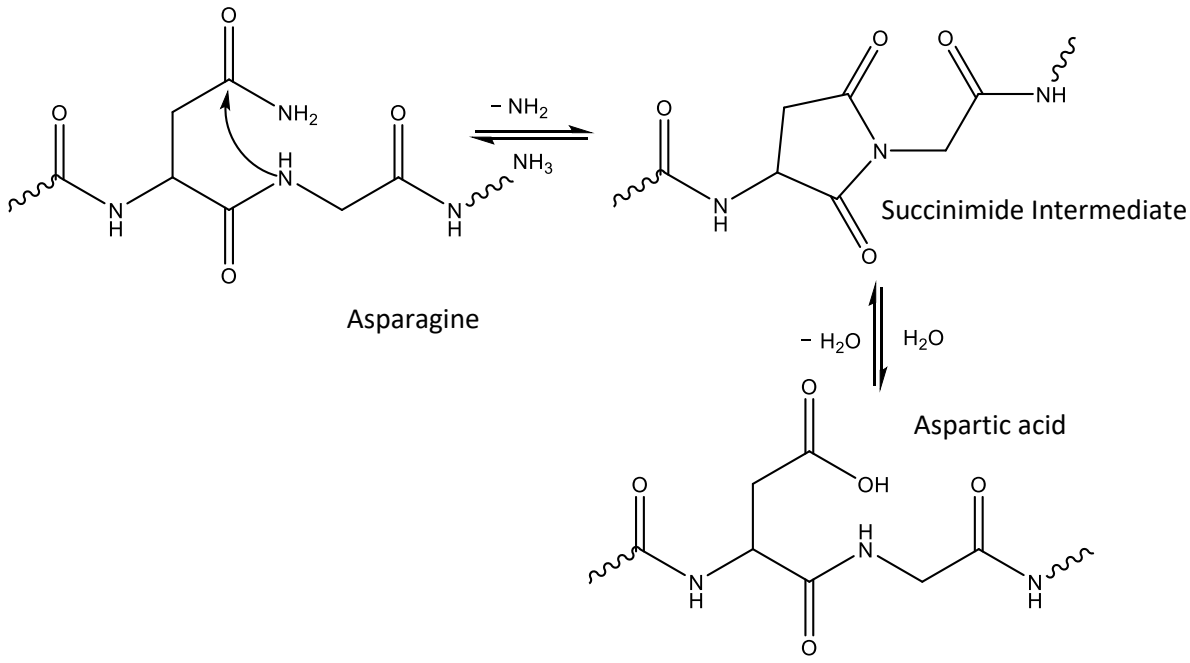

Figure 1.10. Deamidation of asparagine to aspartic acid (Stephenson & Clarke, 1989). Note, iso-aspartic acid can also be formed from the succinimide intermediate but is not shown on this schematic.

A key pathway to aspartic acid racemisation in a peptide chain is via the succinimide intermediate (Stephenson & Clarke, 1989; Collins *et al*., 1999). At neutral pH it has been suggested that the racemisation of the succinimide intermediate occurs via the formation of an enolate, which is assisted by a mechanism involving two molecules of water (Figure 1.11). The two water molecules mediate the relay of the proton, lowering the thermodynamic energy of the intermediate species (Radkiewicz *et al*., 1996; Takahashi, 2013).

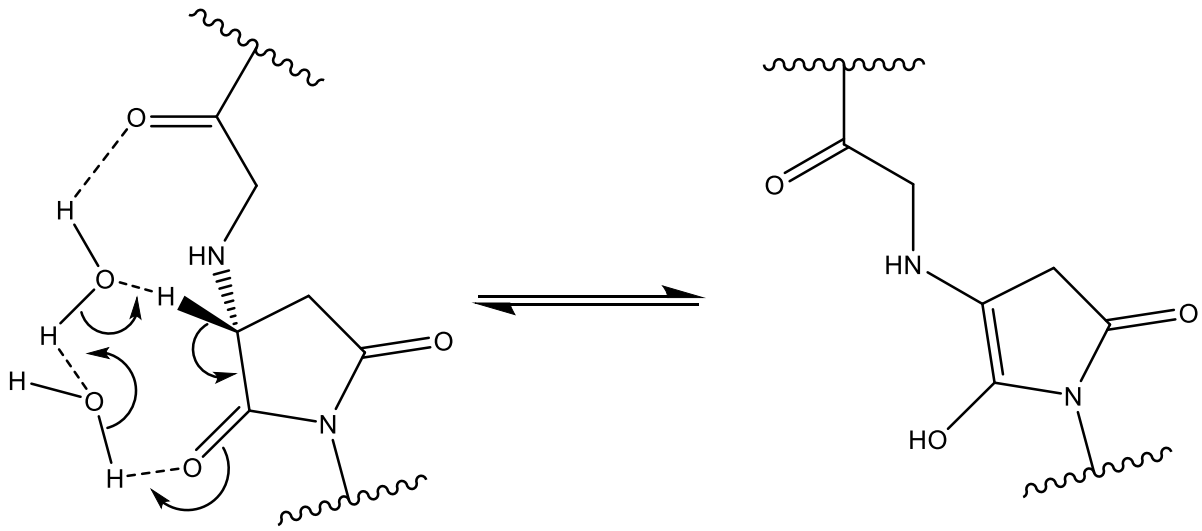

Figure 1.11. Two-water assisted formation of an enolate A proposed pathway to in chain racemisation of aspartic acid (Takahashi, 2013)

The racemisation of amino acids via the enolisation mechanism assisted by two water molecules is not only plausible for the succinimide intermediate, but also for non-cyclic amino acids such as serine. Serine is a relatively unstable amino acid because after elimination of the α-proton, the serine carbanion can undergo subsequent decomposition by β-elimination to form the enamine, dehydroalanine, the product of which irreversibly forms alanine (Steinberg *et al*., 1984). Kinetic studies of serine in the closed system fraction of biominerals reveal an atypical model for racemisation, with a rapid initial increase in racemisation followed by a decline (Penkman *et al*., 2008; Crisp *et al*., 2013; Tomiak *et al*., 2013). This has led to the assertion that serine may be able to racemise in-chain. Computational insight into the energy profiles of the proposed mechanism indicate that this occurs due to the stabilising effect of serine's side chain (-OH) on the enolisation intermediate (Takahashi, *et al*., 2010; Demarchi *et al*., 2013a).

1.5.2. Diketopiperazine and N-terminal racemisation

Studies have shown that peptides can undergo reversible cyclisation to form diketopiperazines (DKPs). DKPs are formed by nucleophilic attack of the lone pair of electrons of the nitrogen of the N-terminal amino group on an internal carbonyl, forming a 6-membered ring (Figure 1.12). Internal amylolysis via the formation of a DKP can result in the cleavage of a terminal dipeptide and is thought to be a major pathway to peptide scission (Steinberg & Bada, 1983). The rate of racemisation of amino acids in a DKP is thought to be orders of magnitude faster than in free amino acids when at neutral pH (Steinberg & Bada, 1981; Collins & Riley, 2000). The exclusive pathway to racemisation via

this mechanism at the N-terminus of peptide chains does in part explain the different rates of racemisation experienced by amino acids at each terminus (N vs C).

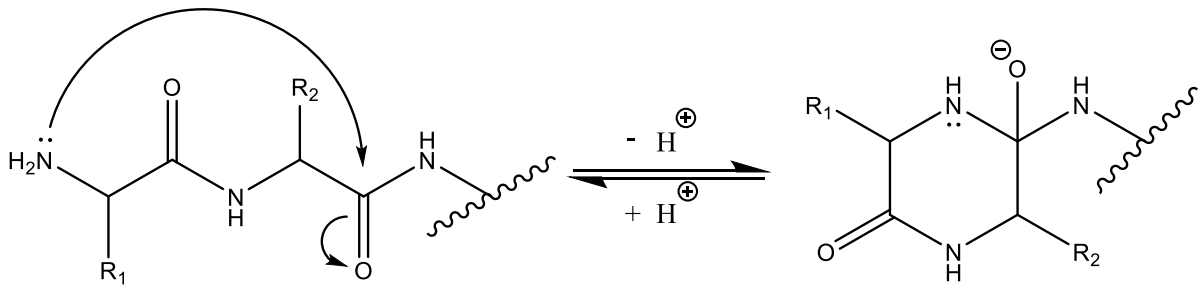

Figure 1.12. Diketopiperazine formation (Steinberg & Bada, 1981)

1.5.3. Free vs bound racemisation and the impact of hydrolysis

In fossil biominerals it is often observed that the free amino acid fractions are more racemised than their bound counterparts (Wehmiller & Hare, 1971; Penkman *et al*., 2008; Hendy *et al*., 2012). Free amino acids are likely to constitute a small fraction of the total amino acid content of young biominerals. Over time, if all the amino acids are retained, the free amino acid content will increase due to the gradual hydrolysis of proteins and peptides. There is evidence that amino acids situated at the terminal position of peptides have the lowest activation for racemisation (for example via the formation of DKP) and thus racemisation here occurs rapidly (Stephenson & Clarke, 1989). Free amino acids will have once been situated at a terminus of a peptide before becoming a free amino acid. The extent of racemisation in the free fraction is therefore most likely higher than in the bound, despite the slow rates of racemisation when free (Wehmiller & Hare, 1971).

The rate of hydrolysis therefore influences the relative extents of racemisation in the free compared to bound fractions in biominerals. If the hydrolysis of a peptide bond linkage to a particular amino acid is preferred, then the generation of terminally bound residues of that amino acid will be faster, leading to enhanced levels of racemisation. As peptide bonds containing hydrophobic amino acids are more resistant to hydrolysis than bonds contain hydrophilic ones (Smith & Evans, 1980), the peptide sequence is likely to influence the overall rates of racemisation.

Base-catalysed racemisation forms a carbanion that is stabilised by the peptide linkage's resonance structures (Figure 1.13) and thus the barrier for racemisation is lowered. It is this stabilisation effect that is thought to increase racemisation in terminally bound amino acids.

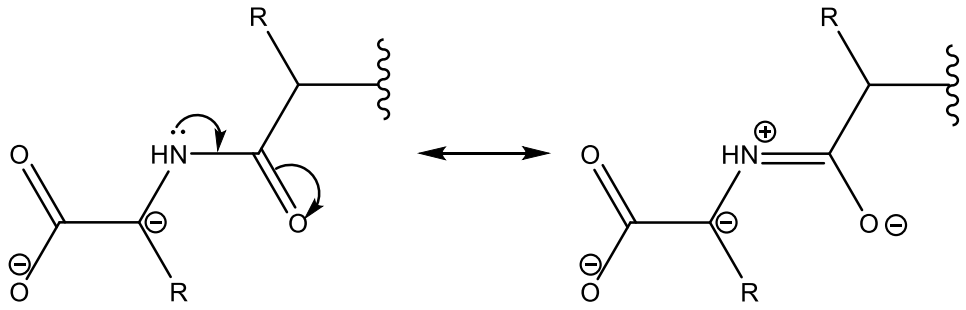

Figure 1.13. The resonance structures of a base-catalysed racemisation of a C-terminus amino acid.

Peptide chains have two chemically different ends, the carboxyl (C) and amino (N) termi. The rate of racemisation has been shown to vary between termini (Kriausakul & Mitterer, 1978; Smith & Evans, 1980). The N-terminus of a peptide chain does not have the destabilising effects of the carboxylate group and thus racemisation (in principle) is favoured in this position, as it is benefited by resonance stabilisation (Smith & Evans, 1980). However, studies have shown that dipeptides containing alanine, leucine, phenylalanine, aspartic acid and methionine racemise faster at the C-terminus than at the N-terminus. Conversely, proline, as well as the sterically-hindered amino acids isoleucine and valine, showed the reverse trend (N > C; Smith & De Sol, 1980). The rates of racemisation at each of these termini is better described by considering multiple factors such as the inductive effect of the NH_3^+ and CO_2^- groups and solvation and steric effects (Kriausakul & Mitterer, 1978).

1.5.4. Physical factors affecting amino acid racemisation

1.5.4.1. The effect of temperature

Kinetic studies of amino acids and proteins have shown that the rate of racemisation is a function of temperature (Wehmiller *et al*., 2012). Therefore, relative chronologies of samples based on extents of racemisation in biominerals have focused on regions that can be assumed to have had the same thermal history (Wehmiller *et al*., 2012; Penkman *et al*., 2013). Models constructed from Arrhenius parameters have been used to estimate the temperature history of samples based on the observed extent of racemisation in fossils, and thus approximate the associated climate when the samples were deposited (Schroeder & Bada, 1973). However, these calculations are highly sensitive to the projected rate

constants and thus require a good understanding of the kinetic pathways (Tomiak *et al*., 2013).

Burial depth can affect the temperature experienced by the sample and therefore the extent of racemisation, potentially making accurate relative dating challenging (Wallace *et al*., 1988). Very shallow or exposed burials (such as those associated with marine terraces) can expose fossils to solar heating, impacting the ability to directly compare sites within a region (Wallace *et al*., 1988). Whilst these local heterogeneous influences can rarely be accounted for, it is vitally important that sites with a higher risk of this type of variability are highlighted and if necessary appropriate steps are taken, such as analysing larger sets of samples or fossils.

1.5.5. Chemical factors affecting amino acid racemisation

Since racemisation is a chemical reaction, in addition to a number of intrinsic factors affecting amino acid racemisation, there is also a range of complex external environmental variables that can influence the rates of racemisation.

1.5.5.1. The effect of pH, ionic strength and buffers on racemisation

The rate limiting step in the base-catalysed racemisation of amino acids is thought to be the abstraction of the α-proton by an Arrhenius base (Neuberger, 1948; Bada, 1985). The rate of reaction is therefore likely to be influenced by the concentration of the catalyst, which in the case of base-catalysed racemisation, is OH^-. However, the overall extent of interconversion between L and D- amino acids is an amalgamation of multiple rates and involves several forms of amino acids in different charge states. Therefore, the effect of factors such as pH, ionic strength and buffers on racemisation is complex and dependent on the amino acid studied (Smith & Evans, 1980).

Experimental data has shown that the rate of racemisation of aspartic acid in dentine increases as pH increases (pH 4-9; Bada, 1972a). Shou & Bada (1980) found that the rate of racemisation of aspartic acid in bone is independent of pH over a similar pH range (pH 3-9), the lack of influence of pH on racemisation was attributed to potential buffing effects of the bone material (Shou & Bada, 1980). Studies over a broader range of pH (pH 0-12) indicated that the rates of racemisation of alanine, leucine and proline plateau over certain pH ranges, thus rendering racemisation independent of pH over certain ranges (Shou & Bada, 1980). High temperature simulations testing the effect of pH on the rates of amino acid racemisation show clear evidence that the rate of racemisation does increase at higher

pH (Orem, 2011; Bright & Kaufman, 2011a), but that the influence of pH on racemisation is minor when compared to the effects of temperature.

Experiments documenting the effect of ionic strength on the racemisation of unbound alanine at pH 7 showed that racemisation was independent of ionic strength, but when the pH was adjusted to 10, an increase in racemisation with increase in ionic strength was observed (Smith *et al*., 1978). This was attributed to the increase in the more negatively charged alanine species ($RCH(NH_2)COO^-$) at the higher pH. The same study revealed that racemisation of free alanine was also increased (~5 %) with increasing buffer concentration (from 0 – 0.1 M phosphate buffer) when pH and ionic strength were constant, supporting the general base-catalysed mechanism for racemisation.

1.5.5.2. The effect of metal ions on racemisation

Metal ions (usually originating from detrital or chemical mineral grains in the surrounding sediment and ground waters) can also accelerate the rates of free amino acid racemisation through chelation, but their impact on bound amino acids/peptides is much less (Smith & Evans, 1980). Metal cations are thought to stabilise the carbanion intermediate via field effects due to their localised charge and thus lead to enhanced racemisation (Smith & Evans, 1980). Studies on alanine-glycine dipeptides chelated to copper and cobalt metal ions showed that the presence of these metals increased racemisation, but the affects were stereoselective; amino acids bound at the C-terminus racemised faster than those at the N-terminus, however, there have been a limited number of studies. (Gillard & Phipps, 1970).

1.5.5.3. The effect of water on racemisation

Early studies showed that apparent rates of epimerization of isoleucine in bone are a function of water concentration (Hare, 1974). In Hare's study, fresh bovine bone was heated in varying amounts of water for up to 3 days. The extent of racemisation in anhydrous conditions (dried to remove water prior to the experiments) was considerably lower than when water was present. The study also showed that in samples where water was present, the extent of racemisation decreased with increasing water content. Bone is an open system, and thus much of the protein and amino acids leached out during the experiments, making the exact relationship between water content and rates of racemisation difficult to establish. However, based on this study the presence of water greatly affects the observed extent of racemisation in bone.

1.5.6. How extrinsic chemical factors are addressed in AAR dating

The effects of extrinsic chemical influences can greatly alter the rates or observed extents of racemisation, however they can only influence the portion of proteins and amino acids that they are able to access. Recent work has isolated proteinaceous material from molluscs that exhibits closed system behaviour in laboratory experiments and over geological time scales (Sykes *et al*., 1995; Penkman *et al*., 2008). Analysis of this fraction is likely to therefore overcome the problems caused by these factors, potentially explaining the increased reliability of amino acid racemisation data obtained after removing non-closed system amino acids (Sykes *et al*., 1995; Penkman *et al*., 2008)

1.6. Closed system

Biomineral formation is coordinated by organic molecules, and as such they play a pivotal role in the properties of the biomineral (Towe & Thompson, 1972). Most of the proteinaceous material in non-degraded biominerals is thought to be located between crystal planes (inter-crystalline). This organic matter is understood to be open system and thus prone to leaching, contamination and alteration by external chemical factors (such as discussed in section 1.5.5; Sykes *et al*., 1995; Penkman *et al*., 2008). However, transmission electron microscopy (TEM) and electron diffraction analysis of calcium carbonate shells of bivalves has indicated the presence of water and organic material inclusions inside crystallites (intra-crystalline; Towe & Thompson, 1972). This early study suggested that the observed 'frothy' structures within single crystals were a consequence of trapped water and organics expanding as a result of heating by the electron beam. This work has been supported by more recent studies using TEM, energy-dispersive X-ray analysis (EDX) and electron energy-loss spectroscopy (EELS) to chemically assess the intra-crystalline voids (Gries *et al*., 2009). Gries *et al*. (2009) used 3D tomography to elucidate the structure of the intra-crystalline voids and a combination of EDX and EELS revealed that they contain increased amounts of carbon in comparison to the surrounding matrix, suggesting the presence of organic matter in the voids.

The extensive exposure of shell powders to bleach has been shown to remove most of the organic matter present but leaves a fraction that is chemically resistant (Crenshaw 1972). This observation supports the evidence for the propensity of organic matter to become trapped within crystallites (intra-crystalline) and indicates that this fraction can be isolated after using prolonged exposure to a strong oxidant. The incorporation of proteins into the crystal structure of biominerals has been linked to modulating crystal shape and its

mechanical properties (Weiner & Addadi, 1997). This “chemically protected” fraction is likely to exhibit more closed system like behaviour than the more easily accessible, inter-crystalline fraction and thus is potentially valuable for geochemical analysis (Penkman *et al*., 2008).

Diffusive loss experiments have been used to test the closed system behaviour of the fraction of organic matter removed after prolonged exposure to bleach in molluscs (Penkman *et al*., 2008; Demarchi *et al*., 2013), ostrich eggshell (OES; Crisp *et al*., 2013) and corals (Tomiak *et al*., 2013). These studies compared samples that had undergone bleaching treatment prior to simulating long term degradation through heating, to those that had not. These studies found that bleaching reduced the concentration of amino acids lost through leaching during the simulation of long term degradation. Moreover, it was shown that bleaching of samples reduces the variability of D/L values data for a single-age population of gastropods by 50 % when compared with unbleached shells (Penkman *et al*., 2008). This is thought to be due to the removal of open system amino acids during the bleaching step, which are more susceptible to external chemical influences and thus, increased variability in extents of racemisation.

Two measures of intra-crystalline protein degradation (IcPD) can be routinely measured in calcium carbonate-based biominerals: the unbound, free amino acid (FAA) and that of the total hydrolysable amino acid (THAA) fractions. In a closed system where all the degradation products are retained, the extent of racemisation in these two fractions should be highly correlated (Collins & Riley, 2000). IcPD experiments simulating long term degradation of the proteins in mollusc shells and ostrich eggshell have shown that the FAA and THAA D/L values for most amino acids were highly correlated (Penkman *et al*., 2008; Crisp *et al*., 2013). It was also observed that analysing the intra-crystalline fraction remaining after bleaching yielded stronger correlations than unbleached material (Penkman *et al*., 2008). These observations provide weight to the theory that the intra-crystalline fraction represents a closed system and can be isolated following extensive bleaching of calcium carbonate based biominerals.

The correlation of the FAA and THAA D/L values can help identify if a sample has undergone unexpected mineral diagenesis. Preece & Penkman (2005) noted that some of the molluscan assemblage from the Lower Palaeolithic site at East Farm, Suffolk, had undergone significant recrystallisation. Analysis of the FAA and THAA values indicated that a single operculum, that had undergone obvious signs of deformation, had THAA D/L values

which indicated a younger than expected age for the sample. However, this was not the case for the FAA values. This lack of agreement between the THAA and FAA D/L values led to the conclusion that post-mortem protein contamination or leaching had occurred and that this sample should be excluded from the subsequent geochronological assessment. This observation provides a mechanism for identifying potential open system samples and creates a tool for identifying and excluding anomalous data.

1.7. Calcium carbonate-based biomineral

Calcium carbonate-based biominerals have been the focus of geochemical analysis for AAR studies, in part because several have been shown to have a chemically resistant fraction that can be isolated following bleaching (Crenshaw 1972; Sykes *et al*., 1999; Penkman *et al*., 2008; Crisp *et al*., 2013; Tomiak *et al*., 2013).

1.7.1. Molluscs

Mollusc shells are useful geochronological tools that have been used to estimate the age of a variety of deposits (Wehmiller 1982; Bowen *et al*., 1985; Penkman *et al*, 2010). An assortment of mollusc species' shells has been shown to contain closed system proteins and amino acids that are prevented from leaching by their crystalline calcium carbonate structure (Sykes *et al*., 1999; Penkman *et al*, 2008). Studies originally focused on whole shell experiments which utilise the proteins in the aragonite shells. However, during diagenesis the thermodynamically unstable aragonite structure of the shell converts to calcite; this process has been attributed some of the variability in some of the data (Penkman *et al,* 2013). Calcite and aragonite are both comprised of calcium carbonate, but their crystal lattices differ; calcite forms a trigonal crystal system whereas aragonite forms an orthorhombic system (Smyth & Ahrens, 1997). Advances in the methodology have now greatly improved the precision of the technique by using the opercula found alongside the shells, as opercula are composed of calcite, the more thermodynamically stable form of calcium carbonate.

1.7.2. Avian eggshell

The extent of AAR in the eggshells of African ostriches has been used to estimate the age of archaeological remains, showing good agreement with already established radiocarbon dates (Brooks *et al*., 1990). Further investigations into the racemisation kinetics and closed system nature of the biomineral indicate that ostrich egg shell has the potential for age estimation of samples in geological contexts (Brooks *et al*., 1990; Crisp *et al*., 2013).

1.8. Calcium phosphate-based biominerals

Mammals mineralise their hard tissues using calcium phosphate, and therefore these are potential targets for amino acid dating. The two potential biominerals are bone and the components of teeth (which has three main components: enamel, dentine and cementum). Bone is dominated by the protein collagen, while dentine and enamel contain different extra-cellular matrix proteins; dentine is collagenous, and enamel is non-collagenous.

1.8.1. Bone

The application of AAR as a direct dating technique for age estimation of bone material would be very desirable. Bone is often found in large quantities (compared to other biomineral remains by weight) and therefore can more readily be made available for destructive sampling. Additionally, it is often skeletal remains that are the most valued finds and accurate dating is imperative to their interpretation. Bone was consequently one of the biominerals initially targeted for AAR studies (Bada, 1972b, 1985; Bada *et al*., 1973; Belluomini, 1985; Belluomini & Bada, 1985). Generally, in these early studies, aspartic acid was used to date material from the Holocene and late Pleistocene, and isoleucine to date older samples (Bada, 1985). The epimerisation of isoleucine was often used to determine age because the diastereomeric isomers allowed for more facile separation (through ion exchange liquid chromatography) and quantification than the enantiomers formed by the other amino acids (e.g. Bada, 1985).

Much of the early work relied on the calculation of activation energies and rate constants to convert racemisation values into chronological dates. However, substantial inconsistencies were identified in the derived age of bone material when a broader range of amino acids were compared (Kessels & Dungworth, 1980), as well as when AAR-derived dates were compared to those obtained from radiocarbon dating (Taylor, 1983). More recent kinetic studies have shown that the racemisation of amino acids in collagen is difficult to model (Collins *et al*., 1999). It is thought that some of the conformationally-free amino acids in the telopeptide on the N-terminus of collagen are able to racemise, giving rise over time to an initial increase in D/L value, after which most of the in-chain racemisation occurs only once the collagen triple helix structure has unwound (Collins *et al*., 2009; Dobberstein *et al*., 2009). This degradation model is difficult to predict and is likely to greatly influence inferences about derived age estimation, especially for those amino acids that can racemise in-chain e.g. aspartic acid and serine.

Bacterial activity in fossil bone has been attributed to anomalously high D/L values for glutamic acid and alanine due the use of certain D-amino acids in some bacterial organelles, casting further doubt on the reliability of AAR dating of bone (Kessels & Dungworth, 1980). Unlike a portion of the proteins in molluscan opercula, bone collagen does not exist in a closed system environment (Hare, 1974). Secondary amino acids from the surrounding environment and contaminating organisms can affect the overall amino acid signal, as well as losses of amino acids by leaching of the original amino acids from the bone (Hedges & Wallace, 1980, Bada, 1987). Early work on bone collagen elucidated the inconsistencies in using the proteins found in bone for age estimation and emphasises the need for targeting endogenous, closed system material when applying AAR for age estimation.

1.8.2. Dentine

The principal protein component of dentine is also collagen and the biomineral shares similar structural properties to bone. Therefore, comparable concerns can be applied to the use of dentine-based biominerals for AAR dating. However, it is proposed that dentine may exhibit more closed system-like behaviour than bone and thus be less prone to contamination and leaching (Torres *et al*., 2000). However, this theory has not yet been robustly investigated.

1.8.3. Enamel

Enamel is heavily mineralised and comprises a densely packed arrangement of hydroxyapatite crystals. It is therefore thought to be more resistant to diagenetic changes and be more chemically resistant than the less dense biominerals, bone or dentine (Hillson, 2005), and it is therefore anticipated to be a more robust repository for stable closed-system proteins and amino acids.

1.9. Mineral composition of enamel

There are three main biomineral components of mammalian teeth: enamel, dentine and cementum. Dentine and enamel contain different extra-cellular matrix proteins; dentine is collagenous, and enamel is non-collagenous. Enamel is the most resilient mammalian biomineral, necessitated by its role in mastication, and because it is acellular and therefore unable to repair damage (Hillson, 2005). Like other mammalian biominerals, the inorganic component of enamel is predominantly calcium hydroxyapatite ($Ca_{10}(PO_4)_6(OH)_2$). However, the proportion of inorganic material in enamel is much higher than in other mammalian biominerals. Mature dental enamel contains ~96 % inorganic material, less

than 1 % organic material and the rest water; in comparison, mature dentine typically comprises 70 % inorganic mineral, 20 % organics and 10 % water (Hillson, 2005).

The hydroxyapatite crystals in enamel are non-stoichiometric (calcium deficient). Within the basic hydroxyapatite structure, OH^- ions or $[PO_4]^{3-}$ can be substituted with $[CO_3]^{2-}$ (Ivanova *et al.*, 2001). The carbon content of mature enamel typically represents ~6 wt.% and the variations in substituted ions and their respective positions aids in fine-tuning the properties of teeth (Sabel *et al.*, 2012). Enamel crystallites are of nanometric sizes (~12 -38 nm) which enables them to occupy all orientations; this permits a tight packing formation and thus contributes to the mineral's mechanical properties (Moradian-Oldak *et al*., 1998; Ouladdiaf *et al*., 2015). In enamel, crystallites organise into rod-like structures termed prisms. These prisms are often inclined to the occlusal plane and run through the enamel, providing strength.

Enamel mineralisation occurs in two phases, apposition (development) and maturation (Robinson *et al*., 1995). During apposition, mineralisation initiates at the occlusal surface (the surface of the teeth that is used for mastication) and advances towards the root of the tooth. The appositional matrix is ~25 wt.% mineral bioapatite (a form of calcium phosphate that comprises the major mineral component of a bone, tooth or scale; Passey & Cerling, 2002), and is comparatively rich in carbonate when compared to mature enamel (Robinson *et al*., 1979). Maturation also progresses from the occlusal surface to the root, with inner and central enamel layers mineralising prior to the outermost enamel (Trayler & Kohn, 2017).

This high degree of organisation and control is orchestrated by an organic fraction (proteins). The combination of mineral and organic material has been found to govern the characteristic properties of many biominerals, such as strength, resistance to fracture, and elasticity (He *et al*., 2006, Kim *et al*., 2016).

1.10. Organic composition of enamel

The protein content of unerupted, developing enamel in vertebrates comprises a range of proteins, some of which are unique to enamel (e.g. Robinson *et al*., 1995; Carneiro *et al*., 2016). Amelogenins make up ~90 % of the total extracellular organic matrix; they are a series of proteins involved in amelogenesis (the process of forming enamel; Termine *et al*., 1980). Other organic matrix proteins (such as tuftelin) comprise the other ~10 % and are also thought to influence the formation of enamel, contributing to: nucleation, growth, cell signalling, support of growing crystals, control of secretion, and protection of the mineral

phase (Robinson *et al*, 1998). Of these, enamelin is the most abundant and constitutes approximately 5 % of the protein component of enamel.

Amelogenesis occurs in two phases: matrix production, and maturation. During production, epithelial-mesenchymal cells aligned along the dentine-enamel junction secrete amelogenins which form supramolecular assemblages. These assemblages, which are regulated by pH and temperature, are thought to control the growth, organisation and structure of the hydroxyapatite crystals in enamel (Wiedemann-Bidlack *et al.*, 2007). Immature mineral crystallites are seeded during this phase but contain only one third of their final mineral content; the rest is made up of water and protein.

Maturation involves the removal of the protein and water which is concurrent with an increase in the size of crystallites. Ameloblasts break down the proteins and once fully matured, the organic content of enamel is only ~1-2 % (Robinson *et al*., 1998). Amelogen proteins are characterised by an amino acid content dominated by proline, glutamic acid, leucine and histidine (Robinson *et al*., 1977). Lower levels of proline and histidine in mature enamel has led to the suggestion that amelogens are selectively removed during maturation (Robinson *et al*., 1977; Robinson *et al*., 1995).

The composition of the proteinaceous matrix material in mature enamel is complex and not yet fully understood (He & Swaine, 2008). It predominantly consists of non-amelogenin proteins and hydrophobic smaller chain peptides, possibly originating from both amelogenin and non-amelogenin proteins (Robinson *et al*., 1995).

Little is known about the exact distribution of organic material in mature enamel, but studies have shown that there is a local heterogeneous distribution of proteins, with much of the organic material found at rod-prism boundaries (Figure 1.14; Hillson, 2005; Hu *et al*., 1997). However, the distribution of organic material across a whole tooth is likely to be more homogeneous. This is an important consideration in AAR geochronology as an uneven distribution of proteins might cause intra-tooth variability. The presence of minute quantities of protein at the rod-prism boundaries allows limited differential movement between adjacent rods, limiting slippage and reducing stress (He & Swain, 2007).

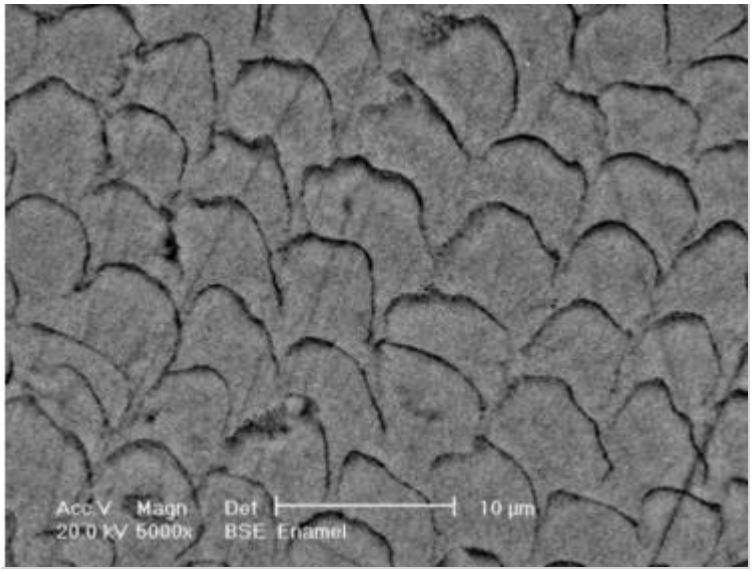

Figure 1.14. Back scattered SEM image of mature enamel. The 'fish scale' structure prevents cracks propagating straight through the enamel. Proteins are believed to be present at boundaries based on immunolocalisation analysis (He et al.*, 1997). Image taken from He & Swain (2008).*

Polarised light microscopy has indicated that a fraction of water in dental enamel is not readily removed by dehydrating methods (Carstrom *et al*., 1963; Myers 1965) and nuclear magnetic resonance spectroscopy indicates that this water fraction is potentially bound between crystallites (Myers 1965). These early studies indicate that a fraction of organic material equivalent to those found within some calcium carbonate-based biominerals may also exist in enamel.

1.11. *In vivo* racemisation in teeth

Amino acids in living organisms can racemise and if they are not actively removed, D-isomers may accumulate (Bada, 1984). The protein-secreting cells which line the enamel-dentine junction in teeth do not become incorporated into the biomineral and thus enamel is acellular (Hillson, 2006). This means that once mature, the trapped organic matrix proteins are not replaced or removed and thus D-isomer amino acids are able to build up (Helfman & Bada, 1976; Ohtani *et al*., 1988). The average temperature of teeth *in vivo* is ~35 °C; at this temperature the rate of racemisation is much greater than in the burial environment. The accumulation of D-amino acids *in vivo* can be used to calculate the age-at-death of modern samples for forensic purposes (Ogino *et al*., 1985).

Aspartic acid has been targeted for age-at-death estimation because it shows appreciable levels of racemisation over the course of an individual's lifetime. D-aspartic acid constitutes ~8 % of the total aspartic acid content in enamel, 60 years after tooth formation (Helfman

& Bada, 1975). This has applications in forensic science where adult human remains can be aged to within ±3 years, typically using the collagenous proteins in dentine (Waite *et al*., 1999).

The extent of aspartic acid racemisation in enamel has also been used to estimate the age-at-death of archaeological remains that have been buried for a short period of time (Griffin *et al*., 2008; Griffin *et al*., 2009). When tested on modern and known aged medieval populations, the correlation between the aspartic acid D/L value and the age-at-death of these populations was good, but there were high levels of variability (Griffin *et al*., 2009). This was partly due to chromatographic issues during reverse-phase high performance liquid chromatography (RP-HPLC), caused by high levels of inorganic species derived from the mineral matrix. These issues are discussed in more detail in Chapter 2.

The extent of *in vivo* racemisation in fossil samples is likely to be negligible in the context of geochronological studies and only particularly relevant when comparing mammalian species which have long lifetimes and maintain their teeth for a large proportion of them. Moreover, the length of time the tooth is likely to have been in the jaw can often be estimated and thus accounted for when building geochronological models.

1.12. Geochronological application of enamel AAR

Amino acid racemisation in mammalian enamel has been used to estimate the ages of paleontological finds with little success (Belluomini & Bada 1985; Blackwell & Rutter, 1990; Bada *et al*., 1991). Blackwell & Rutter (1990) compared AAR dates obtained from enamel of a range of species, to a pre-established chronology based on $^{230}Th/^{234}U$ dating. AAR dating of these samples was calculated based on experimentally-derived rate coefficients which assume the degradation of proteins and amino acids can be accurately extrapolated from kinetic experiments at increased temperatures. The effects of taxonomy, tooth fragment size, geochemical environment, fossil porosity, permeability, diagenetic alteration, and preservation were all assumed to be negligible. It was concluded that the dates obtained in this study were not precise enough for enamel AAR dating to be a useful tool for geochronological study. However, the assumptions made about the degradation of proteins in enamel are likely to the cause of this discrepancy between the two estimates of age. More recent studies based on other biominerals have shown that taxonomy can affect rates of racemisation (Penkman *et* al., 2008; Ortiz *et al*., 2013) and most importantly extrapolation of rate coefficients to calculate absolute ages is not always appropriate (Tomiak *et al*., 2013). Advances in analytical and preparative procedures (such as isolation

of closed system amino acids and the analysis of a greater range of amino acids using an RP-HPLC method) may resolve many of the issues plaguing these earlier studies, and whilst enamel AAR may not be appropriate for calculating absolute age estimates using experimentally-derived rate constants, a relative approach may be valid

Placing mammalian remains in chronological context is fundamental to a broad range of studies, including climate change, evolutionary biology and palaeoreconstruction. Enamel AAR has the potential to contribute to the building of geochronological frameworks through relative dating of mammalian tooth remains. Therefore, the aim of this study was to build a novel procedure for the RP-HPLC analysis of closed system amino acids from enamel, focusing on understanding the diagenetic processes of enamel proteins and amino acids.

1.13. Thesis aims

The work described in this thesis therefore covered the following key objectives:

- Development of a novel method for the isolation of amino acids from phosphate biominerals, so that routine analysis of enamel amino acids can be conducted by RP-HPLC (Chapters 2 & 3)
- Testing the closed system behaviour of amino acids in enamel through:
    - exposure to prolonged oxidative treatment (Chapter 3)
    - simulated degradation experiments, focusing on leaching of amino acids (Chapter 3)
- Testing the behaviour of amino acid degradation over geological timescales through elevated temperature experiments (Chapter 3)
- Evaluation of intra-tooth variability (Chapter 4)
- Evaluation of taxonomic effects between different taxa of Elephantidae (Chapter 4)
- Development of a UK Proboscidean geochronology (Chapter 4)
- A pilot study, building a Sicilian elephant chronology (Chapter 5)

Chapter 2: Isolation of amino acids from phosphate species by HILIC–SPE

2.1. Introduction

Early studies investigating the relationship between the extent of protein degradation in biominerals and age targeted one or two amino acids, typically alloisoleucine/isoleucine using ion exchange chromatographic methods (Bada, 1972b; Hare, 1975; Wehmiller, 1984a). Techniques such as gas chromatography were also employed, which can analyse multiple amino acids, however, also require additional preparative work and costs (Wehmiller, 1984a; Torres *et al*., 1997). A variety of different biominerals has been analysed by these methods (Wehmiller, 1984b; Wehmiller, 2013), including calcium phosphate-based material (Bada *et al*., 1973; Bada, 1985; Belluomini & Bada 1985; Blackwell *et al*., 1990). In the late 1990s an automated reverse-phase HPLC procedure was developed that enabled sub-picomole detection, simple sample preparation and quantification of nine D and L amino acid isomers (Kaufman & Manley, 1998). However, the application of this RP-HPLC protocol to the analysis of amino acids in phosphate-based biominerals presents challenges. High concentrations of inorganic phosphate species are believed to cause peak suppression, poor baseline resolution and reduce the working lifetime of HPLC columns (Griffin, 2006) and thus ideally require removal prior to analysis.

2.1.1. Problems of peak suppression

The RP-HPLC procedure used for the separation and fluorescence detection of DL-amino acids from biominerals typically use pre-column derivatisation with *o*-phthaldialdehyde (OPA; Bruckner *et al*., 1991; Kaufman & Manley 1998). Separation of DL-isomers on a non-chiral column is accomplished through the addition of a second chiral centre (*N*-isobutyryl-L-cysteine; IBLC) and the formation of an isoindole structure supports fluorescence detection at pmol concentrations (Kaufman & Manley 1998).

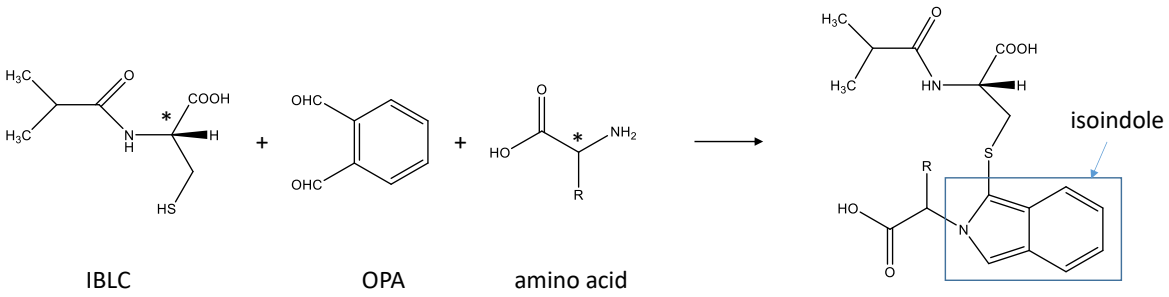

*Figure 2.1. Online derivatisation of an amino acid with OPA and IBLC. * denotes a chiral centre*

L-homo-arginine (LhArg) is used as an internal standard for the quantification of amino acids because it does not co-elute with other naturally occurring amino acids, and LhArg is not present in most biological samples (Bruckner *et al*., 1991; Kaufman & Manley 1998). Changes to the reaction efficiency or the occurrence of competitive side reactions during the pre-column derivatisation are likely to affect the analytical detection of the internal standard. When this reduces the peak area of the internal standard (LhArg) relative to blanks in the chromatogram, this is described as peak suppression.

Previous studies analysing calcium carbonate-based biominerals using the RP-HPLC method outlined by Kaufman & Manley (1998) have not reported observing peak suppression of their internal standards (Penkman *et al*., 2008; Crisp *et al*., 2013; Ortiz *et al*., 2013; Tomiak *et al*., 2013). However, calcium carbonate-based biominerals do not retain the high levels of inorganic species in solution because degassing of the carbonates as CO_2 occurs upon addition of acid during the demineralisation step. In contrast, when enamel (calcium phosphate based) samples are analysed using this method, high concentrations of inorganic phosphate species remain in solution. This correlates with a large reduction in the fluorescence response of the internal standard, affecting quantification of the amino acid concentrations (Figure 2.2). Assuming the inorganic phosphate species present in solution are responsible for the phenomenon of peak suppression, the RP-HPLC fluorescence response to the internal standard can be used as a rough guide to the phosphate species relative concentrations.

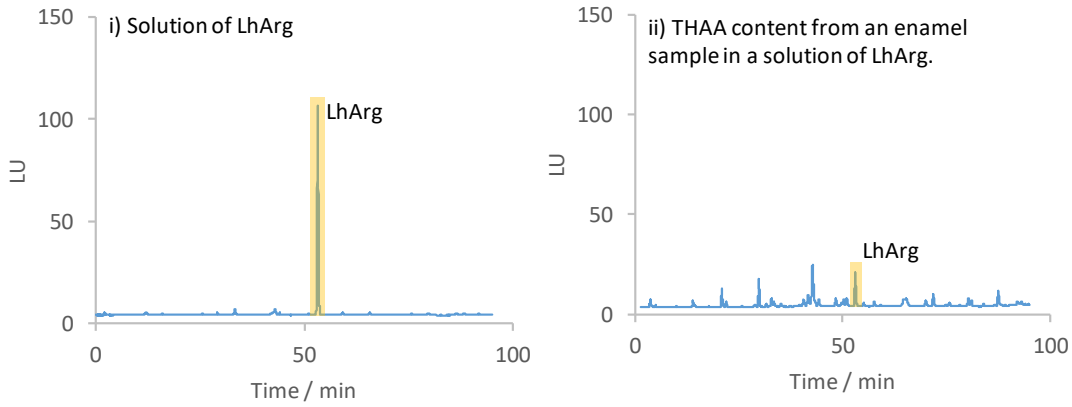

Figure 2.2. HPLC chromatograms of: i) an LhArg blank, which indicates an average LhArg peak response and ii) an enamel sample that has had no treatment to remove the high levels of inorganic phosphate and which contains the same concentration of LhArg. The contrast in LhArg peak height indicates the degree of peak suppression.

2.1.2. Hydrophilic interaction liquid chromatography (HILIC)

Solid phase extraction (SPE) is a common technique used to purify compounds prior to further analysis (Simpson, 2000). Early studies of ancient amino acids in phosphate-based biominerals used cation exchange chromatography prior to gas chromatography (GC) and ion-exchange chromatography (IEX; Bada, 1972; Belluomini & Bada 1985; Blackwell *et al*., 1990), but attempts to use these, and SPE methods using similar principles, prior to RP-HPLC analysis have not been successful for enamel (Morris, 2011; Harriman, 2012).

Hydrophilic interaction chromatography (HILIC) provides an alternative approach to conventional normal and reverse-phase mechanisms for separating polar compounds, as it separates by normal phase chromatography using reverse-phase-type eluents (Gregor *et al*., 1951; Alpert, 1990). Amino acids and the phosphate species are both polar compounds, and thus this mode of separation could potentially provide a mechanism that could separate phosphate species from the amino acids whilst retaining the necessary compositional integrity of the amino acid profile.

HILIC-type separations require the column to be preconditioned with water, which forms a water-rich layer on the surface of the adsorbent. Hydrophobic mobile phases (predominantly organic) are used to separate and elute analytes, with retention times increasing with analyte hydrophilicity. HILIC was initially developed to separate carbohydrates (Linden & Lawhead, 1975) but has since grown to be used to separate a range of molecules, including amino acids, peptides and proteins, nucleic acids and

herbicides (Alpert, 1990; Kaczynski, 2017). Amino acids and phosphates have different affinities for water; whilst both can be described as generally hydrophilic, the varying extents to which they are retained by a stationary water phase may provide a means for separation.

HILIC has been used to separate individual amino acids (Gama *et al.*, 2012), which may therefore hinder their separation from phosphate species; if some amino acids have similar stationary phase affinities to the phosphates than others, then their recovery efficiency may alter the apparent composition of the amino acid profile. Suitable conditions must therefore be discovered which minimise unwanted separation between amino acids whilst still providing the required environment for removal of phosphate species.

Controlling the order of elution in HILIC is challenging, as a number of different interactions can influence retention (McCalley, 2010; Guo, 2015; Figure 2.3). HILIC stationary phases have multimodal retention mechanisms which include ion-exchange, hydrogen bonding, hydrophilic and hydrophobic interactions (Naidong, 2003; Grumbach *et al*., 2010). Altering the separation/elution parameters can vary the predominant retention mechanism and even reverse the retention mechanism from hydrophobic to hydrophilic interactions on the same column (Dong & Huang 2007). Polarity and electrostatic properties are often good indicators of how an analyte will interact with the water layer and therefore suggest the necessary conditions for elution (Periat *et al.*, 2015). However, the contribution of each interaction to the total retention can make fine tuning properties difficult, especially if a comprehensive understanding of the mechanism for retention is not established. Additionally, there is a range of potential equilibrium species present in solution, the proportions of which are dependent on pK_a values and the pH value of the mobile phase. This makes pH an important variable in fine tuning the retention of species, as well as providing a means for improved resolution for the separation of amino acids from phosphate species. However, pH and pK_a values in environments with significant organic content may be very different from those in aqueous solutions, making understanding of the physiochemical properties and interactions challenging.

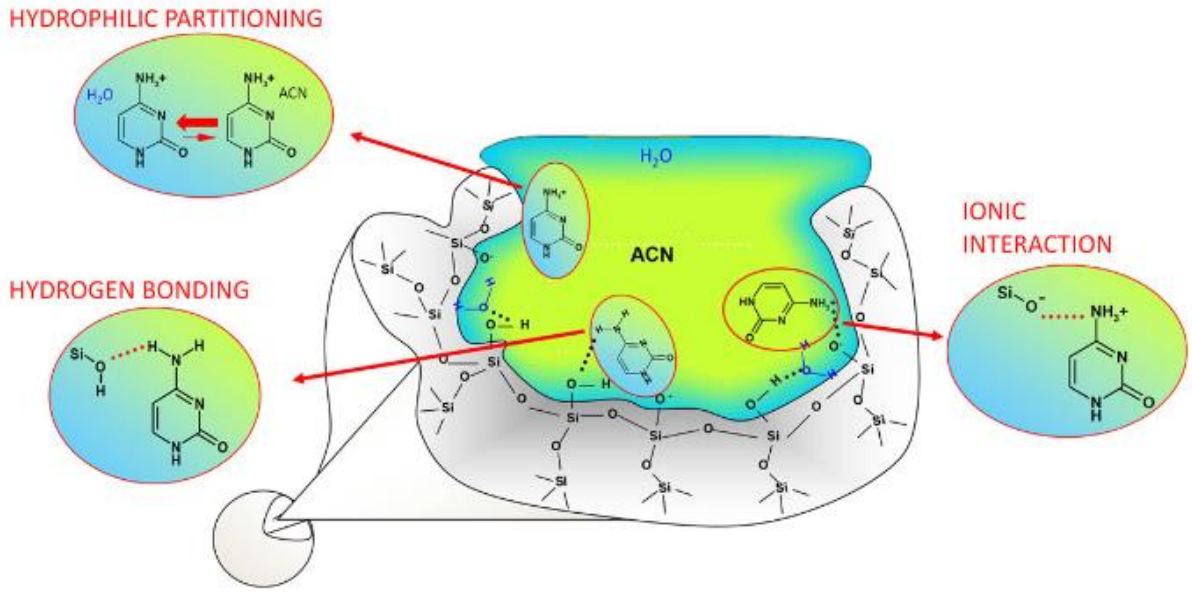

Figure 2.3. The variety of HILIC retention mechanisms (from Grumbach et al., 2010).

By reducing some of the modes used to separate the amino acids from each other and optimising those interactions that separate the total amino acid content from inorganic phosphate species, a mixed mode approach (e.g. HILIC combined with ion exchange) to separation may yield positive results.

2.1.2.1. Importance of pH for HILIC/ionic-exchange separation of phosphate species from amino acids

For the series of experiments outlined in this chapter, a zwitterionic HILIC SPE cartridge was selected, in which the silica stationary phase has polar functional groups of a quaternary ammonium and sulfonic acid covalently attached (Figure 2.4, shown in orange). This allows the use of separation modes based on both hydrophilic and ionic interactions to separate analytes (Kato *et al.*, 2009). If optimised, this stationary phase may be able to give enough selective retention of the amino acids, enabling their separation from phosphate species.

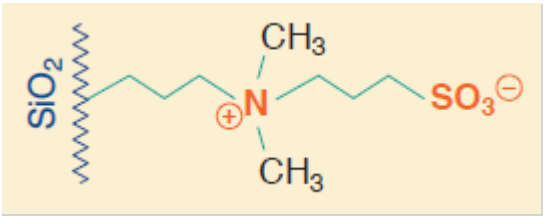

Figure 2.4. Chemical representation of the modified silica surface of the HILIC SPE cartridge used in this study (Grumbach et al., 2010)

The charge state of both the stationary phase and ionisable compounds can lead to dramatic changes in retention (Gou & Gaiki, 2011). Solubilised phosphate can exist in four

forms, the ratio of which is dependent on the pH of its environment (Figure 2.5a). Amino acids also exist in a series of forms (example: Ala, Figure 2.5b); each amino acid has a unique set of pK_as and some amino acids have more than three forms due to doubly charged states (e.g. Asp, Glu).

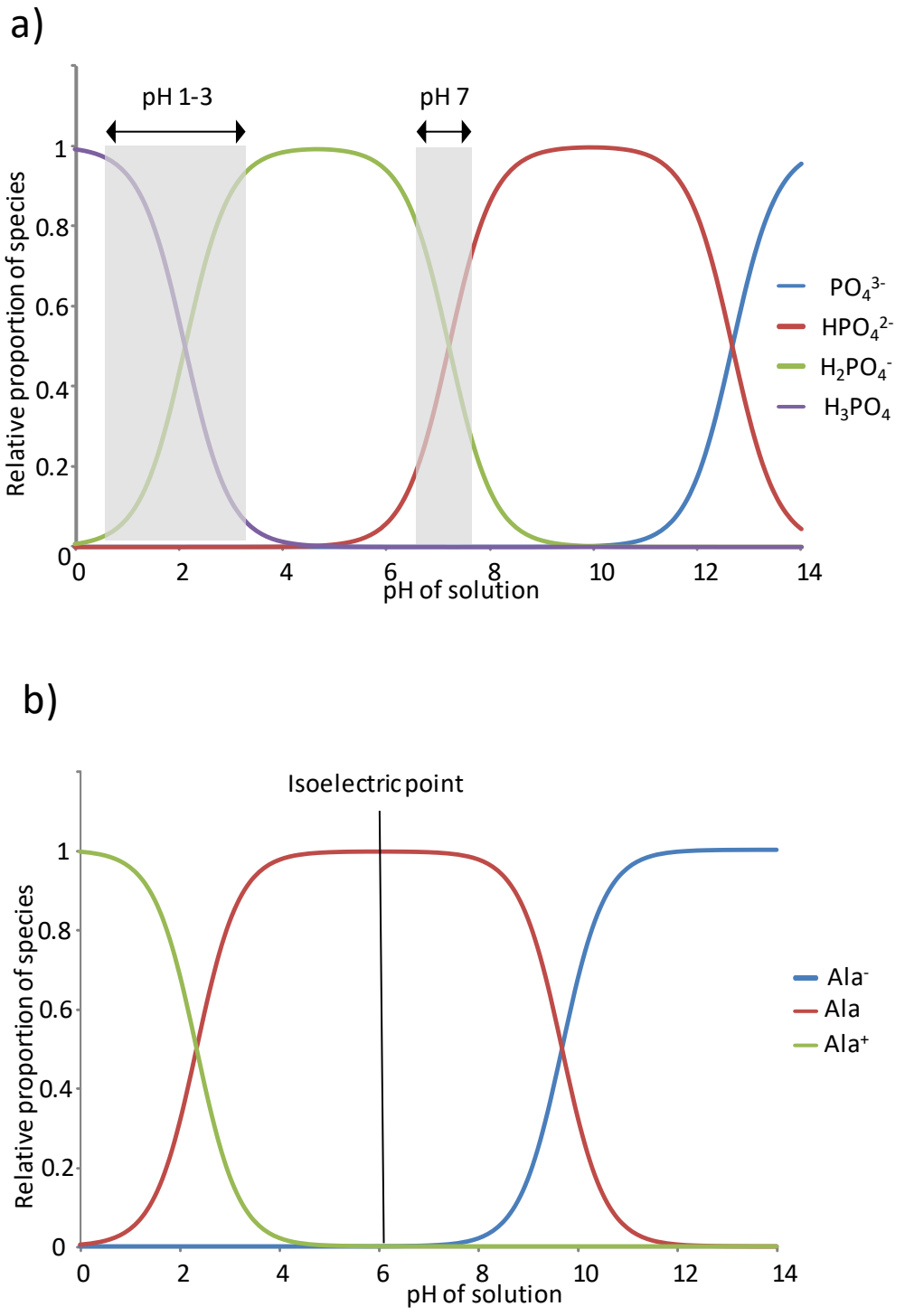

Figure 2.5. Proportion of phosphate (a) and alanine (b) species at different pHs in aqueous solutions. Derived from pK_a values. Note: Alanine has been shown as an example of a neutral amino acid but some amino acids (e.g. Asp, Glu) have more than three species.

Controlling the charge states of the phosphate species present in solution is likely to impact their retention by the stationary phase, especially in terms of their capacity for ionic interactions (Kopaciewicz *et al.*, 1983). Ionic-exchange retention is largely controlled by the

strength of electrostatic interactions. This force can in simplistic terms be described by Coulomb's law:

$$F = \frac{q_1 q_2}{dr^2}$$

Equation 3. Where q_1 and q_2 are point charges of opposite sign, r is the distance between the point charges and d is the dielectric constant of the medium.

Increasing the point charge of the phosphate or amino acid species increases electrostatic interactions and thus is likely to increase the retention of the species. Changes in pH can also impact the charge state of the stationary phase, potentially influencing the retention of analytes. The other modes of separation occurring during this multi-modal separation are also likely to be influenced and thus experimental trials testing the effects of changing the pH of the eluent were needed to optimise the interactions for separation.

The aim of the work described in this chapter was therefore to investigate mechanisms for the removal of phosphate ions from solution prior to injection onto the RP-HPLC column. This focused on the separation of amino acids from inorganic phosphates by HILIC SPE. It is essential that the preparative step does not significantly impact on the amino acid composition and D/L values which are important for the ultimate application of AAR geochronology. A range of different pH and mobile phase compositions was trialled to optimise the separation of amino acids from hydroxyapatite in standards containing amino acids:

- Fixed composition acetonitrile / H_2O mobile phase at low pH
- Fixed composition acetonitrile / H_2O mobile phase at neutral pH
- Variable composition acetonitrile / H_2O mobile phase at neutral pH
- Variable composition methanol / H_2O mobile phase at neutral pH
- Fixed composition methanol / H_2O mobile phase at pH >7

Then the optimised method was tested on fossil mammoth enamel. During these fossil tests it became clear that the method optimised for the standards containing amino acids was not appropriate for preparation of peptide-bound amino acids, and therefore further experiments were undertaken to investigate this.

2.2. Materials and standard procedures

As various methods are discussed over the course of this chapter, those procedures are detailed in the relevant experimental methods sections. However, throughout the study aspects were not changed; these are detailed here.

2.3. Chemicals and reagents

HPLC-grade water was prepared using a Millipore Simplicity system. HPLC-grade acetonitrile and methanol were purchased from VWR Chemicals. Analytical reagent grade HCl (~36%) was purchased from Fisher Scientific, UK. Hydroxyapatite powder was purchased from Sigma Aldrich, UK.

2.4. 1:1 reference samples

A 1:1 D:L amino acid reference solution was used to provide a sample with known amino acid composition. This solution contained the free amino acids Arg, Asp, Glu, Gly, His, Ile (D-isomer D-alle), Leu, Lys, Met, Phe, Ser, Thr, Tyr and Val and the internal standard (LhArg). To mimic an enamel sample, 1:1 amino acid reference solution (10 µL) was added to hydroxyapatite powder (~2 mg) and dried by centrifugal evaporation.

2.5. Powdering and bleaching (fossil samples only)

Fossil samples were powdered with an agate pestle and mortar, and the powder cleaned by bleaching. Samples were submerged in 12 % (w/v) NaOCl (50 mL mg^{-1} of enamel) for 48 h and agitated every 24 h to aid exposure to the bleach (Sykes *et al*., 1995; Penkman *et al.* 2008). The bleach was removed, and the enamel powder washed five times in HPLC-grade water; an additional wash with HPLC-grade methanol was used to remove left-over bleach. The samples were air-dried overnight.

2.6. Hydrolysis of peptide-bound amino acids (fossil samples only)

For fossil samples where the total hydrolysable amino acid (THAA) content was determined: bleached enamel (~2 mg) was hydrolysed in HCl (7 M, 20 µL mg^{-1}) and heated at 110℃ for 24 h in N_2-purged vials, following the methods of Penkman (2005). The samples were dried by centrifugal evaporation, removing the acid.

2.7. Demineralisation/dissolution of samples for use with neutral pH eluents

HCl (1 M, 20 µL mg^{-1}) was added to 1:1 reference samples and fossil samples to demineralise the crystal matrix. Prior to loading onto a HILIC SPE cartridge (see section 2.8) the pH of the solution was raised using KOH solution (1 M, 20 µL mg^{-1}) to better match the

pH of the eluent. Upon addition of the KOH, a monophasic cloudy solution with gel-like properties formed. An excess of ethylenediaminetetraacetic acid (EDTA; 2.5 mg) was added to sequester Ca^{2+} ions and re-dissolve the inorganic species, the solution was agitated until the solution was clear. Samples were then centrifuged at 13,000 rpm for 3 min and the clear solution pipetted off remaining undissolved solid EDTA.

2.8. HILIC SPE general protocol

HILIC SPE cartridges (HiChron, Chromobond) with ammonium – sulfonic acid modification, pore size 60 Å, particle size 45 µm, specific surface 500 m^2/ g, pH stability 2-8, carbon content 7 % (Anon, 2012) were used where specified in this study. HILIC SPE columns were pre-conditioned with 500 µL of distilled water (Macherey-Nagel, 2012), followed by 3 mL of the specified eluent.

The sample was dissolved in 50 µL eluent (according to their specific procedures, see sections 2.12.2, 2.13.1, 2.14.2, 2.16, 2.18.1 & 2.19.1) and then loaded onto the pre-conditioned column. Once the solution reached the column bed, eluent (500 µL) was loaded onto the column and the eluting solution collected in sterilised 2 mL glass vials; this process was repeated 3-4 times. HPLC grade water was used to remove remaining amino acids and collected; this process was repeated 3-4 times (Figure 2.6). The fraction collection was not very reproducible, because SPE flow rates were highly variable between columns. However, although the volumes were not identical between replicates, their relative order was consistent. The conditioning of the column and the collection of all fractions was done under atmospheric pressure. The contents of the vials were dried by centrifugal evaporation overnight at 25 °C.

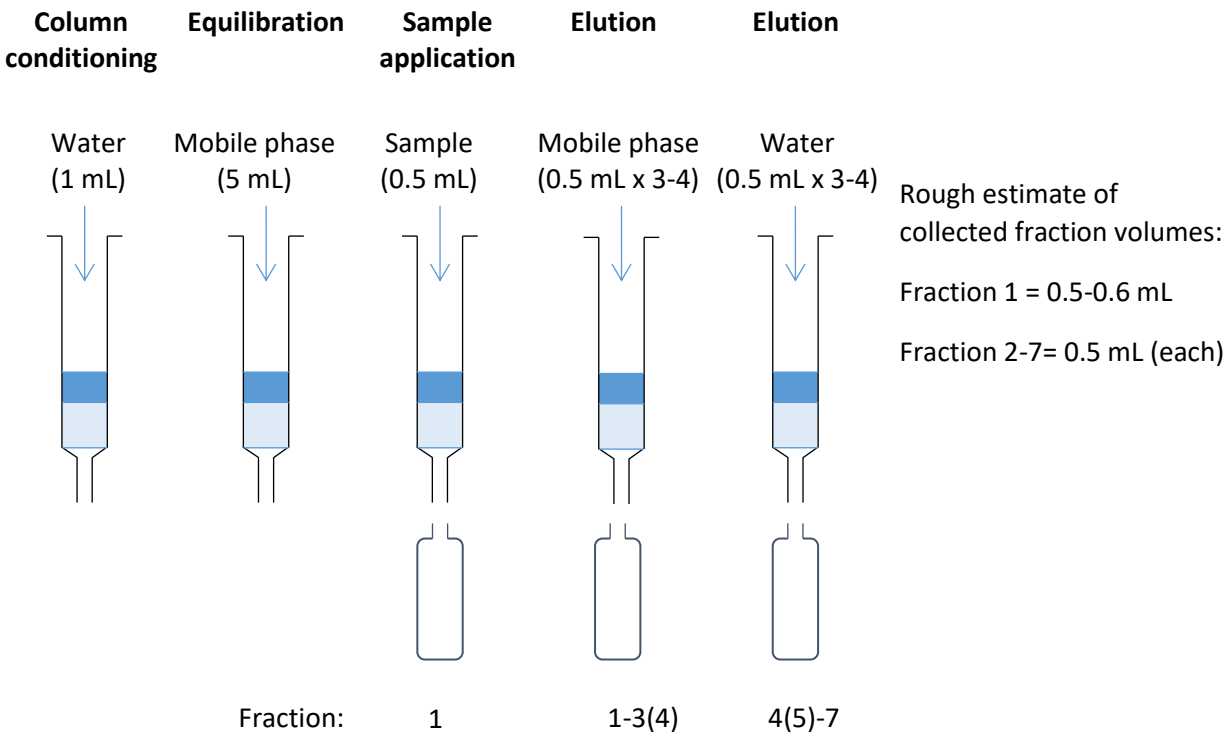

Figure 2.6. Protocol for HILIC SPE column conditioning and fraction collection

2.9. RP-HPLC analysis

Samples were rehydrated in a weak acid solution containing L-homo-arginine (LhArg) which acted as an internal standard for the quantification of amino acids. The solution contained a non-protein amino acid (L-homo-arginine; 0.01 mM), sodium azide (0.01 mM) and HCl (0.01 M) in HPLC grade water.

An Agilent 1100 series HPLC fitted with a HyperSil C18 base deactivated silicone (BDS) column (5 µm, 250 x 3 mm) and fluorescence detector was used for analysis of the chiral amino acid pairs. 2 µL of sample solution was injected and mixed online with 2.2 µL of derivatising reagent (260 mM *n*-Iso-L-butyryl L-cysteine (IBLC), 170 mM *o*-phthaldialdehyde (OPA) in 1 M potassium borate buffer, adjusted to pH 10.4 with potassium hydroxide pellets. The column temperature was controlled at 25°C and a tertiary solvent gradient method used (sodium acetate buffer, acetonitrile and methanol) modified from Kaufman & Manley (1998). Sodium acetate buffer was prepared by dissolving sodium acetate tri-hydrate (6.26 g, Fisher Scientific, UK), EDTA (200 mg, VWR Chemicals) and sodium azide (750 mg, VWR Chemicals) in HPLC-grade water (2 L), adjusted to pH 6.00 ±1 with 10% acetic acid and sodium hydroxide. The fluorescence detector used a xenon-arc flash lamp at a

frequency of 55 Hz, with a 280 nm cut-off filter and an excitation wavelength of 230 nm and emission wavelength of 445 nm.

2.10. LhArg peak response

The amino acid reference solutions (section 2.4) used in the set of experiments outlined in this chapter contained a known concentration of the internal standard LhArg. However, the total amount of LhArg in the amino acid reference solutions is likely to elute in multiple fractions during HILIC SPE and the concentration of LhArg in these fractions was therefore unknown. Upon rehydration, a known concentration of LhArg was subsequently added to each of the collected fractions (section 2.9) but due to the additional amount of LhArg from the amino acid reference solutions, the total concentration of LhArg in each of the fractions could not be accurately determined. Changes in the LhArg HPLC peak areas have been used in the chapter to estimate the effects of peak suppression using the HPLC peak areas of LhArg. Comparisons to samples run without the additional contribution from the amino acid reference solutions (samples run with LhArg rehydration fluid only) have been made, but as these values represent a minimum range for responses, the effects of peak suppression are likely to be underestimated.

2.11. Analysis of D/L values

Where D/L values have been cited for specific mobile phases (e.g. Figure 2.9), the mean value from the two collected fractions that contained the majority of amino acids has been quoted.

2.12. Fixed composition acetonitrile / H_2O mobile phase at low pH

2.12.1. Choice of acetonitrile as mobile phase solvent

Acetonitrile is often used in HILIC-type separations because it is an aprotic polar solvent, it is miscible in water, and it has limited effect on disrupting hydrophilic interactions between substrate molecules and the water partition (Krumpochova *et al*., 2015; Ruta *et al.*, 2010). HILIC retention is proportional to the percentage of organic solvent in the mobile phase; thus, the sample is loaded in an organic-rich solution, and then water is used to elute amino acids because increasing the aqueous content of the eluent diminishes the retention of the polar analytes. With a zwitterionic stationary phase operating under HILIC conditions using a pH-controlled mobile phase, it was hypothesised that the phosphates would elute later in the water-washing stage (Figure 2.6), as they are more polar than the amino acids. Trialling a range of different organic mobile phase compositions may enable a better

understanding of the retention mechanism to be established and an optimum mobile phase composition to be determined.

2.12.2. Fixed composition acetonitrile / H_2O mobile phase at low pH: Background

In general, charged compounds are more hydrophilic than neutral compounds and therefore more readily retained in HILIC (Periat *et al*., 2015). Experiments were conducted at low pHs (1 and 2), as this provides an environment in which the phosphate species would be predominantly in an uncharged state (H_3PO_4) and the amino acids would be charged (Figure 2.5). In theory, low pH should increase the retention of the amino acids through ionic-exchange interactions (in tandem with hydrophilic partitioning) whilst decreasing retention for phosphates (Kopaciewicz *et al*., 1983). Moreover, hydroxyapatite is readily dissolved in acidic conditions, therefore would be in solution at low pH.

However, understanding the pH environment the analytes are exposed to is challenging. Whilst the pH of the water component of the mobile phase can be controlled using an aqueous buffered system, once mixed with an organic modifier, the pH will change and can become much harder to quantify (McCally, 2010). Measuring the pH of an aqueous fraction of the mobile phase with an electrode calibrated in aqueous standard buffers and subsequently adding an organic solvent does not yield a pH value that represents the true concentration of hydrogen ions. Furthermore, measuring the pH of a solvent mix with electrodes calibrated in aqueous buffers also does not yield the true value. To accurately measure the pH of an organic mixed mobile phase, calibration solutions with the same composition as the solution to be measured need to be used. However, this is difficult, as calibration solutions of a range of different solvents are not readily available. Therefore, the pH data reported in this study are not precise but do provide a qualitative measure of the relative acidity / alkalinity of the solutions used.

2.12.3. Fixed composition acetonitrile / H_2O mobile phase at low pH: Experimental

Hydroxyapatite with 1:1 D:L amino acid reference solution (section 2.4) was dissolved in eluent (120 µL) and loaded onto a pre-conditioned HILIC SPE cartridge. Three different low pH acetonitrile/water eluents with were trialled (Table 2.1). Fractions were eluted according to the standard protocol (section 2.8) with three portions (3 x 500 µL) of ACN/water eluent and 4 x 500 µL of water used to elute the analytes. Eluent composed of 75 % acetonitrile in water was used for all three experiments.

Table 2.1. Composition and pH of mobile phase in the experiments with fixed composition mobile phase at low pHs. The pH of the eluent was recorded using pH indicator strips (Fisherbrand, pH-Fix 4.5-10).

Desired pH	% of acetonitrile in water	HCl concentration / mol dm^{-3}	Recorded pH
1	75	0.4	1.0 ± 0.5
2	75	0.04	2.0 ± 0.5
3	75	0.004	3.5 ± 0.5

Elevated pressure was used during elution for pH 1 and 2 eluents and only the first five fractions were collected as it was thought that all the amino acids would have eluted in this volume. Gravity dripped collection was used for pH 3 eluents and all seven fractions were collected. Collected fractions were analysed for their amino acid content by RP-HPLC (section 2.9). The pH of the mobile phase was adjusted with HCl and assessed with pH strips (Fisherbrand, pH-Fix 4.5-10).

The eluent was removed from collected fractions by centrifugal evaporation. Samples were rehydrated in a solution containing LhArg prior to analysis by RP-HPLC (section 2.9).

2.12.4. Fixed composition acetonitrile / H_2O mobile phase at low pH: Results and discussion

SPE experiments with eluents at pHs 1 and 2 yielded very poor recoveries for most of the amino acids. Most of the more hydrophobic amino acids (Try, Val, Phe, Leu, Ile) were not recovered at high enough concentrations to enable quantification of both the D and L peaks (Figure 2.7). The poor recovery of amino acids may be due to the elevated pressures used during the column conditioning, washing and elution. These conditions used to equilibrate the column may have not have been suitable for establishing the stationary water layer need for HILIC and therefore led to poor retention of the amino acids. Additionally, the recommended working pH range of the HILIC SPE cartridge is > pH 2 (Macherey-Nagel, 2012) so at these low pHs, the cartridge may not be working as proposed. At these pHs the column may begin to degrade and thus the stationary phase may not retain analytes as intended.

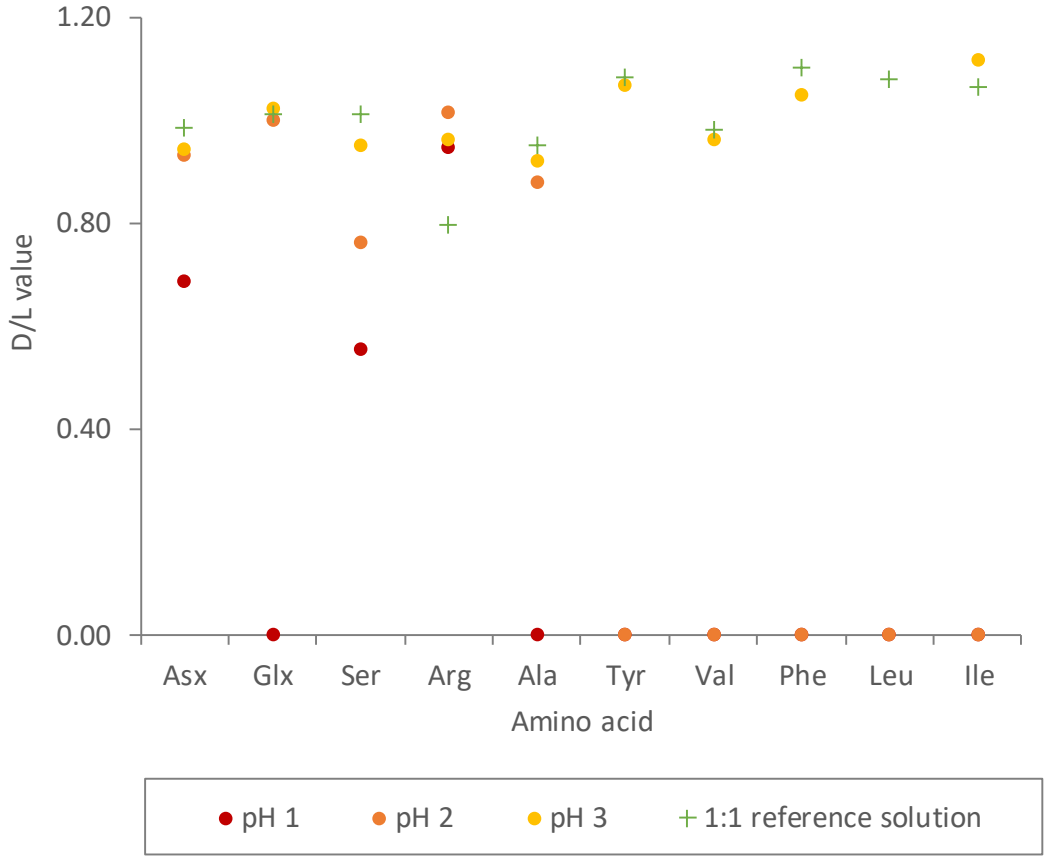

Figure 2.7. D/L values of amino acids recovered from hydroxyapatite-containing amino acid reference solutions after HILIC SPE. Separations used three different low pH mobile phases (pH 1 = red, pH 2 = orange, pH 3 = yellow). Amino acids that could not be resolved to baseline resolution have been plotted along the x-axis. The mean D/L value from the two fractions that contained the most amino acids is shown. A 1:1 reference solution, not subjected to HILIC SPE has been shown for comparison (green cross).

At pHs 1 and 2 there were visual signs of residue in the vials after centrifugal evaporation (Table 2.2). This residue is thought to be calcium phosphate that is co-eluting with the fractions that also contain amino acids. This indicates that at these pHs there is insufficient separation of the amino acids from the phosphate species.

Table 2.2. Visual signs of residue in the vials of fractions after centrifugal evaporation. Y = present, N = not present. The residue was a white solid and thought to be calcium phosphate.

Fraction	Eluent composition	Visual residue in vial		
		pH 1	pH 2	pH 3
1	ACN/water	N	N	N
2	ACN/water	Y	Y	N
3	ACN/water	Y	Y	N
4	Water	Y	Y	Y
5	Water	N	Y	Y
6	Water	-	-	Y
7	Water	-	-	N

A pH 3 mobile phase was trialled under atmospheric pressure, which generated a much higher recovery of all the amino acids studied, with D/L values broadly unaltered (most amino acid D/L values have been altered by <6%, only Arg and Leu are alter by >6%) by the HILIC SPE purification (Figure 2.7). However, the amino acids eluted in multiple fractions. In general, polar amino acids had a greater affinity for the stationary phase and eluted in later fractions (fractions 4-7), with more apolar amino acids eluting earlier (Val, Phe, Leu & Ile, fractions 1-5; Figure 2.8). However, this cannot be the only important interaction, as Asx, even though it is not the most polar amino acid, was more prevalent in later fractions. This may indicate a role of the acidic side chain of Asx or reflect the role of the organic modifiers in the solutions involved. To achieve high recoveries of the amino acids in a single fraction with this mobile phase composition, several of the collected fractions would need to be combined. Moreover, visual inspection of the vials (Table 2.2) suggests that phosphates are co-eluting in the same fractions as some of the amino acids, which may pose concerns if these fractions were to be combined.

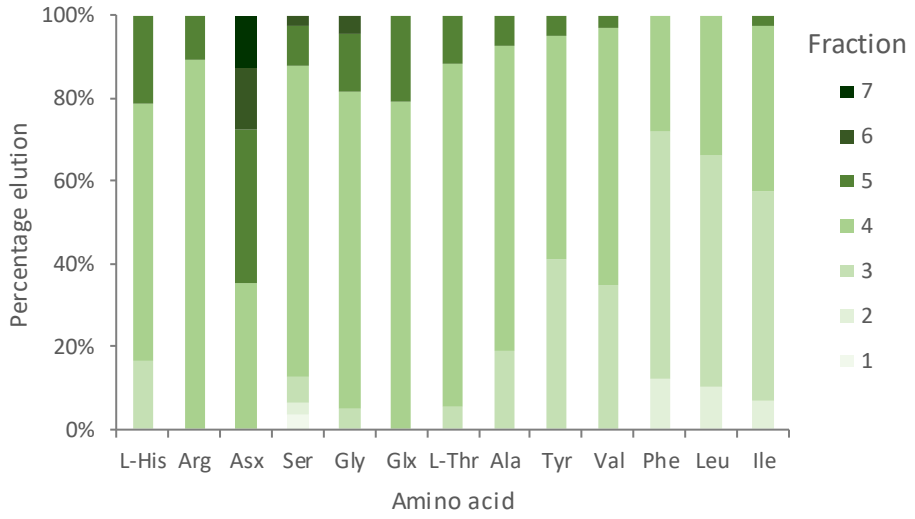

Figure 2.8. Proportion in each of the collected fractions of the total recovered amino acids from an amino acid standard containing hydroxyapatite and purified with HILIC SPE using pH 3 mobile phase (section 2.8). Amino acids are ordered in decreasing polarity (Taylor, 1986).

The use of low pH eluents under these conditions does not appear to sufficiently separate the amino acids from the inorganic species present in solution. Poor amino acid recovery was obtained at pH 1 and 2 but improved at pH 3. This indicates that increasing the pH may improve separation.

2.13. Fixed composition acetonitrile / H_2O mobile phase at neutral pH

As the low pH experiments indicated that phosphate species were eluting in the same fractions as some of the amino acids and improvements were observed when the pH was increased (section 2.12), a mobile phase at neutral pH was trialled. Prior to loading the sample on the SPE column, enamel samples were demineralised to break down the hydroxyapatite structure and release the amino acids. However, this lowers the pH of the mobile phase and therefore may alter the mode of separation. To control the pH of the mobile phase prior to loading onto HILIC SPE cartridges, an additional step was therefore added. Base was added to the demineralised hydroxyapatite solution to increase the pH of the sample solution to match that of the mobile phase (~pH 7). Potassium hydroxide (KOH) was chosen as a suitable base for pH control as it was hoped that potassium phosphate would be formed upon addition, which is more soluble than calcium phosphate and thus would remain in solution.

At close to neutral conditions the amino acids are predominantly in their zwitterionic form with no net charge and therefore least soluble (Figure 2.5). Phosphate ions form

approximately equal amounts of their $H_2PO_4^{1-}$ and HPO_4^{2-} species (Figure 2.5). However, these assumptions are made based on pK_a data in aqueous solutions and may not be accurate for solutions with an organic content. The charge states of the phosphates make ionic interactions with the stationary phase more likely, and therefore the phosphate species are likely to be retained longer by the stationary phase than at low pH. The elution of the amino acids is more complex as there is a range of different charge states present in solution. However, the amino acids should elute earlier than at low pHs and the phosphate species should elute later.

2.13.1. Fixed composition acetonitrile / H_2O mobile phase at neutral pH: Experimental

A sample of hydroxyapatite with a 1:1 amino acid reference solution was used (Section 2.4). The sample was demineralised in HCl (1 M, 40 µL) and then the solution was neutralised with KOH (1 M, 45 µL) to match the pH of the mobile phase prior to loading on to the HILIC SPE cartridge. Upon addition of KOH, a cloudy, monophasic, 'gel like' solution formed. The solution was unsuitable for SPE separation and therefore EDTA was added to bind to the Ca^{2+} ions and bring the sample back into solution.

EDTA (2.5 mg) was added and agitated until the solution was clear. Samples were then centrifuged at 13,000 rpm for 3 min and the clear solution pipetted off remaining undissolved EDTA. The pH of the extracted supernatant was recorded (pH 6.5 ±0.5) using indicator strips.

The samples were loaded onto a pre-conditioned HILIC SPE cartridge and eluted according to the standard protocol (see section 2.8). 75 % acetonitrile in water mobile phase composition was used with pH recorded at 7 ±0.5 using pH indicator strips. Collected fractions were analysed for their amino acid content by RP-HPLC (section 2.9).

2.13.2. Fixed composition acetonitrile / H_2O mobile phase at neutral pH: Results and discussion

2.13.2.1. Gel formation

Hydroxyapatite dissociates in acidic aqueous solutions and the ions can take part in various reactions with water and the other solutes present. The solubility of ions is often highly sensitive to their charge state and thus the pH of the solution. The addition of a base to increase the pH of solution appears to rapidly precipitate the inorganic ions. However, the high concentration of inorganic ions and nature of the solutes leads to the formation of a

gel, thought to be a colloid in which the inorganic ions are 3-dimensionally cross-linked giving it properties like a solid (Furukawa & Tanaka 2010).

2.13.2.2. Separation

The pH 7 mobile phase yielded similar amino acid recoveries to the mobile phase at pH 3 and the D/L values were also comparable (Figure 2.9). This indicates that there is negligible improvement in these measures when raising the pH of the mobile phase to pH 7. However, the retention of the amino acids in the stationary phase increased (Figure 2.8 cf.Figure 2.10). The majority of amino acids eluted in fractions 5 and 6, with only minimal elution of amino acids in fraction 7. The more polar amino acids eluted in later fractions, which is consistent with the experiments conducted at low pH (Figure 2.8). The majority of amino acids eluted in fewer fractions at the higher pH; this may indicate that there is less separation between the amino acids which should aid in the separation between the amino acids and the phosphate species

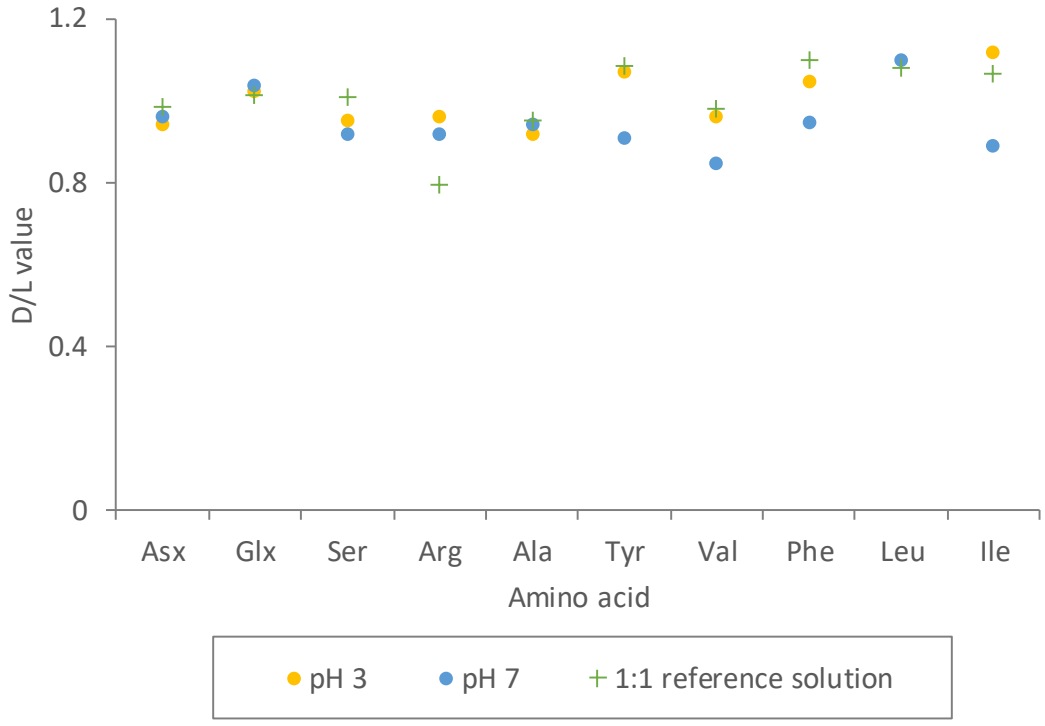

Figure 2.9 D/L values of amino acids recovered from hydroxyapatite with amino acid reference solutions after HILIC SPE. Separations shown have been run with different pH mobile phases (pH 3 = yellow, pH 7 = blue). Amino acids that could not be resolved to baseline resolution have been plotted along the x-axis. D/L values. The mean D/L value from the two fractions that contained the most amino acids is shown. A 1:1 reference solution has been shown for comparison (green cross).

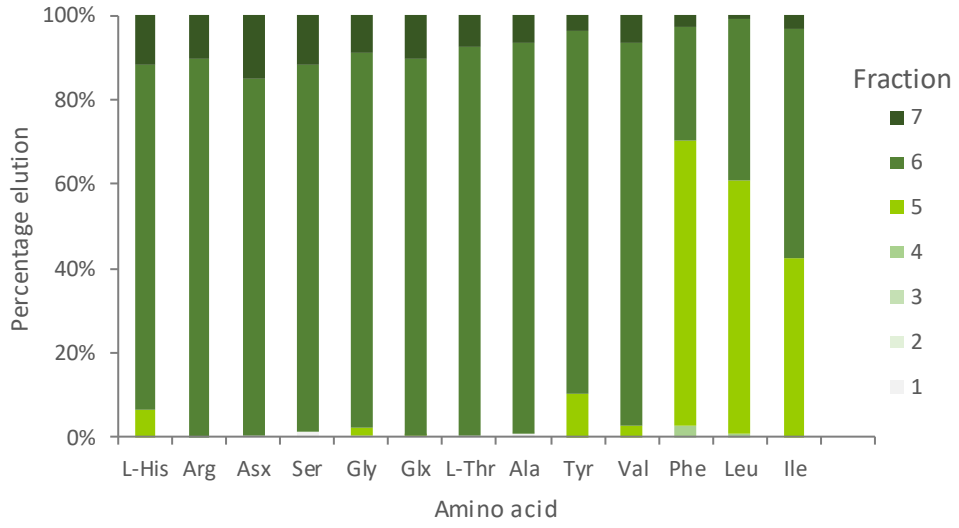

Figure 2.10. Proportion in each of the collected fractions of the total recovered amino acids from an amino acid reference solution with hydroxyapatite and purified with HILIC SPE using neutral pH mobile phase. Amino acids are ordered in decreasing polarity (Taylor, 1986).

Using neutral pH eluent yields similar amino acid recovery rates and D/L values to those eluted at pH 3. However, using a pH 3 mobile phase would potentially require a buffered system and as it provides no additional benefits (apart from dissolution of the sample in the eluent directly), further experiments were conducted using neutral or >pH 7 mobile phases.

2.14. Variable composition acetonitrile / H_2O mobile phase at neutral pH

2.14.1. Elution of amino acids

Trialling a range of different organic mobile phase compositions at neutral pH may enable a better understanding of the retention mechanisms and the optimum mobile phase composition to be determined. Amino acids are hydrophilic and therefore should be retained longer by the water-rich stationary phase upon increasing organic content of the mobile phase. If the separation is predominantly occurring via this mechanism, then the amino acids would be expected to elute in later fractions when using a higher percentage acetonitrile composition, with phosphates eluting earlier.

2.14.2. Variable composition acetonitrile / H_2O mobile phase at neutral pH: Experimental

A sample of hydroxyapatite with a 1:1 amino acid reference solution (section 2.4). The sample was demineralised in HCl (1 M, 40 µL) then the solution was neutralised with KOH to match the pH of the mobile phase prior to loading on to the HILIC SPE column. Upon

addition of KOH, a precipitate formed, and the solution become gel like. EDTA (2.5 mg) was added and agitated until the solution became clear. Samples were then centrifuged, and the clear solution pipetted off remaining undissolved EDTA.

The samples were loaded on to a pre-conditioned HILIC SPE cartridge, and eluted according to the standard protocol (section 2.8) with three portions (500 µL) of ACN/water eluent and four of water used to elute the analytes. The percentage of acetonitrile/H_2O in the mobile phase was varied (20%, 30%, 40%, 85% or 95%; Table 2.3). The pH of the mobile phases was recorded to be 7.0 ±0.5 using pH indicator strips (Fisherbrand, pH-Fix 4.5-10). Collected fractions were analysed for their amino acid content by RP-HPLC (section 2.9).

Table 2.3. The eluent used to generate each fraction (see Figure 2.6). xx = 20, 30, 40, 85 or 95

Fraction	Mobile phase	Total loaded/collected volume / µL
1	sample (50 µL) and ACNxx (300 µL)	350
2-3	ACNxx	500
4	ACNxx or water*	500
5-7	Water	500

* water was used in AcN85 and 95

2.14.3. Variable composition acetonitrile / H_2O mobile phase at neutral pH: Results & discussion

Experiments undertaken with mobile phases of 1:1 acetonitrile/water or less (ACN25 and ACN50) eluted the majority of the amino acids with the organic eluent (fractions 3 and 4), while mobile phases of 3:1 acetonitrile/water or higher (ACN75, ACN85 and ACN95) required water washes to elute the amino acids (fractions 5 and 6; Figure 2.11). This therefore fits with the previous assumption, with amino acid retention increasing with organic content.

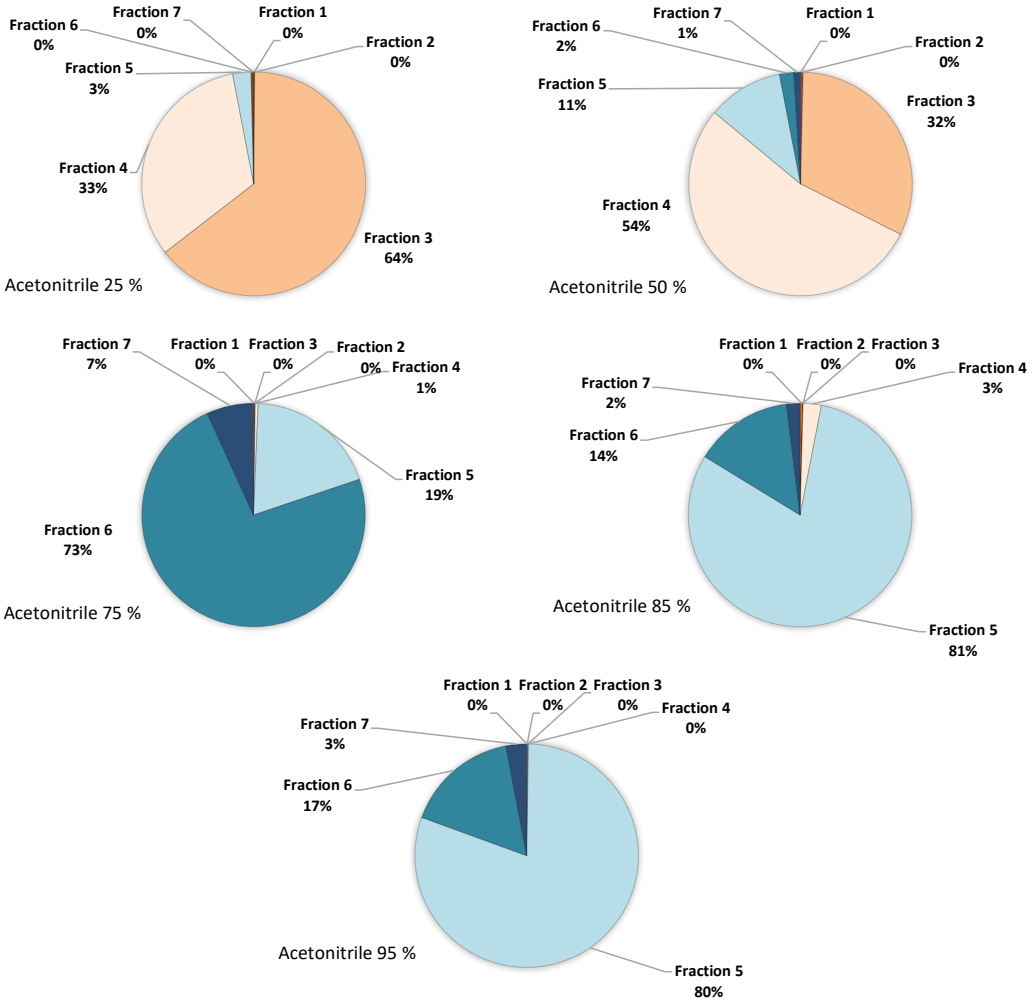

Figure 2.11. Total amino acid content of each of the seven, 500 µL fractions collected at the different acetonitrile compositions. Fractions collected after an acetonitrile-rich mobile phase was loaded are shades of red, fractions after distilled water was loaded are shades of blue

The presence of inorganic phosphate species in solution prior to injection onto the HPLC instrument has been linked with a reduction in the peak areas of amino acids when compared to amino acids analysed without phosphate species (Figure 2.2). The internal standard (LhArg) is added prior to HPLC analysis in a known concentration and is used as a standardised measure of the detector response. It can therefore be inferred that a reduction in the peak area of the internal standard indicates the presence of high concentrations of inorganic phosphate species (section 2.10). Peak suppression above 15 % was present in fraction 5 of ACN25, 85 and 95 (Figure 2.12). Fraction 5 also contained a large portion of the total amino acid content for the higher percentage organic content eluents (ACN85 & 95; Figure 2.11). This level of peak suppression is likely to impede accurate and precise quantification of the DL-isomers of the amino acids. Indications that

the phosphate species are eluting in fraction 5 suggest that early elution of amino acids, such as in lower acetonitrile composition mobile phases, is preferred.

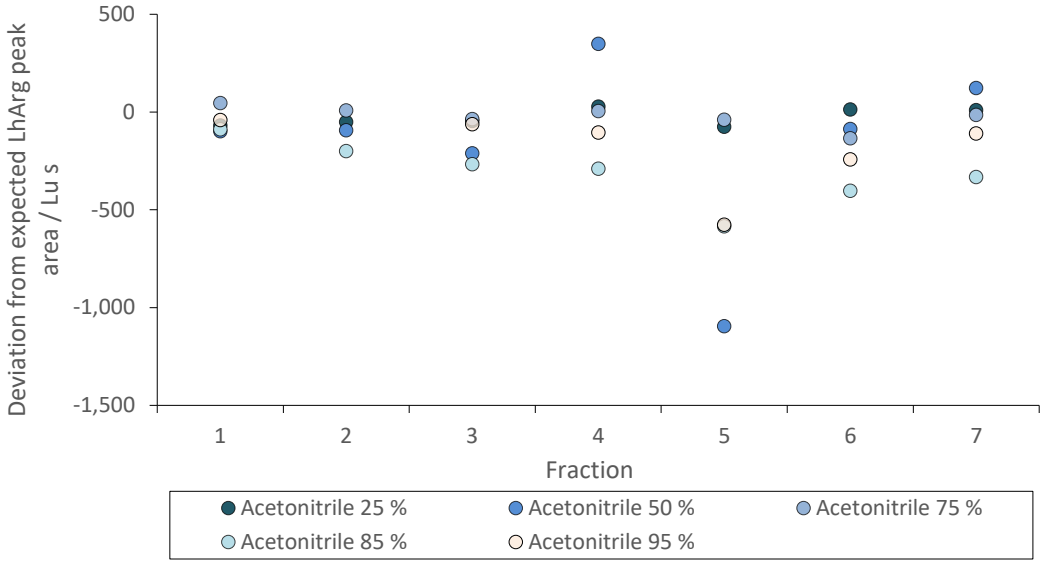

Figure 2.12. Deviation from the expected mean calculated from hydroxyapatite blanks analysed with an appropriate mobile phase for each of the collected fractions. Peak suppression is indicated by negative values, which are greatest in fraction 5 and imply the presence of phosphate species in solution. Fraction 1 for all the eluent compositions (ACN25-95) had similar peak areas to the LhArg blanks, which contained only LhArg in solution and indicates a rough estimate of the expected variability of the LhArg areas.

The impact the separation process has on altering amino acid D/L values is a key factor in assessing the usability of a method on fossil samples. The consistency of amino acid D/L values directly influences the ability to temporally resolve fossil material. Compared to the variability expected from D/L values analysed by this RP-HPLC method (~2-3 %; Kaufman & Manley, 1998), for some amino acids there was relatively high variability in the D/Ls, often for the low (25 %) and high (>75 %) ACN percentages (Figure 2.13). This decreased accuracy correlates with amino acid fractions that also had higher levels of peak suppression (Figure 2.12).

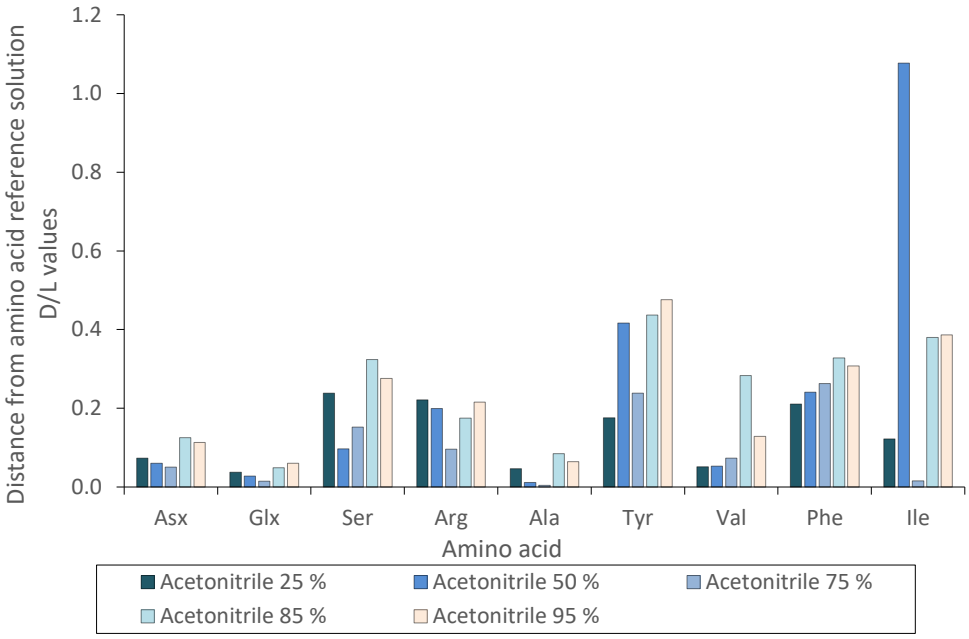

Figure 2.13. Numerical distance from the expected D/L value for the different mobile phase compositions based on the expected value calculated from amino acid reference standards run without hydroxyapatite (section 2.4). The mean D/L value is derived from the two fractions that contain the highest overall levels of amino acids.

Baseline resolution was not obtained for many of the amino acids peaks past ~ 66 min in the RP-HPLC, making the quantification of Val, Phe, Ile & Leu difficult. This lack of baseline resolution was due to co-eluting contaminant compounds which are probably present due to phosphate species or EDTA in solution. The combination of peak suppression and the poor reproducibility of known D/L values shows that there is potential bias in the resulting data.

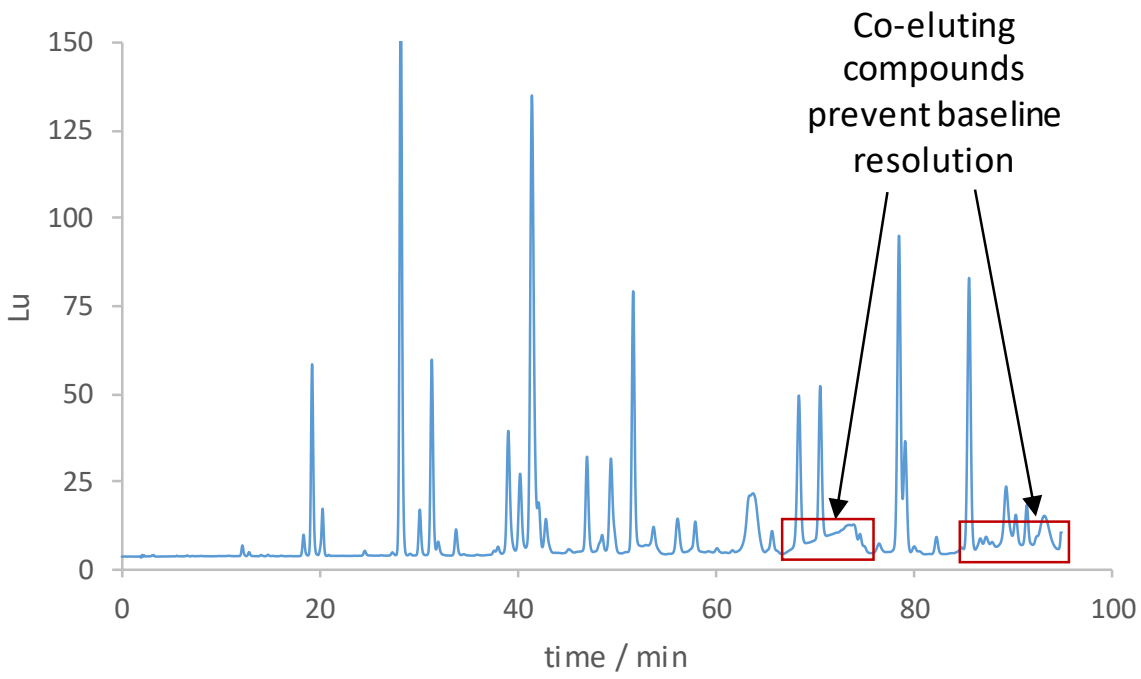

Figure 2.14. Example HPLC chromatogram: red boxes highlight the areas of the chromatogram that are unable to resolve the peak areas to baseline resolution. This prevents accurate determination of concentrations and D/L values for some of the later-eluting amino acids (e.g. Val, Ile and Leu).

This set of experiments highlights the sensitivity of the HILIC retention to the percentage organic in the eluent. This enables a more targeted approach for amino acid isolation from phosphates. The potential bias in D/L values measured and the poor baseline in the analysis indicates that it was worth exploring alternative mobile phase parameters.

2.15. Variable composition methanol / H_2O mobile phase at neutral pH

Methanol is a polar protic solvent and therefore is traditionally considered less suitable for HILIC mode separations than aprotic solvents such as acetonitrile (Perelra *et al.*, 2009). When polar protic functional groups such as -OH and –NH are present in an analyte, retention by a hydrogen-bonding mechanism is often observed when using a HILIC column (Tolstikov & Fiehn, 2002; Yanagida *et al.*, 2007). Polar protic solvents can more effectively compete for polar active sites on the surface of the stationary phase, thus creating a more hydrophobic stationary phase and decreasing HILIC type interactions. Hydrogen-bonding of the MeOH to the H_2O in the water layer of the stationary phase also destabilises the boundary between the mobile phase and the water layer (Figure 2.15). If the separation of amino acids and phosphates is influenced by the strength of hydrogen bonding retention, then switching ACN for MeOH would be expected to reduce its strength and provide poorer

separation (Hao *et al*., 2007). However, if the dominant separation is due to ionic/polar interactions rather than HILIC, then use of MeOH is likely to be similar to that seen with the aprotic ACN. Although MeOH has therefore been reported as being less powerful for HILIC separations (Hao *et al*., 2008), by testing it as an alternative to ACN this may provide insight into the mechanisms of the separation required, and/or improve the baseline issues. Additionally, MeOH is a cheaper and safer solvent than ACN.

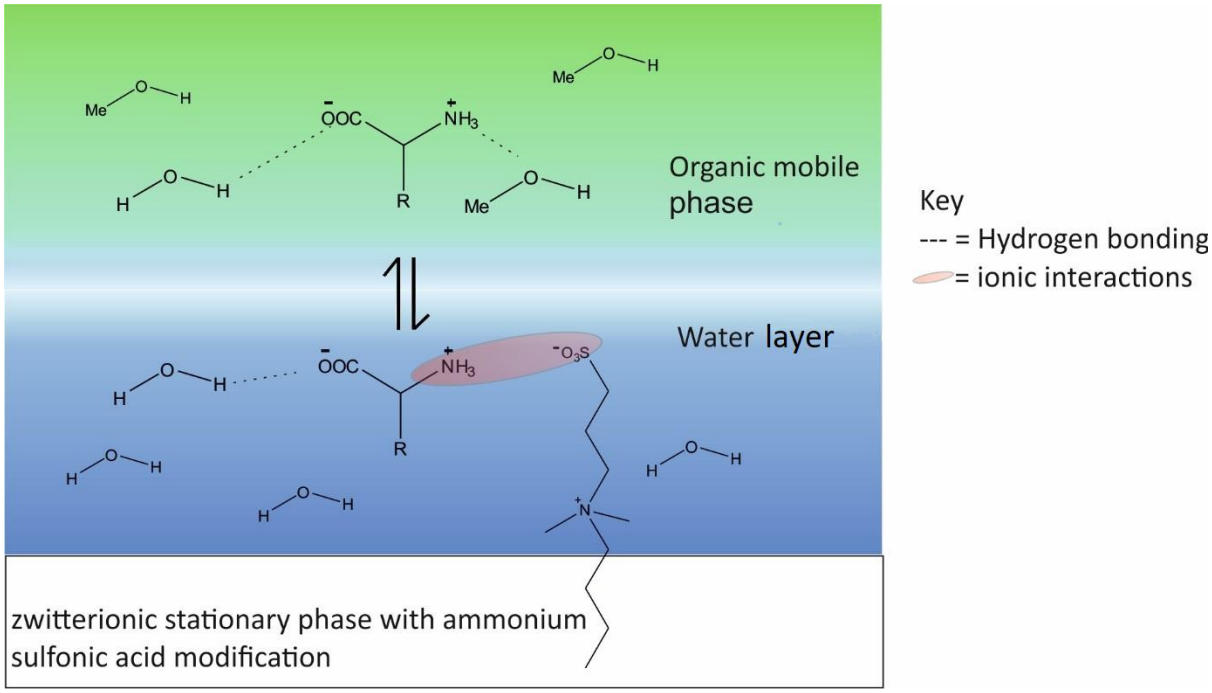

Figure 2.15. Some of the supramolecular interactions potentially influencing the retention of a general amino acid in HILIC with methanol/water mobile phase.

To test the effects of using methanol as the organic component of the HILIC mobile phase, a series of experiments was set up using three different strength mobile phase compositions: 20, 30 and 40 % methanol/water. A control sample was also analysed without the presence of hydroxyapatite to establish the effects of phosphates on the separation. The ACN mobile phase composition that yielded the most promising results in terms of recovery, separation of phosphates and impact on D/L values was at lower ACN % when using a neutral mobile phase (~pH 7). As methanol is a less powerful organic solvent in terms of eluent strength, the most comparable methanol composition to 25 % ACN (iso-eluotropic) is 30 % methanol (Harris, 2007).

2.16. Variable composition methanol / H_2O mobile phase at neutral pH: Experimental

A sample of hydroxyapatite with a 1:1 amino acid standard was used to mimic fossil tooth enamel (section 2.4). The sample was demineralised and then neutralised with KOH; EDTA was added to chelate to the calcium ions and re-dissolve the gel that forms (section 2.7). The samples were loaded onto a HILIC SPE cartridge, pore size 60 Å, particle size 45 µm (Chromabond, HiChrom). A variety of methanol mobile phase solutions (total volume 2.5 mL) were used to elute the amino acids (section 5.6, table 4); subsequent water washes were used to elute more strongly retained polar analytes. Fractions were evaporated, rehydrated and analysed by an RP-HPLC system (section 2.9).

Table 2.4. The eluent used to collect each fraction (see Figure 2.6). xx = 20, 30 or 40

Fraction	Mobile phase	Total volume loaded/collected / µL
1	Sample (50 µL) and MeOHxx (450 µL)	500
2-4	MeOHxx	500
5-7	Water	500

2.17. Variable composition methanol / H_2O mobile phase at neutral pH: Results & discussion

2.17.1. Effects of phosphate

The visible residue in the vials of collected dried fractions was reduced when compared with that using ACN as the organic component in the mobile phase (Table 2.2). Additionally, no peak suppression of the internal standard LhArg was observed with MeOH (Figure 2.16). The LhArg peak areas are also in good agreement with those acquired from the sample run without added hydroxyapatite (MeOH control), suggesting that there was reduced phosphates in the collected fractions.

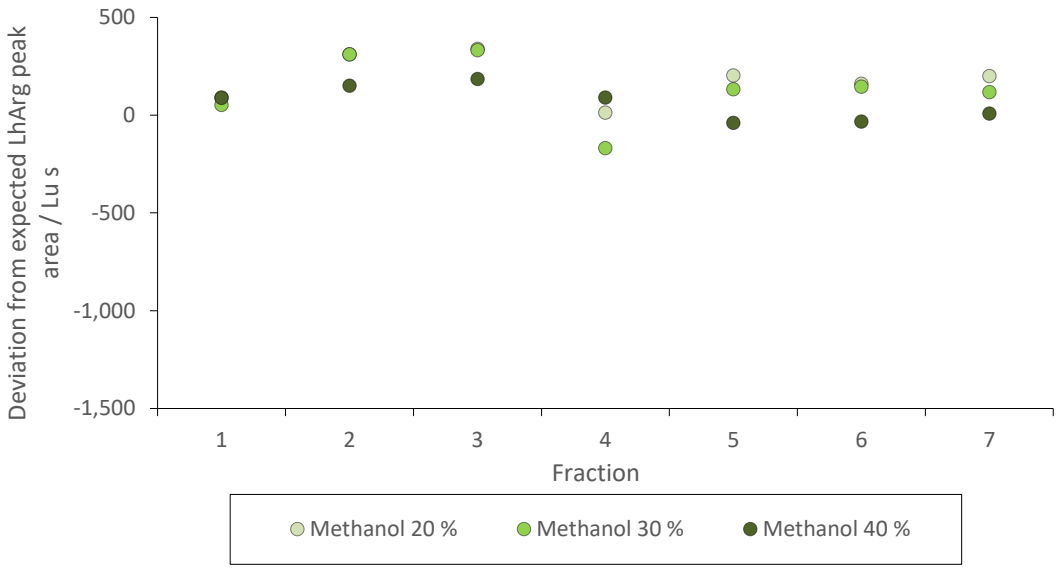

Figure 2.16. LhArg peak areas (eluting at ~51 min) for each of the fractions for each of the different methanol compositions (20%, 30% and 40%). Eluents using MeOH (20-40%) have similar LhArg peak areas to the control (which has no HA) indicating no peak suppression.

2.17.2. Amino acid composition and D/L values

The amino acid compositions of fractions 2 and 3 (the fractions containing most of the eluting amino acids; Figure 2.17 a-c) are consistent with those of the standard starting compositions (Figure 2.17 d); this is a good indicator that amino acids have not been preferentially lost and that co-eluting contaminant peaks have not greatly impaired individual amino acid quantifications. In comparison, the amino acid profile acquired for the experiments using acetonitrile in the mobile phase (ACN25; Figure 2.17 e) were more altered.

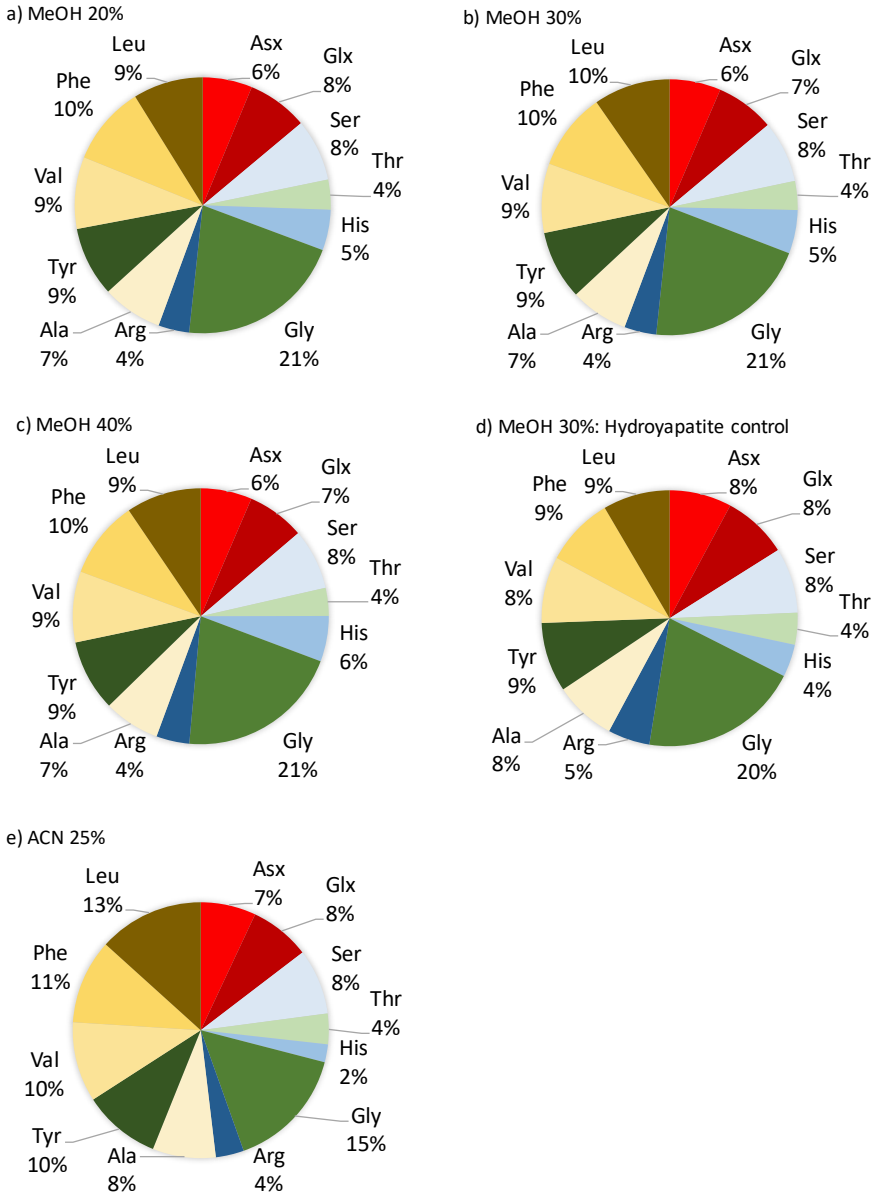

Figure 2.17. Amino acid composition, calculated from their respective peak areas, eluted with different methanol mobile phase compositions (a) 20, b) 30 and c) 40 % methanol/water). Hydroxyapatite control and 25 % Acetonitrile mobile phase at neutral pH has been shown for comparison. Data represents average values from the two fractions that contain the highest overall levels of amino acids.

The D/L values for the fractions generated with a methanol-based mobile phase show good agreement with the expected values (Figure 2.18). Small improvements of the HPLC baseline past 66 min were observed in the analytical chromatography for separations eluted with 20 and 30 % methanol, resulting in a better adherence to the expected Leu D/L value. However, this was not observed when using a 40 % methanol mobile phase during HILIC SPE, which is reflected in increased deviation from expected values for late-eluting Leu and Ile (Figure 2.18). For experiments conducted with methanol, higher amounts of amino acids were recovered in the two fractions that contained the most amino acids,

than for experiments conducted using ACN. This is likely to have caused the change in composition in the ACN fractions analysed (Figure 2.17), indicating that MeOH is a more useful solvent for this study. Further method development optimising the volume of eluent collected may resolve some of these issues but were not explored in these experiments due to later developments (section 2.19.2).

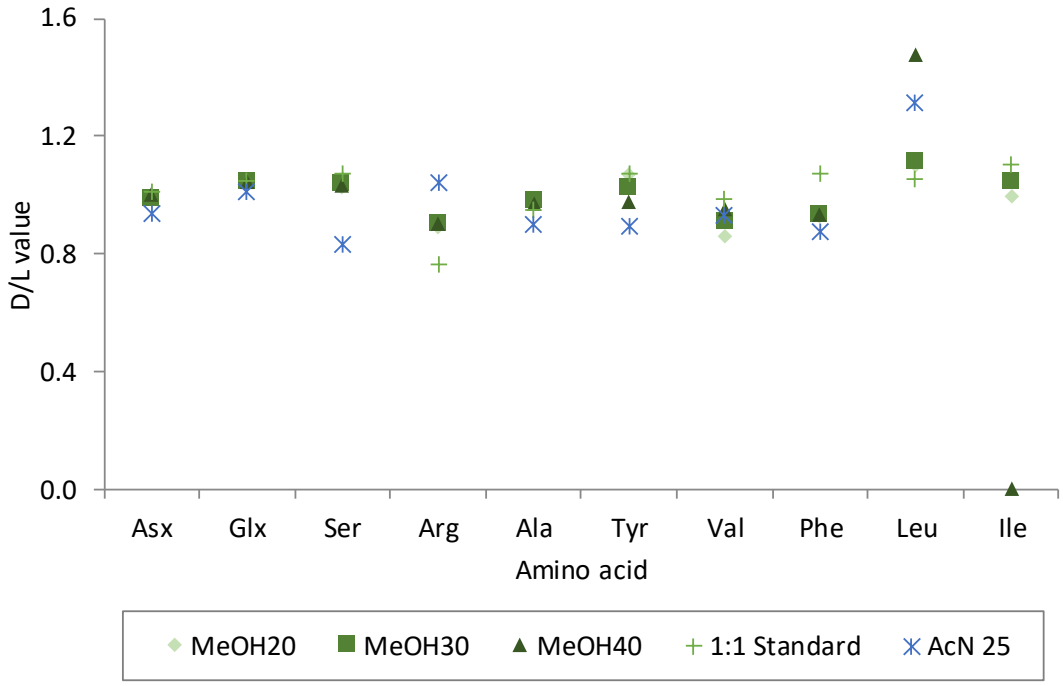

Figure 2.18. D/L values for different methanol mobile phase composition experiments. 1:1 amino acid standard and 25 % acetonitrile mobile phase at neutral pH has been shown for comparison. The mean D/L value from the two fractions that contain the most amino acids is shown.

2.17.3. MeOH at pH7: Conclusions

The three methanol /water mobile phase compositions showed little variation in both the profile and D/L value of the resulting amino acid analysis. Replacement of acetonitrile with methanol in the mobile phase yielded amino acid peak areas in better agreements with the amino acid standard starting compositions (Figure 2.20). Using a protic solvent (MeOH) rather than aprotic (ACN) in HILIC liquid chromatography would be expected to reduce the hydrophilic interactions with the stationary phase, potentially yielding poorer separation (Perelra *et al.*, 2009). The improvement observed with MeOH therefore indicates that hydrogen bonding and hydrophilic interactions are not dominating the mechanism for retention of the analytes. Combined with the lower cost and safety aspects, it was decided to proceed with MeOH in the mobile phase. However, as the co-eluting contaminants that were preventing baseline resolution of several amino acids (after ~66 min; Figure

2.14)were not entirely resolved, it was decided to explore the impact of pH of the MeOH mobile phase.

2.18. MeOH mobile phase optimisation at pH > 7

The co-eluting contaminant compounds in the HPLC analysis that prevent baseline resolution of some amino acids (amino acids eluting after ~66 min; Figure 2.14), may be due to phosphates still present in significant concentrations in the fractions containing the amino acids (although not high enough to cause peak suppression). Increasing the polarity of the phosphates by increasing their charge state could lead to better separation. This would potentially increase the retention of the phosphates as they will be better able to compete for polar active sites and they should have a greater affinity for the stationary phase water layer through ionic and hydrophilic interactions. The variable mobile phase composition methanol and acetonitrile experiments discussed so far in this chapter (Sections 2.13 & 2.14) have used neutral pH mobile phases. Assuming the pK_a values of the phosphate species in these mobile phases are roughly analogous to those in aqueous systems, there should be a 1:1 ratio of dihydrogen phosphate ($H_2PO_4^-$) to monohydrogen phosphate (HPO_4^{2-}) present in solution at pH 7 (Figure 2.5). By increasing the pH to 9, almost all the phosphate species in solution should be present as the di-anion (formal charge of -2) monohydrogen phosphate. If (as suspected) HILIC is not the dominant mechanism of retention using this set of parameters, then ionic/polar interactions are likely to be important (Hao *et al*., 2008). In that case, presence of the phosphate in the dianion form is likely to increase its retention on the stationary phase, thereby eluting in a later fraction than the amino acids. Changing pH will also affect the amino acid speciation, but they will not be as negatively-charged as the phosphate species (Figure 2.5). As previous experiments have indicated that the majority of phosphates are eluting after the amino acids (sections 2.14.3) by increasing the formal charge on the phosphate ions, increased retention of this species is hoped to be achieved.

2.18.1. MeOH mobile phases at pH > 7: Experimental

To test the effects of changing the pH of the mobile phase, a series of experiments was set up using 30% methanol/water solution with two different pHs (8 and 9). A sample of hydroxyapatite with a 1:1 amino acid reference solution was used to mimic fossil tooth enamel (section 2.4). The sample was demineralised with HCl and then neutralised with KOH; EDTA was added to chelate the calcium ions and re-dissolve the gel that forms (section 2.7). The samples were loaded onto a HILIC SPE cartridge with an ammonium

sulfonate modification, pore size 60 Å, particle size 45 µm (Chromabond, HiChrom). Columns were analysed with an eluent adjusted to pH 8 or 9 with KOH (0.01 M) and subsequent water washes were used to elute any more strongly retained polar analytes. Fractions were rehydrated and analysed on an RP-HPLC system (section 2.9). Experiments were run in triplicate so that standard deviations could be calculated and used to assess the variability in LhArg peak areas, amino acid recoveries and D/L values.

2.18.1.1. Effects of phosphate on the internal standard peak area

There was no evidence of peak suppression in the analytical chromatograms (Figure 2.19), although the variability of some dried fractions contained a white residue indicating that inorganic phosphate species may be present. This evidence is consistent with the experiments run at neutral pH (section 2.13).

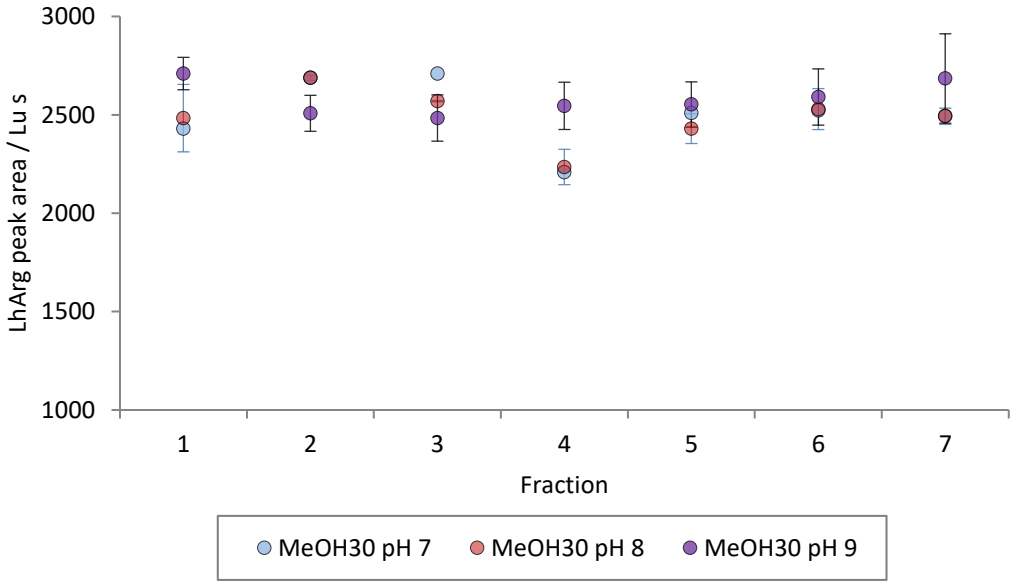

Figure 2.19. Averaged LhArg peak areas for the seven fractions collected post HILIC SPE conducted using a 30% methanol/water mobile phase at three different pH values (pH 7, 8 and 9). The error bars depict one standard deviation about the mean.

2.18.1.2. Amino acid composition and D/L values

At elevated pHs, the amino acids predominantly eluted in fractions 2 and 3, which was comparable to experiments run with no pH control (~pH 7; experiments in section 2.17). The composition of the amino acids in these fractions was broadly similar to the expected composition(Figure 2.20). This indicates that there is little/no preferential loss of amino acids during SPE purification using these parameters.

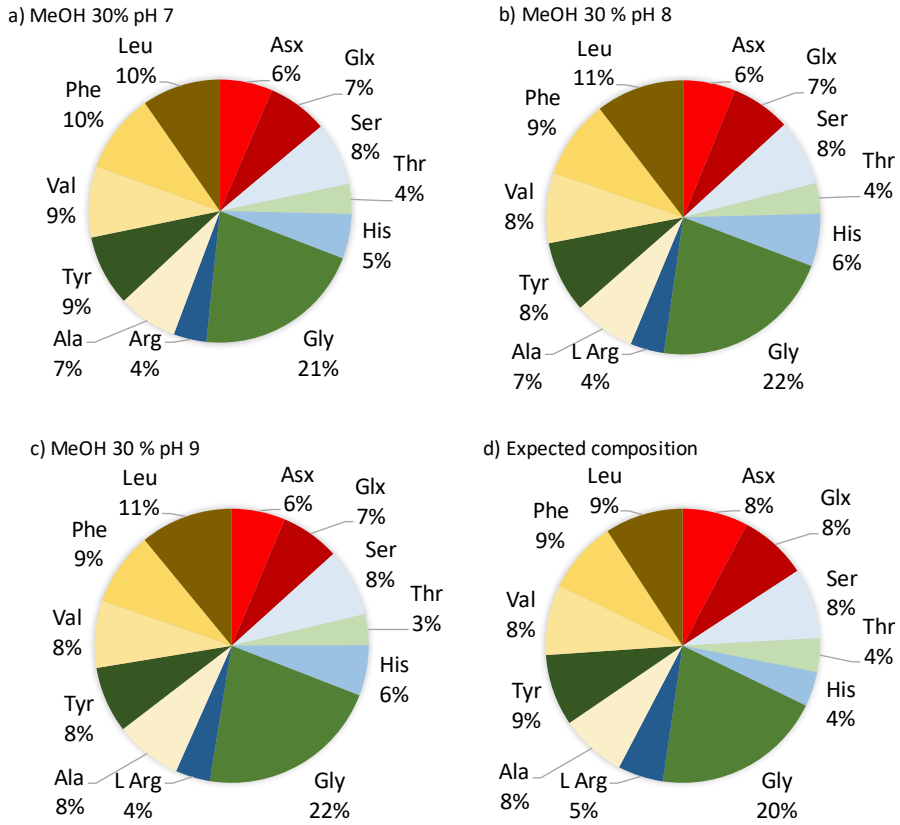

Figure 2.20. Amino acid composition, calculated from their respective peak areas, run at different 30 % methanol mobile phase pHs (a-c). Expected composition (d) was calculated from amino acid reference solutions analysed without hydroxyapatite.

The D/L values for the elevated pH experiments were similar to the expected values calculated from the amino acid reference solutions analysed without hydroxyapatite (1:1 amino acid reference; Figure 2.21). The standard deviation of LhArg peak areas (Figure 2.19) and D/L values (Figure 2.21) for experiments conducted with a pH 9 mobile phase is larger in than for experiments conducted with a pH 8 mobile phase (); however, caution must be used when assessing variability between experiments with a limited number of repeats (n=3). The co-eluting compounds preventing baseline resolution of several amino acids by HPLC (Figure 2.13),were not improved at higher pH and this is likely to be responsible for much of the variability observed in the values for the later eluting amino acids (Ala, Tyr, Val, Phe and Leu).

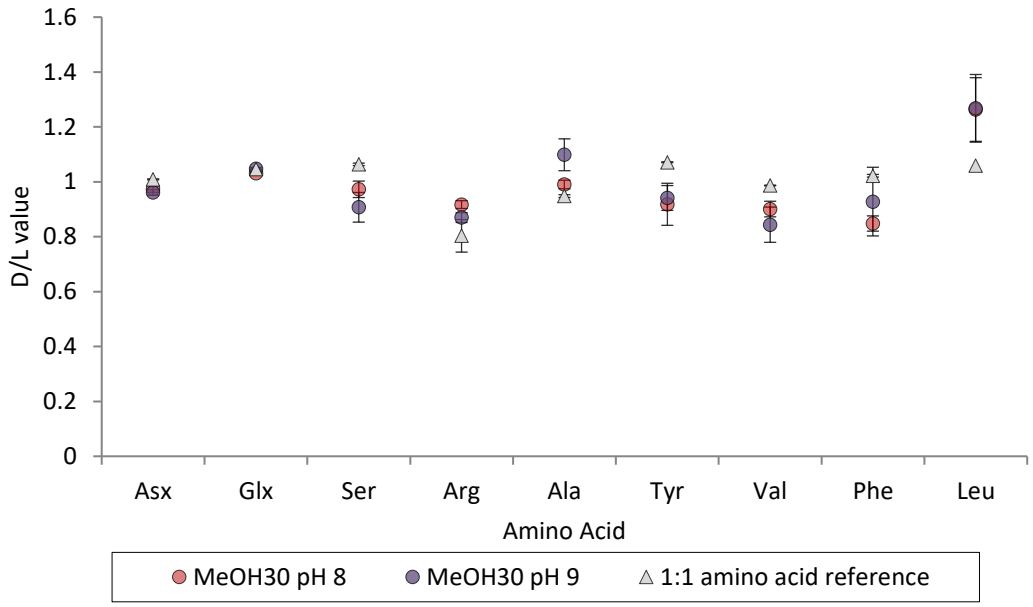

Figure 2.21. Mean D/L values for a range of amino acids eluted using a 30% methanol/water mobile phase at two different pH values (pH 8 and pH 9, compared to the original standard). The mean D/L value is derived from the two fractions that contain the highest overall levels of amino acids. The error bars depict one standard deviation about the mean.

2.18.1.3. MeOH mobile phases at pH > 7: Conclusions

The data acquired from this set of experiments suggest that the optimised method using 30% methanol / water mobile phase, adjusted to pH 8 provides the most accurate and precise amino acid data. This mobile phase composition was therefore used in subsequent experiments described in this chapter. However, the concerns regarding the co-eluting contaminant compounds occurring after ~66 min during the HPLC were not resolved and potentially still inhibit the accurate determination of D/L values for amino acids eluting in that region.

2.19. Testing the optimised HILIC SPE protocol on fossil material

Previous experiments described in this chapter (sections 2.12- 2.18) have used amino acid reference solutions with hydroxyapatite to mimic an enamel sample. However, two amino acid fractions are routinely analysed for biomineral AAR geochronology: the free amino acids (FAA) and the total hydrolysable amino acid fraction (THAA), which also includes those that had been peptide bound (Figure 2.22; Penkman *et al*., 2005). The experiments using hydroxyapatite containing amino acid reference solutions (sections 2.12-2.18) mimic the sample preparation of FAA fractions, where samples are demineralised in 1 M HCl to break down the inorganic matrix and release the free amino acids. However, in order to

liberate the amino acids bound in the peptides in fossil samples, a hydrolysis step using 7 M HCl at 110°C is needed to break peptide bonds (Section 2.6). It was hoped that HILIC SPE using the FAA and THAA fractions would be comparable and thus the method developed would be suitable for both analyses. Therefore, to test this, fossil enamel has been used in subsequent experiments to determine the effects of the protocol on the THAA fraction as well as the FAA.

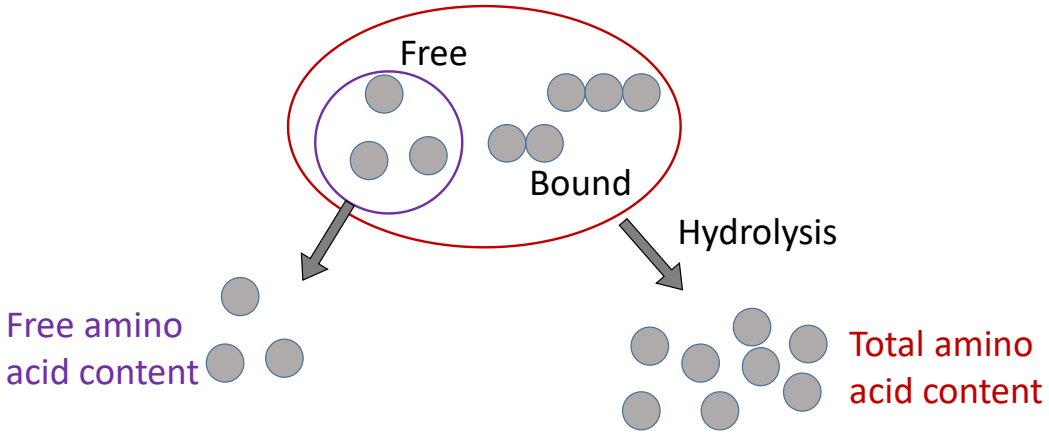

Figure 2.22. Origin of the free amino acid (FAA) and total hydrolysable amino acid (THAA) fractions

The D/L values and amino acid composition of the fossil samples are unknown and thus unavailable for quantitative comparison but should be consistent within the sample. In addition, changes in the LhArg peak area may provide insight into the efficiency of the protocol.

2.19.1. Method

To test the optimised HILIC SPE method, an enamel fossil tooth from the Pleistocene deposits at Witham (for site information see section 4.3.1.6.1) was analysed for its FAA and THAA content (NB. Fossil material by definition does not contain endogenous organic material, as to be a fossil the organic material has to have been petrified (Anon, 2018). A more accurate term to describe the semi-fossilised remains analysed in this thesis would be sub-fossil; however, this term is not routinely used in the literature in this field (Blackwell *et al.*, 1990; Belluomini & Bada, 1985) and thus the term fossil will be used in this thesis to include the remains that have not undergone complete petrification).

The fossil enamel from a *Mammuthus sp.* tooth from Witham was powdered and bleached for 24 h (Section 2.5). Bleached enamel was then split into two fractions (~ 2 mg each); one was analysed for its FAA content and the other for the THAA content. The THAA fraction

was hydrolysed for 24 h in a 110°C oven (section 2.6) and then the acid was removed by centrifugal evaporation. Dried samples were then rehydrated in HCl (1 M, 20 µL mg^{-1}). FAA fractions were demineralised in HCl (1 M, 20 µL mg^{-1}). Both the THAA and FAA fractions were neutralised with KOH (1 M, 20 µL mg^{-1}); solid EDTA was added to sequester calcium ions and reincorporate the gel into solution (section 2.7). The pH of the solutions was tested using pH strips (Fisher brand).

The samples were loaded onto a HILIC SPE cartridge with an ammonium sulfonate modification (section 2.8). The optimised preparative protocol using eluent containing 30% methanol/water adjusted to pH 8 was used to prepare this fossil material. Fractions were dried and rehydrated with an internal standard (LhArg) and analysed on an RP-HPLC system (section 5.7).

2.19.2. Results and discussion

2.19.2.1. LhArg peak areas

A white residue was observed in the vials after drying vials containing fractions 2 and 3 from both the FAA and THAA portions (indicated by the Xs in Figure 2.23). For the THAA portion, these visual signs of inorganic phosphate species also correlate with considerable peak suppression of the internal standard (LhArg; Figure 2.23). Additionally, these fractions also contained most of amino acids, indicating that the amino acids and phosphate species were eluting together, this made the data from this set of experiments more challenging to interpret. There was also a small amount of peak suppression for the FAA sample fraction 3, but this level is unlikely to impact on the interpretation of the amino acid data (Figure 2.23).

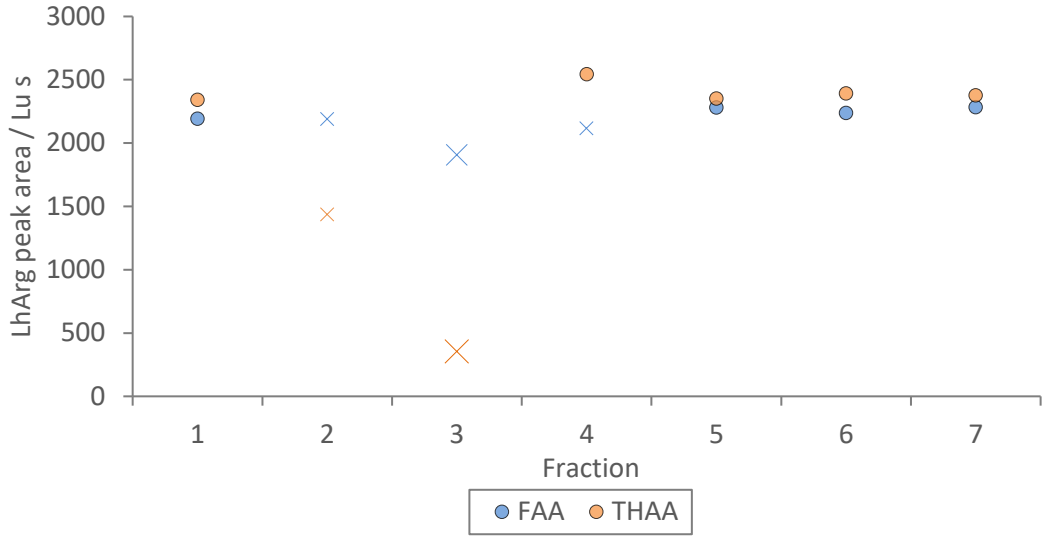

Figure 2.23. LhArg peak areas for the seven fractions collected post HILIC SPE for the experiments conducted using a 30% methanol/water mobile phase at pH 8. FAA fractions are coloured blue; THAA fractions are coloured orange. The Xs represent vials that contained a white residue after the fractions were dried. The larger the X, the more residue was present

2.19.2.2. pH of the THAA sample prior to loading onto the HILIC SPE

7 M HCl was added to samples prepared for their THAA content to liberate bound amino acids (Section 2.6). Most of this acid was removed by centrifugal evaporation, but tests of the pH of the samples after KOH neutralisation and the addition of EDTA suggest that the residue left behind was more acidic (~pH 1) than that formed in the samples treated for their FAA content (~pH 6.8).

The neutralisation procedure involving the addition of KOH prior to dissolving the sample in HCl was designed to increase the pH of the sample solution that was loaded onto the HILIC SPE cartridge to match that of the mobile phase. The lack of pH control during elution may alter the separation of the amino acids from the phosphate species and potentially accounts for the reduced efficiency of separation observed here for the THAA fraction.

2.19.2.3. Amino acid D/L values of the enamel from Witham, UK

Many of the amino acid peaks were not baseline resolved due to co-eluting peaks and thus the reported D/L values (Table 2.5) may not be accurate. The extent of IcPD in the mammoth enamel from Witham (~500 ka) is less than that reported in opercula of similar age (Penkman *et al*., 2013); the reported extent of THAA racemisation of Asx in opercula from the Sidestrand, Upper *Unio*-Bed (MIS 13; ~533 ka) is 0.72 ±0.01 (Penkman *et al*., 2013), compared to 0.25 from the Witham mammoth tooth. A similar difference is seen for the other amino acids. Biomineral amino acids from different species are known to

racemise at different rates (e.g. Miller *et al*., 1983), so this observation does not mean that the values obtained here are incorrect.

Table 2.5. D/L values for the ten amino acids recovered in both enantiomeric isomers in both the FAA and THAA fractions from a Mammuthus sp. tooth from Witham, UK.

	Asx	Glx	Ser	Arg	Ala	Tyr	Val	Phe	Leu	Ile
FAA	0.20	0.06	0.23	0.34	0.21	0.17	0.10	0.12	0.33	0.31
THAA	0.25	0.08	0.14	0.26	0.23	0.08	0.07	0.05	0.19	0.20

2.19.3. Conclusions

The unsuitability of the method for the separation of amino acids from phosphate species in fossil samples treated for the THAA content make the optimised protocol developed for the FAA unusable for THAA fractions. The difference in the pH of FAA and THAA samples prior to separation via HILIC SPE suggests that the neutralisation with KOH and dissolution with EDTA procedure may not be sufficiently optimised for THAA samples. The protocol's impact on both the FAA and THAA fractions of fossil material has therefore been investigated further.

2.20.Effects of the neutralisation and EDTA step on the analysis of amino acids from fossil samples

Experiments have shown that the HILIC SPE method optimised on amino acid reference standards is not suitable for analysis of the THAA fractions of fossil material (section 2.19). Additionally, the optimised MeOH method still exhibits poor analytical baseline resolution for some of the more hydrophobic amino acids, limiting the efficacy of the method even for FAAs.

The development of a method for the isolation of amino acids from the inorganic phosphate species described has focused on optimising the parameters of the mobile phase used in the HILIC SPE. Experiments using a pH mobile phase with a pH > 7 have included an additional neutralisation step that led to the formation of a gel-like solution and the addition of EDTA to resolve this (Section 2.13). The impact this additional step may have on the recovery and D/L values obtained from fossil enamel has been evaluated.

The binding of calcium ions with EDTA to re-incorporate calcium phosphate into solution may cause issues with the RP- HPLC method outlined by Kaufman and Manley (1998).

However, calcium carbonate-based biominerals also contain high concentrations of calcium ions but publications studying these biominerals have not reported similar issues of peak suppression and poor chromatographic resolution (Penkman, 2008; Hendy *et al*., 2012; Crisp 2013; Tomiak *et al*., 2013; Ortiz *et al*., 2013). Moreover, the RP-HPLC mobile phase buffer contains EDTA (3.75 g dm^3) to bind to calcium ions, so EDTA is already present (although at lower concentrations than in the HILIC SPE samples). However, some of the difficulties analysing some of the later eluting amino acids using RP-HPLC, caused by a lack of baseline resolution and presence of contaminant peaks are still present, which cannot be explained if the amino acids had been sufficiently purified. A series of experiments have been conducted to test the impact of the neutralisation step on the concentration of LhArg and amino acid D/L values, to investigate the potential cause(s) of the lack of baseline resolution and presence of contaminating peaks.

2.20.1. Method

To test the optimised HILIC SPE method, an enamel fossil sample from the Witham member deposits, UK (for additional site information see section 4.3.1.6.1), was analysed for its FAA and THAA content. Fossil enamel from a *M. trogontherii* tooth was powdered and bleached for 48 h (Section 2.5). Bleached enamel was then split into two fractions (~ 2 mg each): one was analysed for its FAA content and the other for the THAA content. The THAA fraction was hydrolysed for 24 h in an oven (section 2.6) and then the THAA and FAA fractions were demineralised in HCl (1 M, 20 µL mg^{-1}) and then a series of different purification methods were applied to each fraction.

Three sample preparation procedures have been tested post-demineralisation (and post-hydrolysis for the THAAs):

1:

   The demineralised sample was neutralised with KOH (1 M, 20 µL mg^{-1}); EDTA was added to chelate to the calcium ions and reincorporate the gel back into solution (section 2.7). This protocol is identical to the optimised method used on the Witham mammoth enamel sample described in section 2.19.

2:

   The demineralised sample was neutralised with KOH (1 M, 20 µL mg^{-1}); the gel precipitate was then centrifuged at 15000 rpm for 3 mins whereupon two phases were observed: a clear solution on top of the opaque gel. The clear solution was

pipetted off the gel and analysed for its amino acid content. This step therefore does not use EDTA.

3.

No attempt was made to control the pH of the sample solution.

The samples were each loaded onto a HILIC SPE cartridge. The optimised preparative protocol using a 30% methanol/water adjusted to pH 8 eluent was used to fractionate this fossil material. Collected fractions were rehydrated in an internal standard solution (LhArg) and analysed on an HPLC system (section 5.7).

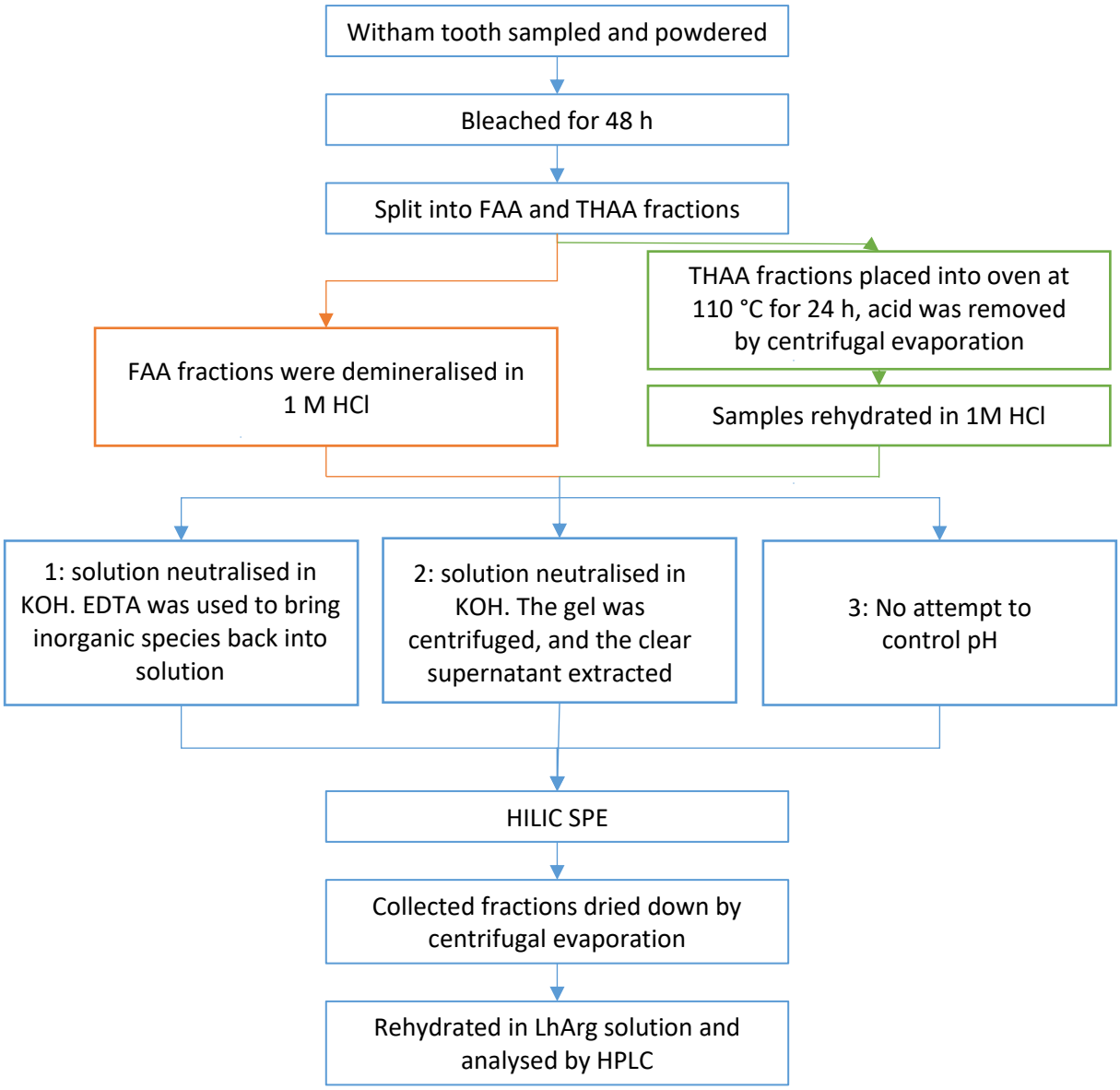

Figure 2.24. Schematic of the experimental protocol for the three different approaches to sample preparation

2.20.2. The effects of the neutralisation and EDTA step on fossil data

2.20.2.1. 1: Neutralisation and Ca^{2+} ions reincorporated with EDTA

The experiments termed 1 (section 2.20.2.1) followed the optimised protocol for FAA, developed on amino acid reference standards. The LhArg peak areas for the collected fractions were similar to those reported in the previous experiments conducted on mammoth enamel from Witham (section 2.19). Peak suppression was observed in the LhArg peak areas for the A1 experiments in both the FAA and THAA portions (Figure 2.25). The extent of peak suppression in the THAA fractions was greater than in the FAA fractions, which is also consistent with the previous observations.

The two fractions most affected by peak suppression in the A1 experiments were FAA Fraction 6 and THAA fraction 4 (Figure 2.25); however, low levels of amino acids eluted in those fractions so it is unlikely that the cumulative amino acid peak areas calculated were significantly affected. The magnitude of peak suppression of LhArg in the A1 THAA fractions was less than when previously analysed under the same conditions (section 2.19; Figure 2.23). The reason is unclear at this stage, but inconsistencies in the HILIC SPE are likely responsible (e.g. inconsistent collection volumes and large differences in flow rates, due to the high variability between SPE columns).

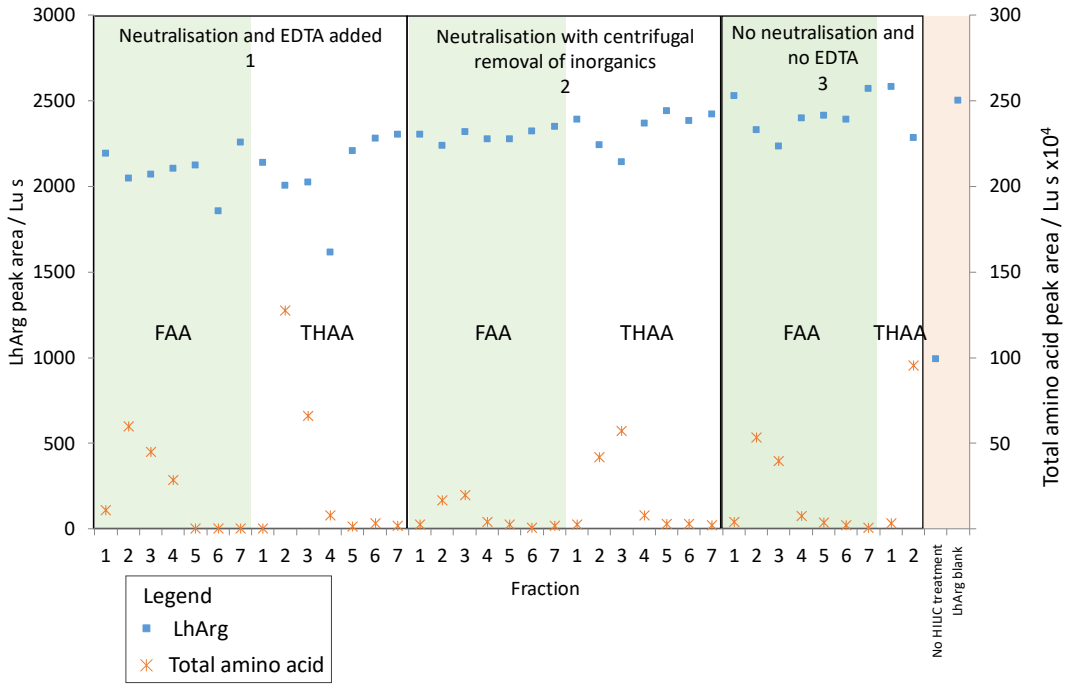

Figure 2.25. LhArg peak area (eluting at ~51 min) for each of the collected fractions for both the FAA and THAA from fossil mammoth enamel analysed using different preparative protocols prior to HILIC SPE of the amino acids. The summed peak areas of Asx, Glx, Arg, Ala and Phe have also been included to indicate in which fractions the amino acids elute.

2.20.2.2. A2: Neutralisation with centrifugal removal of Ca^{2+} ions

The A2 experiments were conducted without the use of EDTA to dissolve the precipitate; instead, centrifugal force was used to create a biphasic system with a clear solution lying above the gel. The clear solution was collected and passed through a HILIC SPE column and the collected fractions analysed for their amino acid content.

The clear solution extracted after centrifugation showed no signs of LhArg peak suppression in the FAA fraction and whilst some suppression was observed in the THAA

fraction, it was considerably less than that observed in the comparable fractions following the previously optimised method (A1, Figure 2.25). This indicates that centrifugal removal of the supernatant prior to HILIC SPE reduces the effects of peak suppression. However, the primary concern with spinning down the "gel" is that amino acids may become entrapped and subsequently lost to the analysis. This is difficult to quantify in these experiments as the theoretical concentrations of the amino acids are not known and because as amino acid concentration was calculated from the internal standard, the effects of peak suppression can impact concentration data. The total amino acid peak area of the FAA and THAA fractions were lower than those collected in the A1 experiments. This might be evidence of amino acids becoming trapped in the gel and thus being lost to the analysis. This reduction in amino acid concentrations therefore poses potential concerns to the ultimate application of a Quaternary dating method.

2.20.2.3. A3: No neutralisation and no chelation of Ca^{2+} ions

The LhArg peak area of the FAA fractions analysed without neutralisation or chelation of Ca^{2+} showed signs of suppression in fractions 2 and 3 (Figure 2.25); however, these were minimal and unlikely to impact negatively on the interpretation of data. The THAA fractions showed substantial visual signs of the presence of inorganic species; no fractions beyond number 2 were analysed because the rehydrated samples were cloudy and therefore not suitable for analysis by HPLC. The HILIC SPE separation of the amino acids and phosphate species in this method was rendered ineffective because the inorganic matrix was not dissolved in the sample solution. However, the impact of LhArg peak suppression for the FAA fractions was lower than expected despite a similar lack of dissolution prior to SPE.

2.20.2.4. Comparison of amino acid D/L values using three different preparative protocols

The D/L values for some amino acids could not be established (Figure 2.26). This was either due to concentrations below the limits of detection (mainly D-isomers) or the co-elution of an amino acid with a contaminant rendering quantification of their peak area/concentration unreliable. Where it was possible to analyse both amino acid enantiomers, the D/L values using the preparative protocols A1 and A2 were broadly in agreement (Figure 2.26). The spread of D/L values for Asx between protocols ranged from 0.15-0.22 and 0.22-0.25 for the FAA and THAA portions respectively. Based on the precision of data from experiments conducted using hydroxyapatite containing an amino acid reference solution (section 2.18), this spread of data is likely to be greater than the analytical/experimental precision (~0.2 ±0.03). This therefore suggests that changes in the preparative protocol influence the D/L values of this amino acid. The spread of D/L values

of Ser were also greater than expected for the FAA portion. However, Ser is a relatively unstable amino acid and therefore is unsuitable for used as a tool of age estimation (Akiyama, 1980).

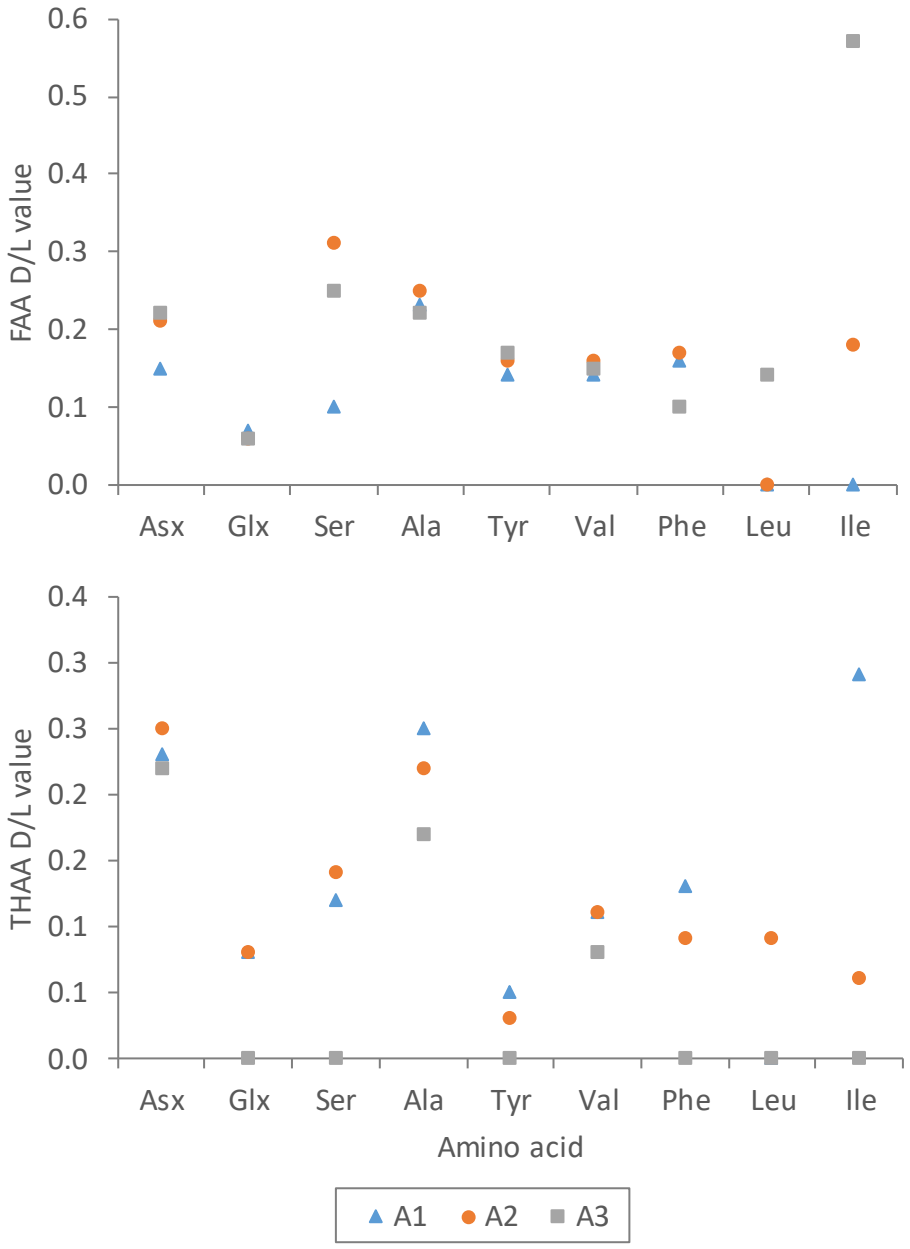

Figure 2.26. Mean D/L values for the FAA (top) and THAA (bottom) fractions of the three different preparative protocols. Fossil enamel analysed in these experiments is from a M. *trogontherii tooth from the deposits at Witham, UK*

2.20.3. The effects of the neutralisation and EDTA step on fossil data: Conclusions

The amino acid recovery and D/L value results from these preparative protocols reinforce the importance of pH prior to HILIC SPE for this method. The use of centrifugation (rather than EDTA) to produce a solution suitable for HILIC SPE resulted in data comparable to the

optimised method using EDTA (A1). The use of centrifugation (A2) also reduced the effects of co-eluting contaminant peaks in the RP-HPLC analysis, enabling reasonable resolution of L and D peaks of Ile. The biphasic solution formed prior to HILIC SPE during method A2, is likely to have formed as a result of pH dependent precipitation of calcium phosphate (Du *et al*., 2000). If this separation captures sufficient concentrations of phosphate species, then removal of the supernatant may provide separation of amino acids from the phosphates without the need for SPE.

2.21. Summary

In this chapter the effects of pH, organic solvent (ACN and MeOH) and neutralisation methods have been tested to develop a method to separate amino acids from phosphate. Although a successful method using amino acid standards was developed and optimised, the dominant separation mechanism did not appear to be via HILIC. When this optimised method was applied to fossil samples, the phosphate species were not successfully separated from the amino acids. Addition of a neutralisation step prior to SPE formed a gel, and the use of centrifugation (to isolate the supernatant from this "gel") resulted in more consistent data. It was therefore hypothesised that if the biphasic solution formation captures the phosphate species, then removal of the supernatant is providing the separation of amino acids from the phosphates without the need for SPE. However, this separation method may result in a proportion of the amino acids becoming trapped in the gel and ultimately lost for analysis. In the next section (Chapter 3), this hypothesis is tested and an optimised method which does not use column chromatography developed.

Chapter 3: A new method for enamel amino acid geochronology: a closed system approach

This chapter has been submitted for publication in the journal Quaternary Geochronology and thus has been presented here in article format.

3.1. Introduction

Mammalian teeth are often found in Quaternary paleontological deposits, providing an excellent target for direct dating. However, mammalian remains older than the limits of radiocarbon analysis (~50 ka, MacPhee *et al*., 2002; Jacobi, 2006) are challenging to date and therefore frequently rely on chronological analysis of associated material (e.g. Frouin *et al*., 2017). Currently, electron spin resonance (ESR) and U-series (which can be used together or separately) are the only commonplace direct dating techniques available for skeletal remains older than ~50 ka and spanning the Middle to Late Pleistocene (Dirks *et al*., 2017; Hershkovitz, *et al*., 2018). Both these techniques require an accurate reconstruction of the U-uptake history, but as teeth (and bones) are open systems for uranium, modelling this uptake is challenging. U-uptake modelling (such as diffusive-absorption models) can, however, provide an age estimation up to ~500 ka on small samples on the order of ~ 10-50 mg (Dirks *et al*., 2017; Hershkovitz, *et al*., 2018), which can be pushed further back (~750 ka) using combined Pa/U and Th/U data. However, at present this is restricted by the requirement for significantly larger sample sizes of up to ~1 g (Grün *et al*., 2010; Duval, 2015). Moreover, it is thought that the best source of material is often from the centre of the sample, thereby requiring relatively destructive sampling methods (Grün *et al*., 2010).

Amino acid racemization (AAR) analysis has proven a valuable technique for age estimation over Quaternary timescales (~2.5 Ma) for a variety of calcium carbonate-based biominerals (Wehmiller *et al*., 2012; Hendy *et al*., 2012; Refsnider *et al*., 2013) and it requires comparatively small sample masses (~10 mg). AAR dating of mammalian collagen-based biominerals (e.g. bone and dentine) has had more limited success (Taylor 1983; Bischoff & Rosenbauer, 1981; Bada 1985; Blackwell *et al*., 1990; Marshall, 1990). Amino acid kinetic studies, conducted on dentine have shown a good adherence between the temperature-induced models and fossil data for some amino acids, but significantly not all (Canoira *et*

al., 2003) and these issues are compounded by the non-linear degradation of collagen (Collins *et al*., 2009). However, critically the concerns associated with leaching and contamination of such open systems preclude accurate dates (Towe *et al*., 1980; Hare, 1988; Bravenec *et al*., 2018).

Early studies postulated that amino acids can become trapped during the formation of certain biominerals (Towe and Thompson, 1972); recent research has shown mineral facets ranging in size from ~2.5-38.4 nm can be found in molluscan nacre (the inner layer of some molluscan shells), with elemental analysis indicating a higher carbon content in these voids (Gries *et al*., 2009). This suggests that organic material is likely to be trapped within the voids and could be more isolated from their external chemical environment than the matter between the crystal planes. Prolonged exposure of powdered mollusc shells to bleach has been shown to isolate a fraction of organic matter that is resistant to oxidative treatment (Sykes 1995, Penkman *et al*., 2007, 2008), defined as the intra-crystalline fraction, with the potential to act as a closed system for protein degradation. (Brooks *et al*., 1990; Penkman *et al*., 2008). As organic matter within the crystal structure contradicts the strictest definition of crystals (which cannot contain large macromolecules), here we define "intra-crystalline" as the fraction of organic matter that is resistant to prolonged oxidative treatment (Sykes *et al*., 1995). Bleach has been used to isolate intra-crystalline proteins and amino acids in mollusc shells (Sykes, 1995; Penkman *et al*., 2008; Demarchi *et al*., 2013b), opercula (Penkman *et al*., 2011) and coral (Hendy *et al*., 2012, Tomiak *et al*., 2013).

These voids imaged in nacre may also be present in tooth enamel, and expansion of AAR analysis to the routine dating of mammalian remains would be highly valuable, for example in helping to elucidate the migration and evolution of fauna in response to Pleistocene climate change. Enamel is composed of a form of hydroxyapatite (HA; calcium phosphate) which is heavily mineralised. The determination of L- and D- amino acids for geochronological purposes is typically achieved by analysis by HPLC with fluorescence detection modified from Kaufman & Manley (1998). However, the application of AAR analysis on enamel is not trivial, as high concentrations of inorganic salts originating from demineralisation of the enamel crystal structure (calcium phosphate) result in peak response suppression, and unstable and raised baselines limiting accurate quantification (Griffin, 2006). Isolation of the amino acids from inorganic salts in enamel therefore requires development of a method for routine application that has good recovery rates of a range of amino acids and does not alter the D/L value.

This paper outlines a method developed for the removal of inorganic salts from the mineral matrix in samples of fossil and modern proboscidean teeth as a potential solution for isolating amino acids for AAR analysis. Through RP-HPLC, FTIR and TEM analyses, we evaluate whether intra-crystalline amino acids and proteins are present in enamel and if they exhibit closed system behaviour. Long term degradation of enamel is simulated through elevated temperatures and compared to results from fossil material to gain a better understanding of the reaction kinetics of racemization.

To this end, a series of experiments was performed on enamel:

1) Optimisation of the biphasic separation of inorganic species from amino acids (Section 3.3), using:
    a. FT-IR analysis of both the supernatant (containing the amino acids) and the underlying gel
    b. optimising the volume of KOH used in the preparation
    c. testing the impact of the optimised method on the relative concentration of amino acids and their D/L values
    d. evaluation of the expected analytical error
2) Optimisation of the oxidation method for the isolation of any intra-crystalline amino acids from the enamel (Section 3.4).
3) Elevated-temperature experiments designed to investigate potential leaching (diffusive loss) of amino acids from both the intra- and inter-crystalline fractions, as well as to study the kinetics of intra-crystalline protein degradation (IcPD; Section 3.5).
4) Analysis of racemization in fossil proboscidean enamel from the UK, providing a pilot relative geochronology (Sections 3.5.5.5 - 3.5.5.6).

3.2. Materials and optimised methods

As some of the methods were optimised over the course of the study (Sections 3.3 & 3.4), the optimised methods are detailed in this section.

3.2.1. Enamel samples

13 teeth were sampled from a range of contexts varying in age from modern to ~2.2 Ma (Table 3.1 and SI); fossil material was selected from sites which had independent evidence of age

Table 3.1. Sample information for the fossil enamel and comparative *Bithynia* opercula, taken from Penkman *et al*., 2013. *E.* = *Elephas*, *P.* =*Palaeoloxodon*, *M.* = *Mammuthus*, *A.* = *Anancus*

Locality	UK grid ref	Species	Samples	Mammal bed	*Bithynia* opercula IcPD*	Other previous dating of site	Estimated age of sampled fossil(s)	n
Asia	-	*E. maximus*	A. Lister coll.	-	-	-	modern	3
North Sea	-	*M. primigenius*	A. Lister coll.	Brown Bank	-	Radiocarbon: ca 34-49 ka (Mol *et al*., 2006)	MIS 4-3	3
Balderton Sands & Gravels, Lincs.	SK 837561	*M. primigenius*	A. Brandon coll. [6A/36]	Cold-stage sands & gravels (Lister & Brandon, 1991)	-	Terrace stratigraphy: MIS 6 (Brandon & Sumbler, 1991; Bridgland *et al*., 2015); ESR: 130-190 ka (Grün, 1991)	MIS 6	3
Tattershall Thorpe, Lincs.	TF 228605	*M. primigenius*	J. Rackham coll. [TTb3]	Cold-stage sands and Gravels (Girling, 1974; Rackham, 1978; Holyoak & Preece, 1985)	-	Mollusc fauna (Meijer & Preece 2000); terrace stratigraphy (Bridgland *et al* 2015): MIS 6.	MIS 6	3
Crayford, Kent	TQ 517758	*M.* sp.	BGS [117009] & [5123]	Lower Brickearth (Chandler, 1914; King & Oakley, 1936)	From the Norris Pit deposits. Late MIS 7 /	Mammal fauna (Schreve, 2001), terrace stratigraphy (Bridgland 2014): late MIS 7	Late MIS 7	2

					early MIS 6			
Ilford, Uphall Pit, Essex	TQ 437860	*M.* cf. *trogontherii* & *P. antiquus*	BGS [114884] & [114892] (*M. t.*); [114881] (*P.a.*)	Brickearths within Taplow/Mucking Formation (Sutcliffe, 1975; Schreve, 2001)	From the Taplow/Muckin g formation at Ilford, Uphall Pit	Terrace stratigraphy (Bridgland, 1994), fauna (Preece, 1999; Coope 2001; Schreve, 2001): MIS 7.	MIS 7	2
Barnfield Pit, Swanscom be, Kent	TQ 595745	*P. antiquus*	BGS [50340] & [50341]	Silts, sands & gravels of Boyn Hill Terrace. BGS [50340] & [50341] from Lower gravel	From Barnfield Pit, Swanscombe	Boyn Hill Gravel above Anglian boulder clay at Hornchurch; terrace stratigraphy & U-series (Bridgland, 1994); thermoluminescence (Bridgland *et al*., 1985), fauna (Schreve, 2001): MIS 11.	MIS 11. Lower Gravel specimen [50341]: MIS 11c (Ashton *et al* 2018).	2
Sidestrand, Norfolk	TG 255405	*P. antiquus*	BGS [6574]	Unknown	From Sidestrand Hall Member (Preece *et al*., 2009) older	*Ex situ* mammal fauna encompasses Early & early Middle Pleistocene but *P. antiquus* limited to mid-late	MIS 15-13	2

					than MIS 11 of Hoxne & Clacton but younger than MIS 15/17 of West Runton	part of early Middle Pleistocene (Lister, 1993; 1996)		
Easton Bavents, Suffolk	TM 518787	*A. arvernensis*	BGS [5988]	Norwich Crag Formation	From Norwich Crag Formation Thorpe at Aldringham, Suffolk Pit	Biostratigraphic correlation based on mammals, molluscs, foraminifera and dinoflagellates (Stuart, 1982; Zalasiewicz *et al*., 1991; Hamblin *et al*., 1997; Lister, 1998): ca. 2.0-1.8 Ma	Antian/Bramertio nian to Baventian/Pre-Pastonian; ca. 2.0-1.8 Ma	2
Holton, Suffolk	Approx. TM 405773	*A. arvernensis*	BGS [1385]					
Whittingha m, Suffolk	Approx. TL 720989	*M. meridionalis*	BGS [7971]					

3.2.1.1. Hydroxyapatite containing an amino acid reference solution

To mimic an enamel fossil sample with a known relative concentration of amino acids and D/L values, 1:1 and 1:4 D:L amino acid reference solutions (10 µL) were added to reagent grade hydroxyapatite (~2 mg; <200 nm particle size; Sigma Aldrich) and dried by centrifugal evaporation. The 1:1 amino acid reference solution mimics an older sample in which the amino acids have reached equilibrium, while the 1:4 amino acid reference solution mimics a younger sample. The reference solutions contain the free amino acids: Arg, Asp, Glu, Gly, His, Ile (D-isomer D-alle), Leu, Lys, Met, Phe, Ser, Thr, Tyr and Val with a D to L-isomer ratio of ~1 (1:1) or 0.2 (1:4) and the internal standard (L-*homo*-arginine).

Table 3.2. Samples used in each series of experiments. Optimisation and testing of the biphasic separation of inorganic species from amino acids method (OBS); Isolation of the intra-crystalline fraction (IIcF); Elevated temperature experiments to test for closed system behaviour (ET); fossil comparison to Bithynia *opercula (F)*

Sample code	BGS number	Species	Site	Experiment
MoE1	-	*E. maximus*	-	ET
NSM1	-	*M. primigenius*	North Sea	ET
BaM1	-	*M. primigenius*	Balderton	IIcF
TaM1	-	*M. primigenius*	Tattershall Thorpe	OBS
CrM1	117009	*M. sp.*	Crayford	F
CrM2	5123	*M. sp.*	Crayford	F
IlP1	114881	*P. antiquus*	Ilford	F
IlM1	114884	*M. trogontherii*	Ilford	F
IlM2	114892	*M. trogontherii*	Ilford	F
SwP1	50340	*P. antiquus*	Swanscombe	F
SwP2	50341	*P. antiquus*	Swanscombe	F
SiP1	6574	*P. antiquus*	Sidestrand	F
NCA1	5988	*A. arvernensis*	Easton Bavents	F
NCA2	7971	*A. arvernensis*	Whittingham	F
NCM1	1385	*M. meridionalis*	Holton	F

3.2.2. Enamel sampling

An enamel chip was removed from each tooth with a Dremel drill and the exposed outside layer removed using an abrasive rotary burr drill bit. Care was taken to remove any visible dark discolouration that was probably due to iron or manganese staining (Turner-Walker, 2007; Garot *et al*., 2017). To eliminate powder resulting from the initial drilling, chips were sonicated for 3 min in HPLC-grade water (Sigma-Aldrich) and then ethanol (VWR, analytical-grade), and air-dried before being finely powdered using an agate pestle and mortar.

3.2.3. Optimised NaOCl procedure

Approximately 30 mg of powdered enamel was weighed into a 2 mL microcentrifuge tube (Eppendorf), and NaOCl (12%, Fisher Scientific, analytical grade, 50 µL mg^{-1} of enamel) was added. Samples were exposed to NaOCl for 72 h and were continuously agitated using a rotary shaker to ensure complete exposure. The NaOCl was removed and the powdered

enamel was washed five times with HPLC-grade water. A final wash with methanol (Sigma-Aldrich, HPLC-grade) was used to remove remaining NaOCl, before the sample was left to air dry overnight.

3.2.4. Preparation of FAA and THAA fractions

Powdered enamel samples were accurately weighed into two fractions. One sample was treated for their free amino acid (FAA) content and the other their total hydrolysable amino acid (THAA) content.

3.2.4.1. Hydrolysis

THAA samples were dissolved in HCl (7 M, 20 µL mg^{-1}), purged with N_2 to prevent oxidation and heated in a sterile sealed glass vial at 110℃ for 24 h. The acid was removed by centrifugal evaporation.

3.2.4.2. Optimised biphasic phosphate ion removal

THAA samples were re-dissolved in HCl (1 M, 20 µL mg^{-1}) and FAA samples were demineralised in HCl (1 M, 25 µL mg^{-1}) in a sterile 0.5 mL microcentrifuge tube (Eppendorf) and sonicated for 10 min or until all visible signs of undissolved material had disappeared. To remove the high concentrations of phosphate ions (thought to impact on the accuracy of the RP-HPLC analysis), an additional protocol to those outlined for the standard analysis of amino acids in calcium carbonate-based biominerals (Kaufman & Manley, 1998; Penkman *et al*., 2008) was developed. The optimised method is as follows: KOH (1 M, 28 µL mg^{-1}, Fisher Scientific, analytical grade) was added to the acidified solutions, whereupon a mono-phasic cloudy solution formed. The samples were then briefly agitated to homogenise the solution. The sample was centrifuged at 13000 rpm for 10 min causing a clear supernatant to form above a gel; the biphasic separation (Figure 3.1). The supernatant was extracted and dried by centrifugal evaporation.

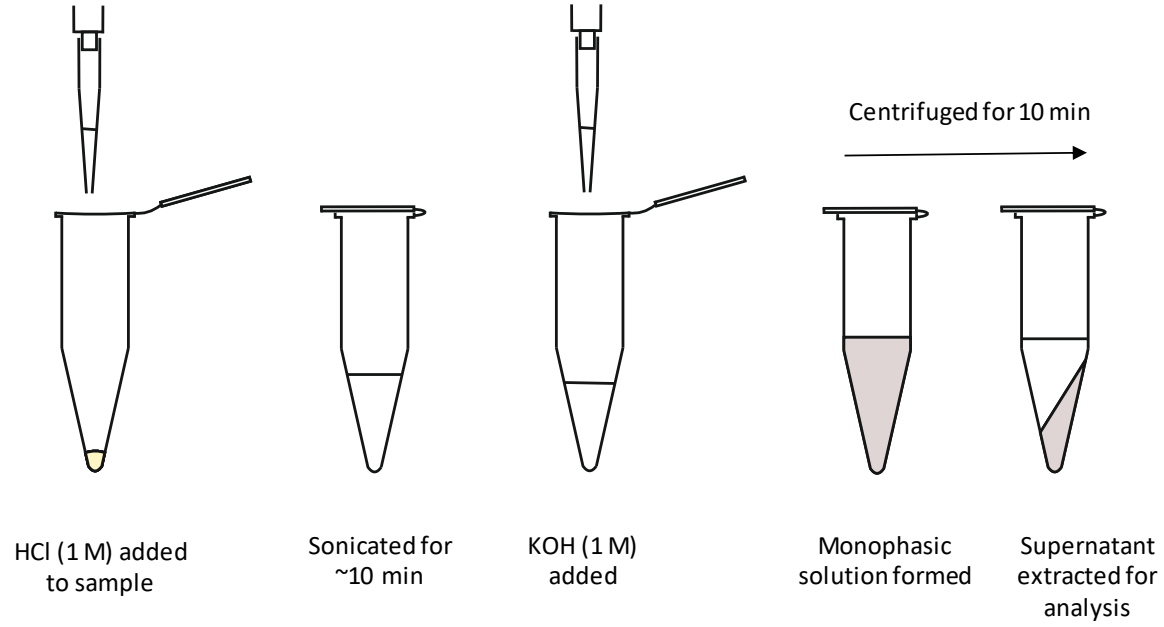

Figure 3.1. Schematic of the biphasic extraction of amino acids, designed to reduce phosphate ion concentration in the samples undergoing RP-HPLC analysis.

3.2.5. RP-HPLC Analysis

Samples were rehydrated with a solution containing an internal standard (L-*homo*-arginine; 0.01 mM), sodium azide (1.5 mM) and HCl (0.01 M), to enable quantification of the amino acids. Analysis of chiral amino acid pairs was achieved using an Agilent 1100 Series HPLC fitted with a HyperSil C18 base deactivated silica column (5 µm, 250 x 3 mm) and fluorescence detector, using a modified method outlined by Kaufman and Manley (1998). The column temperature was controlled at 25 ^{o}C and a tertiary system containing sodium buffer (23 mM sodium acetate trihydrate, sodium azide, 1.3 µM EDTA, adjusted to pH 6.00 ±0.01 with 10 % acetic acid and sodium hydroxide), acetonitrile and methanol was used as a solvent. Sodium azide prevents the build-up of microorganisms and EDTA complexes with excess metal ions.

3.2.6. FT-IR analysis

FT-IR analysis of both the dried gel and supernatant were conducted so the fate of the inorganic phosphate species could be determined. Fossil mammoth enamel from Tattershall Thorpe (Section 4.3.1.4.3) was powdered and bleached according to the optimised protocol (Section 3.2.3). Bleached enamel was treated as if analysing FAAs using the optimised biphasic separation (Section 3.2.4.2). The pellet that formed during the biphasic separation was dried by centrifugal evaporation. Both the dried gel and supernatant produced solids suitable for IR analysis: the gel formed a white powdery pellet,

whist the supernatant formed transparent crystals. To identify the location of the phosphate species, FT-IR analysis was carried out on each fraction as well as on pure hydroxyapatite for reference, using a Perkin Elmer Spectrum two IR spectrophotometer set to scan from 4000 – 350 cm^{-1} with a resolution of 2 cm^{-1}.

3.3. Optimisation and testing of the biphasic separation of inorganic species from amino acids

3.3.1. Biphasic separation optimisation methods

To develop an optimised method for the biphasic separation, three aspects were tested in detail:

a. the impact of the volume of KOH solution used in the preparation
b. the impact of the optimised method on the relative concentration of amino acids and their D/L values
c. evaluation of the expected analytical error

For part a.; testing the impact of KOH volume used) fossil enamel from the Thorpe sand and gravel at Tattershall was powdered and the intra-crystalline amino acids were isolated. THAAs were prepared (Section 3.2.4.1) and re-dissolved in the minimum volume of HCl (1 M, 20 µL mg^{-1}) and FAA samples were demineralised in HCl (1 M, 25 µL mg^{-1}). Different volumes of KOH (1 M, Fisher-Scientific) were added to these sub-samples prepared for their THAA (12 - 65 µL) and FAA (12 - 180 µL) contents to test for the optimum volumes required. A monophasic cloudy solution formed upon addition of KOH. The solution was centrifuged at 13000 rpm for 10 min and a clear supernatant formed above a gel (Figure 3.1). The supernatant was extracted and dried by centrifugal evaporation. Most samples were run in triplicate and were analysed by RP-HPLC (Section 3.2.5). However, upon addition of the rehydration fluid, some samples were insoluble due to the presence of high concentrations of calcium phosphate; in these cases, only one replicate was analysed by RP-HPLC to prevent damage to the HPLC system.

For part b.; (quantifying the impact of the optimised method on amino acid composition) 1:1 and 1:4 amino acid reference solutions were added to powdered hydroxyapatite. Samples followed the optimised protocol outlined for FAA samples post bleaching (Sections 3.2.4 and 3.2.5).

For part c.; estimation of analytical errors), *M. primigenius* tooth enamel from the Thorpe sand and gravel at Tattershall (Section 4.3.1.4.3) was powdered and homogenised (Section

3.2.2). Eight sub-samples were taken and run independently for their THAA and their FAA content as described in sections 3.2.2 - 3.2.5. Each sub-sample was run in duplicate. Some of the amino acids do not have reported D/L values due to low concentrations (Ile) and/or the presence of co-eluting peaks (THAA-Tyr, Leu and Ile), making accurate quantification impossible; in both instances, it is the usually the D-isomer peak that is affected.

3.3.2. Optimising the volume of KOH added during the biphasic separation of phosphate species and amino acids: results and discussion

The conditional solubility of hydroxyapatite ($Ca_5(PO_4)_3(OH)$) is a function of pH (Vasenko & Qu, 2017) but the solubility of amino acids is less sensitive to solution pH (Amend & Helgeson, 1997). Therefore, changing the pH potentially provides a mechanism for separation. A biphasic method for separation of phosphate species from amino acids has therefore been developed to eliminate the chromatographic issues caused by high concentrations of inorganic species during RP-HPLC analysis.

3.3.2.1. FT-IR analysis of the gel and supernatant

The IR spectrum for the dried gel displays absorption bands assigned to phosphate (PO_4^{3-}): vibrational frequencies at 1000 cm^{-1} (v_3), 962 cm^{-1} (v_1) and 561 cm^{-1} (v_4; Paz *et al*., 2012), all of which are also present in the spectrum of pure hydroxyapatite (Figure 3.2). The IR spectrum for the supernatant does not contain any discernible absorption bands (Figure 3.2), indicating that it does not contain detectable concentrations of phosphate species. The crystals formed by the dried supernatant are most likely KCl, which is not detectable by IR analysis. The presence of phosphate absorption bands in the gel and not in the supernatant indicates that phosphate species are removed from solution using this biphasic extraction method.

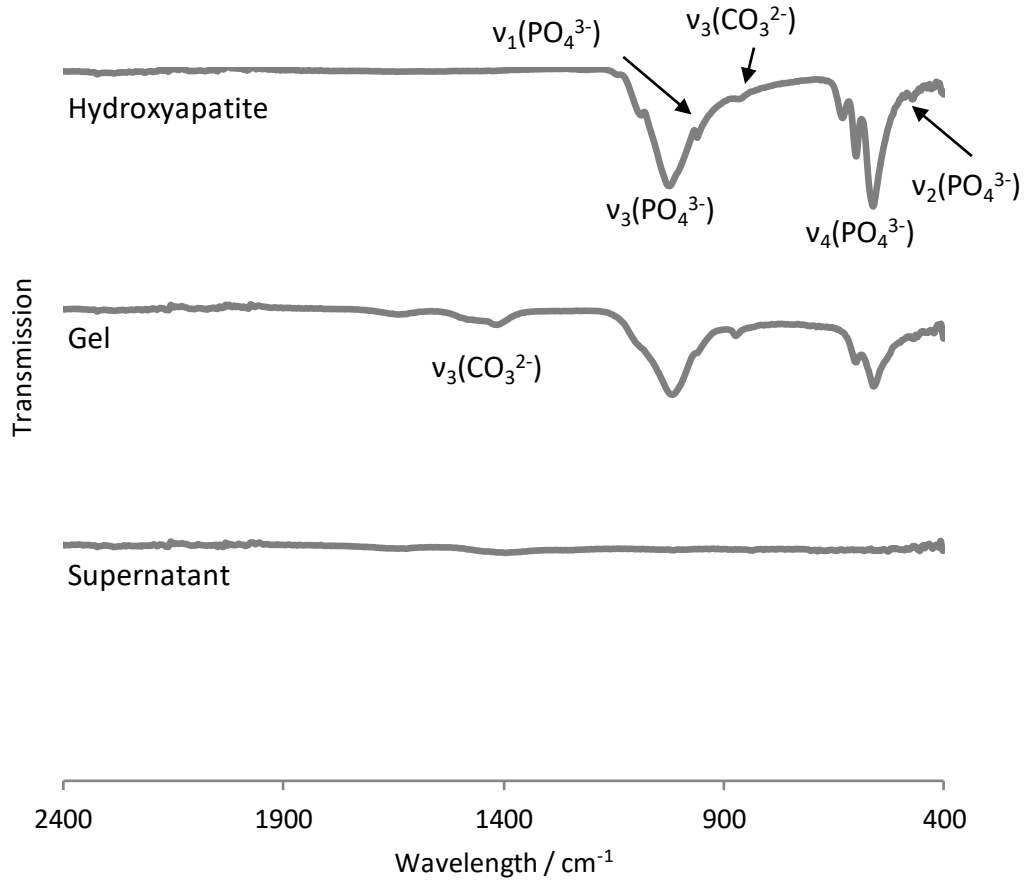

Figure 3.2. Stacked FT-IR spectra of pure hydroxyapatite (top), the gel formed after biphasic separation (middle), exhibiting phosphate absorption bands and the supernatant extracted (bottom). Absorption bands associated with inorganic salts have been labelled based on assignment from Paz et al. (2012). This data indicate that phosphate is incorporated into the gel, with none detectable in the supernatant then used for amino acid analysis. Carbonate peaks are also present due to CO_2 substitution in the hydroxyapatite crystal structure (Paz et al., 2012).

3.3.2.2. Changes in FAA and THAA concentration with increasing KOH volume

For the samples analysed for their FAAs, the measured concentration of Asx, Glx and Ala initially drops with increasing KOH volume (12-20 µL; Figure 3.3); this is most likely due to an increasing HPLC response to the internal standard, as the inorganic phosphates are more effectively removed and peak suppression is reduced. Above 16 µL mg^{-1} of KOH, the internal standard peak response lies within the expected range (i.e. of the rehydration solution alone), but peak area reduces again as excess KOH (> 40 µL mg^{-1}) start to cause peak suppression. The measured concentration of Asx when 180 µL of KOH solution was added is higher than at lower volumes of KOH, but this is not replicated in the other amino acids (Figure 3.3). The LhArg peak response at this concentration is lower than at other concentrations, indicating that Asx has a different response to the higher levels of KOH

than the other amino acids (including LhArg). This might lead to inaccuracies in analysing the relative amino acid composition of fossil samples. Additionally, the samples analysed at the highest and lowest volumes of KOH solution (12, 120 and 180 µL mg^{-1}) induced cloudy solutions prior to HPLC injection, suggesting higher concentrations of inorganic salts. Volumes of 20-65 µL mg^{-1} of KOH used to induce gel formation are therefore most likely to yield reliable amino acid data, and a value of 28 µL mg^{-1} is recommended.

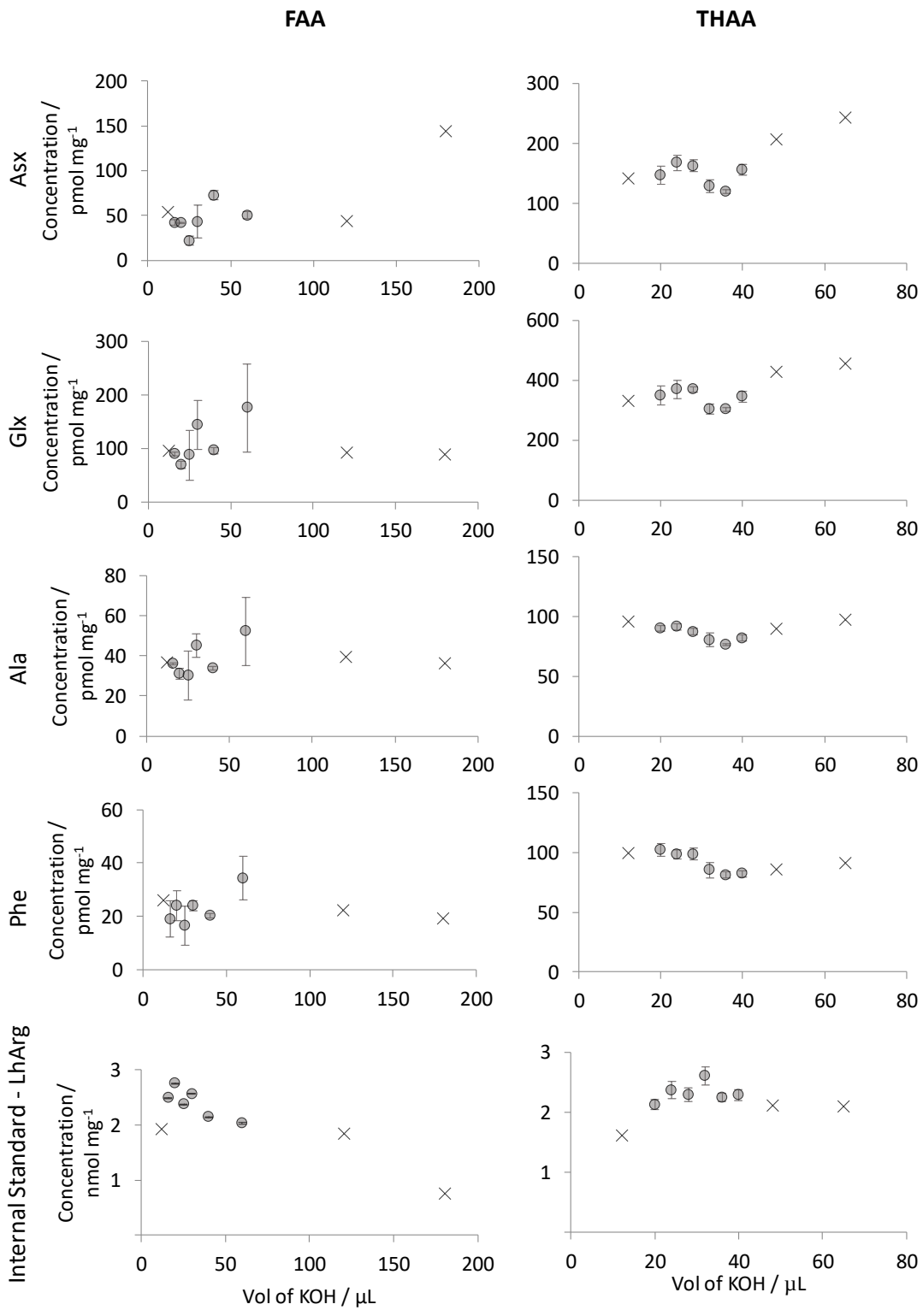

Figure 3.3. FAA (Left) and THAA (right) biphasic separation optimisation: Change in concentration of amino acids when changing the volume of KOH added (top four rows), the change in the HPLC response to the internal standard when changing the volume of KOH (bottom panel). Error bars depict one standard deviation about the mean (n = 3). Samples that were cloudy prior to HPLC injection have been plotted as crosses; only one sample of each of these was analysed.

Generally, a higher precision was observed for the THAA measured concentrations than for comparable FAA fractions (Figure 3.3) and this is most likely due to the higher amounts of amino acids in the THAA fractions, making quantification of integrated HPLC peak areas more precise. The measured concentration for Glx, Ala, and Phe are relatively stable with increasing KOH volume (Figure 3.3). In contrast, the measured concentration of Asx increases at KOH volumes greater than 42 µL, whilst the LhArg peak area response remains relatively stable. The change in Asx concentration with KOH volume alludes to either a bias in the peak suppression when compared to other amino acids (including the internal standard), or that the concentration of Asx could be biased by gel formation.

3.3.2.3. Changes in D/L value with increasing KOH volume

The D/L value for most amino acids is unaffected by changes in KOH volume, except for Ala prepared with 12 µL KOH and the THAA Glx and Phe prepared with 70 µL KOH (Figure 3.4). This suggests the biphasic gel formation does not bias the D/L values at the intermediate volumes (FAA: 16 – 120 µL; THAA: 20 – 65 µL). Whilst a range of volumes of KOH may be appropriate, a standard volume of 28 µL mg^{-1} has therefore been selected for the biphasic separation of amino acids from phosphate species. This volume does not appear to produce data affected by peak suppression and the amino acid D/L values are relatively stable on minor adjustments to the volume of KOH solution used.

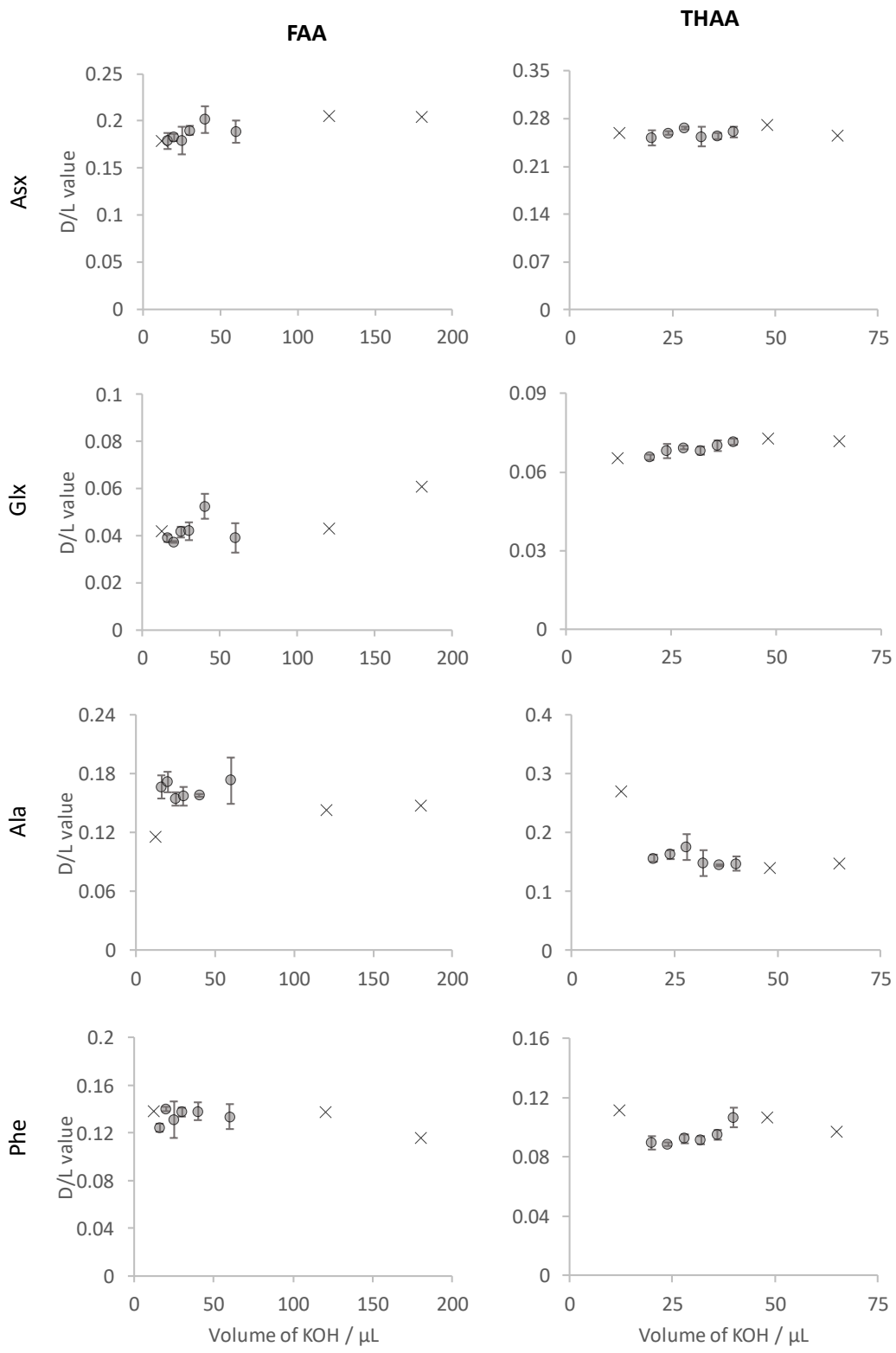

Figure 3.4. FAA (Left) and THAA (right) biphasic separation impact on D/L value of amino acids when changing the volume of KOH added). Error bars depict one standard deviation about the mean

3.3.3. Impact of the biphasic separation on amino acid composition and D/L value

The biphasic separation of amino acids and phosphate species involves the formation of a gel. The structure of the gel most likely contains a network of inorganic phosphate and calcium ions cross-linked with molecules of water (Gash *et al*., 2001). It is therefore likely that a proportion of the amino acid content in solution will be retained by the gel and subsequently unanalysed. As each amino acid is chemically unique, they may be retained by the gel to different extents. To test this, a solution with known amino acid composition but different D:L values (1:1 & 4:1) was added to pure hydroxyapatite (principal mineral component of enamel) and the amino acid composition was analysed after the optimised biphasic separation.

The amino acid composition of the amino acid reference solutions is broadly unchanged by the biphasic separation procedure (Glx, Ser, L-Thr, Ala, Tyr are biased by <6 %; Figure 3.5). However, the percentage contribution of Asx to the total amino acid content is slightly reduced and the contribution of the more apolar amino acids (Leu & Ile) is slightly increased. This indicates that there is a slight preferential retention of the more polar amino acids into the gel complex. This preferential incorporation of some amino acids over others may result in inaccurate amino acid compositional data, but it is consistent between analyses and the magnitude of this is unlikely to impact on the estimation of IcPD in fossil samples.

Quantification of the HPLC peak areas of Leu and Ile have been shown to be vulnerable to co-eluting peaks in samples from calcium carbonate-based biominerals (Kaufman & Manley, 1998; Powell *et al*., 2013; Wehmiller, 2013), and this susceptibility also appears to be true for enamel-derived samples (Figure 3.5; Figure 3.6).

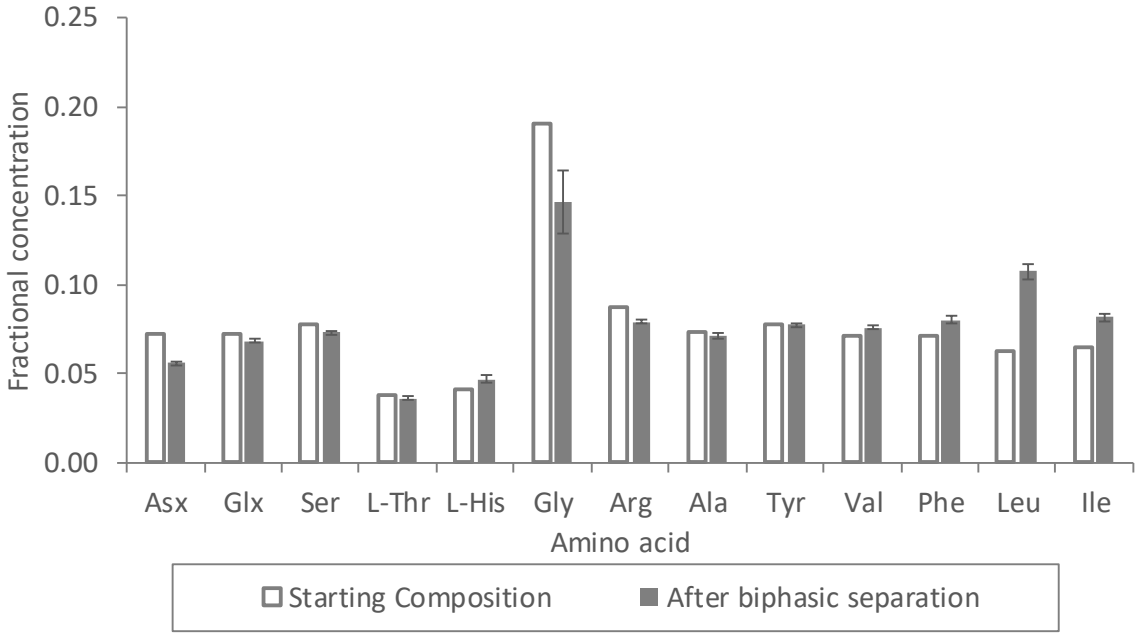

Figure 3.5. Concentration data expressed as a fraction of the total amino acid amount of a 1:1 amino acid reference solutions with hydroxyapatite that has undergone the biphasic separation of the amino acids from inorganic phosphates (solid bars). The starting composition has been shown for comparison (hollow bars). Error bars depict one standard deviation about the mean. Data was slightly skewed by the higher than expected concentration of Leu.

3.3.3.1. Changes in amino acid D/L value induced by biphasic separation

The biphasic separation of amino acids from phosphate species does not alter the D/L value of most amino acids at both low (~0.2) and high (~1) D/L values (Figure 3.6). This, in conjunction with the IR analysis, indicates that this method of separation is suitable for evaluating amino acids from enamel by RP-HPLC. However, the change in Leu concentration and D/L value after the biphasic preparation precludes the use of this amino acid for IcPD enamel studies using the current methods. Kaufman and Manley (1998) reported compounds in some samples that interfered with the resolution of D-Leu when analysing amino acids by RP-HPLC, which may account for the change in the concentration of Leu as well as the increased D/L values (Figure 3.6).

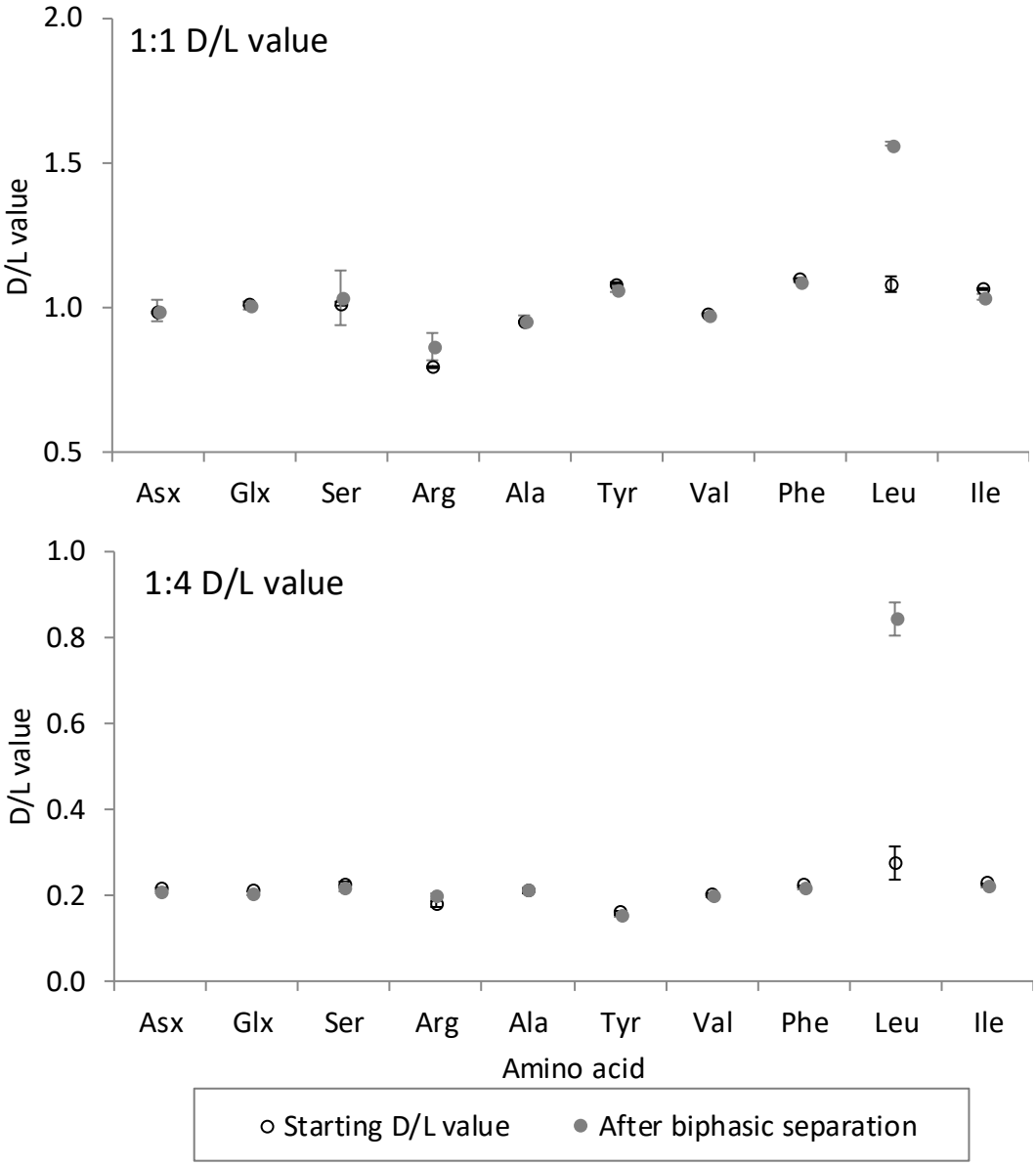

Figure 3.6. Amino acid D/L values for hydroxyapatite containing amino acid reference solutions. Two different D/L values reference solutions were used to mimic both old (1:1 D/L value; top) and young (1:4 D/L value; bottom) fossil samples. Error bars depict one standard deviation about the mean.

3.3.3.2. Estimation of analytical errors

Analytical error here is defined as the variability in amino acid D/L values resulting from the sample preparative procedures and analysis, in this case by RP-HPLC. Most fossil enamel samples can be prepared in duplicate however, due to the precious nature of some of the samples this may not always be possible. It is essential for geochronological applications that the developed protocol is reproducible. The replicate analysis of eight fossil enamel samples and their standard deviations and coefficient of variance is presented in Table 3.3.

Except for Val, the coefficient of variance for most of the amino acids obtained from enamel are on the same order as those values reported for comparably racemized *Bithynia* opercula (Penkman *et al*., 2013). We therefore conclude that the biphasic separation method developed in this section does enable sufficiently precise amino acid data to be obtained. However, it is noted that this degree of precision may not hold true for the entire range of D/L values required for geochronological assessment over Quaternary time scales, so additional analysis of younger and older enamel material would be valuable. Due to the low degree of precision of Val and Tyr D/L values, these amino acids have not been used to build a geochronology.

Table 3.3. Experimental variability for each amino acid of the optimised enamel AAR protocol on an M. *primigenius tooth from the Tattershall Thorpe sand and gravel.*

	THAA			FAA		
	Mean D/L value	Σ	Coefficient of variance	Mean D/L value	σ	Coefficient of variance
Asx	0.248	0.008	3.2 %	0.186	0.003	1.8 %
Glx	0.070	0.003	4.6 %	0.039	0.001	2.7 %
Ser	0.230	0.017	7.2 %	0.413	0.020	4.9 %
Arg	0.225	0.027	12.1 %	0.402	0.031	7.7 %
Ala	0.154	0.009	5.8 %	0.163	0.006	3.7 %
Tyr	-	-	-	0.124	0.051	40.7 %
Val	0.134	0.027	20.2 %	-	-	-
Phe	0.090	0.005	5.9 %	0.169	0.011	6.6 %

3.4. Isolation of the intra-crystalline fraction

3.4.1. Prolonged oxidative treatment

Previous studies have reported that prolonged oxidative treatment of calcium carbonate-based biominerals greatly reduces the amino acid content but leaves a small fraction that is chemically inaccessible (Crenshaw, 1972; Brooks *et al*., 1990; Sykes *et al*., 1995; Penkman *et al*., 2008; Crisp *et al*., 2013). NaOCl is predicted to oxidise all amino acids and proteins it encounters but will be ineffective on material that is inaccessible. Oxidative pre-treatment of mollusc shell has been shown to improve the accuracy and precision of AAR data, which

is vitally important for its application as a tool for geochronology (Penkman *et al*., 2008; Demarchi *et al*., 2013b; Ortiz *et al*., 2018). Powdered enamel was therefore exposed to bleach for increasing lengths of time to test if a similar fraction can be isolated from enamel, and if so, to calculate the optimum length of time to isolate this closed system material.

3.4.2. Optimising the oxidation procedure

3.4.2.1. Optimisation of the oxidation method

Powdered enamel (~30 mg) from Tattershall Thorpe was weighed into sterile 2 mL microcentrifuge tubes (Eppendorf), and samples were submerged in NaOCl (12 %, 50 µL mg^{-1}) for 0, 6, 15, 25, 48, 72 and 238 h. The NaOCl was removed and the powdered enamel washed five times with HPLC-grade water. A final wash with methanol was performed before the samples were left to air dry overnight. Samples were then purified using the optimised biphasic procedure (section 3.2.4.2) and analysed by RP-HPLC (Section 3.2.5). Samples were prepared with 4 replicates.

3.4.2.2. Changes in amino acid concentration with prolonged oxidative treatment

The FAA concentration remains constant up to 6 h, increases by 15 h, before returning to approximately the initial concentrations (Figure 3.7). The concentration of the FAA does not decrease when exposed to NaOCl which indicates that the FAAs are inaccessible to the NaOCl and potentially retained in a closed system. The enamel used in this set of experiments was ~191 ka in age, so it is likely that most of the open system FAAs would have leached out whilst in the depositional environment, thus leaving a mostly closed-system fraction of FAA resistant to oxidative treatment.

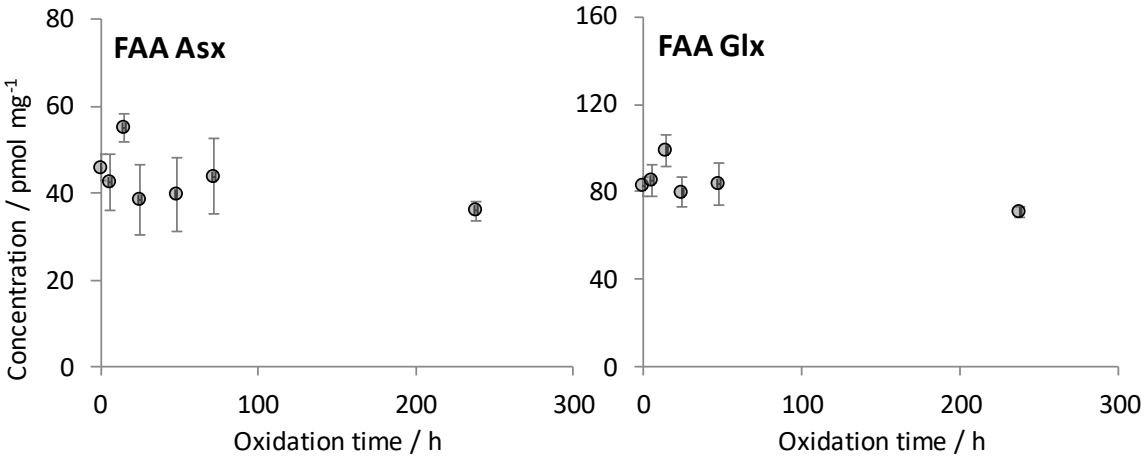

Figure 3.7. FAA concentrations from powdered M. primigenius *enamel of Asx (left) and Glx (right) after prolonged exposure to a strong oxidant (NaOCl). Error bars depict one standard deviation about the mean (n= 4 or 5).*

The concentration of THAA in enamel decreased rapidly by ~25 % during the initial 6 h of exposure to NaOCl (Figure 3.8). This rapid loss of organic matter has been reported for other biominerals (Bright & Kaufman, 2011b; Hendy *et al*., 2012; Crisp *et al*., 2013) and has been attributed to the oxidation of easily accessible organic matter, believed to be present in an open system found between crystallites (Towe and Thomson, 1972). After this point a more gradual decrease in concentration was observed; it is likely that a fraction of organic matter present between crystallites is resistant to the initial exposure of strong oxidant and therefore enamel requires further exposure to fully remove this material. After 72 h of exposure to bleach only minimal additional loss of the THAAs is observed.

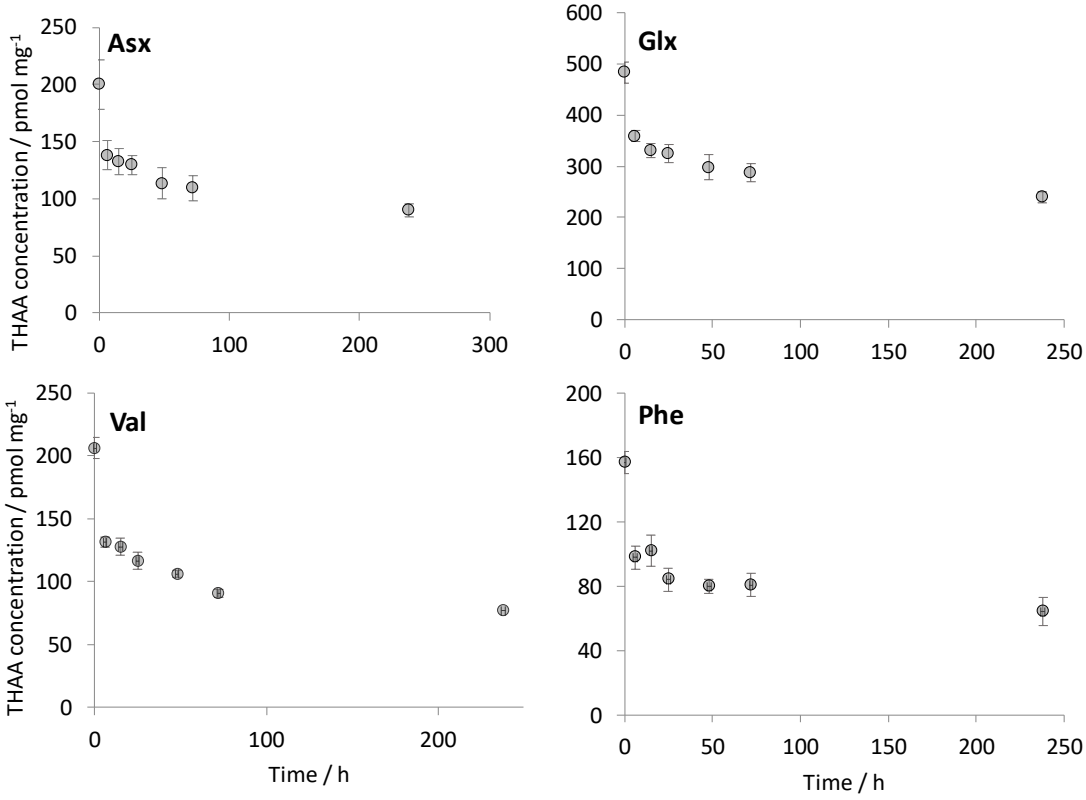

Figure 3.8. THAA concentrations from powdered M. primigenius *enamel of Asx (top left), Glx (top right), Val (bottom left) and Phe (bottom right) after prolonged exposure to a strong oxidant (NaOCl). Error bars depict one standard deviation about the mean (n= 4 or 5).*

3.4.2.3. Effect of increased oxidation time on D/L values

The FAA D/L values for Asx, Glx, Ala and Phe remain relatively constant with increasing exposure time (Figure 3.9), which is consistent with the trends observed for the FAA concentrations (Figure 3.7) and indicate the FAA fraction is in a stable, inaccessible environment.

The THAA D/L values for some of the amino acids does not change (Glx and Phe), indicating that the organic material removed by the prolonged oxidation is at a similar level of degradation to that which has been isolated. However, this will most likely not always be the case (e.g. Penkman *et al* 2007, Ortiz *et al*., 2018).

The THAA D/L values for Asx decline gradually to 72 h and then plateau. The extent of bound Asx racemization is initially greater than for free Asx (Figure 3.9). The Asx THAA concentration decreases and the FAA concentration is stable with exposure to NaOCl up until 72 h (Figure 3.7 and 3) and thus NaOCl is removing the more racemised bound Asx, causing the gradual decrease in Asx THAA racemization.

Studies of molluscan shells and ostrich eggshell have reported that after the intra-crystalline fraction has been isolated, a gradual increase in D/L value is observed with increasing exposure time (Penkman *et al*., 2008; Crisp *et al*., 2013). In aqueous solutions, bleach forms a weak acid and this increase in D/L value is thought to be caused by gradual etching of the calcium carbonate matrix, inducing racemization. This D/L pattern is not observed in the sample of enamel, but gradual loss of amino acids might be caused by the same slow etching of the calcium phosphate mineral matrix.

The extent of Asx and Glx racemization in the FAA fraction is less than in the THAA fraction (Figure 3.9). This is the opposite of the patterns observed in other biominerals (e.g. Penkman *et al*., 2008; Tomiak *et al*., 2013) and indicates that the bound amino acids are more racemised than the FAAs. FAAs are expected to be more racemised than THAAs, because with the exceptions of Asx and Ser, most amino acids are unable to racemise in-chain (Stephenson & Clarke, 1989; Takahashi, *et al*., 2010; Demarchi *et al*., 2013a). Amino acids situated at the terminal position of peptides are thought to have the lowest activation of racemization and thus racemization occurs rapidly (Kriausakul & Mitterer, 1978; Stephenson & Clarke, 1989). Free amino acids form as a result of hydrolysis of these more highly racemised amino acids and thus are expected to have a greater extent of racemization. In enamel, in-chain racemization may account for the reversal of trend for Asx but not for Glx, so this is a very interesting observation that may indicate enamel peptides are breaking down in a different way to other biominerals, possibly due to the maturation process *in vivo,* which breaks down most of the protein content of enamel before the tooth is mature (Robinson *et al*., 1995; 1998).

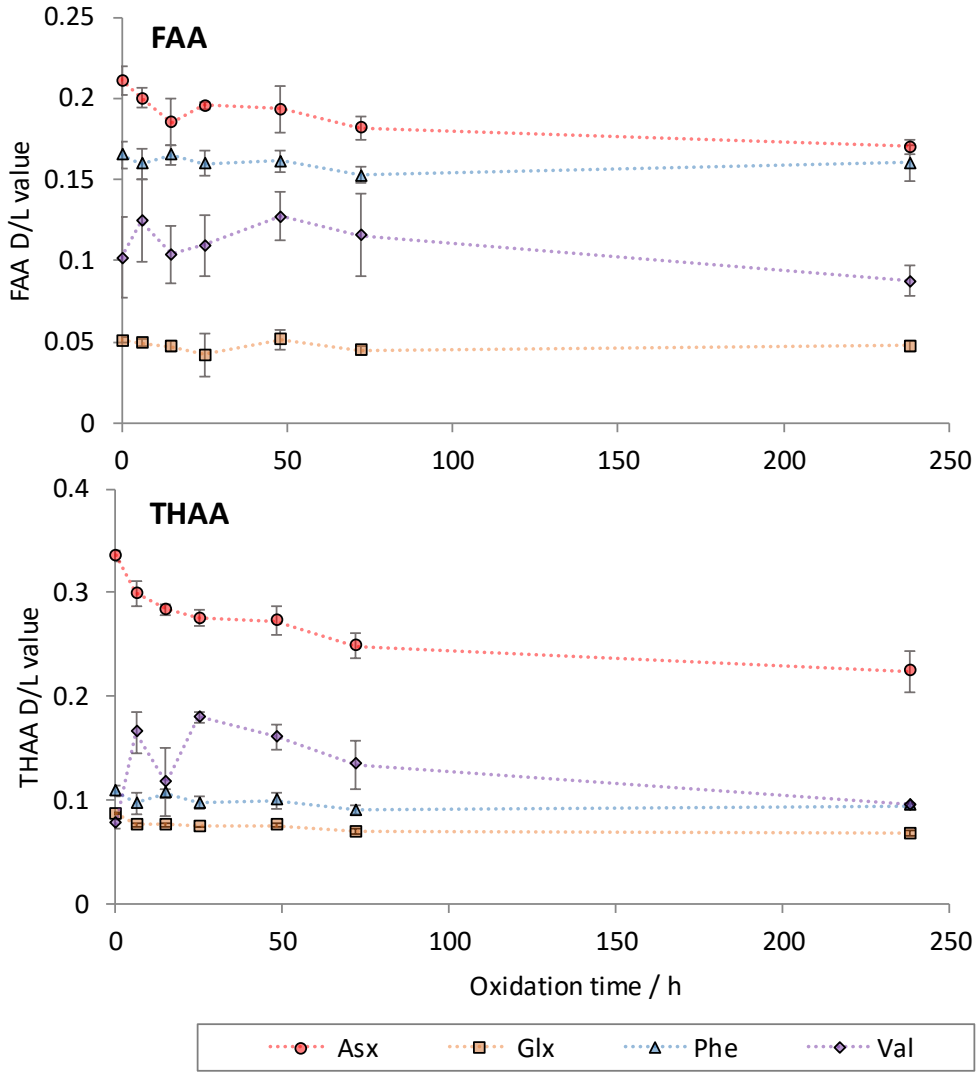

Figure 3.9. Effects of oxidative treatment on the extent of racemization in powdered M. primigenius *enamel for FAA (Top) and THAA (bottom) fractions. Error bars depict one standard deviation about the mean (n= 4 or 5).*

3.4.2.4. Intra-crystalline enamel composition

The composition and role of protein in immature dental enamel have been widely studied (Margolis *et al*., 2006), but little is known about the proteinaceous material that can be recovered from mature/fossil enamel. Mature enamel is acellular and contains a complex mixture of peptides, amino acids and proteins originating from a variety of different dental developmental processes (Robinson *et al*., 1995). Collagen contamination from the surrounding dentine and cementum poses a risk to enamel AAR dating. Collagen has a characteristically high proportion of Gly (~33%), proline (~12%) and hydroxyproline (10 %; Poinar & Stankiewicz, 1999). The method of analysis used in this study cannot detect proline or hydroxyproline, but the relatively low levels of Gly (< 33 %) observed in the bleached THAA fraction of mammoth enamel (Figure 3.10) indicates that the amino acids

analysed by this procedure have likely originated from mature enamel proteins rather than collagen. The enamel profile also matches that of previously reported fossil enamel from a closely related taxon, *Mammut sp.* (mastodon; Figure 3.10).

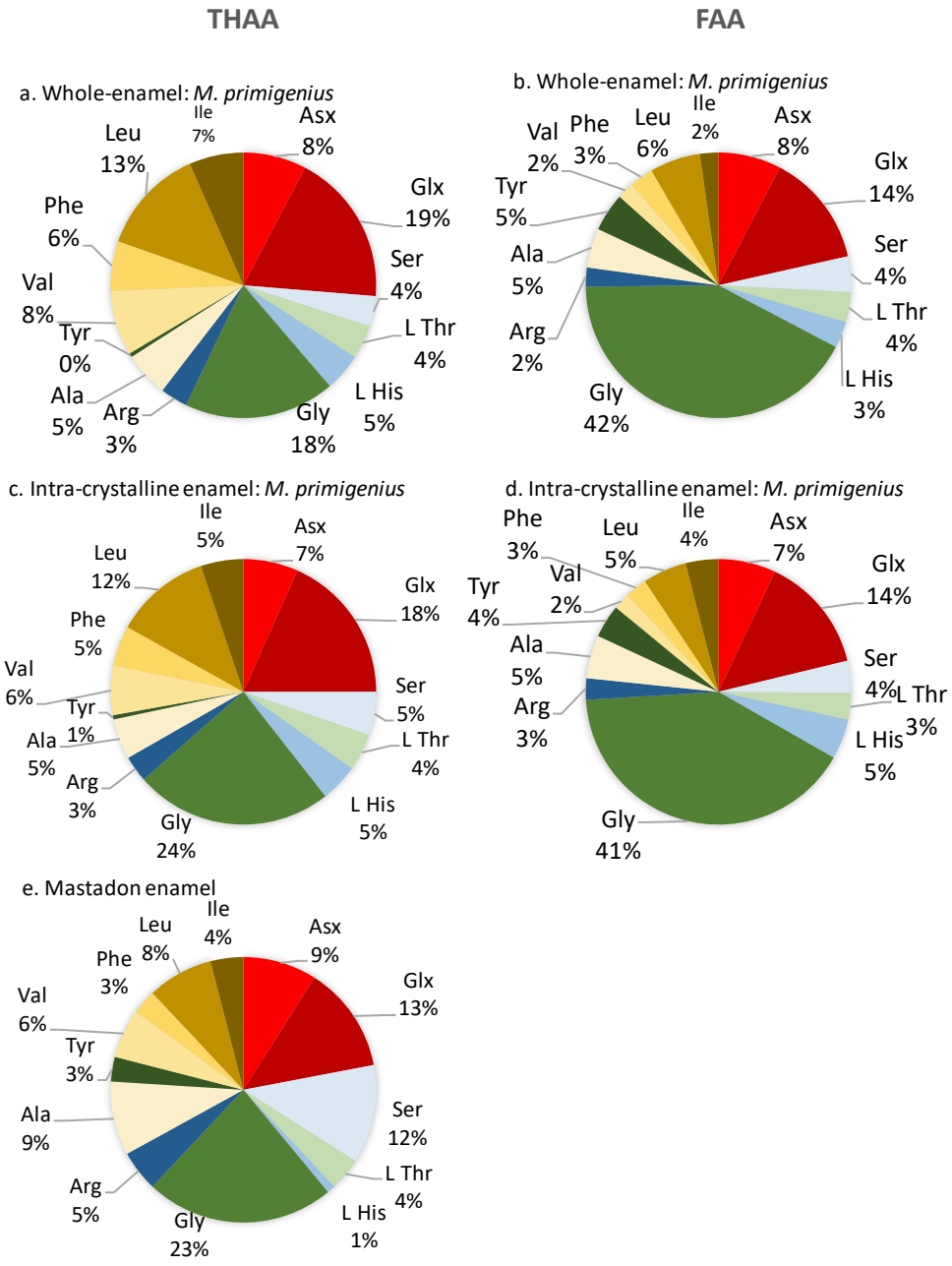

Figure 3.10. FAA (Right) and THAA (left) composition of M. primigenius *enamel from the Thorpe sand and gravel at Tattershall, from both whole-enamel (top), intra-crystalline (middle), and previously reported mastodon enamel (bottom; Doberenz et al., 1969). Amino acids are coloured differently based on their side-chain properties: Ionisable side-chains with a negative charge (red), ionisable side-chains with a positive charge (blue), non-ionisable side-chains that are polar (yellow) and non-ionisable side-chains that are non-polar (green)*

The THAA composition of the unbleached enamel is similar to that of the bleached (intra-crystalline; Figure 3.10). This suggests that they are made up of an analogous set of proteins. However, there is an increase in the relative contribution of Gly in the intra-crystalline fraction. The concentration of the Gly-rich FAA fraction has been shown to be stable upon increased exposure time to bleach (Figure 3.9), whilst the THAA concentration decreases. The THAA content is comprised of both the FAA and bound amino acid fractions therefore, the change in the THAA composition is likely to be due to the loss of the more Gly-poor bound amino acids upon bleaching.

The similar compositional change of amino acids during bleaching has been observed in ostrich eggshell (Crisp *et al*., 2013) but not for other biominerals (Ingalls *et al*, 2003; Penkman *et al*., 2008; Demarchi *et al*., 2013c). It has been observed that acid-rich proteins preferentially bind to calcite, enhancing their contribution to the intra-crystalline fraction (Marin *et al*., 2007). However, this has not been observed for enamel, and is potentially a result of different pathways for the structural formation of enamel or for the degradation of enamel proteins.

3.5. Elevated temperature experiments and fossil analyses to test for closed system behaviour

The process of racemization at ambient depositional temperatures occurs over geological timescales, in some cases taking millions of years to equilibrate (Hare & Mitterer, 1968). To study the reaction kinetics of IcPD/racemization in a laboratory, this process needs to be accelerated and all the amino acids in the system need to be accounted for (Collins & Riley, 2000). Bleached and unbleached samples have been analysed to compare the behaviour of the inter- and intra-crystalline fractions of amino acids in enamel (Sections 3.4.1). However, bleaching treatment may not isolate a purely intra-fraction as bleached biominerals may also contain quantities of highly resilient proteins from the inter-crystalline fraction (Bright & Kaufman, 2011b).

Previous studies of the long-term diagenesis of proteins in other biominerals (e.g. mollusc shells, Penkman *et al*., 2008; OES, Crisp *et al*., 2013; corals, Tomiak *et al*., 2012) have heated samples isothermally in sealed vials containing water; analysis of both the biomineral and the supernatant water thus accounts for all amino acid degradation products. Consideration of the reaction kinetics of the proteins and amino acids in enamel under laboratory conditions can help inform our understanding of some of the trends observed in fossil data. High temperature kinetic and leaching experiments have therefore

been undertaken on both modern and fossil enamel to examine their degradation behaviours.

3.5.1. Methods for testing for a closed system

Approximately 10 mg of bleached and unbleached powdered tooth enamel from both *M. primigenius* from the North Sea and a modern *E. maximus* was weighed into sterile glass ampoules. 500 µL of HPLC grade water was added and the glass vials were sealed. The ampoules were placed in an oven and heated isothermally at 80, 110 or 140 °C for varying times (Table 3.4). Triplicate samples were analysed for each time-point.

Table 3.4. Conditions for the heating of powdered enamel. Triplicate samples were prepared for each time point. Bleached samples were agitated in NaOCl for 72 h according to section 3.4.2.1.

Sample	Bleached	T / °C	Heating time / h											
Modern Elephant	Yes	140	0	1	2	4	6	8	24	48	72	96	120	
Modern Elephant	No	140	0	1	2	4	48							
Modern Elephant	Yes	110	0	24	48	148	240	384	480	720	840	963	1200	2688
Modern Elephant	Yes	80	0	24	96	148	480	720	963	1442	2160	3600	4560	5760
North Sea	Yes	140	0	1	4	6	8	24	48					
North Sea	No	140	0	1	6	48								

After the allotted time, the glass ampoules were unsealed, and the supernatant water split into two aliquots (100 µL). One fraction was analysed for the free amino acids present in the water (FAAw) and the other was analysed for the total hydrolysable amino acid content in the water (THAAw). To THAAw samples, HCl (6 M, 20 µL per maximum theoretical mg equivalent of enamel) was added and placed in an oven for 24 h at 110 °C in N_2 purged vials. To remove the HCl, samples were placed in a centrifugal evaporator. FAAw samples were dried in a centrifugal evaporator with no further sample preparation.

Powder samples were weighed out into two fractions for the analysis of the free and total hydrolysable amino acid content in the powders (FAAp and THAAp respectively) according to the optimised procedure outlined in sections 3.2.4.1-3.2.5. All sub-samples were analysed by RP-HPLC (section 3.2.5).

The supernatant water of bleached modern elephant enamel powder isothermally heated at 140 °C for 48 h was concentrated 10-fold and the resultant residue imaged by transmission electron microscopy (TEM). Formvar/Carbon 200 mesh copper grids were plasma cleaned for 10 seconds in a Harrick Plasma PDC-32G-2. A 3 µL volume of sample was applied to the grid and either removed by blotting after 1 min and left to air dry, or left to dry for 30 min without blotting to increase the sample deposited on the grid. Grids were imaged using a Tecnai G^2 12 BioTWIN microscope operating at 120 kV with a tungsten filament. Some of the TEM plates were overloaded with crystals and thus damaged.

3.5.1.1. Fossil enamel pilot study

Enamel from: a modern elephant, mammoths from the North Sea, Balderton, Tattershall Thorpe, Crayford, Ilford, Swanscombe, Sidestrand and the Norwich Crag formation were individually prepared and analysed for their intra-crystalline amino acid content by RP-HPLC according to the optimised protocols outlined in sections 3.2.2-3.2.5.

3.5.2. Leaching of amino acids into the supernatant water

It is expected that during an accelerated degradation experiment, open system amino acids will leach out of the enamel powder; this diffusive loss would also be relevant in the depositional environment (Collins & Riley, 2000). Previous studies have shown that bleaching can significantly reduce the quantity of leached amino acids in similar IcPD experiments (Penkman *et al*., 2008; Crisp *et al*., 2013; Ortiz *et al*., 2018). To quantify the

extent of leaching, the enamel powder was heated in water so that leached material could be recovered through subsequent analysis of the water (section 3.5.1).

3.5.2.1. Concentration of amino acids in the supernatant water

The concentration of leached amino acids in the waters of bleached enamel is notably lower than observed in the supernatant water of unbleached enamel (Figure 3.11 & Figure 3.12). This implies that most of the amino acids removed by bleaching are open system and thus can leach out of the enamel during these degradation experiments.

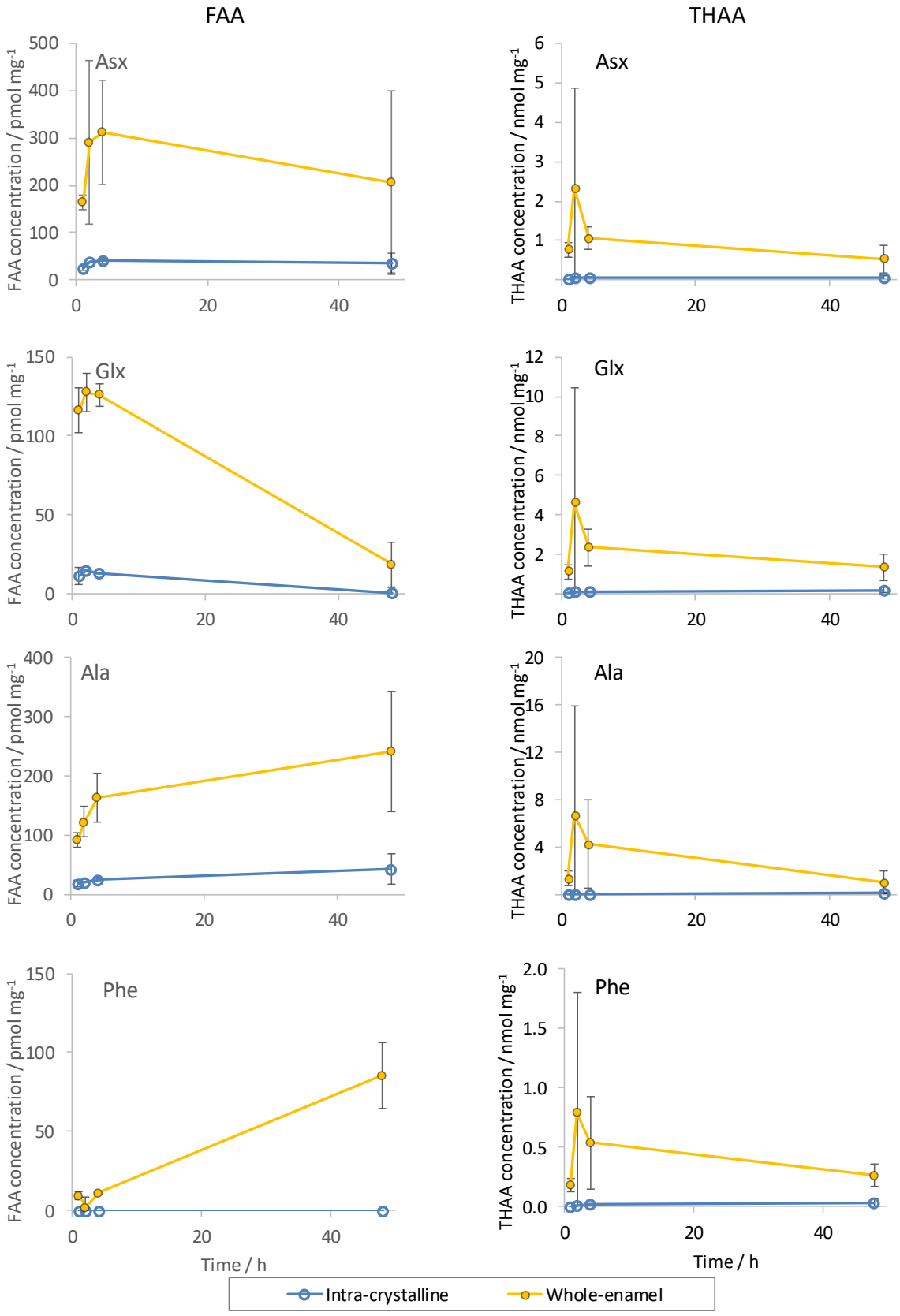

Figure 3.11. Concentration of FAA (left) and THAA (right) in supernatant water from heating experiments conducted at 140 °C for both bleached (blue) and unbleached (orange) modern elephant enamel. Error bars show one standard deviation about the mean (n = 2-6).

Higher concentrations of amino acids were also present in the supernatant waters of unbleached mammoth enamel from the North Sea than in those of bleached enamel (Figure 3.12), which agrees with the trends observed for modern elephant enamel (Figure 3.11). Low concentrations of amino acids were also detectable in the supernatant waters from the bleached modern and North Sea enamel. Mean percentage concentration of Asx, Glx, Ser, Ala, Arg, Ala Tyr, Val & Phe in the supernatant water of enamel after 72 h were ~5 % of the total starting concentration, which is similar to those recorded for gastropod *Phorcus lineatus* (ca. 5%; Ortiz *et al*., 2018).

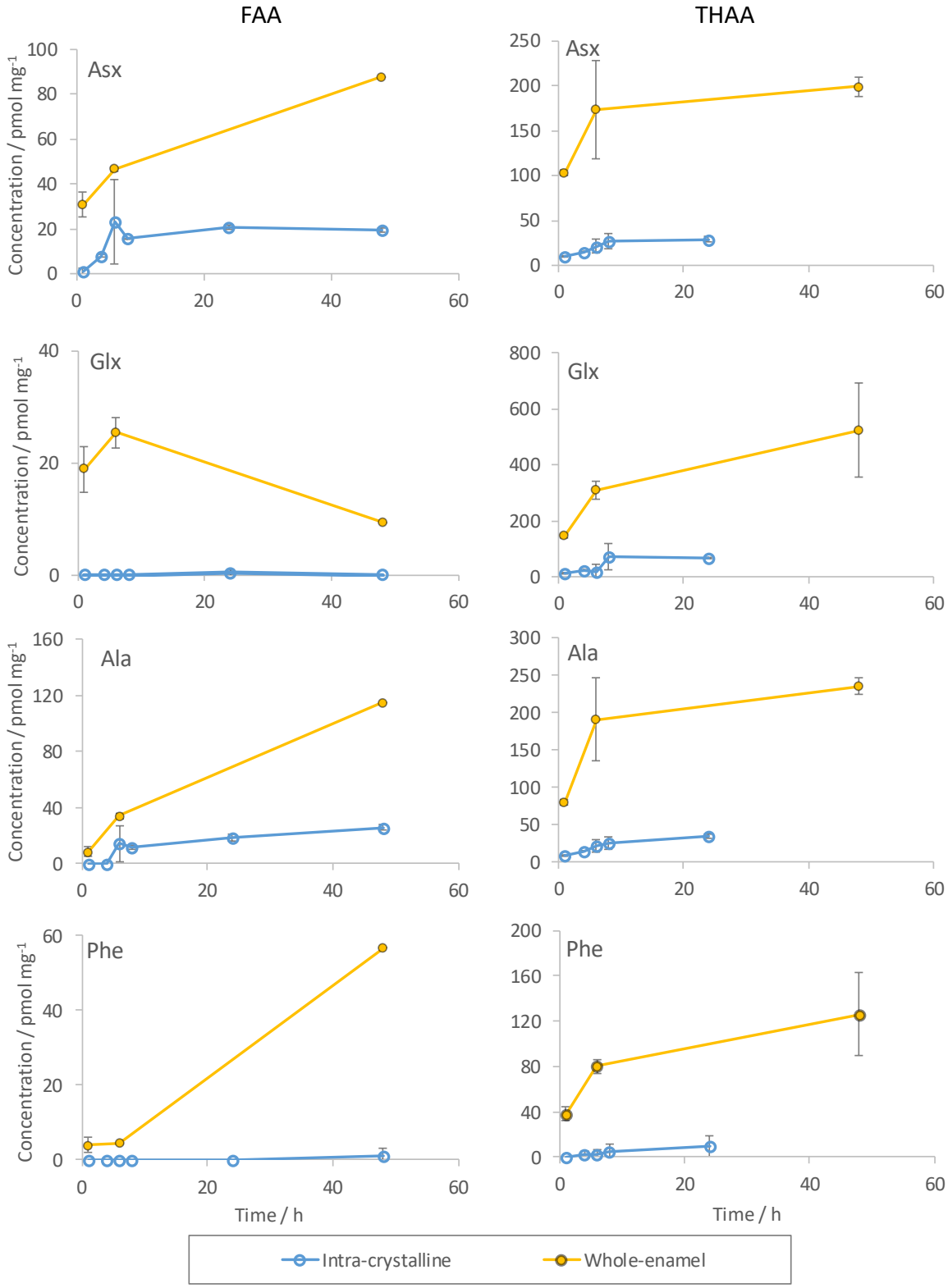

Figure 3.12. Concentration of FAA (left) and THAA (right) in supernatant waters of heating experiments conducted at 140 °C for both bleached (Blue) and unbleached (orange) North Sea M. primigenius. *Error bars depict one standard deviation about the mean (n-2-3).*

The enamel powder used in these elevated heating experiments is very fine and thus small particles can be readily disturbed into the supernatant waters, thereby potentially accounting for some of the amino acids in the water fractions. To combat this, the vials were centrifuged prior to extraction, but this may have not been sufficient. The dried supernatant water of a modern elephant sample was therefore imaged by TEM to investigate if crystalline material was present in the supernatant waters of these experiments.

As the supernatant water was concentrated, the solution became cloudy, indicating the presence of solid material. A large range of crystal sizes from tens of µm to ~10 nm was observed by TEM (Figure 3.13). The abundance of crystalline artefacts indicates that despite the careful attempt to isolate supernatant water only, powdered enamel is still present in the supernatant waters, and thus will contribute to the total FAAw and THAAw contents. This evidence does not preclude the possibility there are leached amino acids in the supernatant waters, but this observation means that we are limited in differentiating leached amino acids from powder contamination of the supernatant water in this study. The concentrations of amino acids in the supernatant water are therefore upper estimates of leaching and the actual percentages of leached amino acids is likely to be lower. The results of these leaching experiments indicate that bleaching does significantly minimise leaching during high temperature diagenesis in both fossil and modern material.

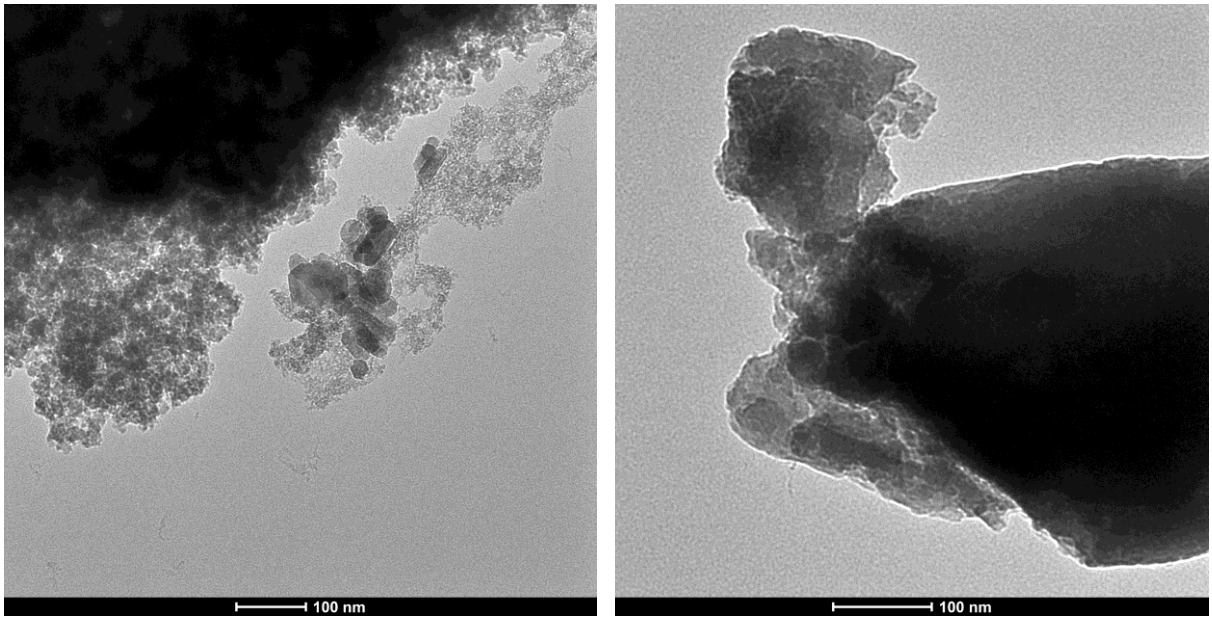

Figure 3.13. TEM images of inorganic crystals in the supernatant water of modern elephant enamel powder isothermally heated at 140 °C for 48 h. Supernatant water was left to dry for 30 min on the copper grid.

3.5.3. Intra-crystalline vs whole-enamel

3.5.3.1. Modern elephant enamel

As expected, in modern elephant enamel, THAA D/L values for intra-crystalline Asx, Glx, Ala and Phe increase over time when heated isothermally at 140 °C (Figure 3.14). However, the D/L values for the whole-enamel (unbleached) proteins initially increased and then plateaued, deviating greatly from the trend observed for the intra-crystalline fraction. Comparable experiments of other biominerals that simulate protein degradation have shown similar observations, which have been attributed to the early leaching of the more highly racemised FAAs from the whole-shell fraction of gastropod and ostrich eggshell (Crisp *et al*., 2013; Ortiz *et al*., 2018). In contrast, this process does not occur in the intra-crystalline fraction because it exhibits closed system behaviour. The precision of the intra-crystalline D/L values are higher than of the whole-enamel data (Figure 3.14), with the higher variability for the whole-enamel data likely to be a consequence of differential leaching of open system material.

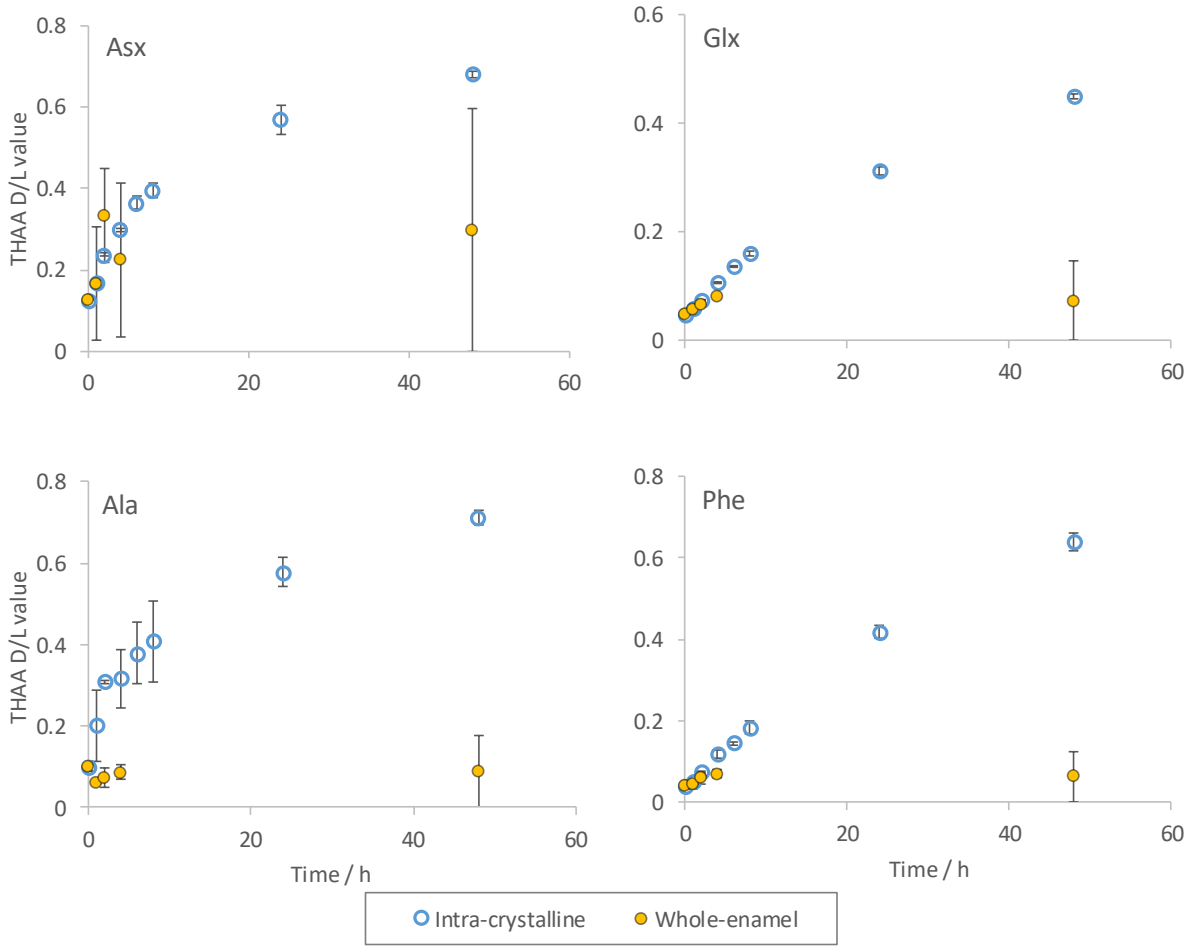

Figure 3.14. THAA D/L value of Asx, Glx, Ala, and Phe for bleached (intra-crystalline) and unbleached (whole-enamel) modern elephant enamel with increasing time when isothermally heated at 140 °C. Error bars depict one standard deviation about the mean (n = 2-6).

3.5.3.2. North Sea mammoth enamel

In contrast to the modern enamel (Figure 3.15), for the amino acids studied, there is no significant difference in extent of THAA racemization between bleached and unbleached North Sea enamel heated at 140 °C (Figure 3.15). It is likely that the fossil enamel has already lost most of the leachable organics and thus the whole-enamel protein composition is instead dominated by the intra-crystalline amino acids, and thus the bleached and unbleached fractions are behaving in a similar manner.

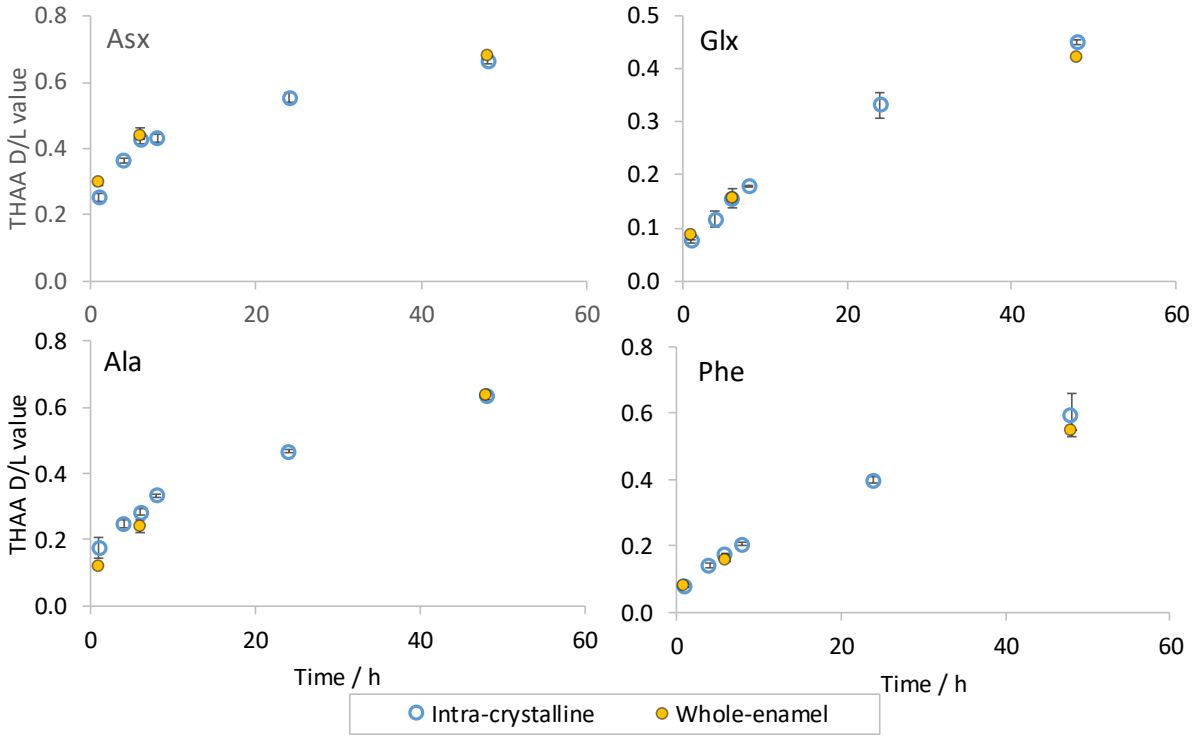

Figure 3.15. THAA D/L value of Asx, Glx, Ala, and Phe for bleached (intra-crystalline) and unbleached (whole-enamel) North Sea *M. primigenius* enamel with increasing time when isothermally heated to 140 °C. Error bars depict one standard deviation about the mean (n = 2-3).

3.5.4. Elevated temperature FAA vs THAA D/L

In a closed system, all the diagenetic products of protein degradation are retained within the biomineral up until analysis (Collins & Riley, 2000), the implication of which is that FAA and THAA D/L values should be highly correlated, if enamel is a closed system.

The FAA and THAA D/L values of Asx, Glx, Ala and Phe are highly correlated at all the temperatures studied (Figure 3.16). The D/L values for some of the least racemised FAAs could not be determined due to very low concentrations of the D isomer and have therefore been plotted along the axis. The high degree of correlation indicates that the FAA are retained by the biomineral and that leaching is not occurring. This supports the assertion that the enamel proteins isolated via bleaching are effectively operating as a closed system.

In calcium carbonate based-biominerals, the extent of FAA racemization is greater than for the THAA, because most amino acids (except Asx and Ser; Stephenson & Clarke, 1989; Demarchi *et al*., 2013b) are unable to racemise when bound in chain (Mitterer &

Kriausakul, 1984). Except for Phe, this trend has generally not been observed to be true for enamel during these degradation experiments (Figure 3.16). The extent of racemisation observed for the FAA and THAA fractions of Glx and Ala are very similar and increase in a roughly 1:1 ratio (Figure 3.16). Mature enamel contains shorter chain peptides than most biominerals due its maturation processes (Robinson et al., 1995); the lower average chain length peptides in enamel might explain the similar rates of racemisation between the THAA and FAA fractions. The Asx THAA D/L values are greater than the corresponding FAA values (Figure 3.16), likely to be due to in-chain racemization (Stephenson & Clarke, 1989).

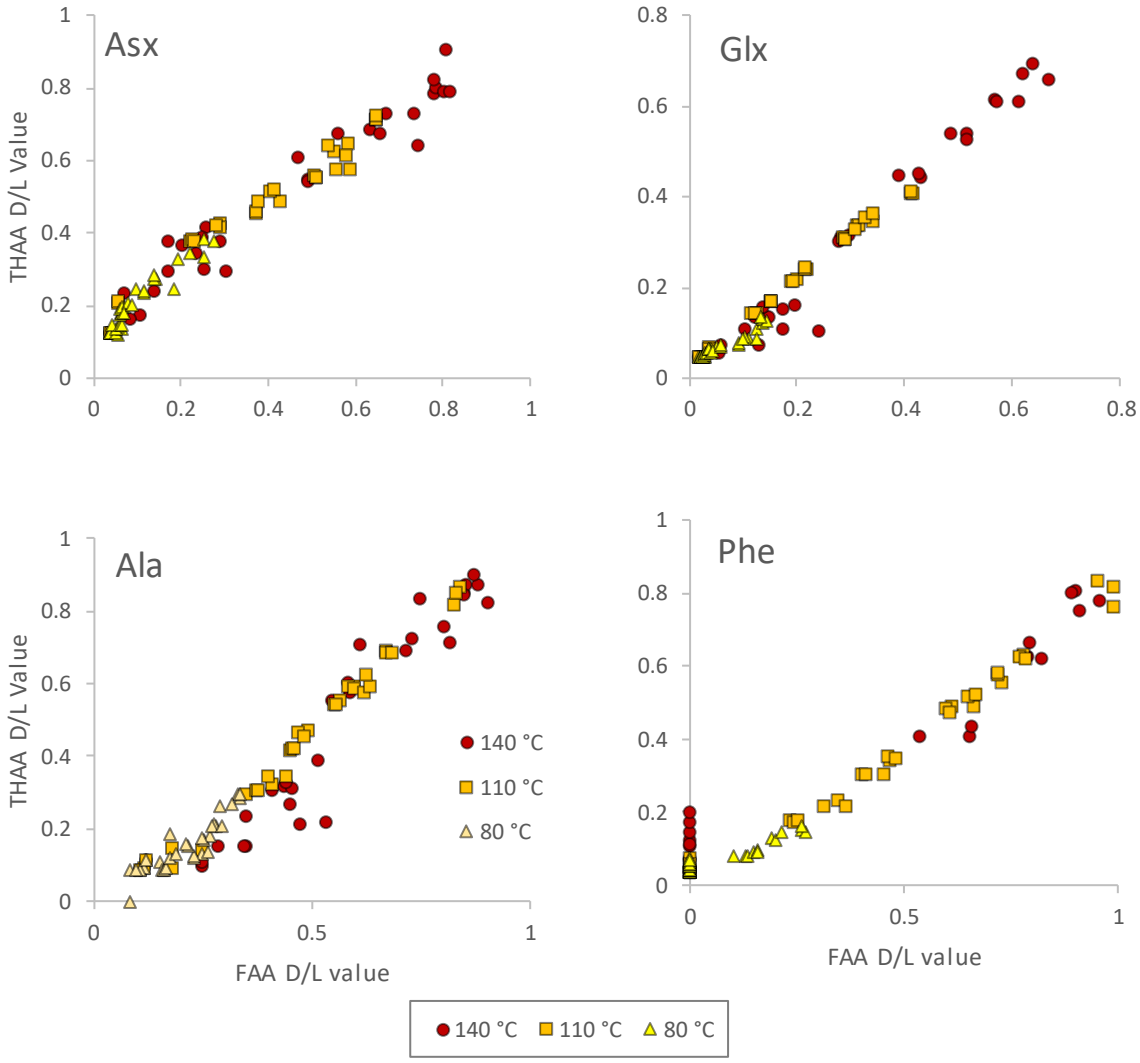

Figure 3.16. FAA D/L vs THAA D/L values for bleached enamel in 140 °C, 110 °C and 80 °C heating experiments for Asx (top left), Glx (top right), Ala (bottom left) and Phe (bottom right). Points plotted on the y-axis are due to concentration of the D isomer being below the limits of detection.

3.5.5. Intra-crystalline enamel amino acids: kinetic behaviour

Except for Ser, a predictable increase in the extent of racemization was observed in all the amino acids studied (Asx, Glx, Ala, Val and Phe) across the range of temperatures (80, 110 and 140 °C; Figure 3.17). The racemization of Ser increases rapidly and then falls to lower levels of racemization, which is linked to in-chain racemization and chemical instability of Ser respectively (Akiyama, 1980; Takahashi *et al*., 2010). This trend of Ser racemization in the intra-crystalline fraction has been observed in elevated temperature studies of other biominerals (Kaufman, 2000; Penkman, *et al*., 2008; Demarchi, *et al*., 2013c; Orem & Kaufman, 2011) and is supported by observations in the fossil record (Preece & Penkman, 2005).

The mechanism for the racemization of FAAs is thought to predominantly proceed by a carbanion intermediate. The electron-withdrawing and resonance stabilisation capabilities of the substituents attached to the α-carbon are the principal factors in determining the relative order of rates of racemization (Shou & Bada, 1980). However, in a biomineral, the complexity of peptide-bound amino acid diagenesis means that the primary sequence and the chemical environment can also influence relative rates of racemization (Collins *et al*., 1999). The observed relative order of the rates of racemization of FAAs in solution has been reported to be Asp > Phe > Ala > Glu > Val (Smith & Evans, 1980) and the heating experiments conducted on enamel in this study show broadly similar trends (Figure 3.17).

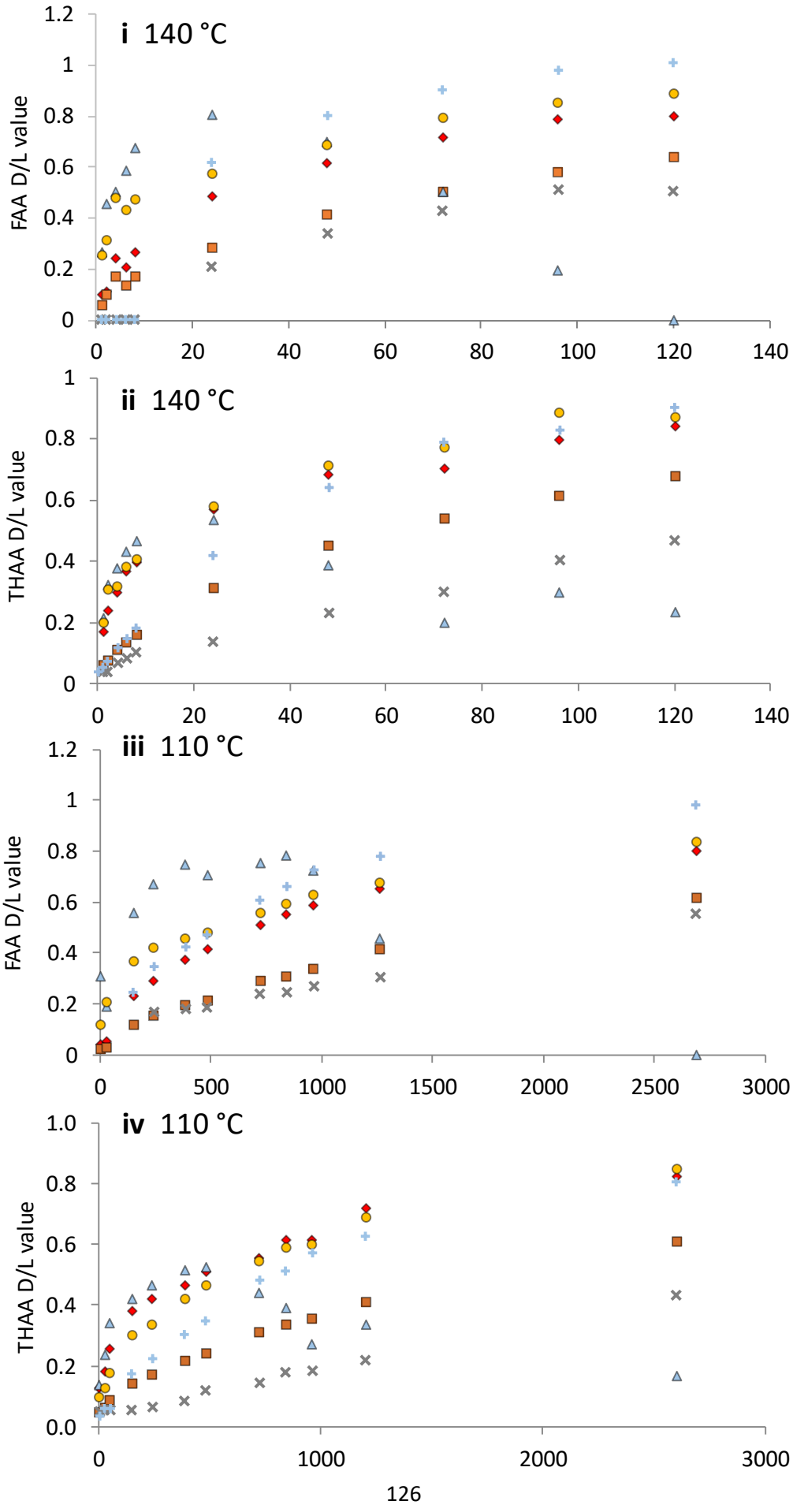
i 140 °C
FAA D/L value
1.2
1
0.8
0.6
0.4
0.2
0
0
20
40
60
80
100
120
140
ii 140 °C
THAA D/L value
1
0.8
0.6
0.4
0.2
0
0
20
40
60
80
100
120
140
iii 110 °C
FAA D/L value
1.2
1
0.8
0.6
0.4
0.2
0
0
500
1000
1500
2000
2500
3000
iv 110 °C
THAA D/L value
1.0
0.8
0.6
0.4
0.2
0.0
0
1000
2000
3000

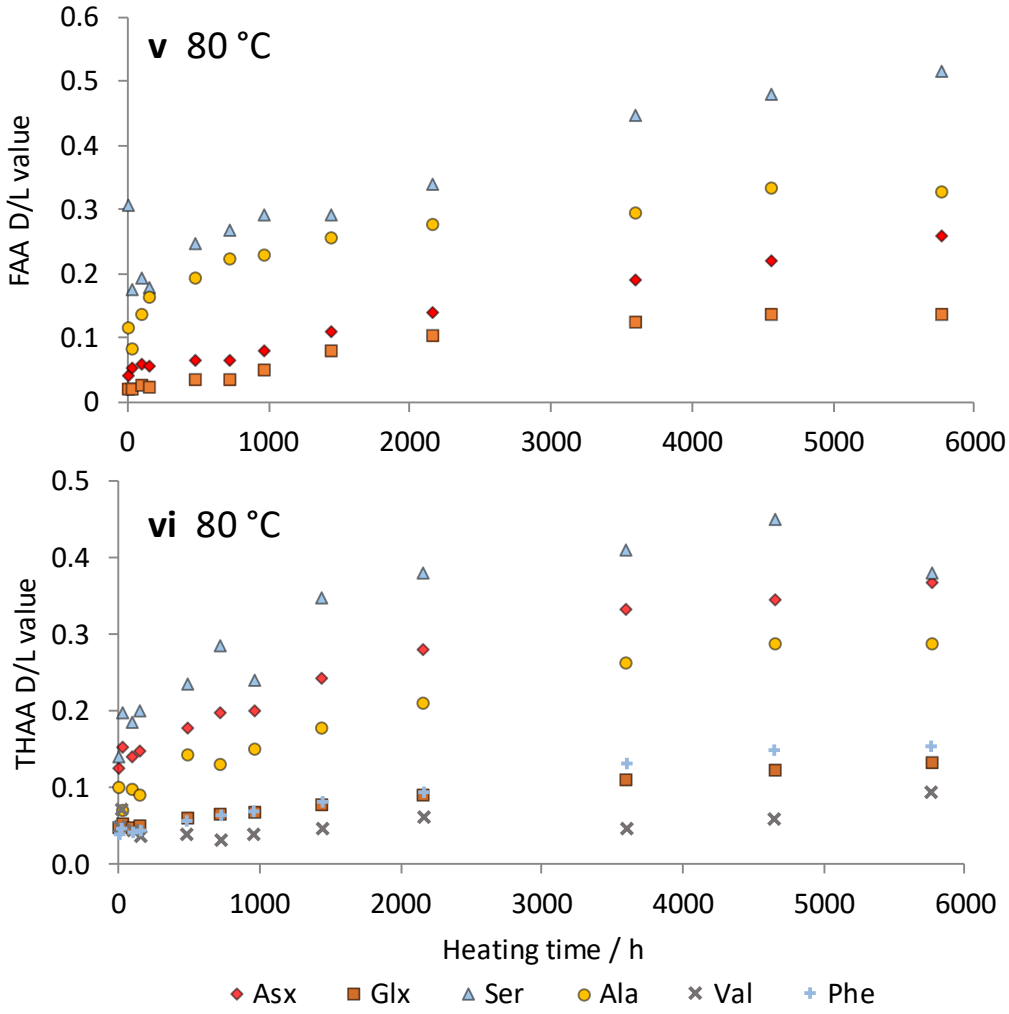

Figure 3.17. Extent of racemization of FAAs and THAAs in the intra-crystalline fraction of enamel during 140 (i & ii), 110 (iii & iv) and 80 (v & vi) °C elevated temperature experiments.

3.5.5.1. Calculation of reaction parameters using elevated-temperature data

The use of AAR as a tool for absolute age estimation requires the relationship between the age and extent of racemization to be described. This can be achieved through mathematically modelling accelerated degradation experiments, coupled with calibration using direct dating (e.g. radiometric dating) and/or indirect geochronological evidence from the same geographic region (Miller & Mangerud, 1985; Murray-Wallace & Bournman, 1990; Wehmiller *et al.*, 2013). Methods using high temperature experimental data assume that the mechanisms for racemization *in situ* are synonymous with the process occurring at elevated temperatures, which is not the case for all biominerals (Tomiak *et al.*, 2013). To mathematically describe the kinetic behaviour of enamel proteins, two models have been tested: reversible first order rate kinetics (RFOK) and constrained power law kinetics (CPK; Clarke and Murray-Wallace, 2006).

3.5.5.2. Reversible first order reaction kinetics (RFOK) to describe racemization in enamel

Racemization of FAAs is theoretically described by reversible first-order kinetics (RFOK), assuming no thermal decomposition of amino acids or additional side reactions (Bada & Schroeder, 1972; Shou & Bada, 1980). This behaviour has been shown to predict the racemization of aqueous FAAs relatively well (Bada & Schroeder, 1975; Smith and Reddy, 1989), but does not always accurately describe the intra-crystalline racemization of amino acids in biominerals (Penkman *et al*., 2008; Crisp *et al*., 2013; Tomiak *et al*., 2013). This is not unexpected, as the complexity of the inter- and intra- molecular interactions involved in the degradation of peptide-bound amino acids in biominerals would be highly unlikely to follow RFOK (Collins & Riley, 2000; Clarke & Murray-Wallace, 2006).

RFOK dictates that:

$$Ln\left(\frac{1+D/L}{1-D/L}\right)+constant=2kt$$

Equation 4. Where k *is the rate of racemization and is equal in both the forward and backward reaction, and* t *is time.*

If ln{(1+D/L)/(1-D/L)} has a linear relationship with time, then the mechanism for racemization can be described by RFOK. The strength of the correlation has been assessed based on coefficient of determination values (R^2). To model RFOK in fossil biominerals, Crisp *et al*. (2013) suggested excluding data that yielded R^2 values < 0.97, as it was not appropriate to linearize the data below this grade of correlation. When including the full range of time points for enamel, the R^2 values for most of the plots was < 0.97, even when restricted ranges of D/L were used (Table 3.5). The amino acids with the highest conformity to RFOK were Glx and Phe (Table 3.5; Figure 3.18). Val also yielded correlations higher than the 0.97 threshold for heating experiments run at 110 and 140 °C, but not for 80 °C. The rate of racemization of Val in enamel is very slow and thus the extent of racemization observed within the time frame of the 80 °C experiment was not long enough to acquire a high degree of correlation.

The plot of ln[(1+D/L)/(1-D/L)] vs. t for Asx exhibits two D/L ranges which can be linearised with dissimilar gradients and therefore kinetic behaviours (Figure 3.18; Table 3.5). This lack of conformity to RFOK is likely to be a consequence of the complex nature of Asx racemization, which is a composite signal encompassing both aspartic acid and asparagine (Glx is also a composite signal).

Table 3.5. R^2 values from the plot between the transformed D/L values against time, constrained D/L ranges have been used to optimise correlation. R^2 values test for conformity to RFOK.

	140 °C		110 °C		80 °C	
Amino acid	D/L range	R^2	D/L range	R^2	D/L range	R^2
Asx	0.13 – 0.38	0.9826	0.38 – 0.72	0.9514	0.14 – 0.29	0.9682
Glx	0.05 – 0.69	0.9738	0.05 – 0.61	0.9763	0.05 – 0.14	0.9629
Ala	0.09 – 0.91	0.9019	0.16 – 0.69	0.9735	0.09 – 0.30	0.9050
Phe	0.04 – 0.90	0.9762	0.04 – 0.63	0.9888	0.04 – 0.16	0.9606
Val	0.03 – 0.51	0.9740	0.03 – 0.45	0.9841	0.03 – 0.09	0.7889

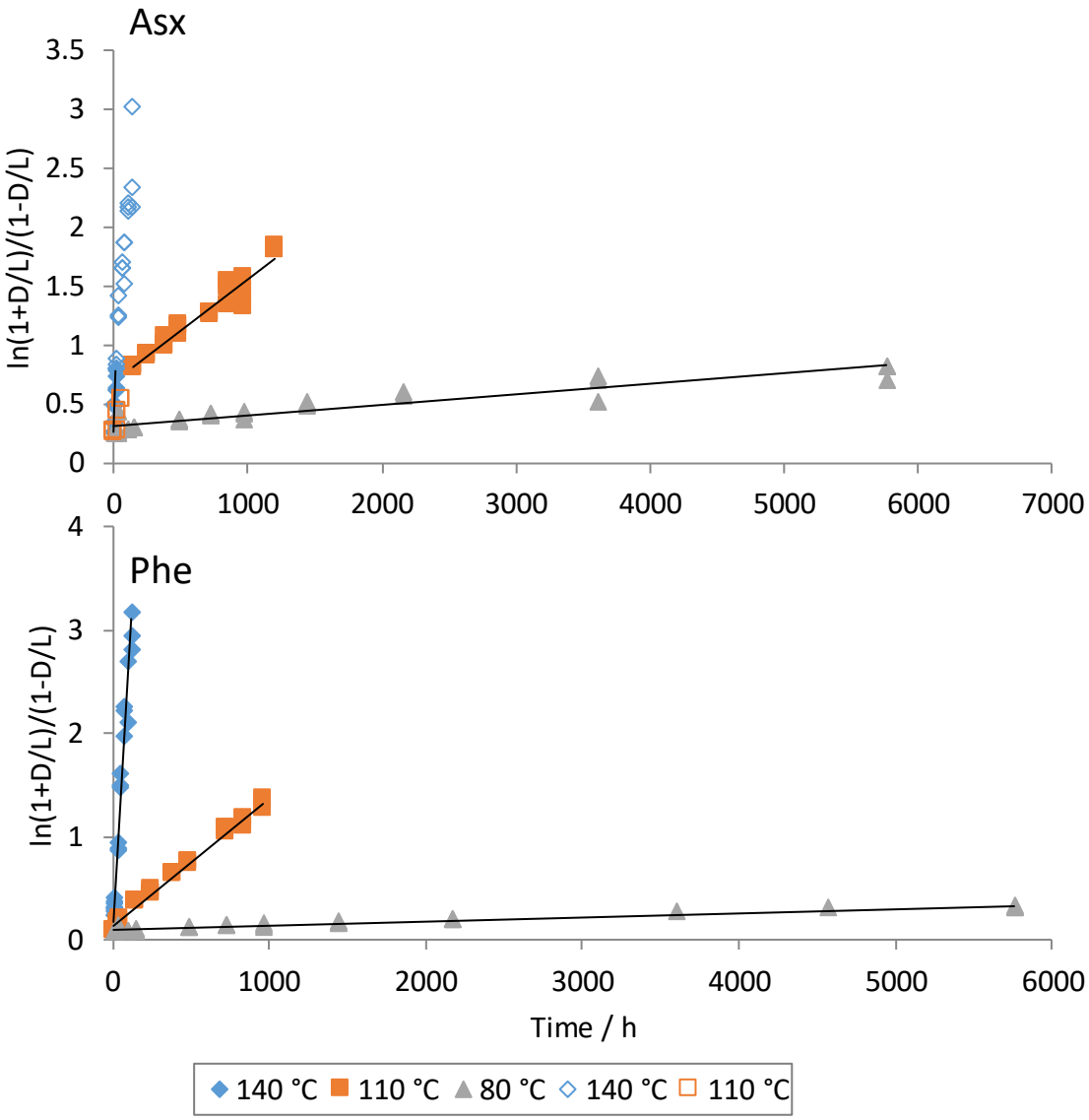

Figure 3.18. Transformed D/L data on increasing heating time at three different temperatures. Linearity of the plot indicates adherence to RFOK; an R^2 cut-off of 0.97 is used in this study. The gradient is proportional to the rate of reaction. Block colour data points were used to calculate rates and assess correlation. Outlined data points were not used to calculate the rates of reactions as they reduced the strength of the correlation.

3.5.5.3. Constrained power-law kinetics (CPK) to describe racemization in enamel

The lack of adherence between RFOK and heating experiments in other biominerals has led to the use of alternative, experimentally derived functions to describe amino acid racemization (e.g. Manley *et al.*, 2000; Kaufman *et al.*, 2000; Clarke & Wallace 2006; Allen *et al.*, 2013; Crisp *et al.*, 2013; Tomiak *et al.*, 2013). Constrained power-law kinetics (CPK) can be used to improve the description of a trend by raising one of the terms to a power

(Equation 5). This power (n) is varied to maximise the R^2 value and thus improve the mathematical description of the trend (e.g. Figure 3.19). CPK has been used with the most success to better describe the racemization of Asx and Glx (Kaufman, 2000, Manley *et al*., 2000; Crisp *et al*., 2013).

$$Ln\left(\frac{1 + D/L}{1 - D/L}\right)^{n} + constant = 2kt$$

Equation 5*:* k *is the rate of racemization and is equal in both the forward and backward reaction,* t *is time and n is varied to improve the description of the relationship between D/L and time.*

The use of CPK can better describe the rate of racemization in enamel for most of the amino acids at a specific temperature (Table 3.6). However, for most amino acids there is little concordance between the optimised power values the transformed D/L value are raised to at each of the different temperatures. For example, the optimum value of n to maximise the linear fit of Phe using CPK at 140 and 110 °C is 1.2 and for 80 °C is 1.7 (Figure 3.19). This indicates that across different D/L value ranges/temperatures the data are exhibiting a different relationship between transformed D/L value and time. This lack of coherence between temperatures indicates that trend fitting in this way may not be appropriate for most amino acids in enamel.

Table 3.6. R^2 values from the plot between the transformed D/L values against time; constrained D/L ranges have been used to optimise correlation. R^2 values test for conformity to CPK at the specified value of n. Values in bold signify the highest R^2 for that temperature and specific amino acid.

		140 °C		110 °C		80 °C	
Amino acid	n	D/L range	R^2	D/L range	R^2	D/L range	R^2
Asx	0.3	0.13 – 0.38	0.9569	0.38 – 0.72	**0.9555**	0.14 – 0.29	0.9496
Asx	1.5	0.13 – 0.38	**0.9881**	0.38 – 0.72	0.9326	0.14 – 0.29	0.9745
Asx	1.8	0.13 – 0.38	0.9863	0.38 – 0.72	0.9205	0.14 – 0.29	**0.9755**
Glx	1.7	0.05 – 0.69	**0.9972**	0.05 – 0.61	**0.9972**	0.05 – 0.17	**0.9787**
Ala	1.1	0.09 – 0.95	**0.9140**	0.16 – 0.69	0.9779	0.09 – 0.30	0.9117
Ala	1.5	0.09 – 0.95	0.9434	0.16 – 0.69	**0.9858**	0.09 – 0.30	0.9329
Ala	2.2	0.09 – 0.95	0.9441	0.16 – 0.69	0.9699	0.09 – 0.30	**0.9479**
Phe	1.3	0.04 – 0.90	**0.9816**	0.04 – 0.63	**0.9945**	0.04 – 0.16	0.9728
Phe	1.7	0.04 – 0.90	0.9689	0.04 – 0.63	0.9849	0.04 – 0.16	**0.9780**

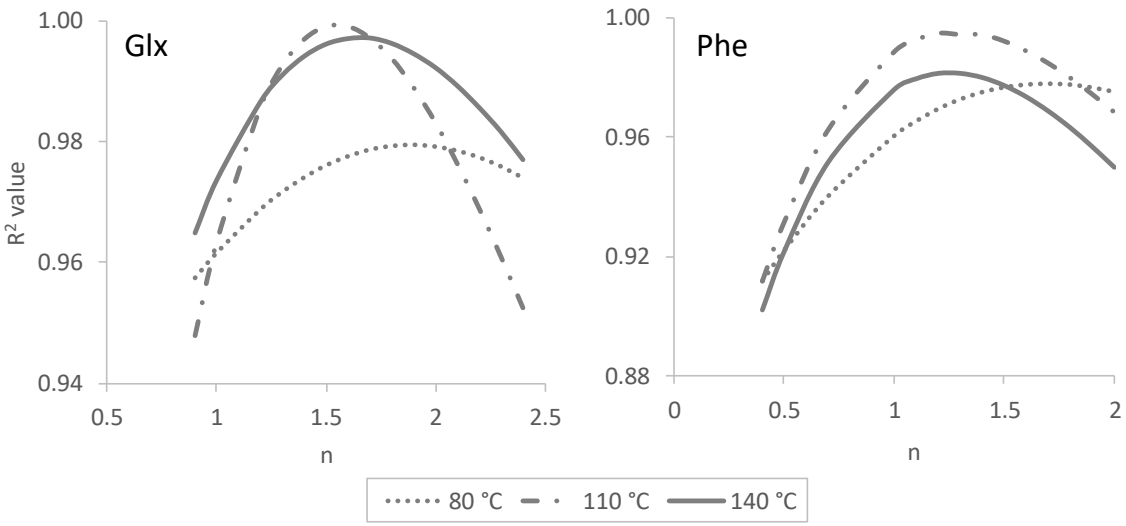

Figure 3.19. R^2 values for the three different temperature heating experiments when D/L values are transformed using CPK. R^2 values have been plotted against the power (n) ln{(1+D/L)/(1-D/L)} has been raised to (Equation 5).

3.5.5.4. Arrhenius parameters

The calculated rate constants at the various temperatures can be used to determine kinetic parameters using the Arrhenius equation (Equation 6). This calculation is reliant on accurate calculated rates of racemization and assumes a consistent mechanism for racemization across the studied range of D/L values and temperatures.

$$k = A\, e^{-E_a/RT}$$

Equation 6: k is the rate constant, A is the frequency factor, E_a is the activation energy, R is the gas constant and T is the temperature.

Table 3.7. Activation energies, frequency factors (A) and Arrhenius plot R^2 values for the four studied amino acids. Ranges and R^2 values for the RFOK and CPK data used are shown in Table 3.5 & Table 3.6 respectively.

Amino acid	Model	Arrhenius plot R^2 value	E_a / kJ mol^{-1}	ln(A)
Asx	RFOK	0.9790	121	25.7
Glx	RFOK	0.9984	123	30.7
Glx	CPK	0.9999	143	37.1
Ala	RFOK	0.9882	109	27.1
Phe	RFOK	0.9998	128	33.1

In contrast to the other amino acids studied, the R^2 values for Glx can roughly be optimised using CPK (n = 1.7), yielding a good linear relationship between the transformed D/L values and heating time between 0.05 – 0.69 D/L values (Table 3.6). Some of the kinetic

parameters of the degradation of Glx have therefore been calculated and methods for trend fitting have been compared to assess the potential for using high temperature studies to estimate absolute age and palaeotemperature reconstruction with enamel AAR.

The activation energy for racemisation for Glx calculated using a CPK method for ostrich eggshell was 147 kJ mol^{-1} (Crisp *et al*., 2013) and *Patella vulgata* was 141 kJ mol^{-1} (Demarchi *et al*., 2013c), compared to 123 kJ mol^{-1} using RFOK and 143 kJ mol^{-1} using CPK for enamel. The activation energies for different biominerals are likely to be diverse, so it is not surprising that the value calculated for enamel would be different to those of ostrich eggshell and *Patella vulgata*. The divergence in the values between the models for enamel are significant however; it is therefore difficult to assess the true value for the activation energy.

3.5.5.5. Palaeothermometry using Glx

The relationship between rate of racemization and ambient temperature of the reaction medium (T_{eff}) can be extrapolated to the burial environment provided the kinetics of the racemization reaction and temperature sensitivity of the rate constants are known (Miller *et al*., 1983; Oches *et al*., 1996). To highlight the sensitivity and importance of the choice of mathematical model for estimating kinetic parameters, 13 proboscidean enamel samples with well constrained temporal assignments from the UK, plus a modern Asian elephant tooth (*E. maximus*), have been used to estimate the ambient temperature of the reaction medium (T_{eff}) in the UK over the last 2 Ma using RFOK (Figure 3.20) and CPK. Using RFOK, T_{eff} is calculated to be -10 °C and using a CPK model T_{eff} is 1 °C (Figure 3.21). These predicted temperatures are unlikely; comparable experimental data and palaeoclimatic data indicate ranges of 8-10 °C are more realistic (BGS report, 2011). Not only is there a significant discrepancy between the temperatures obtained using the different models, the absolute values indicate that the assumption of similar kinetics over these temperature ranges may not be valid.

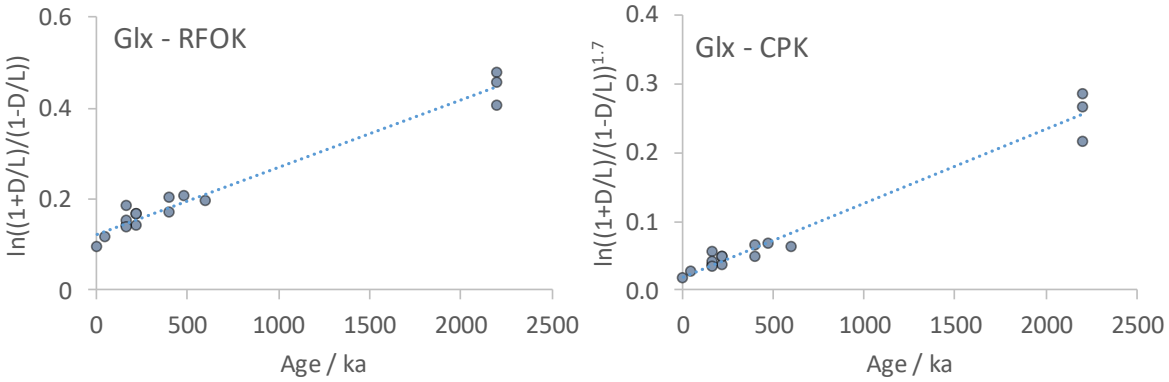

Figure 3.20. Linearised relationship between age of fossil enamel from UK sites and transformed D/L value assuming RFOK (left) and CPK (right). Gradient of the liner trend is proportional to the rate of racemization.

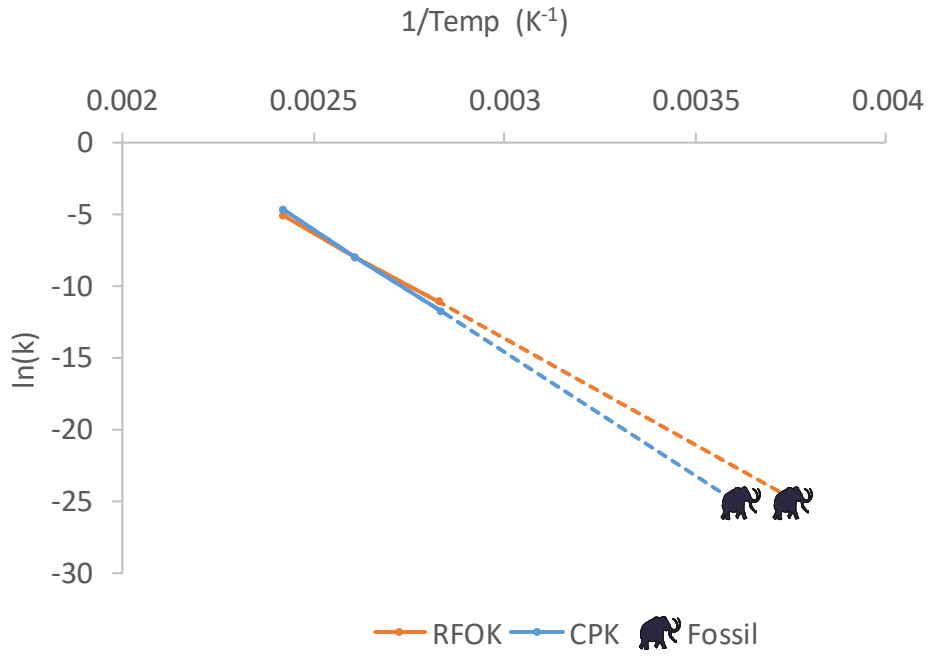

Figure 3.21. Arrhenius plot used to calculate the activation energies using RFOK and CPK. Effective temperatures of the fossil UK samples have been calculated using each of the models using the rate of reaction of enamel fossil material.

3.5.5.6. Enamel fossil data and comparison to Bithynia opercula heated experiments

To understand the kinetics in more detail, the patterns of racemization in enamel were compared to those obtained from *Bithynia* opercula, using both fossil samples and elevated temperature experimental data. The extent of racemization in fossil proboscidean enamel increases with independent evidence of age but is considerably lower than in *Bithynia* opercula when compared to samples from the same deposits (Figure 3.22). The lower rates

of racemisation in enamel (cf. *Bithynia*) suggest that the enamel AAR may be able to be used as a relative dating technique over longer time scales than *Bithynia.* *H*owever, this will likely be balanced by a lower temporal resolution due to the slower rates yielding smaller incremental changes over time.

The rates of racemization are very similar between the two biominerals in the elevated-temperature experiments (Figure 3.23). This indicates that the rates of racemization in enamel and opercula are not behaving in comparable ways at elevated temperatures and in the depositional environment. The lack of consistency between the two data sets indicates these elevated temperature experiments do not fully describe the degradation mechanisms in the depositional environment for enamel. If the rates of reaction calculated in elevated temperatures are not appropriate for extrapolation to the burial environment, then irrespective of how accurately a mathematical model is describing those rates, derivation of absolute age using kinetic parameters is inappropriate.

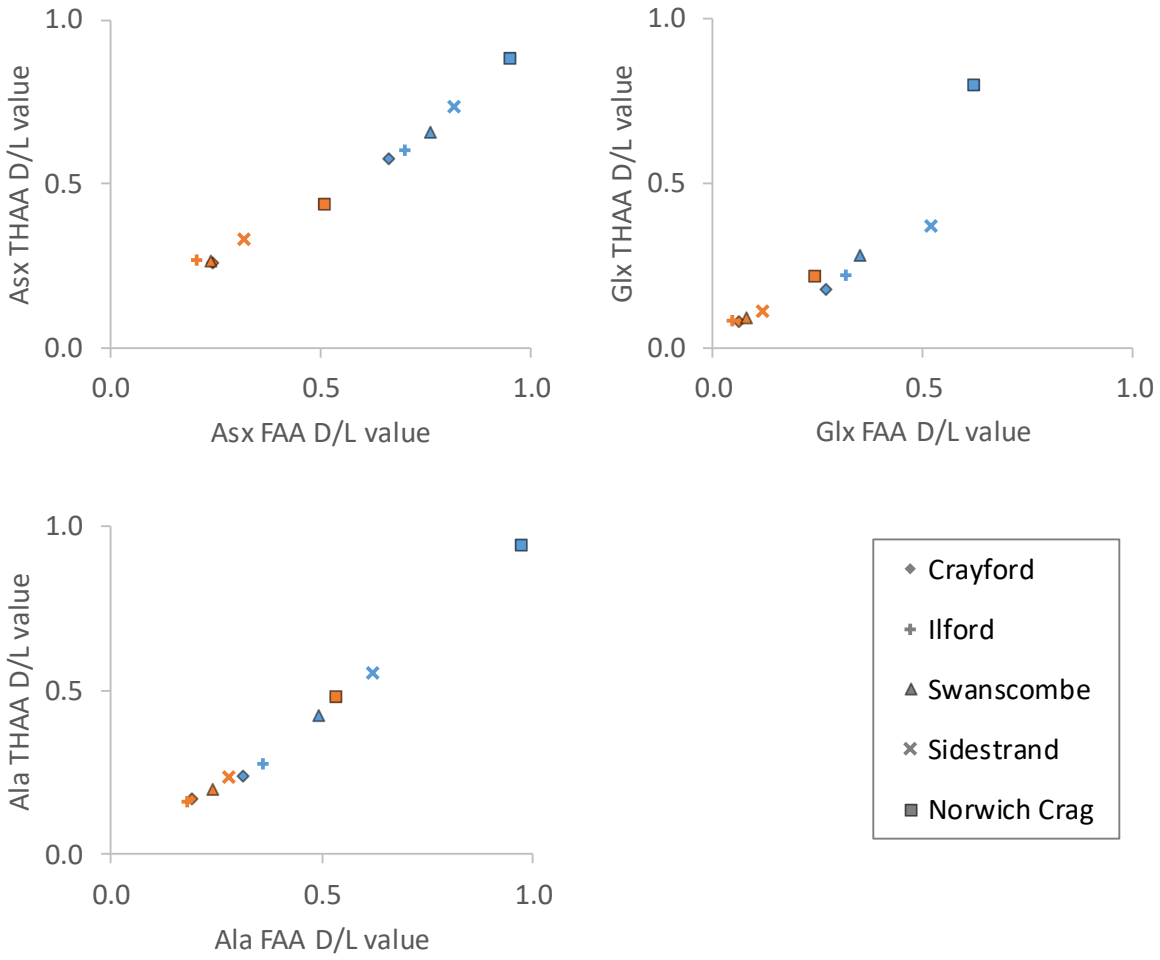

Figure 3.22. Extent of racemisation in fossil enamel (orange) and Bithynia *opercula (blue) IcPD from a range of UK sites. Sites have been selected to give a broad range of ages spanning the Quaternary.*

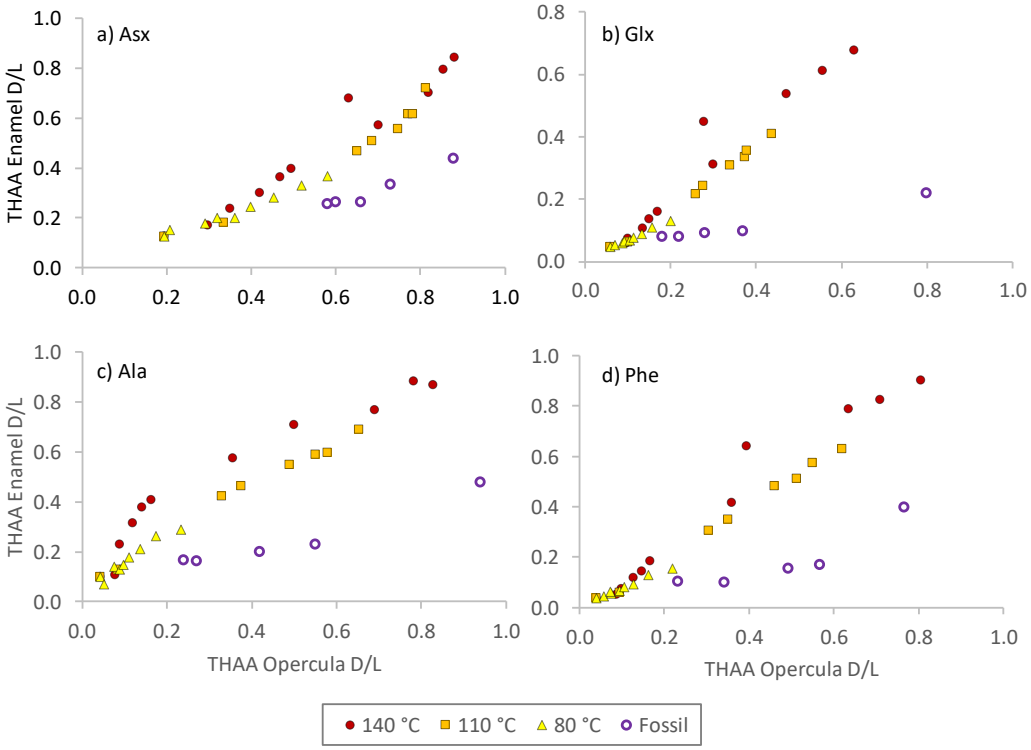

Figure 3.23. Extents of THAA racemization in proboscidean enamel plotted against Bithynia *opercula values for both elevated temperature experiments at 140, 110 and 80 °C (blue, orange and grey respectively), and for fossil data from sites where both opercula and enamel could be compared. Opercula elevated temperature data points have been plotted against their equivalent time point from the enamel study (at the same temperature).*

3.6. Conclusions

A simple protocol for amino acid analysis of enamel has been developed, involving a biphasic separation of the inorganic species (originating from the mineral matrix) from the amino acids. This enables the routine analysis of fossil enamel proteins via a RP-HPLC method. Crucially the method does not greatly influence the amino acid composition and does not alter the amino acid D/L values.

A fraction of amino acids, stable to prolonged exposure to a strong oxidant has been isolated (ca. 72 h exposure to NaOCl) and has been shown to exhibit effectively closed system behaviour during simulated degradation experiments. Only minimal leaching of amino acids into the supernatant water was observed during diagenetic experiments (ca. 5%), and at least part of that total is due to the presence of small crystals of enamel suspended in solution.

Elevated temperature studies have shown that enamel intra-crystalline amino acids follow predictable trends of racemization and breakdown, but the divergence with patterns

observed in fossil enamel indicate that different mechanisms are prevailing at lower diagenetic temperatures. This therefore limits the ability to use high temperature experiments to calculate relevant kinetic parameters. However, the predictability of the diagenetic behaviour of enamel amino acids in both the fossil and elevated temperature experiments, indicate that analysis of the intra-crystalline protein fraction of enamel is suitable for amino acid geochronology over Quaternary timescales.

In conclusion, we present here a new preparative method for the routine analysis of closed system amino acids from fossil enamel. The application of this technique has the potential to be able to build geochronologies on the order of millions of years' time scales and therefore to directly estimate the age of material where there previously has not been an applicable technique.

Chapter 4: Direct aminostratigraphic dating of Elephantidae enamel from UK deposits

4.1. Overview of the chapter

This chapter describes work aiming to assess if enamel IcPD can be used as a geochronological tool. To achieve this, the potential effects of intra-tooth amino acid heterogeneity on D/L values will be explored, focusing on *in vivo* racemisation as a potential source of the heterogeneity. This chapter also presents a UK Proboscidean geochronology using the IcPD patterns in enamel. This work focused on using samples from sites with well constrained chronologies to provide a template on which to test the enamel geochronology.

4.2. Intra-tooth variability

AAR dating depends on the natural bias towards one chiral form of amino acids in living organisms (L-form). Biotic proteins are replaced and maintained during the course of an organism's lifetime and thus the dominance of the L-amino acid is maintained. However, once tooth enamel reaches maturity, there is no replacement of proteins (Hillson, 2005) and as such, any racemisation products that form are retained if a closed system is present (Collins *et al*., 1999). An individual Elephantid tooth can be in the mouth for 30+ years and, whist alive, the temperature inside the oral cavity is ~35 °C, leading to *in vivo* protein degradation. This property has been utilised in the forensics of human teeth for age-at-death estimations (Helfman & Bada, 1975; Griffin *et al*., 2008; Timme *et al*., 2017) but may present a challenge when assessing the AAR rates in fossil enamel for building a geochronology. However, these changes are likely to only affect the faster racemising amino acids such as aspartic acid.

Elephantidae teeth are composed of a series of enamel folds surrounding a dentine core. Elephantids can grow six sets of molariform teeth in each quadrant of the mouth over the course of their lifetime, with each set of teeth taking a different length of time to fully mature (Laws, 1966; Shoshani, 1996). Elephantidae teeth are deciduous and are referred to as M1 to M6 in order of development (Laws, 1966). Elephantid teeth form in the back of the jaw, moving each enamel fold forward and pushing the previous tooth out (with the exception of M1 plates). Therefore, the enamel folds at the anterior of the tooth have

spent longer in the mouth than those at the posterior (Hillson, 2005). Elephantidae enamel plates develop from the occlusal enamel-dentine junction and grow downwards towards the basal region (Shoshani, 1996). Once formed, the enamel begins to mature, becoming thicker and denser (Metcalfe *et al*., 2010). Intra-tooth variability has been observed in the protein concentration of dentine from bovine mandibles, with lower concentrations in the root of the tooth when compared to the middle and crown (Procopio *et al*., 2018).Samples from different sections of a *M. primigenius* tooth were analysed for their D/L values to evaluate the intra-tooth IcPD variability. Replicate preparative analysis enabled estimations of the standard deviation in amino acid concentrations and D/L values to be obtained.

4.2.1. Intra-tooth variation sampling

Six enamel chips were taken from different locations (Figure 4.1) on a single *M. primigenius* tooth from the Thorpe sand and gravel deposits at Tattershall (Section 4.3.1.4.3), a site correlated with MIS 6 based on biostratigraphy (Holyoak & Preece, 1985; White *et al*., 2010). Locations were targeted to represent areas that might have different extents of *in vivo* racemisation due to disparities between their times of formation.

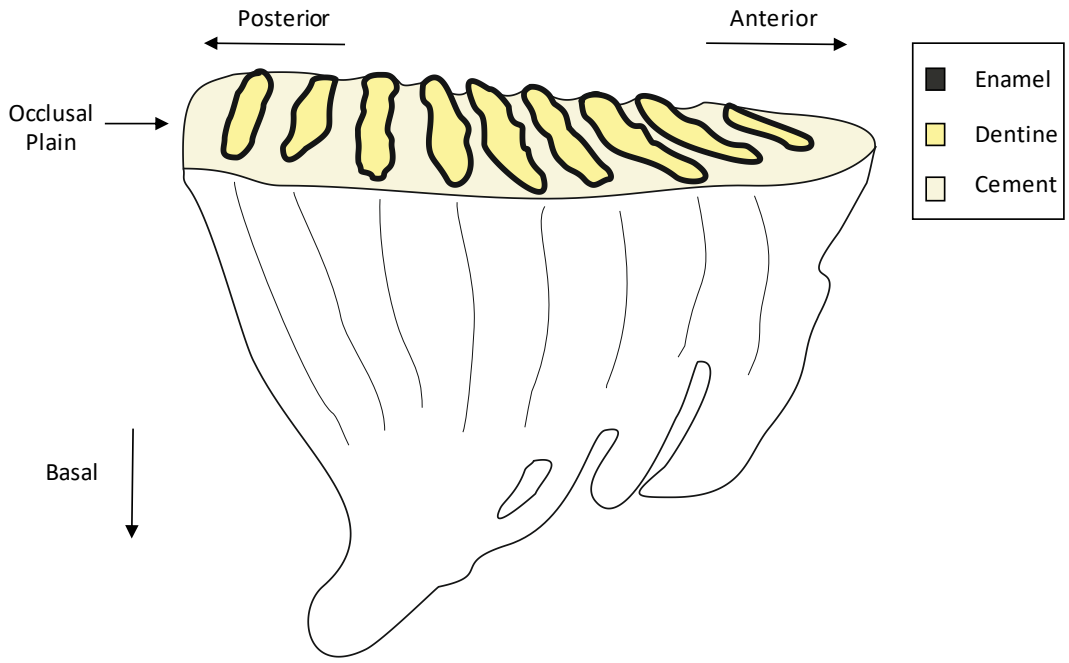

Figure 4.1. Diagram of a mammoth tooth, highlighting some of the key dental components.

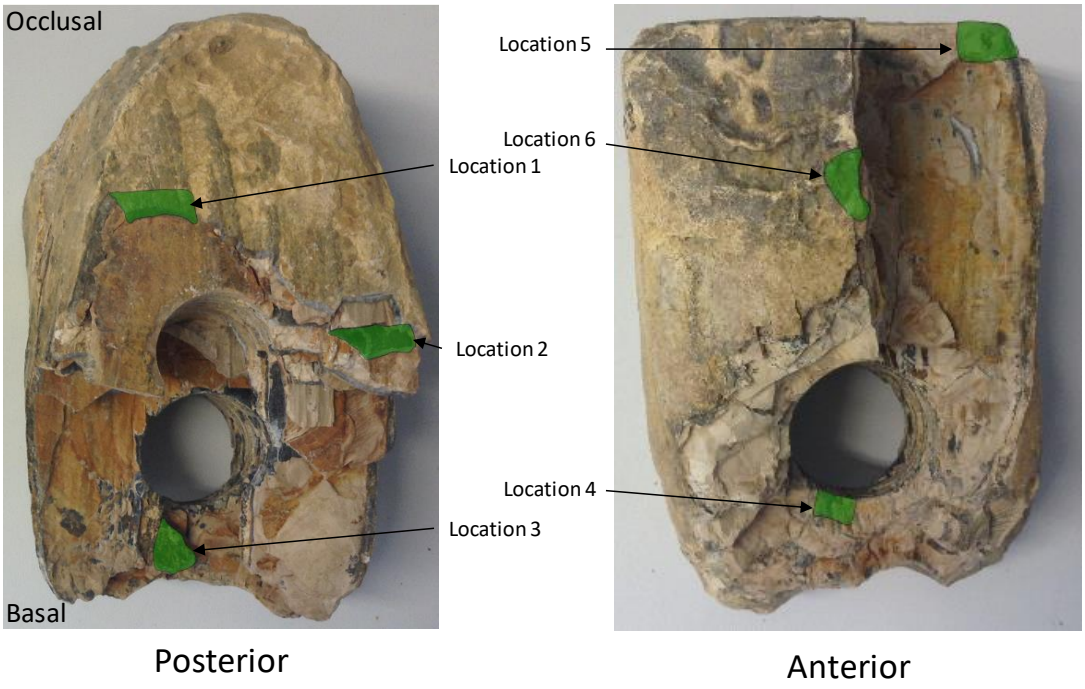

Figure 4.2. Sampling locations from the M. primigenius *tooth from the Thorpe sand and gravel deposits at Tattershall. Images were taken prior to removal of the enamel chips and the green areas indicate where enamel chips were removed. The large circular hole cut through the middle of the tooth was previously cut for ESR dating.*

Table 4.1. Sampling locations of the M. primigenius *tooth from the Thorpe sand and gravel deposits at Tattershall. Plate number starts from the anterior side (younger). *a and p denote the anterior (a) and posterior (p) sides of the plate.*

Code	Location	Lateral position	*Plate number	Distance from occlusal plane / cm	
PH1	1	Posterior	1a	4.5	(halfway)
PH2	2	Posterior	1p	6.5	(halfway)
MB3	3	Middle	5a	12.0	(basal)
AB4	4	Anterior	7a	10.5	(basal)
AO5	5	Anterior	8a	0.5	(occlusal)
AH6	6	Anterior	11p	3.0	(basal)

Enamel chips were bleached and prepared using a biphasic separation method according to the standard protocols outlined in Chapter 3 (Section 3.2). Amino acid analysis was conducted using RP-HPLC according to the protocol outlined in section 3.2.5. Analysis of each chip was conducted in preparative triplicate.

4.2.2. Overall intra-tooth AAR variation

The overall precision, including intra-tooth variability, is highly dependent on the amino acid studied (Figure 4.3). Glx and Phe have the highest precision and are therefore likely to yield a greater resolution across their respective time ranges when applied to geochronology. Asx, Ala and Val are also considered good candidates for AAR dating due to their predictable patterns of IcPD (Penkman *et al*., 2011; 2013). The overall levels of variability of Asx and Ala do not preclude their application to AAR geochronology but may hamper the temporal resolution. In contrast, the large variability observed for Val is likely to greatly impact on the temporal resolution of enamel AAR geochronology and therefore further investigations into the causes of this variability would need to be conducted to enable this amino acid to be used for geochronological applications. Ser and Arg do not racemise predictably in the geological context due their instability, and thus are not used in geochronology (Vallentyne, 1964).

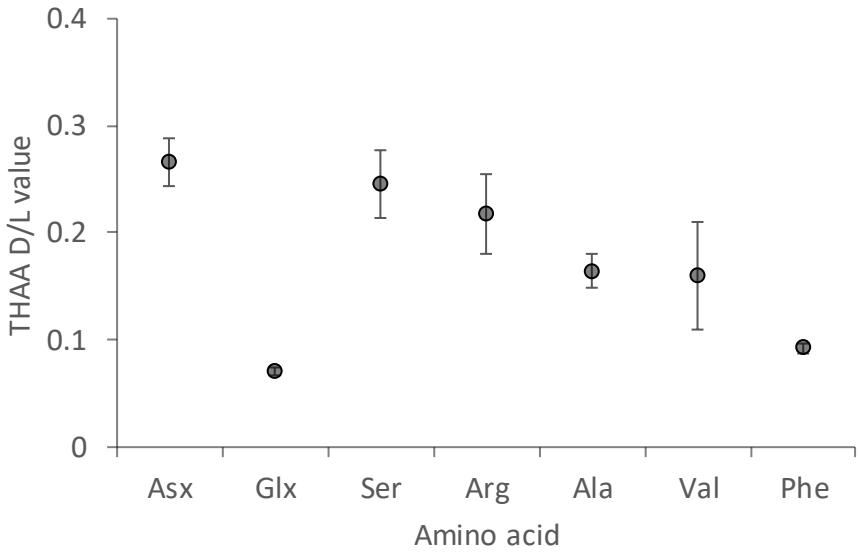

Figure 4.3. Mean THAA D/L values across all six sampling locations intra-tooth, error bars depict one standard deviation about the mean.

The intra-sample variability has been compared to the variability between the six sampling locations (Table 4.2) to evaluate which amino acids exhibit greater variability between sample locations than would be intrinsically expected within a single sample. Asx has the greatest difference between intra-sample and intra-tooth variability, whilst Phe exhibits no notable additional variability between sample locations (Table 4.2). The intra-tooth variability for Glx is small (~5%) and is likely to be negligible when placed within the context

of its application to AAR geochronology (Figure 4.3). The intra-tooth variability observed for Asx could be due to differences in *in vivo* racemisation.

Table 4.2. Intra-tooth and intra-sample standard deviations for amino acid D/L values. An estimation of the analytical variability (calculated from replicate analysis of reference solutions) has been included for comparison. Intra-tooth standard deviations greater than either twice the analytical or intra-sample variability are highlighted in bold.

	FAA			THAA			Amino acid reference
	D/L value	Intra-sample (1σ)	Intra-tooth (1σ)	D/L value	Intra-sample (1σ)	Intra-tooth (1σ)	Analytical (1σ)
Asx	0.216	0.007	**0.038**	0.267	0.005	**0.026**	0.013
Glx	0.111	0.113	0.152	0.069	0.001	0.004	0.010
Ala	0.181	0.012	0.021	0.164	0.009	0.014	0.001
Phe	0.165	0.010	0.010	0.092	0.005	0.003	0.026

4.2.3. Lateral and vertical variation in D/L value

The precision of data may be improved by controlling the variables accounting for intra-tooth variability. This could be achieved by avoiding certain sample areas known to give lower precision, or by consistently sampling from a single region of a tooth. The extent of racemisation in an Elephantidae tooth would be expected to increase from the posterior to the anterior due to increased time spent in the oral cavity when the animal was alive. However, it is anticipated that the *in vivo* racemisation caused by this difference would be minor and thus below the limits of detection. Asx is a relatively fast racemising amino acid in mature enamel (Chapter 3) and thus is likely to be the most sensitive indicator of *in vivo* racemisation (Helfman & Bada, 1975). No significant trend was observed in THAA D/L values when compared to plate number in the *M. primigenius* tooth from the Thorpe sand and gravel at Tattershall (e.g. Asx: Coefficient=0.003, P=0.058; Figure 4.4). This supports the expectation that lateral differences in *in vivo* racemisation are below the limits of detection for this technique.

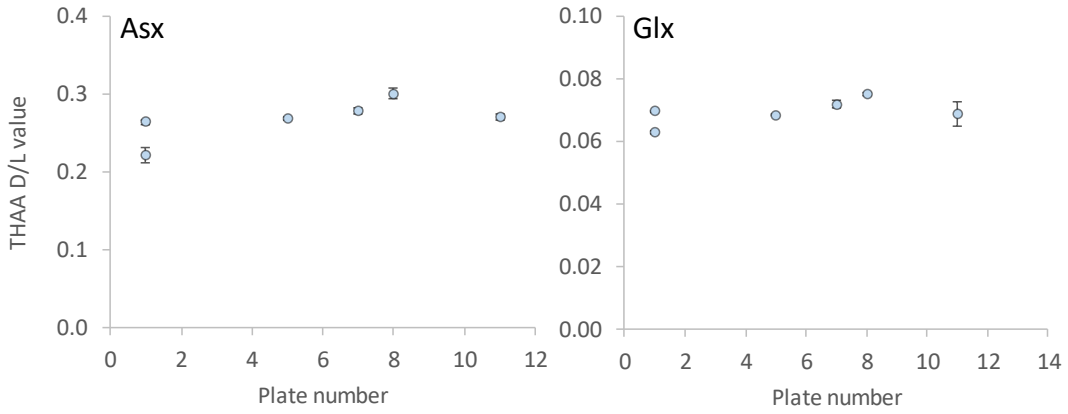

Figure 4.4. Extent of Asx (left) and Glx (right) THAA racemisation in different enamel plates. Plate numbers are counted consecutively starting from the posterior. Error bars depict one standard deviation about the mean.

The extent of racemisation may also be expected to decrease with vertical distance from the occlusal plan, in addition to lateral differences. The enamel closer to the occlusal plane develops first and grows downwards towards the root of the tooth (Hillson, 2005). The maturation processes occurring in enamel may also mean that the enamel that has spent longer *in vivo,* may be at a different stage of development, which may impact the rates of racemisation both *in vivo* and in the burial environment. The extents of racemisation

observed in this study have found no significant correlation between vertical distance from the occlusal plane and extent of racemisation of the studied amino acids (P values > 0.05; Figure 4.5).

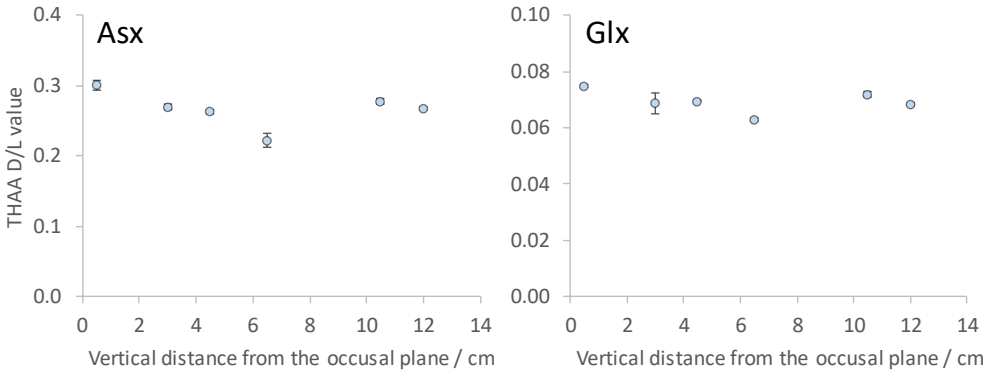

Figure 4.5. Asx THAA D/L values with vertical distance from the occlusal plane. Error bars depict one standard deviation about the mean.

4.2.4. Intra-tooth amino acid composition

The rate of amino acid racemisation in fossil biominerals is dependent on the primary amino acid sequence (Kriausakul & Mitterer, 1978); as such, differences in the amino acid composition may correlate with differences in amino acid D/L values and help explain the lack of homogeneity of intra-tooth Asx D/L values. However, the amino acid compositions of the six sampling locations are similar and therefore do not account for the intra-tooth D/L variability.

The mammoth tooth analysed in this set of experiments was heterogenous with respect to the extent of Asx racemisation. However, the extent of racemisation between sample locations did not correlate with latitudinal nor vertical position. Therefore, reasons for the heterogeneity maybe more complex than initially expected and factors other than *in vivo* racemisation may be influencing the extent of IcPD. Intra-tooth variability is expected reduce the precision (and thus the temporal resolution) of Asx AAR relative dating. However, the levels of variability are low enough for Asx to still be useful for relative dating comparisons.

Table 4.3. Percentage amino acid compositions from six sampling locations taken from a M. primigenius *tooth from the Thorpe sand and gravel deposits at Tattershall.*

Sample location	Percentage composition												
	Asx	Glx	Ser	L-Thr	L-His	Gly	Arg	Ala	Tyr	Val	Phe	Leu	Ile
1	8	18	5	5	3	27	4	5	1	6	5	11	4
2	8	17	4	4	6	26	3	5	1	6	5	11	5
3	8	17	4	4	5	27	4	4	1	6	5	11	5
4	8	17	4	4	3	25	3	5	2	7	5	11	5
5	8	17	4	4	4	26	4	5	2	6	5	11	5
6	8	18	4	4	2	25	4	4	1	7	6	12	5

4.3. Enamel IcPD geochronology

Once synthesised by an organism, proteins and their constituent amino acids break down through a series of complex biochemical reactions. Geochronologies based on protein breakdown have demonstrated a strong correlation between IcPD and age (e.g. Penkman *et al*., 2011; 2013). For each new biomineral application of AAR-based chronology, the biomineral must first be independently tested. Most of the enamel analysed in this study was from deposits thought to have been laid down during the Pleistocene, and thus most of the sites have been dated based on: radiocarbon (up to ~ 50 ka), U-series, electron spin resonance dating, optically stimulated luminescence and biostratigraphical comparisons. Crucially, some of the oldest material in this study can only broadly be assigned to large time periods, highlighting the need for the development of a direct dating method. A description of each of the sites (in age order) with the relevant independent evidence of age is discussed, along with a brief assessment of the racemisation values. Most of the samples analysed in this study are from the British Geological Survey (BGS) and their collection reference number is quoted in square brackets. Several different species of Proboscidean were present in the UK during the Quaternary and no single species is ubiquitous, therefore, a variety of species from this single family have been analysed. A few sites contain multiple species of Proboscidean and thus have been used to test if substantial taxonomic effects can be detected.

All samples were prepared using the methods outlined in section 3.2 and analysed by the RP-HPLC method outlined in section 3.2.5. The locations of most the sites are shown in *Figure 4.6* and the precise sample information can be found in Appendix Table 1.


1
22
5 & 24
18
13
24
16
10
15
14
8
2
17
11
20
23
7
19
3
9
23
7
19
12
4
21
6

Figure 4.6. A map of Southern England and Wales highlighting the locations of the sites analysed to build a proboscidean geochronology.

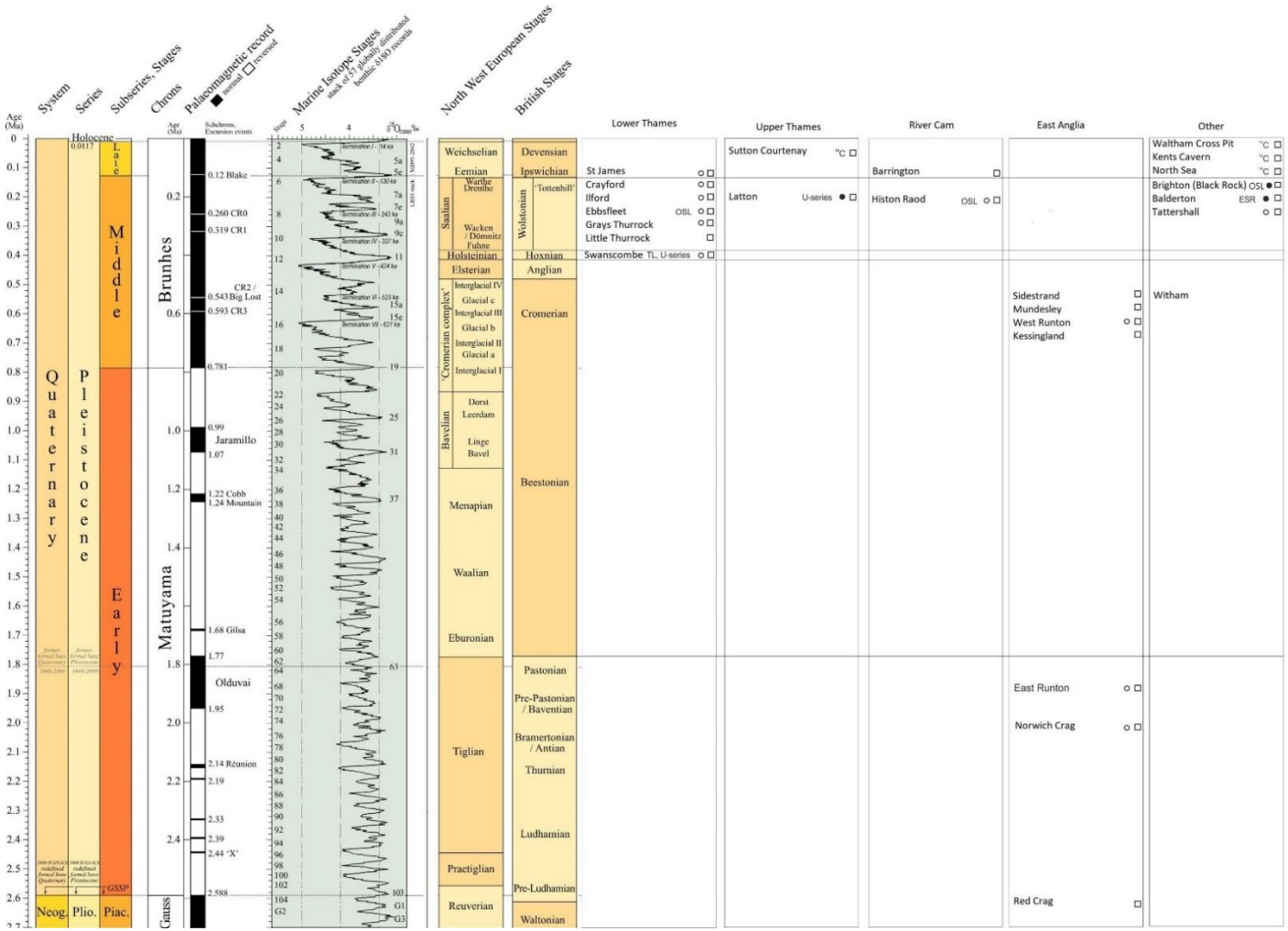

Figure 4.7. Global chronological correlation (last 2.7 Ma) with UK sites. Legend: Square = biostraigraphical correlations, circle = AAR analysis (open= Bithynia *opercula; closed=* Valvata*). Based on Gibbard & Cohen (2010).*

4.3.1. Racemisation in the enamel from UK sites

Racemisation is the most widely used diagenetic reaction for age estimation, and the extent of both FAA and THAA racemisation are routinely obtained for IcPD-geochronological studies, thus affording the opportunity to compare two proxies for IcPD (e.g. Preece & Penkman, 2005; Penkman *et al*., 2013). The rate of AAR is highly dependent on the chemical situation; terminal amino acids are thought to racemise faster than those that are in-chain, or those free in solution (Smith & Evans, 1980). FAAs have once formed part of a protein/peptide chain, and through continuous iterations of peptide hydrolysis form FAAs. Within a closed system, where all of the degradation products are retained, a strong positive relationship between FAA and THAA racemisation should be observed. This enables the identification of samples compromised by open system behaviour. Significant deviation from the expected FAA vs THAA trend can indicate leaching or contamination of amino acids (typically of the more labile FAAs) from the sample and thus compromise the interpretation of data (Preece & Penkman 2005; Penkman *et al*., 2013).

In this study four key amino acids were compared for their amino acid D/L values: Asx, Glx, Ala and Phe. They have been selected because they have shown predictable trends of IcPD in elevated-temperature experiments (Chapter 3) and replicate analysis of fossil material has shown they have a relatively high degree of precision (Figure 4.3

Table 4.4. FAA and THAA D/L values for the Proboscidean enamel samples from a range of UK sites analysed in this study. Location of each site is shown in Figure 4.2.

Sample code	Location	FAA								THAA							
		Asx	1 σ	Glx	1 σ	Ala	1 σ	Phe	1 σ	Asx	1 σ	Glx	1 σ	Ala	1 σ	Phe	1 σ
MoEE1		0.04	0.003	0.019	0.003	0.099	0.014	-	-	0.126	0.00	0.048	0.00	0.116	0.007	0.039	0.000
WCME1	Waltham Cross	0.124	0.006	0.031	0.003	0.117	0.043	0.028	-	0.214	0.014	0.058	0.001	0.103	0.003	0.053	0.002
WCME2	Waltham Cross	0.085	0.005	0.028	-	0.112	0.010	-	-	0.164	0.007	0.050	0.001	0.092	0.003	0.052	0.005
KCME1	Kents Cavern	0.088	-	0.032	-	0.113	-	0.058	-	0.173	0.000	0.059	0.001	0.113	0.005	0.048	0.002
SCME1	Sutton Courtney	0.113	0.005	0.031	0.001	0.13	0.02	0.055	0.004	0.187	0.007	0.052	0.001	0.115	0.034	0.05	0.000
BaPE1	Barrington	0.120	0.002	0.034	0.001	0.169	0.017	0.122	0.000	0.232	0.001	0.067	0.000	0.128	0.015	0.068	0.003
BaPE2	Barrington	0.152	0.003	0.061	0.000	0.134	0.004	0.106	0.011	0.252	0.000	0.074	0.001	0.109	0.007	0.067	0.001
BaPE3	Barrington	0.159	0.000	0.04	0.002	0.129	0.004	0.116	0.002	0.251	0.003	0.072	0.000	0.14	0.012	0.066	0.003
SJPE1	St James	0.122	0.004	0.416	0.002	0.144	0.016	0.137	0.004	0.239	0.005	0.065	0.000	0.122	0.002	0.076	0.003

Table 4.4. continued. FAA and THAA D/L values for the Proboscidean enamel samples from a range of UK sites analysed in this study. Location of each site is shown in Figure 4.2.

Sample code	Location	FAA								THAA							
		Asx	1 σ	Glx	1 σ	Ala	1 σ	Phe	1 σ	Asx	1 σ	Glx	1 σ	Ala	1 σ	Phe	1 σ
SJPE2	St James	0.242	0.019	0.118	0.000	0.244	0.028	0.165	0.018	0.313	0.008	0.093	0.001	0.137	0.021	0.081	0.002
BBME1	Brighton Raised Beach	0.215	0.002	0.040	0.001	0.180	0.013	0.138	0.007	0.227	0.004	0.070	0.001	0.162	0.013	0.084	0.005
BaME1	Balderton	0.213	0.004	0.066	0.000	0.186	0.017	0.169	0.014	0.253	0.006	0.076	0.001	0.153	0.002	0.089	0.001
TaME1	Tattershall Thorpe	0.186	0.007	0.039	0.045	0.163	0.018	0.169	0.005	0.248	0.012	0.070	0.003	0.154	0.026	0.090	0.005
CrME1	Crayford	0.225	0.000	0.055	0.004	0.174	0.011	0.153	0.014	0.226	0.007	0.071	0.001	0.155	0.006	0.095	0.003
CrME2	Crayford	0.257	0.008	0.070	0.002	0.201	0.005	0.202	0.012	0.284	0.008	0.092	0.000	0.182	0.001	0.111	0.003
HRME1	Histon Road	0.295	0.003	0.053	0.001	0.169	0.009	0.155	0.011	0.287	0.007	0.069	0.001	0.142	0.015	0.091	0.002
IlPE1	Ilford	0.189	0.000	0.056	0.003	0.196	0.024	0.173	0.012	0.263	0.012	0.084	0.002	0.159	0.005	0.104	0.003

Table 4.4. continued. FAA and THAA D/L values for the Proboscidean enamel samples from a range of UK sites analysed in this study. Location of each site is shown in Figure 4.2.

Sample code	Location	FAA								THAA							
		Asx	1 σ	Glx	1 σ	Ala	1 σ	Phe	1 σ	Asx	1 σ	Glx	1 σ	Ala	1 σ	Phe	1 σ
IlME1	Ilford	0.196	0.003	0.045	0.000	0.152	0.010	0.165	0.020	0.233	0.006	0.072	0.001	0.153	0.015	0.095	0.007
IlME2	Ilford	0.228	0.006	0.061	0.004	0.199	0.007	0.183	0.004	0.295	0.005	0.084	0.005	0.177	0.004	0.102	0.006
EbPE1	Ebbsfleet	0.188	0.000	0.064	0.004	0.185	0.011	0.195	0.005	0.237	0.004	0.084	0.000	0.180	0.006	0.108	0.009
LaME1	Latton	0.162	0.001	0.039	0.003	0.172	0.006	0.128	0.005	0.227	0.001	0.059	0.000	0.174	0.009	0.081	0.000
GTPE1	Grays Thurrock	0.220	0.000	0.068	0.002	0.224	0.001	0.246	0.001	0.257	0.000	0.085	0.001	0.228	0.013	0.12	0.007
LTPE1	Little Thurrock	0.263	0.006	0.077	0.002	0.254	0.008	0.224	0.007	0.312	0.000	0.105	0.000	0.235	0.013	0.144	0.007
SwPE1	Swanscombe	0.235	0.004	0.07	0.001	0.249	0.009	0.27	0.001	0.24	-	0.085	-	0.193	-	0.148	-
SwPE2	Swanscombe	0.238	0.001	0.08	0.001	0.252	0.007	0.266	0.007	0.289	0.000	0.101	0.000	0.207	0.002	0.163	0.002
WiME1	Witham	0.288	0.006	0.103	0.009	0.275	0.035	0.282	0.012	0.291	0.009	0.103	0.003	0.197	0.025	0.142	0.005

Table 4.4. continued. FAA and THAA D/L values for the Proboscidean enamel samples from a range of UK sites analysed in this study. Location of each site is shown in Figure 4.2.

Sample code	Location	FAA								THAA							
		Asx	1 σ	Glx	1 σ	Ala	1 σ	Phe	1 σ	Asx	1 σ	Glx	1 σ	Ala	1 σ	Phe	1 σ
SiPE1	Sidestrand	0.302	0.004	0.094	0.002	0.269	0.016	0.308	0.004	0.332	0.02	0.098	0.000	0.231	0.004	0.170	0.008
MuME1	Mundersley	0.392	0.001	0.087	0.000	0.262	0.013	0.278	0.012	0.398	0.016	0.095	0.005	0.234	0.016	0.153	0.007
WRME1	West Runton	0.392	0.019	0.129	0.008	0.335	0.056	0.345	0.03	0.362	0.004	0.109	0.001	0.25	0.005	0.209	0.001
KeME1	Kessingland	0.279	-	0.105	-	0.106	-	0.313	-	0.404	0.026	0.110	0.002	0.251	0.004	0.180	0.005
KeME2	Kessingland	0.378	0.011	0.110	0.002	0.304	0.022	0.339	0.045	0.376	0.035	0.110	0.002	0.263	0.003	0.203	0.005
ERME1	East Runton	0.450	0.016	0.208	0.003	0.490	0.022	0.622	0.008	0.421	0.004	0.199	0.001	0.460	0.006	0.389	0.009
NCME1	Norwich Crag	0.544	0.002	0.255	0.001	0.504	0.072	0.667	0.024	0.468	0.003	0.221	0.001	0.536	0.007	0.599	0.001
NCAE1	Norwich Crag	0.468	0.003	0.221	0.001	0.536	0.007	0.599	0.001	0.387	0.01	0.201	0.001	0.464	0.021	0.369	0.012
NCAE2	Norwich Crag	0.509	0.009	0.268	0.001	0.556	0.005	0.689	0.002	0.443	0.002	0.225	0.000	0.48	0.004	0.409	0.011

Table 4.4. continued. FAA and THAA D/L values for the Proboscidean enamel samples from a range of UK sites analysed in this study. Location of each site is shown in Figure 4.2.

Sample code	Location	FAA								THAA							
		Asx	1 σ	Glx	1 σ	Ala	1 σ	Phe	1 σ	Asx	1 σ	Glx	1 σ	Ala	1 σ	Phe	1 σ
RCAE1	Red Crag	0.667	0.008	0.312	0.000	0.658	0.002	0.699	0.004	0.639	0.007	0.297	0.004	0.606	0.037	0.506	0.018
RCAE2	Red Crag	0.611	0.000	0.311	0.003	0.646	0.019	0.734	0.016	0.591	0.015	0.309	0.008	0.618	0.034	0.526	0.025

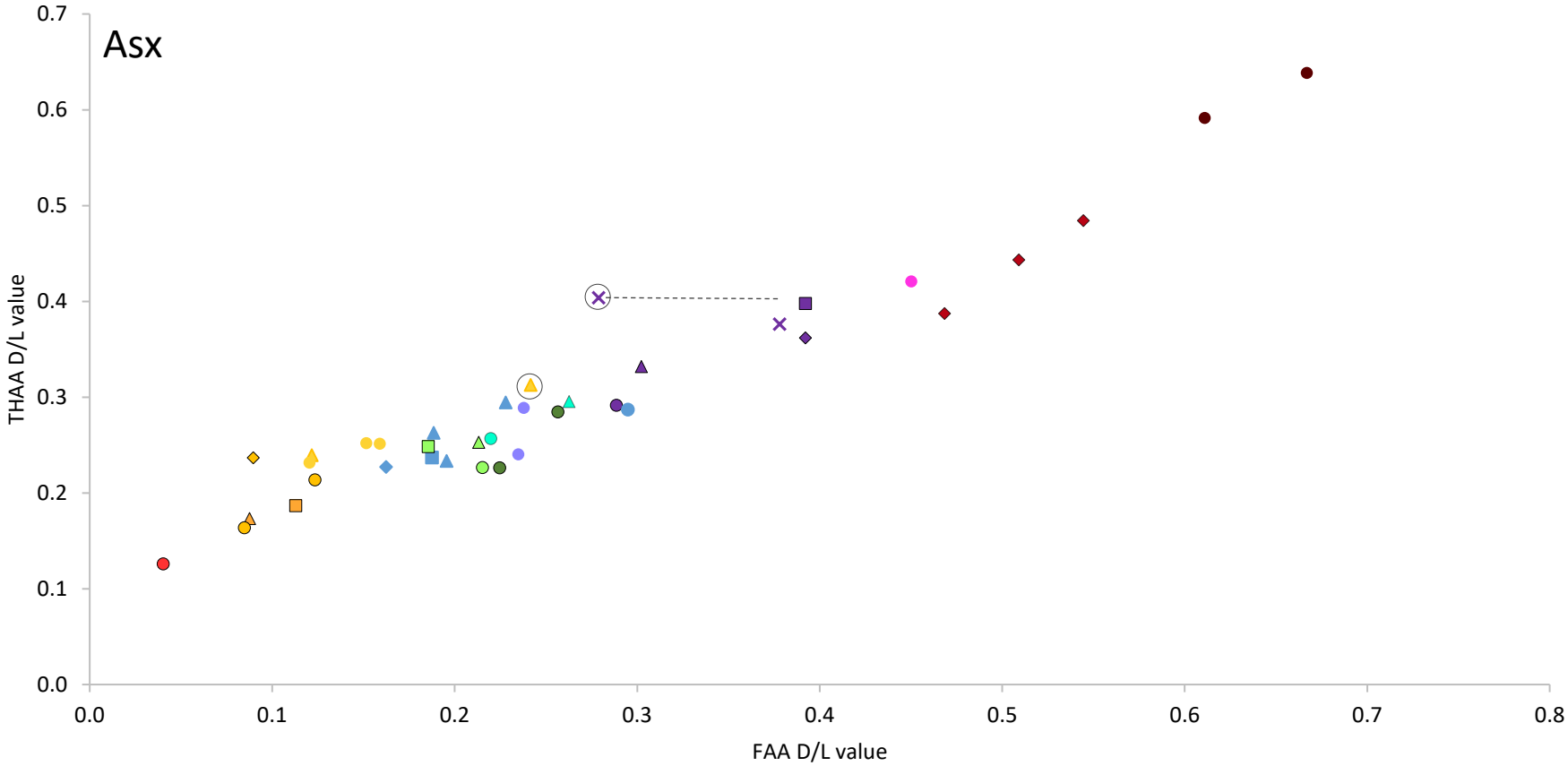

Figure 4.8. Proboscidean enamel, FAA D/L vs THAA D/L plots for four different amino acids: Asx, Glx, Ala and Phe. Most of the dental material originates from UK sites with well constrained chronologies. Different colours have been used to highlight sites thought to correlate to a comparable age based on their independent geochronology (red=modern; orange=Devensian; yellow=Ipswichian; green=MIS 6; blue=MIS 7; turquoise=MIS 9; light purple=Hoxnian; dark purple= Cromerian; pink/dark red= Early Pleistocene/Pliocene). The independent evidence of age for each site can be found in section 4.3.1.1.1-7). Data points that do not fit the general trend are circled.

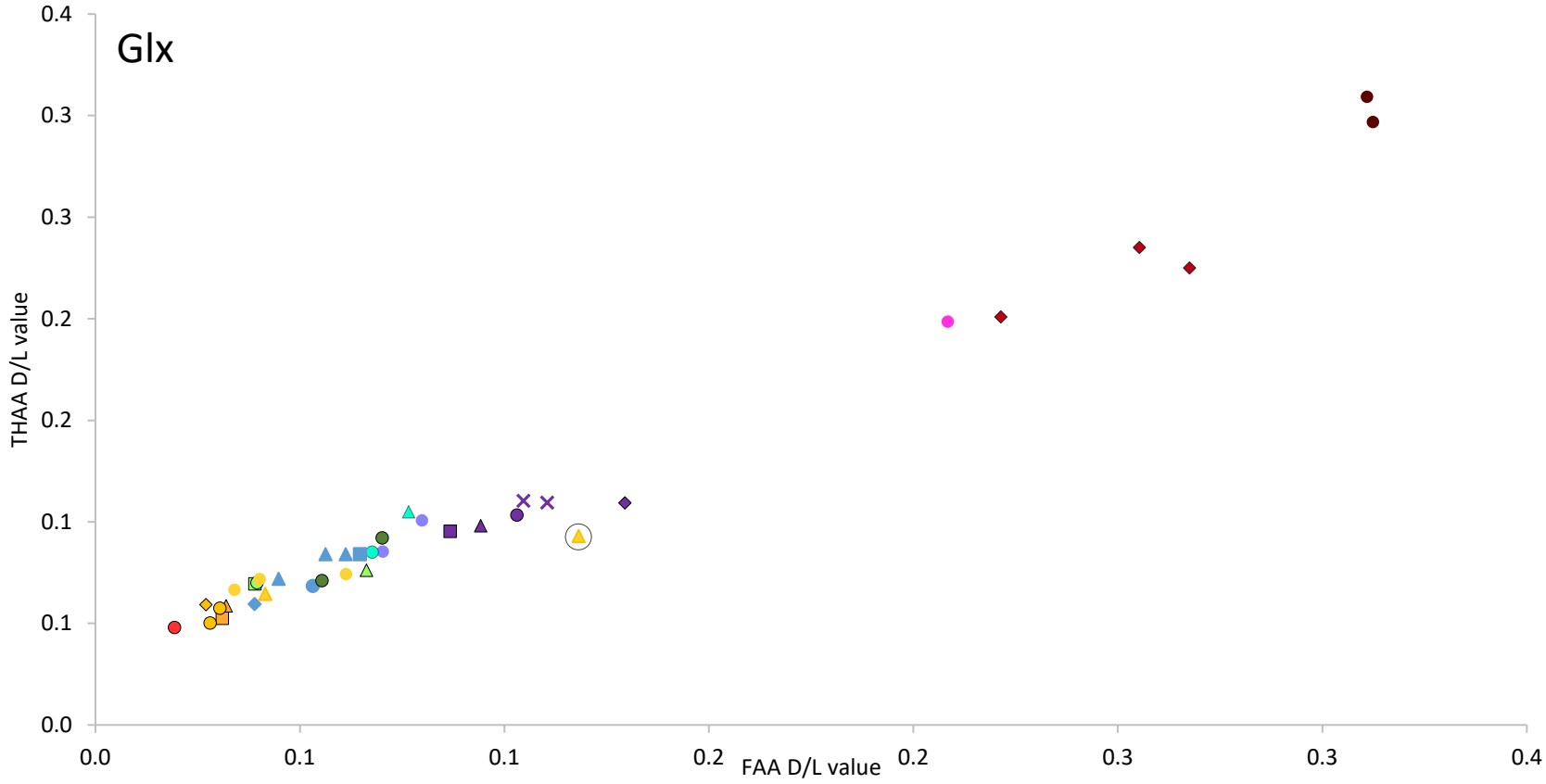

Figure 4.8 continued. Proboscidean enamel, FAA D/L vs THAA D/L plots for four different amino acids: Asx, Glx, Ala and Phe. Most of the dental material originates from UK sites with well constrained chronologies. Different colours have been used to highlight sites thought to correlate to a comparable age based on their independent geochronology (red=modern; orange=Devensian; yellow=Ipswichian; green=MIS 6; blue=MIS 7; turquoise=MIS 9; light purple=Hoxnian; dark purple= Cromerian; pink/dark red= Early Pleistocene/Pliocene). The independent evidence of age for each site can be found in section 4.3.1.1.1-7). Data points that do not fit the general trend are circled.

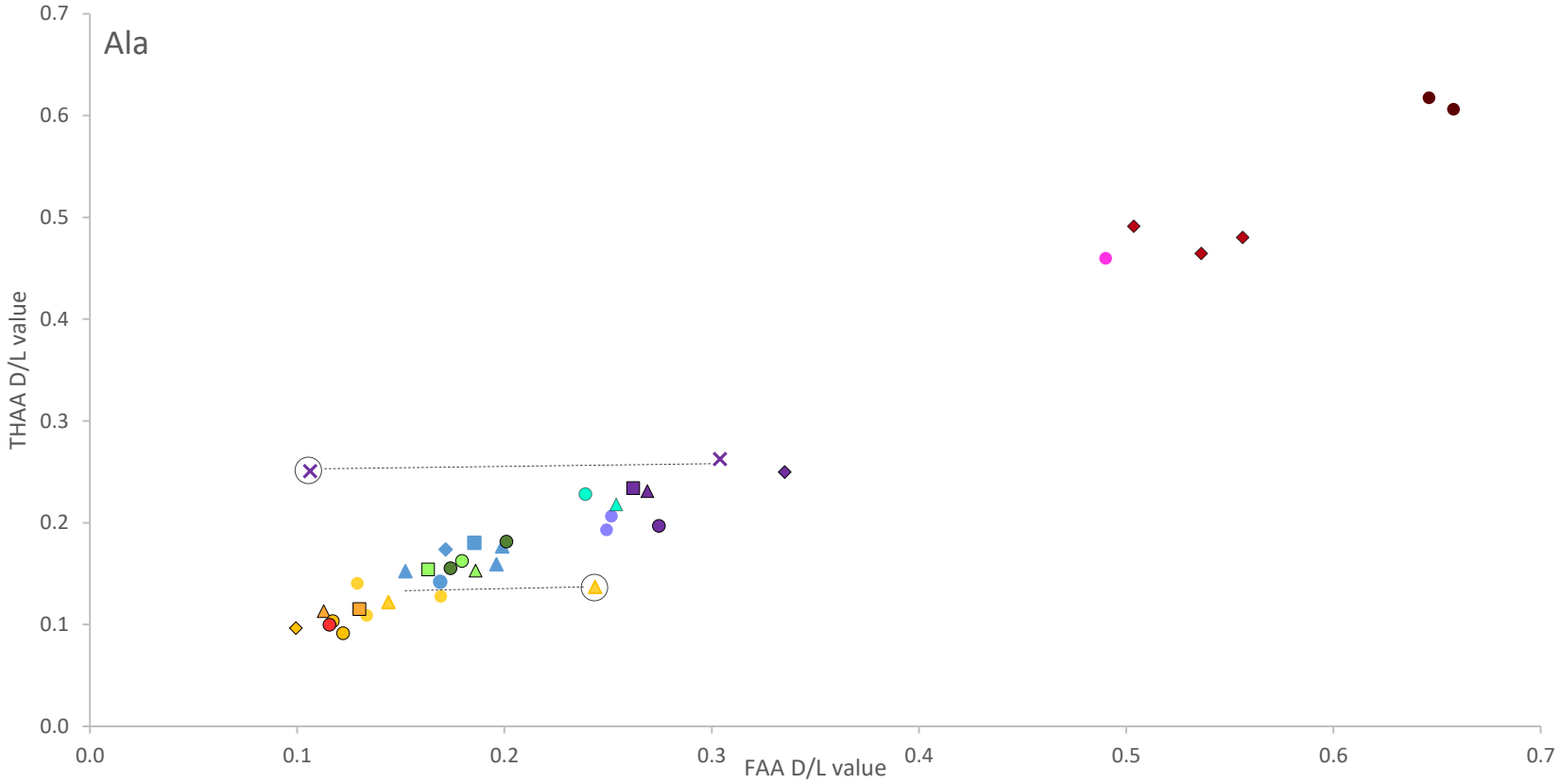

Figure 4.8 continued. Proboscidean enamel, FAA D/L vs THAA D/L plots for four different amino acids: Asx, Glx, Ala and Phe. Most of the dental material originates from UK sites with well constrained chronologies. Different colours have been used to highlight sites thought to correlate to a comparable age based on their independent geochronology (red=modern; orange=Devensian; yellow=Ipswichian; green=MIS 6; blue=MIS 7; turquoise=MIS 9; light purple=Hoxnian; dark purple= Cromerian; pink/dark red= Early Pleistocene/Pliocene). The independent evidence of age for each site can be found in section 4.3.1.1.1-7). Data points that do not fit the general trend are circled.

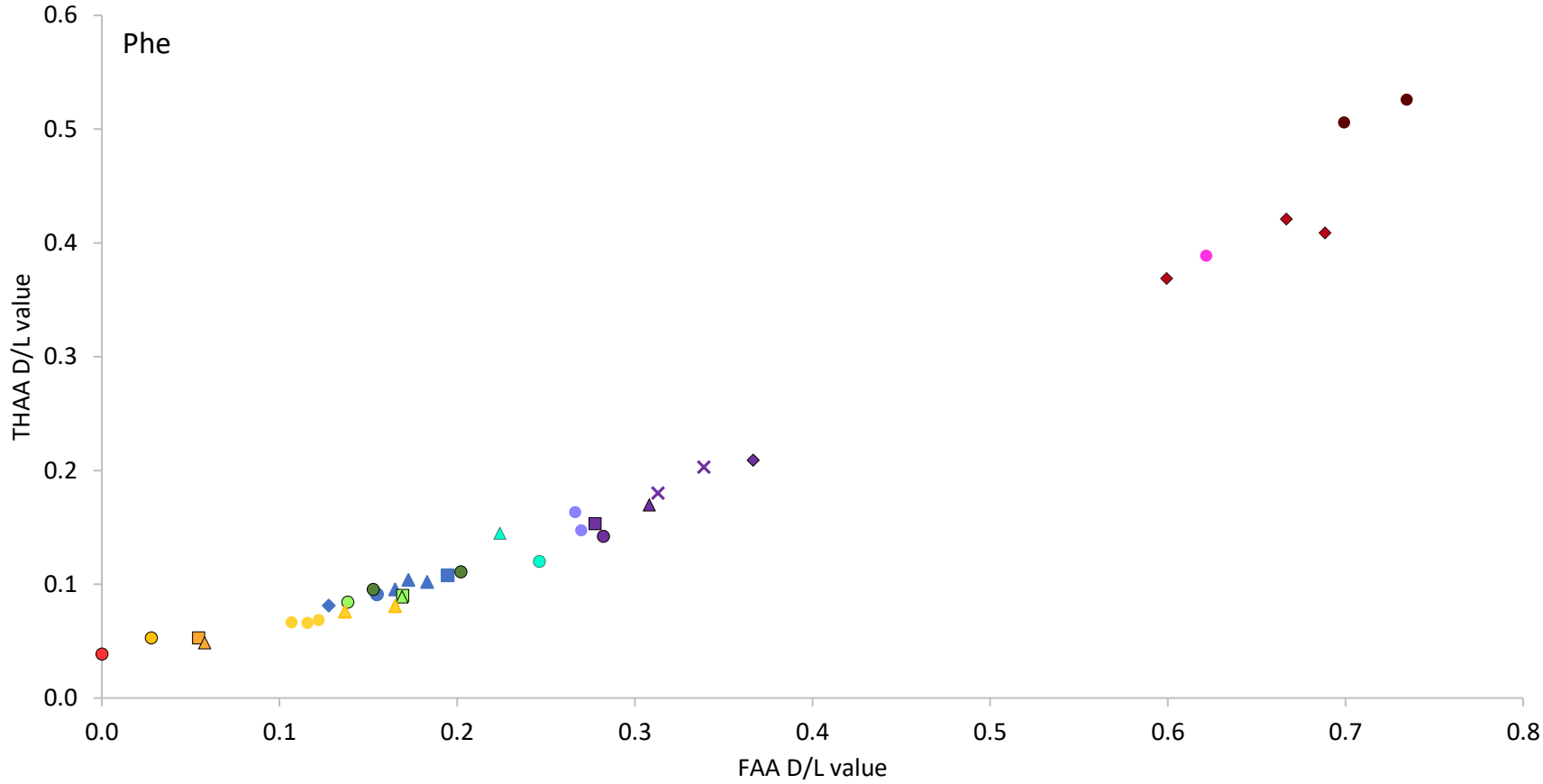

Figure 4.8 continued Proboscidean enamel, FAA D/L vs THAA D/L plots for four different amino acids: Asx, Glx, Ala and Phe. Most of the dental material originates from UK sites with well constrained chronologies. Different colours have been used to highlight sites thought to correlate to a comparable age based on their independent geochronology (red=modern; orange=Devensian; yellow=Ipswichian; green=MIS 6; blue=MIS 7; turquoise=MIS 9; light purple=Hoxnian; dark purple= Cromerian; pink/dark red= Early Pleistocene/Pliocene). The independent evidence of age for each site can be found in section 4.3.1.1.1-7). Data points that do not fit the general trend are circled.

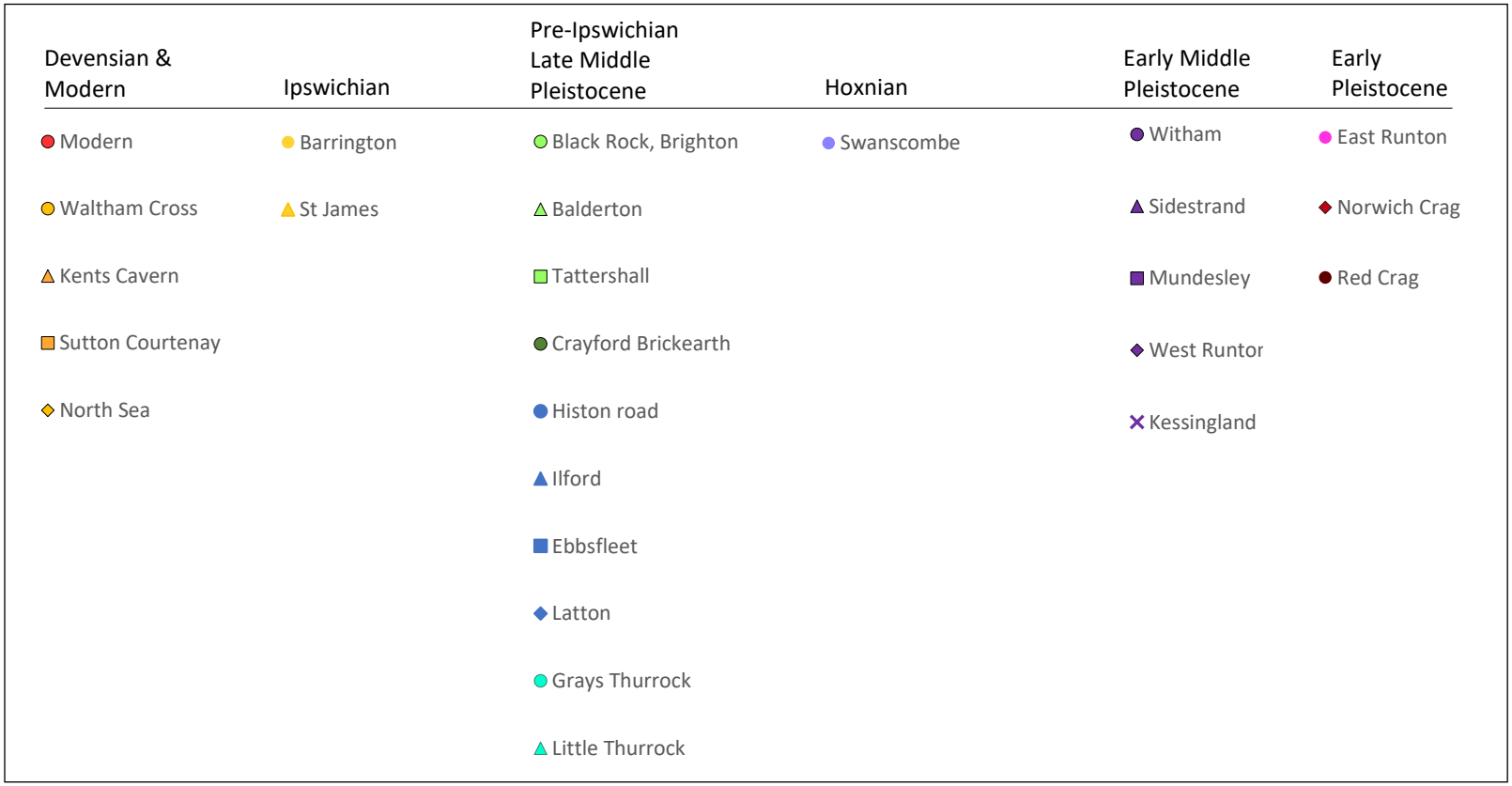

Figure 4.8 continued Proboscidean enamel, FAA D/L vs THAA D/L plots for four different amino acids: Asx, Glx, Ala and Phe. Most of the dental material originates from UK sites with well constrained chronologies. Different colours have been used to highlight sites thought to correlate to a comparable age based on their independent geochronology (red=modern; orange=Devensian; yellow=Ipswichian; green=MIS 6; blue=MIS 7; turquoise=MIS 9; light purple=Hoxnian; dark purple= Cromerian; pink/dark red= Early Pleistocene/Pliocene). The independent evidence of age for each site can be found in section 4.3.1.1.1-7. Data points that do not fit the general trend are circled.

4.3.1.1.1. Modern elephant enamel: *E. maximus*

Sample name: MoEE1

Enamel was obtained from an upper left M1 tooth of a modern Asian elephant (*E. maximus*) that died at around 8-10 years of age. The original provenance of the tooth is unknown, but now resides as part of Adrian Lister's personal collection.

As expected, the lowest extent of racemisation in this geochronology (Figure 4.8) was observed in MoEE1. MoEE1 has had the least time to degrade and therefore most of the racemisation of L-amino acids should have occurred *in vivo* or during the preparation of the sample.

4.3.1.2. Devensian sites

In the British Isles, the Devensian is the term used to describe the last glacial period (Mitchell *et al*., 1973; Bowen, 1999), and encompasses the period 115 – 11.7 ka, which correlates with stages 5a-2 in the marine oxygen isotope stratigraphy. ^{14}C dating is applicable to the later part of the Devensian (up to ~50 ka) and thus most of the sites in this study are supported by radiocarbon dates. The type site for the Devensian is the Four Ashes Pit in Staffordshire (SJ 914083; Bowen, 1999). During this time period the first anatomically modern humans are thought to have reached northwestern Europe (ca. 44.2-41.5 ka BP; Higham *et al*., 2011).

4.3.1.2.1. Waltham Cross Pit, Hertfordshire: *M. primigenius*

UK national grid reference: TL 366010

Sample name: WCME1 [BGS: GSM50289], WCME2 [BGS: GSM50288]

The deposits at Waltham Cross Pit form part of the low terrace gravels of the River Lea. It is thought that the Lea Valley contains two separate deposits: one older, with fossiliferous channel sediments and a younger infill of gravel and sands (Gibbard, 1994). The fossiliferous channel deposits (Ponders End formation) in the Lea Valley have yielded cold-adapted mammalian fauna including *M. primigenius*, *Coelodonta antiquitatis*, *Rangifer tarandus* and *Dicrostonyx torquatus* (Lister, 2001a). Radiocarbon dating of the organic matter in the Lea Valley indicates an age of c. 28 ka (Allison *et al*., 1954; Stuart, 1982), and although the dates should be treated with caution as they were undertaken in the early days of radiocarbon dating, they are supported by the palynology of the sites, which indicates a cold climate, including some sites yielding Arctic flora (Reid, 1949). The two teeth analysed are from the flood plain gravels at the Waltham Cross Pit, which form part

of the Ponders End Formation and were presented to the Natural History Museum (London) as part of the Twickenham Gravel Co. Ltd collection in 1932. Based on the radiocarbon dates and palynology of the site, the *M. primigenius* teeth recovered from this site are likely to have been laid down during MIS 2-3.

Two *M. primigenius* teeth have been studied from the Waltham Cross Pit deposits and analysis was conducted in preparative duplicate.

4.3.1.2.2. Kents Cavern, Torquay: *M. primigenius*

UK national grid reference: SX 9356415

Sample name: KCME1 [BGS: GSM63]

Kents Cavern near Torquay is a cave system of large chambers in Devonian limestone that has provided the earliest evidence for anatomically modern humans in northwestern Europe (Higham *et al*., 2011). Stratified deposits of material ranging from Middle Pleistocene to Holocene in age have been recovered from this site. The faunal remains at Kent's Cavern have been spilt into three distinct assemblages: the Breccia, which lies at the base of the stratigraphy, dated to the Middle Pleistocene (Proctor, 1996), the Late Pleistocene Cave Earth which lies above the Breccia and the late-glacial Black Band (Campbell & Sampson, 1971). The tooth analysed in this study is from the Cave Earth which has been divided into the lower A2 Loamy and upper B2 Stony Cave earths. The B2 Stony Cave Earth assemblage is dominated by *Crocuta crocuta, Bison priscus* and *Rangifer tarandus* with an absence of *Mammuthus*, but it is possible that some *Mammuthus* teeth were recovered from this layer but not adequately recorded (Lister, 2001b). The A2 Loamy Cave Earth assemblages, which are dominated by *Mammuthus* and *Coelodonta*, are also associated with human artefacts (*c.* 60 – 35 ka; Currant & Jacobi, 1997). Radiocarbon dates from hominin material found in the Cave earth initially dated the remains to 36 - 34 ka cal BP (Hedges *et al*., 1989) but owing to improvements in radiocarbon dating (use of ultrafiltration during the extraction), it has been more recently revised to 41-39 ka cal BP (Higham *et al*., 2011). A lower age limit of MIS 4 for the Cave Earth deposits has been suggested based on faunal changes during the Devensian (Currant & Jacobi, 1997). The B2 Stony Cave Earth broadly correlates with MIS 4 owing to the abundance of *Bison priscus* and *Rangifer tarandus*, which is then succeeded by the A2 Loamy Cave Earth dominated by *Mammuthus* and *Coelodonta,* which based on the faunal model proposed by Currant and Jacobi (1997), and the radiocarbon dates (Higham *et al*., 2011), supports a correlation with MIS 2-3.

The exact provenance within the Cave Earth sequence of the *M. primigenius* tooth analysed in this study is not known but the bulk of the faunal remains from these deposits originated from the "A2 Loamy Cave Earth" (Lister, 2001b) as defined by Campbell and Sampson (1971) and therefore most likely date to *c.* 60-25 ka (MIS 2-3). There was only enough sample for three individual analyses, so the THAA analysed were conducted in preparative duplicate and a single analysis of the FAAs was undertaken.

4.3.1.2.3. Sutton Courtenay, Oxfordshire: *M. primigenius*

UK national grid reference: SU 511947

Sample name: SCME1 (SC1240)2

The deposits at Sutton Courtenay form part of a series of fluvial terraces in the Upper Thames valley and have been defined as forming part of 'the Flood-plain Terrace' (Briggs & Gilbertson, 1980). Radiocarbon dating of the Flood-plain terrace has indicated that the deposits were lain down during the late Middle and Late Devensian (Briggs & Gilbertson, 1980), i.e. ca. 35- 12 ka. Large mammalian grazers have been recovered from the Flood-plain terrace deposits at Sutton Courtenay including *M. primigenius*, *C. antiquitatis* and *Bison priscus*. Based on biostratigraphy, the deposits at Sutton Courtenay have been correlated with MIS 3 (Scott & Eeles, in prep). One *M. primigenius* tooth from Sutton Courtenay was analysed in preparative duplicate.

4.3.1.2.4. North Sea (Brown Bank region): *M. primigenius*

Sample name: NSME1

During glacial periods, the southern part of the North Sea formed a land bridge between Britain and continental Europe (Coles, 2000). Terrestrial mammalian remains are frequently found in this now marine region through commercial fishing or dredging of the seabed. *M. primigenius* skeletal remains have been radiocarbon dated from the Brown Bank region in the southern part of the North Sea from 34 ka cal BP to the upper limits of the radiocarbon dating (48,500 years cal BP; Mol *et al*., 2006). Faunal evidence from both marine and terrestrial species indicate cold stage fauna was intermittently present in this region from 48,500 – 28,000 years cal BP (Mol *et al*., 2006). Mammoths are thought to have vacated Britain during the last glacial maximum (Stuart *et al*., 2004), so the *M. primigenius* tooth analysed in this study, which was recovered via dredging near the Brown Bank region in the North Sea, is therefore most likely to have been deposited during MIS 4 or 3 (71 - 29 ka BP; Mole *et al*., 2006; Stuart *et al*., 2004). One *M. primigenius* tooth from the Brown Bank

region in the North Sea has been studied and analysis was conducted in preparative triplicate.

4.3.1.2.5. Devensian sites results summary

In general, all of the Devensian sites in this study have similar extents of racemisation in both the FAA and THAA fractions (Figure 4.8), which is consistent with them being broadly contemporaneous. The extent of Asx, Glx and Phe (not all Phe FAA D/L values were obtained due to low concentrations of the D-isomer) racemisation in the enamel of teeth from Devensian sites is greater than in the modern elephant sample (section 4.3.1.1.1), with the greatest separation obtained in Asx. This indicates that the extent of Asx racemisation might be able to best distinguish between modern and Devensian age teeth.

Two teeth were analysed from the deposits at Waltham Cross (WCME1 & WiME2). The extent of Glx and Ala racemisation are very similar, suggesting a low intra-site variability for these two amino acids (Table 4.4; Figure 4.8). However, the intra-site variation in the extent of Asx racemisation is greater than expected. Asx is the fastest racemising amino acid studied over this time period, the extent of Asx racemisation is therefore likely to have the greatest sensitivity to age. This potentially indicates that the two teeth are of different ages (but both still originating from the Devensian). However, the previous experiments evaluating intra-tooth variability, indicated that the greatest variability was observed for Asx (section 4.2) and thus, the range of Asx D/L values for the Waltham Cross site may be a reflection of the intra-site variability at Waltham Cross. To more comprehensively understand intra-site variability, additional experiments analysing a greater number of enamel samples from the same bed are required and would aid in distinguishing between these two interpretations.

4.3.1.3. Ipswichian sites

In the British Isles, the Ipswichian is the formal name for the last interglacial (Mitchell *et al*., 1973), and encompasses the period 130-115 ka, correlating with MIS 5e (NEEM community members, 2013). The type site for the Ipswichian in the UK is Bobbitshole in Ipswich (TM 148414). It is thought that the Ipswichian was on average warmer than the present-day (Phillips, 1974; Schreve and Candy, 2010; Candy *et al*., 2016)), with mammalian assemblages dominated by species such as *Hippopotamus amphibius*, *Panthera leo*, *Palaeoloxodon antiquus* and *Crocuta crocuta*, with an absence of *Homo sp.* and their associated artefacts (Schreve, 2001).

4.3.1.3.1. Barrington, Cambridgeshire: *P. antiquus*

UK national Grid Reference: TL 381491 – 406498

Sample numbers: BaPE1 [BGS: GSM925], BaPE2 [BGS: GSM919-920], BaPE3 [No BGS number]

The Barrington beds form part of the terrace deposits of a tributary of the river Cam in Cambridgeshire. The Barrington beds occur as remnants of a high terrace lying at maximum height of about 6 m above the modern floodplain alluvium where the river has cut through chalk marl and gault (Gibbard & Stuart 1975). The deposits contain a rich assemblage of interglacial mammalian fauna including *Ursus arctos, Panthera leo, Stephanorhinus hemitoechus, Palaeoloxodon antiquus, Hippopotamus amphibious* and an absence of *Equus ferus*. Some of the bone material shows clear indications of chewing, almost certainly from spotted hyena, *Crocuta crocuta,* which indicates that the bones were not incorporated into the channel sediments immediately. The presence of *Hippopotamus amphibius* and absence of *Equus ferus* strongly indicates the material was deposited during the Ipswichian interglacial, MIS 5e (Turner, 1973; Stuart, 1975; Schreve, 2001). Pollen analysis from the sediments at Barrington supports correlation with the Ipswichian zone IIb, which is consistent with the mammalian biostratigraphy (Gibbard & Stuart, 1975).

Three *Palaeoloxodon antiquus* teeth have been analysed in duplicate: a lower M1 [GSM925], upper right M2 [GSM 921], while the type of the third tooth [unnumbered] is unknown.

4.3.1.3.2. St James, Westminster: *P. antiquus*

UK national Grid Reference: TQ 300804 (Trafalgar Square)

Sample name: SJPE1 [BGS: GSM6399], SJPE2 [BGS: GSM60236]

The St James enamel samples are from the Trafalgar Square interglacial deposits, which form part of the Kempton Park Formation (Bridgland, 1994, 2006) formerly known as the 'Upper Floodplain Terrace' of the Thames (Bowen *et al*., 1999). The terrace lies upon London Clay and comprises: basal gravels named the Spring Gardens Gravels which are thought to have formed during a cold climate, overlain by finer-grained interglacial sediments (Trafalgar Square deposits), which are in turn overlain by the Kempton Park Gravel, which contain cold-climate sands and gravels (Gibbard, 1985; Preece, 1999). The diagnostic presence of *Hippopotamus amphibius* and the absence of *Equus ferus* in the interglacial sediments strongly supports assignment to MIS 5e (Stuart, 1976; Preece, 1999;

Schreve, 2001). This is supported by palynology, which correlates the deposits with Ipswichian pollen zone Ip IIb (MIS 5; Stuart, 1976) and IcPD dating of *Bithynia* opercula (Penkman *et al*., 2011).

The two *P. antiquus* teeth from the Trafalgar Square interglacial deposits were analysed in preparative duplicate. SJPE1 is a lower left M1 and was recovered during the excavations of Cleveland House and presented by J. W. Read in 1898. SJPE2 is an upper right M1 and was recovered as part of sewer excavations; it has an unknown history prior to forming part of the collections at the BGS.

4.3.1.3.3. Ipswichian sites results summary

The extent of racemisation in all three teeth from Barrington (BaPE1-3) and one of the teeth from St James (SJPE1) is greater than that for the teeth from the Devensian sites. For these teeth, the spread of data in the Glx FAA is relatively large, but the Glx THAA values are more consistent (Table 4.4; Figure 4.8), suggesting that Glx FAA does not have high enough temporal resolution in this time range to distinguish between MISs. The extent of racemisation in Phe is relatively consistent and there is a good degree of separation between the three teeth for Barrington and the younger Devensian sites. This indicates that Phe may be better suited for differentiating between MIS in the Late Pleistocene. Asx also displays reasonable separation between these teeth and the younger teeth from Devensian sites, but there is greater intra-site variation.

The extent of Ala and Phe THAA racemisation in SJPE2 is also similar to that for samples from the other Ipswichian sites, but the extent of Asx and Glx THAA, and Asx, Glx and Ala FAA racemisation is much greater. The relationship between the extent of FAA and THAA racemisation of Ala and to a lesser extent Glx does not follow the same trend as for other teeth recovered from UK sites. In a closed system, the relationship between the FAA and THAA racemisation should follow a predictable trend (Preece & Penkman, 2005; Penkman *et al*., 2013), but morphologically distorted biominerals can result in non-concordance (Preece & Penkman, 2005). This is likely to be due to contamination and/or leaching at a point in the depositional demineralisation. The non-conformity of SJPE2 to the predictable degradation of amino acids in enamel may indicate that this tooth (or this small section of tooth) has undergone mineral changes during its depositional history, which has temporarily exposed the amino acids to open system circumstances. Alternatively, bacteria are known to synthesise D-enantiomer amino acids, in particular D-Ala and D-Glx, to modulate the production of peptidoglycan, which acts as a stress-bearing component of

their cell walls (Lam *et al*., 2009). It therefore follows that the higher than expected FAA D/L values may be caused by bacterial contamination. It is unclear exactly why the extent of racemisation in SJPE2 is markedly different to that of SJPE1 and the other MIS 5e samples from Barrington. Further investigation (potentially focusing on possible mineral changes) is therefore required to establish the cause of this anomalous result.

4.3.1.4. Pre-Ipswichian Late Middle Pleistocene sites

The pre-Ipswichian Late Middle Pleistocene began 352 ka and ended at the start of MIS 5e(130 ka; Lisiecki & Raymo, 2005). The Pre-Ipswichian Late Middle Pleistocene correlates with MIS 6-10.

4.3.1.4.1. Brighton/Norton Raised Beach, Sussex: *M. primigenius*

UK national Grid Reference: Unknown

Sample name: BBME1 [BGS: 654]

A series of Pleistocene deposits spanning the West Sussex Coastal Plain have yielded a range of fossil mammalian remains. It has been recognised that these deposits and the wider Solent Basin form four discrete groups of sediments (Bates *et al.,* 2010):

- Marine sands/gravels/silts which are associated with sea-level highstands during interglacials and fine-grained terrestrial sediments which are thought to have accumulated under low energy fluvial conditions.
- Coarse angular flint gravels associated with sea-level low stands during periglacial climates which often overly interglacial marine deposits
- Flint gravels deposited by river action
- Abandoned/buried sediment channels

The Brighton/Norton raised beach deposits were originally thought to have been laid down during a single high-sea-level stand during the Ipswichian interglacial (Hodgson, 1964), but subsequent research suggested the high-sea-level aggradations had occurred earlier (Bates *et al*., 1997). D-alloisoleucine/L-Ile values of 0.31 ±0.003 from whole-shell molluscs (*Macoma balthica*) led to a tentative attribution of the material to MIS 7 or 9 (Bowen & Sykes 1985). This is supported by the faunal assemblage from the Brighton/Norton raised beach which, based on diagnostic dental morphological data from a northern vole species (*M. oeconomus*), is thought to restrict the site to MIS 7 and 6 (Parfitt, 1998; Westaway *et al*., 2006). The cold stage deposits of Coombe Rock contained the faunal remains of *Coelodonta antiquitatis*, *Equus ferus* and *Bison priscus* (provenance uncertain) and were

most likely deposited during MIS 6 (Parfitt, 1998). OSL dating has been conducted at several sites from the West Sussex Coastal Plain with dates from bore holes in the Brighton/Norton raised beach deposits at Norton Farm yielding age estimates indicating correlation with MIS 6-7 (Bates *et al.,* 2010). Analysis of the *M. primigenius* tooth (BBME1) from Brighton, which formed part of the G. Mantell collection, was conducted in preparative duplicate.

4.3.1.4.2. Balderton Sands and Gravels, Nottinghamshire: *M. primigenius*

UK national Grid Reference: SK 837561

Sample Name: BaME1

The Balderton sand and gravel deposits comprise poorly-sorted gravel with medium- to coarse-grained sand matrix (Brandon & Sumbler, 1991). The deposits contain one of the largest assemblages of mammalian fauna from the Trent system, rich in cold stage mammals (Lister & Brandon, 1991). The composition of the mammalian assemblage includes *Canis lupus, Ursus sp., Panthera leo* and *Mammuthus primigenius,* and is comparable to many Devensian sites. However, its position in the Trent terrace system (altitudinally higher than a terrace containing a *Hippopotamus* fauna and interpreted as Ipswichian (MIS 5e) in age) indicates the site is older (Figure 4.9; Brandon & Sumbler 1991; White *et al*., 2010; Bridgland *et al* 2015). ESR dating of multiple elephantid teeth (using two alternative models of uranium uptake) yielded ages of 130-190 ka (Grün, 1991), supporting correlation of the deposits with MIS 6 and 7. Amino acid epimerisation values from whole-shell *Valvata piscinalis* yielded D-alloisoleucine/L-isoleucine ratios of 0.13 ±0.01, which when compared to the Ipswichian stratotype and the MIS 7 deposits at Stanton Harcourt, indicate an age of MIS 6 (Brandon & Sumbler, 1991). Analysis of the *M. primigenius* from Balderton sands and gravels was conducted in preparative triplicate.

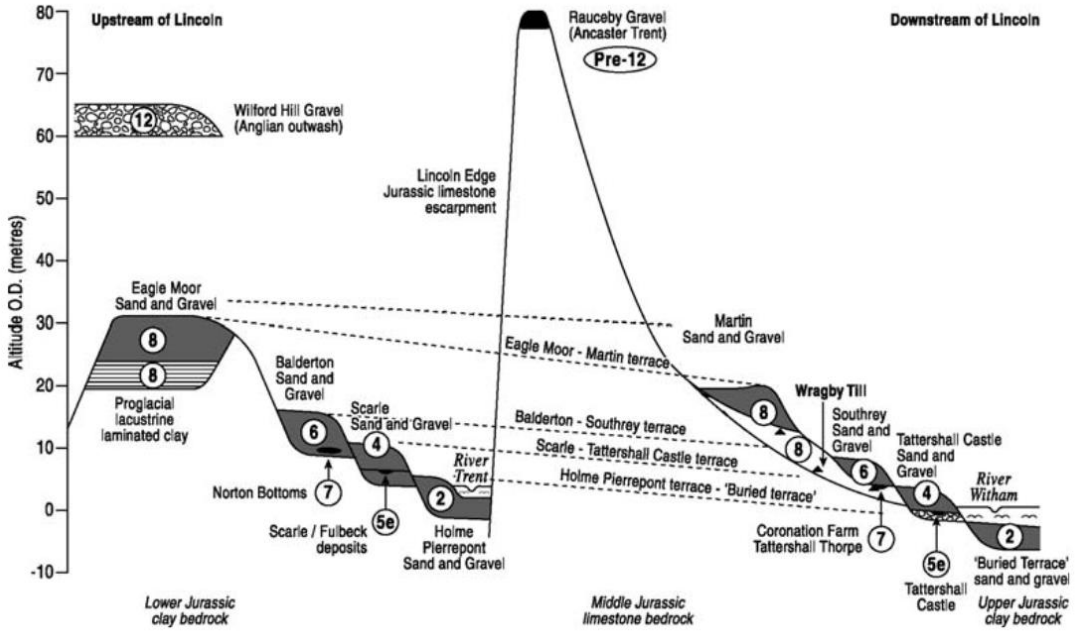

Figure 4.9. An idealised composite cross section comparing the Trent terraces and glacial deposits Composite upstream (west) and downstream (east) of the Lincoln Gap. Figure taken from White et al., (2010). Figure shows the position of the Balderton Sand and Gravel within the Terrace sequence, and how these deposits relate to the Tattershall Thorpe deposits.

4.3.1.4.3. Tattershall Thorpe, Sands and Gravels, Lincolnshire: *M. primigenius*

UK national Grid Reference: TF 211571 or TF 230602

Sample name: TaME1

Tattershall Thorpe forms part of the Trent terraces and lies within the Wragby Till (Figure 4.9). Girling (1974) described the deposits at two gravel pits at Tattershall Castle and Kirkby-on-Bain. The Tattershall Thorpe sand and gravel pits are located along the western side of the River Bain valley and are contemporaneous with the deposits at Kirkby-on-Bain (Bridgland *et al*., 2015). They comprise deposits from *c.* 13 – 5 m O.D., encompassing sands and gravels with post-depositional ice wedge casts that overlie clays and detritus muds (Holyoak & Preece, 1985). Based on radiocarbon dates and faunal remains at Tattershall Thorpe and Castle, Rackham (1978) suggested that they represented two different intervals in the Devensian Cold Stage, with the Thorpe member forming during a cooler climate. However, most of the dates were near radiocarbon saturation (which would be expected from a sample over 50 ka) and the samples that did yield radiocarbon dates within the Devensian, were suspected to have done so as a result of contamination with Holocene rootlets (Girling, 1980). The Tattershall Thorpe deposit has yielded cold-stage large fauna dominated by woolly mammoth (*Mammuthus primigenius*) and woolly rhino (*Coelodonta*

antiquitatis), with rarer horse, *Equus sp.* and other species, similar in composition to the upstream Balderton Sands and Gravel deposits (Section 4.3.1.4.2).

The palynology of interglacial deposits underlying the sands and gravels at the two Tattershall sites was originally interpreted as indicating an Ipswichian age (Rackham, 1979), but Holyoak and Preece (1985) described dissimilarities between the two beds, notably the presence of the molluscan fauna *Planorbis planorbis* and *Bathyomphalus contortus* at Tattershall Thorpe but not at Tattershall Castle. Differences in height above sea level (Figure 4.9) and the presence of the mollusc *Corbicula fluminalis* indicates the deposits from Tattershall Thorpe are more likely to be pre-Ipswichian (Meijer & Preece, 2000; Bridgland *et al.,* 2015). IcPD dating of *Bithynia* opercula from Kirkby-on-Bain (interglacial sediments) indicates a slightly greater extent of racemisation than seen in MIS 5e sites, and thus is consistent with an MIS 7 assignment (Bridgland *et al*., 2015). The sand and gravel deposits at Tattershall Thorpe are thought to be contemporaneous with the Balderton sand and gravel and thus the glacial deposits are thought to be MIS 6 in age. Analysis of the *M. primigenius* from the sand and gravel at Tattershall Thorpe was conducted in preparative triplicate.

4.3.1.4.4. Crayford, London (lower Crayford Brickearths): *M. trogontherii/primigenius*

UK national Grid Reference: TQ 517758

Sample name: CrME1 [BGS: GSM117009], CrME2 [BGS: GSM5123]

The deposits at Crayford comprise a large accumulation of 'brickearths' which consist of sand flood-loams and laminated loess-like deposits and have a maximum thickness of about 11 m (Chandler, 1914). These brickearths overlie the Taplow/Mucking Gravels of the Lower Thames in south-east London (Chandler, 1914; Bridgland & Schreve, 2004; Bridgland 2014). The deposits at this site have been sub-divided into two horizons: the upper and lower brickearths and are thought to have been deposited during two separate stages (King & Oakley, 1936). The lower brickearth consists of yellow calcareous loams and has yielded mammalian fauna including temperate elements such as straight-tusked elephant *Palaeoloxodon antiquus* and the interglacial rhino *Stephanorhinus hemitoechus*, but also open-ground elements like *Mammuthus, Coelodonta* and *Ovibos*, as well as numerous molluscan remains. Based on the faunal remains, the lower brickearths are thought to have accumulated during relatively temperate but open conditions. The mammoth may be transitional between steppe and woolly species (*M. trogontherii/primigenius*) (Lister & Scott, in prep.). The upper brickearth consists of reddish-brown clayey loam, which has

probably formed due to weathering in which calcareous material has been removed in solution and redeposited in the lower brickearths in the form of calcareous nodules (King & Oakley, 1936). The deposits are thought to have been laid down during MIS 6 and 7 (Schreve, 2001; Bridgland, 2014). IcPD data from *Bithynia* opercula from the Brickeaths (layer unknown) at Crayford (Norris Pit) indicates an age of late MIS 7 / early MIS 6 (Penkman *et al*., 2011). The *M. trogontherii/primigenius* enamel, CrME1, is from the Lower Crayford Brickearths. The exact provenance of the upper right M1, CrME2, is unknown. Analysis of both teeth from the lower Crayford Brickearths was conducted in preparative duplicate.

4.3.1.4.5. Histon Road/Pumping Station, Cambridge: *M. cf. trogontherii*

UK national Grid Reference: TL 445663

Sample name: PSME1 [BGS: GSM424]

The site at Histon Road (also referred to as the pumping station in the collection at the BGS) is situated north of Cambridge and comprises a series of interglacial gravels, silty sands and marls, rich in plant and molluscan fossils which have been deposited by the river Cam (Sparks & West, 1959). Based on pollen biostratigraphy and the molluscan fauna, the site was originally thought to consist of deposits from the last interglacial (Sparks & West, 1959). The vertebrate assemblage at the sewer excavations near Histon Road (Histon Road Member) is absent of hippopotamus, however, it contains major element of the 'hippopotamus fauna' associated with MIS 5e (Boreham *et al*., 2010). The deposits also contain *Equus ferus* and the bivalve *Corbicula fluminalis*, both of which are thought to have been absent from Britain during MIS 5e. However, more recent studies of the coleopteran assemblages at Histon Road and other MIS 7 sites, indicate that the deposits more likely correlate with MIS 7 (Coope, 2001). This is supported by IcPD dating of *Bithynia* opercula from Histon Road, which exhibit similar extents of AAR to other sites correlated with MIS 7 (Penkman *et al*., 2013). OSL date from the silts has given a minimum age estimate of 121.55 Ka BP ±20.08 (Boreham *et al*., 2010). Analysis of a single *M. cf. trogontherii* tooth form the sewer excavations near Histon Road (Histon Road Member) was conducted in preparative duplicate.

4.3.1.4.6. Ilford (Uphall Pit), London: *M. trogontherii* & *Palaeoloxodon antiquus*

UK national Grid Reference: TQ 437860

Sample Name: IlPE1 [BGS: GSM114881], IlME1 [BGS: GSM114884], IlME2 [BGS: GSM114892]

The interglacial deposits at the Uphall brickearth pit comprise silts and clays and are contained within the chronologically well-constrained Taplow/Mucking formation, which forms part of the Lower Thames terraces (Bridgland, 1994). Contained within this formation are sedimentary sequences attributed to two cold and one warm climatic episode. These sediments are situated in a higher terrace than those attributed to the Ipswichian and are thus thought to be older (Sutcliffe, 1975; Bridgland, 1994). The interglacial deposits found at Ilford (as well as Aveley), have been recognised as part of MIS 7 on the grounds of molluscan (Preece, 1999), coleopteran (Coope, 2001) and mammalian assemblages (Sutcliffe, 1975; Bridgland & Schreve, 2004), as well as aminostratigraphy (Bowen, 1995; Penkman *et al*., 2011). *Equus ferus*, *Corbicula fluminalis, Palaeoloxodon antiquus* and *Mammuthus trogontherii* have been recovered from the site and there is an absence of *Hippopotamus amphibius* (Schreve, 2001). The mammoths found in the interglacial deposits at Ilford are of particular interest due to their abundance and their significance in mammoth evolution. The Ilford mammoths have molars that are smaller in size and have a lower enamel plate count than typical *M. primigenius* teeth, due to a late persistence of mammoths adapting to a more temperate climate and less abrasive vegetation (Lister & Sher, 2001). Enamel samples from two *M. trogontherii* and one *P. antiquus* from the Ilford brickearths at the Uphall Pit were analysed in preparative duplicate. IlME1 was from a *M. trogontherii* upper left MIII, IlME2 was from a *M. trogontherii* upper left MII and IlPE1 was from a *P. antiquus* lower MI.

4.3.1.4.7. Ebbsfleet, Kent: *Palaeoloxodon antiquus*

UK national Grid Reference: TQ 611735

Sample name: EbPE1 [BGS: GSM5031]

The Ebbsfleet site is situated south of the river Thames and lies on the western side of the Ebbsfleet valley. Beneath the Pleistocene horizons are a series of Palaeocene and Eocene deposits (Thanet Sand, Woolwich Beds and Blackheath Beds) which overlie Cretaceous Chalk (Wenban-Smith, 2013). The Pleistocene deposits at Ebbsfleet have yielded multiple finds of Clactonian technology, the dating of which is predominantly reliant on associated

dating of the mammalian fauna (Parfitt, 2013). Due to irregularities in the lateral deposition of material, different exposures have been difficult to date, and thus dating of the site has required a multifaceted approach (e.g. OSL, biostratigraphy, IcPD of *Bithynia* opercula; see Wenban-Smith, 2013).

One *P. antiquus* tooth from Spurrell's 'Tramway Cutting' excavation (roughly corresponding to Wenban-Smith's (2013) Trench D) has been analysed in this study. The deposits at Ebbsfleet are complex, and as no additional horizon information was recorded with this sample it could potentially have derived from a number of different age horizons. However, Wenban-Smith's Trench D is thought to include horizons dating to MIS 11-6. The *P. antiquus* tooth from the deposits at Ebbsfleet has been analysed in preparative duplicate.

4.3.1.4.8. Latton, Wiltshire: *M. cf. trogontherii*

UK national Grid Reference: SU 081965

Sample name: LaME3 (LQ95)

The deposits at Latton consist mainly of fluvial medium to coarse limestone gravels originally derived from Middle Jurassic rocks (Lewis *et al*., 2006). Additionally, there are minor quantities of flint, quartz, quartzite and chert, which probably are derived from glacial and/or fluvial sediments (Lewis *et al*., 2006). The sequence at Latton has been subdivided into three facies associations; A–C (Lewis *et al.,* 2006). The enamel specimen analysed in this study was from association A. The deposits at Latton have yielded *Equus ferus* and *Mammuthus primigenius* ('Ilford type') which indicate correlation with MIS 7. The deposits at Latton have yielded a relatively impoverished diversity of large fauna when compared to other sites correlated with MIS 7 (Schreve, 2001; Scott, 2001), which led Scott & Buckingham (2001) to conclude that the deposits at Latton probably accumulated during a short time period, perhaps late in the interglacial (MIS 7a). U-series dating of *Equus ferus* tibia has yielded a minimum age of 147.4 ±20 ka, assuming the bone was a closed system with respect to uranium (Lewis *et al*., 2006). IcPD dating of *Valvata piscinalis* yielded AAR values consistent with other sites correlated with MIS 7 (Penkman *et al*., 2007). Analysis of enamel from a single *M. cf. trogontherii* was conducted in preparative duplicate.

4.3.1.4.9. Grays Thurrock, Essex: *P. antiquus*

UK national Grid Reference: unknown

Sample name: GTPE1 [BGS: GSM11520]

Grays Thurrock lies within the Lynch Hill/Corbets Tey gravels and is part of the Lower Thames terrace sequence. This set of gravels is believed to correlate with MIS 9 and lies above the Taplow/Mucking gravels assigned to MIS 7 (Schreve, 2002; Penkman *et al*., 2013; Bridgland, 2006). Mammalian assemblages from sites such as Purfleet (which lie within the Corbets Tey formation and have similar faunal assemblages to Grays Thurrock), are distinct from other interglacial deposits and have enabled the development of diagnostic fauna for MIS 9 deposits in the UK (Schreve, 2002). For example, *Ursus arctos* has replaced *Ursus spelaeus* which is thought to be characteristic of the Hoxnian (MIS 11) interglacial (Schreve, 1997). IcPD-stratigraphy of *Bithynia* opercula based on the THAA fraction for Ala places Grays Thurrock in the more racemised end of MIS 9 (Penkman *et al*., 2013). Analysis of a single *P. antiquus* milk molar from the interglacial deposits at Grays Thurrock was conducted in preparative duplicate.

4.3.1.4.10. Little Thurrock, Essex: *P. antiquus*

UK national Grid Reference: TQ 625783

Sample name: LTPE1 [No BGS number]

The Little Thurrock Gravel Member contains cold climate gravels with Clactonian technology artefacts and is the term given to the basal Corbets Tey cold-climate gravels (Bridgland & Harding, 1994; Schreve *et al*., 2001). The Little Thurrock Gravel Member at Globe Pit is well developed and is stratigraphically constrained by the overlying Grays Thurrock Member (MIS 9). The deposits contain chalk and irregular intervals of flint with individual clasts up to 120 mm in length, indicating periodic scouring out of the smaller material (Schreve *et al*., 2002). The mammalian biostratigraphy is very similar to the assemblages from Purfleet, Grays Thurrock and Cudmore Grove. Based on the terrace stratigraphy and biostratigraphical evidence, the Little Thurrock deposits at Globe Pit are thought to have formed during the earlier part of MIS 9 or 10 (Bridgland *et al*., 2014). Analysis of enamel from a single *P. antiquus* from the Little Thurrock Gravels was conducted in preparative duplicate.

4.3.1.4.11.Pre-Ipswichian Late Middle Pleistocene site results summary

The extent of racemisation in the teeth from the pre-Ipswichian late Middle Pleistocene sites is generally greater than in the samples from *Hippopotamus amphibius* containing sites thought to correlate with the Ipswichian (Figure 4.8; Section 4.3.1.3). This is consistent with the current understanding of the presence of this species in the UK during the Ipswichian and its absence from the fossil record during the pre-Ipswichian late Middle Pleistocene (Shreve, 2001). The degree of separation between sites that correlate with the Ipswichian and those that correlate with MIS 7-6, is relatively small. This potentially indicates that enamel AAR may not be able to robustly differentiate between MIS 5e and MIS 7/6 when analysing a limited number of samples from a single site. In contrast, AAR of *Bithynia* opercula is able to differentiate between MIS 5e and 7 (Penkman *et al*., 2011; 2013); this likely due to the faster rates of racemisation in this biomineral (Figure 3.22).

The enamel from the Balderton Sand and Gravel and Thorpe Sand and Gravel (at Tattershall) have yielded similar extents of racemisation, which is consistent with the current understanding of stratigraphy at the two sites (Bridgland *et al*., 2015).

The extent of racemisation in the tooth from Histon Road (PSME1) is consistent with its assignment to MIS 7. The extent of racemisation in Glx, Ala and Phe is similar to other MIS 6 and 7 sites (e.g. Ilford, Crayford, and Balderton), however, the extent of Asx FAA racemisation is most similar to that of the tooth from the late Cromerian age deposits at Witham. This may indicate the low temporal resolution of Asx racemisation in Proboscidean enamel in the UK.

The extent of racemisation in the tooth from Latton is similar to that of teeth from other sites thought to correlate to MIS 7. The extent of racemisation in Asx, Glx and Phe is the lowest of all the MIS 7 sites in this study, which is consistent with its assignment to MIS 7a, but enamel AAR does not have the temporal resolution to assign material to marine isotope sub-stages and this is therefore likely to be a coincidence.

The extent of Glx, Ala and Phe racemisation in the enamel of teeth from Grays and Little Thurrock is greater than amino acids in enamel from sites thought to correlate with MIS 7-6. In particular, Phe racemisation has a higher degree of separation between MIS 7 sites and Grays and Little Thurrock than the other amino acids studied. This indicates that enamel AAR may be able to distinguish between interglacials MIS 7 and 9. However, given the limited number of replicate MIS 10/9 samples, the spread of D/L values of MIS 10/9 sites is unknown and thus additional samples are required to test this theory.

The provenance of the tooth from the deposits at Ebbsfleet (EbPE1) was unknown and thus, this sample is not chronologically well constrained. However, the extent of racemisation in EbPE1 is similar to the samples from Ilford and Crayford and therefore the samples likely correlate with MIS 7/6.

4.3.1.5. Hoxnian sites

The Hoxnian interglacial correlates with MIS 11 which spans 425 - 360 ka with ice and deep-sea records illustrating a complex climate within this stage (EPICA Community members, 2004). The Hoxnian began with a particularly warm interglacial climate, which was terminated by rapid cooling at ~390 ka (Parfitt, 2013). The latter cooling period is thought to comprise several stadials and interstadials.

4.3.1.5.1. Swanscombe, Barnfield Pit, Kent: *P. antiquus*

UK national Grid Reference: TQ 598745

Sample name: SwPE1 [BGS: GSM50340], SwPE2 [BGS: GSM50341]

The site at Barnfield Pit near Swanscombe, contains a complex sequence of fluvial sediments which form part of the Thames terrace staircase and principally comprises gravels, sands and loams attributed to the Boyn Hill Gravel (Bridgland, 1994; Wenban-Smith, 2013). The sequence of sediments at Barnfield Pit lie upon Thanet Sand and comprises Lower Gravel, Lower Loam, Lower Middle Gravel, Upper Middle Gravel Upper Loam and Upper Gravel (Ashton et al., 1995). At Hornchurch, the Boyn Hill Gravel lies directly above the Chalky Boulder Clay of Essex at about 22.5 m O.D., which is accepted as being Anglian (MIS 12) in age, and thus Swanscombe is believed to be younger. The mammalian faunal assemblage at from the fluvial sediments at Swanscombe includes *Ursus spelaeus, Dama dama clactoniana, Talpa minor, Trogontherium cuvieri, Microtus subterraneus* and *Oryctolagus cuniculus* as well as archaeological artefacts, which are diagnostic of MIS 11 (Lister, 1986; Schreve, 2001). Thermoluminescence (Bridgland *et al*., 1985) and U-series dating (Bridgland, 1994) have both supported the assignment of the deposits at Swanscombe to MIS 11. IcPD data from *Bithynia* opercula from the Lower Loam at Barnfield Pit also support correlation of these deposits with MIS 11 (Penkman *et al*., 2013). The site at Barnfield Pit comprises several fossiliferous horizons; one of the *P. antiquus* analysed in this study is from the Lower Gravel (SwPE2), the other is from unspecified terrace gravel (SwPE1). The Lower Gravel at Barnfield Pit is thought to correlate with MIS 11c, due to the increasing relative abundances of horse and bison which are indicative of woodlands interspersed by grasslands (Oakley, 1952; Parfitt, 2013). Analysis of

the two *P. antiquus* teeth was conducted in preparative duplicate (however THAA for SwPE1 was analysed only once due to a crack in the glass vial). The enamel of both teeth was chalky and bright white in appearance, in contrast to the off-white crystalline appearance of most of the other enamel samples in this study. This change in enamel appearance may be caused by degradational changes in the inorganic crystal structure.

4.3.1.5.2. Hoxnian site results summary

The two teeth from Barnfield Pit exhibit similar extents of racemisation and are generally greater than in samples from MIS 7 sites, however this is dependent on the amino acids studied (Figure 4.8). The extent of Asx, Glx and Ala racemisation is very similar in the enamel samples from Grays and Little Thurrock, which are thought to correlate with MIS 9. This indicates that these amino acids are unable to distinguish between MIS 9 and 11. However, the extent of Phe racemisation has a relatively large separation between Swanscombe and Grays and Little Thurrock sites, indicating this amino acid may be better able to temporally assign enamel in this period.

4.3.1.6. Early Middle Pleistocene sites

The Anglian began ~ 478 ka ago and ended at the start of the Hoxnian, ~425 ka ago (). At its maximum, the British Anglian ice sheet covered most of the British Isles and was the most extensive glaciation of the Pleistocene in Britain. The Anglian was preceded by the Cromerian Complex, which began ~866 ka (MIS 21) and consists of multiple glacial and interglacial periods. One of them, the Cromerian Interglacial *s.s.,* has as its type site the West Runton Fresh-water Bed in Norfolk (TG 188432; Lister & Stuart, 2010).

4.3.1.6.1. Witham, Essex: *M. trogontherii*

UK national Grid Reference: TF 030177 (Witham-on-the-Hill)

Sample Name: WiME1 (donated by Jim Rose)

The Witham Member overlies the Castle Bytham Member and consists of cross-stratified, reddish brown to brown sands, derived from Triassic sandstones (Bateman & Rose, 1994). The Witham Member deposits are thought to have been laid down during the Cromerian Complex (Lewis, 1999). The most likely age of the *Mammuthus* tooth from Witham is 450 – 500 ka (Rose, *pers comm*) and thus the sample most likely originates from the Anglian or the latest part of the Cromerian Complex. Analysis of a single *M. trogontherii* tooth was conducted with five preparative replicates.

4.3.1.6.2. Sidestrand, Norfolk: *P. antiquus*

UK national Grid Reference: TG 262401

Sample Name: SiPE1 [BGS: GSM6574]

The deposits at Sidestrand consist of a complex series of geological units, stretching across a large coastal region. The locality comprises a thick glaciogenic sediment pile of Middle Pleistocene age, overlying up to 10 m of preglacial sands, gravels, clays and peats (Larkin *et al*., 2014 see references therein). These preglacial deposits are subdivided into the shallow marine/coastal sediments (forming part of the Crag group) and the freshwater deposits (forming part of the Cromer Forest-bed Formation). The Crag deposits are further subdivided including the Wroxham Crag Formation, thought to date to the late Early and early Middle Pleistocene, and a lower Sidestrand Member (formerly the 'Weybourne Crag') which dates to the Early Pleistocene. The shelly horizons within the upper fresh-water bed are termed the 'Sidestrand *Unio*-bed' (or 'Sidestrand Hall Member') and were originally thought to form part of the Norwich Crag formation (Funnell & West, 1977; West 1980). However, evaluation of the microtine rodent assemblage of the *Unio*-bed suggested that some of the deposits more closely resemble that of the later members of the Cromer Forest-bed Formation (Mayhew & Stuart, 1986). The Sidestrand *Unio*-bed mainly consists of marine laminated clays, sands and gravels, which overlie the shallow marine sediments of the Wroxham Crag. The Sidestrand *Unio*-bed, which stretches from Sidestrand to Trimingham, has been described as comprising two distinct horizons, the 'lower' and 'upper' *Unio-beds*. The lower bed comprises sand and gravel and the upper comprises blue clays; the two beds are thought to have been deformed by glaciotectonic processes (Preece *et al*., 2009). IcPD of *Bithynia* opercula from the two *Unio*-beds suggest the member is older than the MIS 11 sites of Hoxne and Clacton but younger than the MIS 15/17 site of West Runton; supported by the biostratigraphical evidence, the *Unio*-bed has therefore been interpreted as forming during either late MIS 15 or early MIS 13 (Preece *et al*., 2009).

The tooth analysed in this study was from the G. W. Lamplugh collection, housed at the BGS. The mammalian collections from the site at Sidestrand have been shown to be of mixed ages, ranging from Early Pleistocene to early Middle Pleistocene (Lister, 1994; 1996; Preece *et al*., 2009). The exact provenance of the tooth is unknown but based on the known biostratigraphic range of *P. antiquus,* it is very probable that the tooth dates to the later part of the early Middle Pleistocene. Analysis of this *P. antiquus* tooth from the Sidestrand was conducted in preparative duplicate.

4.3.1.6.3. Mundesley, Norfolk: *M. trogontherii*

UK national Grid Reference: TG 319363

Sample name: MuME1 [BGS: GSM7333]

The formation at Mundesley comprises two main bone deposits (West, 1980). The lower deposits below the cliff level contain alternating beds of clay pebbles and laminated clay and gravel. Large quantities of bones and teeth of elephants and antlers of deer were discovered in this deposit. The upper deposits at the base of the cliff comprise gravels, clay pebbles, lignite, and cakes of peat; these deposits are also fossiliferous, containing *Palaeoloxodon antiquus* and other large faunal remains. The deposits below the level of the cliff (bed f; West, 1980) are most likely of Pastonian age and the deposits at the base of the cliff (beds h and I; West, 1980) are of Anglian and Cromerian age (West, 1980; Lister, 1996). The specimen analysed in this study is from a *M. trogontherii* and was from the blue clay at the base of the cliff and is thus thought to be of Anglian/Cromerian Complex age. Analysis of this *M. trogontherii* tooth was conducted in preparative duplicate.

4.3.1.6.4. West Runton, Norfolk: *M. trogontherii*

UK national Grid Reference: TG 189441

Sample name: WRME1, Norwich Museums Service (Sample name unknown)

The interglacial deposits at West Runton consist of *c.* 2 m of freshwater muds and alluvial clays. The deposits lie above 'Wroxham Crag' deposits, which based on the faunal record are believed to be of pre-Pastonian age (Lister, 1998; Lewis, 1999). The interglacial deposits at the base of the cliff at West Runton have been defined as the stratotype for the Cromerian stage (West, 1980). The Cromer Forest-bed was orginally divided into three sets of deposits, the 'Upper-Freshwater Bed', the 'Forest Bed' (Estuarine) and the 'Lower Freshwater Bed'. At West Runton, basal marls recognised as Late Beestonian are overlain by the West Runton Freshwater Bed (formerly 'Upper Freshwater Bed'); based on palynology, the West Runton Freshwayer Bed is thought to cover the first half of the Cromerian Stage (Cr I-II; West, 1980) In contrast to the Late Beestonian deposits, the Cromerian deposits at West Runton have yielded large numbers of large and small mammalian fauna, including: *Mimomys savini, Equus altidens, Mammuthus trogontherii, Megaloceros savini* and *Macroneomys brachygnathus* (Lister & Stuart, 2010; Maul & Parfitt, 2010). One of the largest, nearly complete skeletons of an *M. trogontherii* from a well stratified deposit has been recovered from the West Runton Freshwater Bed (Lister &

Stuart, 2010). Additionally, the bone collagen protein sequence of the *M. trogontherii* has been analysed, demonstrating the longevity of collagen for hundreds of thousands of years (Buckley *et al*., 2011).

Relative IcPD dating of *Bithynia* opercula indicate the West Runton Freshwater Bed is significantly older than the MIS 11 deposits at Clacton and MIS 13 at Waverley Wood (Penkman *et al*., 2010), indicating a pre-MIS 13 age. ESR dating of tooth enamel initially produced an age estimate of 346 ±55 ka but has since been revised using different moisture content values and has produced ages of between and 460 ±80 ka (Rink *et al*., 1996). These dates are thought to under-estimate the antiquity of the site. Analysis of a single *M. trogontherii* tooth from the West Runton Freshwater Bed was conducted in preparative duplicate.

4.3.1.6.5. Kessingland, Suffolk: *M. trogontherii*

UK national Grid Reference: TM 536862

Sample name: KeME1 [BGS: GSM118478], KeME2 [BGS: GSM118477]

The cliff exposures at Kessingland and Pakefield were first described by Blake (1877; 1890). The oldest marine deposits at the base of the cliff consist of laminated marine silts and clays, which were estimated to have been laid down during the Early Pleistocene (West, 1980). Above these deposits lie red-brown sand and gravels (ferruginous) and thenthe Rootlet Bed, which mainly consists of reddish-brown silt with carbonate nodules and contains mammalian remains. The Rootlets Bed is thought to have been formed during the early temperate sub-stage of the Cromerian Complex (Stuart & Lister 2001). Beneath the Rootlet Bed lies which based on the mammalian fauna are thought to have been laid down at a similar time to the Rootlet bed (Stuart & Lister, 2001).

In contrast to many sites that form part of the Cromer Forest-bed Formation, much of the vertebrate remains at Kessingland were recorded *in situ,* enabling a strong provenance. From the Cromerian Complex deposits (Gravel and Rootlet beds) at Kessingland diagnostic mammalian taxa including *Mammuthus trogontherii, Crocuta crocuta, Mimomys savini* have been recovered. The presence of *Palaeoloxodon antiquus, Hippopotamus amphibius* and *Megaloceros dawkinsi* at Kessingland are potentially important biostratigraphical markers as they are absent from the West Runton Freshwater Bed, and thus suggest that the Kessingland deposits are likely from a separate temperate stage (lister & Stuart, 2010; Preece & Parfitt, 2012). Analysis of two *M. trogontherii* teeth were conducted in duplicate.

4.3.1.6.6. Early Middle Pleistocene sites results summary

In general, the extent of racemisation in the enamel from the Early Middle Pleistocene sites is greater than the samples from pre-Ipswichian Late Middle Pleistocene and Hoxnian sites (Figure 4.8), which is consistent with the known chronology. The extent of racemisation in all four studied amino acids is greater in the enamel from West Runton and Kessingland than in the samples from Witham, Sidestrand and Mundesley, suggesting a greater antiquity. This is consistent with the likely ages of the Witham, Sidestrand and Mundesley teeth, which are thought to be younger than the West Runton tooth. The extent of racemisation in the younger teeth from Witham, Sidestrand and Mundesley is similar to specimens from the Hoxnian site of Swanscombe but always higher. It therefore suggests that enamel AAR cannot robustly differentiate between samples from the Hoxnian and the Anglian/late Cromerian. However, it does appear to be able to distinguish between the samples within the Cromerian.

Two *Palaeoloxodon* teeth were sampled from the deposits at Kessingland, which has been independently correlated with MIS 15-17. Both THAA fractions are in good agreement with the rest of the AAR chronology, but the Asx and Ala FAA fractions have lower D/L values than expected (Table 4.4; Figure 4.8). This may indicate that the intra-crystalline fractions of amino acids in the sample may have been compromised (become open system) at some point between deposition and analysis. The relationship between the THAA and FAA racemisation of Asx and Ala does not follow the general patterns for amino acid decomposition. This might indicate that the tooth has lost the more highly racemised free Ala and Asx amino acids, and thus, has not always represented a closed system. The non-conformity to the trend does not follow the same patterns as for SJPE1, as the FAA is lower than expected. In both cases the racemisation of Phe is the least variable of the amino acids studied.

4.3.1.7. Early Pleistocene sites

The western-most region of the Pliocene North Sea Basin extends into eastern England and corresponds to the Crag Basin in East Anglia (Mathers & Hamblin, 2015). The Crag Basin is highly fragmented and has numerous hiatuses, stretching from the Early Pliocene to the late Middle Pleistocene (Lee *et al.*, 2017). The Crag deposits indicate a cooling climate, with a transition to more regular climate cycle. Due to the age of the deposits, estimations of their ages are principally proposed based on biostratigraphy and palaeomagnetic dating (Mathers & Hamblin, 2015).

4.3.1.7.1. East Runton, Norfolk (Wroxham Crag): *M. meridionalis*

UK national Grid Reference: TG 194430 – 205427

Sample name: ERME1 [BGS: GSM116503]

The Early Pleistocene formation at East Runton comprises a bed of cemented sands and marine shells which form part of the Wroxham Crag Formation; these deposits lie upon a platform of chalk and a stone bed (Reid, 1890). The Wroxham Crag is the youngest part of the series of marine sediments encompassing the Red Crag Formation and the Norwich Crag Formation, all of which were laid down in the North Sea basin during the Early Pleistocene (Hamblin *et al*., 1997). The Wroxham Crag has been distinguished from the older Norwich Crag based on the abundance of *Macoma balthica* (Norton, 2000), supported by aminostratigraphic dating of *Bithynia* opercula (Penkman *et al*., 2013). The Wroxham Crag has yielded a pollen record attributed to the cool Pre-Pastonian a Substage (West, 1980). The Wroxham Crag deposits at East Runton contain a rich assemblage of large-mammal fauna including *Mammuthus meridionalis, Eucladoceros spp. Pseudodama rhenana, Equus stenonis* and *bressanus,* and *Stephanorhins etruscus.* The biostratigraphy, in combination with palaeomagnetic data, positions Wroxham Crag as Pre-Pastonian, which roughly correlates with the later part of the Tiglian TC4c of the Dutch succession (Lister, 1998), i.e. ca. 1.8 Ma. One *M. meridionalis* tooth was analysed from the Wroxham Crag deposits at East Runton in preparative duplicate.

4.3.1.7.2. Norwich Crag Formation: *M. meridionalis* & *A. arvernensis*

Sample name: NCME1 [BGS: GSM1385], NCAE1 [BGS: GSM5988], NCAE2 [BGS: GSM7971]

NCME1 - Holton gravel pit (approx. TM 405773)

NCAE1 – Easton Bavents (TM 518787)

NCAE2 – Whittingham (approx. TL 720989).

The Norwich Crag Formation succeeds the older Red Crag Formation, which forms part of the Crag group in East Anglia (Hamblin *et al*., 1997). The East Anglian Crag deposits have been biostratigraphically correlated to the continental European record based on mammals, molluscs, foraminifera and dinoflagellates (Hamblin *et al*., 1997). The Norwich Crag Formation comprises onshore shelly sand deposits, formed in shallow water environments during one or more climatically forced marine transgression/regression depositional cycles. Within the shelly sands of the Norwich Crag are interbedded gravels and clay bodies. The deposits are thought to have been laid down during the Thurnian,

Antian (Bramertonian) and Pre-Pastonian/Baventian stages of the British Early Pleistocene (Funnell, 1998; Mayhew, 2013).

The biostratigraphy of the Norwich Crag Formation correlates with the European Mammalian zone MN17 and includes diagnostic species such as *Lemmus kowalskii* and *Mimomys tigliensis* (Mayhew, 2013). Localities ascribed to the Norwich Crag Formation are not necessarily of identical age and cover a long-time period (Mayhew, 2013), likely to be between ~1.9 and 2.2 Ma (Hamblin *et al*., 1997). IcPD data from *Bithynia* opercula from the Norwich Crag Formation at Thorpe Aldringham, support an early Early Pleistocene age for these deposits (Penkman *et al*., 2013).

The Early Pleistocene deposits at Easton Bavents comprise undifferentiated Norwich Crag deposits overlain by Easton Bavents Clay, which are in turn overlain by the Westleton Beds, all of which form part of the Norwich Crag Formation (Funnell & West, 1962). The Easton Bavents Clay deposits lie between +1 to +3 m O.D. and are less than 3 m thick. They are compositionally similar to the Chillesford Clay, and based on palaeomagnetic polarity and floral and faunal stratigraphies, are thought to have been laid down in a single cold stage during the Pre-Pastonian *a*/Baventian (Zalasiewicz *et al*., 1991). The underlying Crags are of the temperate Antian/Bramertonian Stage. NCAE1 was a lower molar from Easton Bavents [TM 518787] and could be from the Westleton Beds or lower Norwich Crag Formation. The sites of Holton gravel pit and Whittingham are not documented in the literature and therefore little is known about the stratigraphy of these sites. All three teeth from the Norwich Crag Formations were analysed in preparative duplicate.

4.3.1.7.3. Red Crag, Suffolk: *A. arvernensis*

Location: Felixstowe (approx.TM302346)

Sample name: RCAE1 [BGS: GSM116468], RCAE2 [BGS: GSM2204]

The Red Crag Formation is located over parts of Essex and southeast Suffolk, and consists of inshore marine shelly sand deposits containing terrestrial mammalian fauna (Mathers & Zalasiewicz, 1988). It is typically 10 - 40 m thick and lies between elevations of + 40 to – 40 m above sea level (Mathers & Zalasiewicz, 1988). The Red Crag comprises deposits from the Waltonian, Pre-Ludhamian and Ludhamian Stages of the British Late Pliocene (Gibbard *et al*., 1998; Head, 1998). The Red Crag is underlain by the 'Red Crag Basement Bed' that contains reworked fossils (including mammals) of Pliocene age, and these are mixed in the collections with material from the Red Crag proper but can be distinguished by a highly

polished appearance. Biostratigraphy based on dinoflagellates and foraminifera correlates these deposits to ca. 2.6-2.4 Ma (Head, 1998; Funnell, 1998). Therefore, the majority of mammalian material recovered from the Red Crag proper is likely to be of Pre-Ludhamian age (Rivals *et al*., 2015). Proboscidean fauna were recovered from these deposits, including *M. rumanus* and *A. arvernensis* (Lister & van Essen, 2003).

The teeth analysed in this study are from the Red Crag deposits at Felixstowe, the stratigraphy of which has been described by Reid (1890). These teeth from the Red Crag are the oldest samples analysed in the study and should yield the greatest amino acid D/L values. Analysis of two *A. arvernensis* teeth from the Red Crag deposits were conducted in preparative duplicate.

4.3.1.7.4. Early Pleistocene sites results summary:

The extent of racemisation in the tooth from East Runton is much greater than the extent of racemisation in the enamel from next youngest site at West Runton. A large interval in racemisation values is observed for Glx, Ala and Phe and corresponds to the ~million-year time gap between materials analysed in this study. However, this intermission is not observed in the Asx data, indicating that Asx may have very limited temporal resolution over this time period. The temporal range of enamel AAR is dictated by the time taken for each amino acid to reach equilibrium (or close to) in a particular temperature region. Asx is the fastest racemising amino acid in this study, owing to its fast rates of racemisation when free (Smith & Reddy, 1989) and its ability to racemise in chain via a succinimide intermediate (Brennan & Clarke, 1993). The extent of Asx racemisation in the teeth from the Red Crag is only just approaching the upper limits of Asx racemisation. In contrast, Glx has the slowest rate of racemisation of the four amino acids studied and its extent of racemisation is approaching 0.3 in both the FAA and the THAA content. This level of Glx racemisation is comparable the extent of racemisation in Devensian age material from the UK when analysing the IcPD in opercula (Penkman *et al*., 2011; 2013). This indicates that the application of enamel AAR may extend beyond the Pleistocene. AAR analysis of *Bithynia* opercula has indicated that Asx loses temporal resolution at sites older than ~130 ka due to Asx racemisation approaching equilibrium (Penkman *et al*., 2013). The rate of racemisation in enamel is slower than in *Bithynia* opercula (Figure 3.22) and therefore, enamel Asx AAR should be able to temporally resolve material older than ~130 ka, but will still be limited by the same loss of resolution at higher Asx D/L values.

The extent of racemisation in the teeth from the Red Crag formations is greater than observed in the teeth from the Norwich Crag deposits, which stratigraphically lie above the Red Crag and thus, is consistent with a younger age. The separation in D/L values between the Red and Norwich Crag deposits in all four amino acids indicate that enamel AAR is able to effectively distinguish between samples of this age from UK deposits. Glx appears to yield the greatest separation between the three deposits and thus is likely to produce the greatest temporal resolution for this period. However, the separation in Glx racemisation between the least racemised sample from the Norwich Crag Formation (Whittingham; NCAE2) and the sample from the Wroxham Crag (ERME1) is small and thus it is unlikely that enamel AAR will be able to effectively resolve the chronology of these two sets of deposits.

4.3.1.8. Patterns of racemisation within the Lower Thames terraces

The Lower Thames terrace comprises a series of fluvial deposits downstream of central London. Drainage of this area by the river Thames began during the Anglian/Elsterian Stage and was caused by a glacial diversion (Gibbard, 1979; Bridgland & Gibbard, 1997). Four terraces have been identified in this area and comprise primarily flint-rich-cold-climate gravels with corresponding interglacial deposits (Bridgland & Schreve, 2004). The series of deposits that encompass the Lower Thames terraces are well studied (Schreve, 2001; Bridgland *et al*., 2003; Bridgland & Schreve, 2004; Bridgland, 2006) and therefore provide a template with which to interpret a section of the enamel AAR dataset.

In this study, enamel from seven sites from the Lower Thames terraces has been analysed. The extent of racemisation in these samples is relatively low (D/L values 0.1-0.3). Therefore, a faster racemising amino acid, such as Asx would be expected to yield a higher degree of temporal resolution than the slower racemising amino acids, such as Glx. However, the extent of Asx racemisation is not able to place the site from the Lower Thames in the order prescribed by our current understanding of their relative chronology. This potentially indicates that even the extent of Asx racemisation in enamel is not able to temporally resolve sites in this time range.

In general, the extent of Phe racemisation increases with age. In contrast to the other amino acids studied, the two samples from the deposits at St James have yielded similar extents of Phe racemisation (Figure 4.10). The extent of Phe racemisation from the deposits at St James is lower than those observed for enamel from the deposits at Ilford and is therefore in agreement with the current understanding of the relative chronology of the two sites. There is overlap in the extents of Phe racemisation between the sites of

Crayford and Ilford. This indicates that this amino acid is not able to temporally resolve MIS 6 and 7. The samples from Little Thurrock and Grays Thurrock are thought to have been laid down during MIS 9. The extent of racemisation from these sites is intermediate between the MIS 6/7 deposits of Ilford and the MIS 11 deposits at Swanscombe, which fits with the terrace stratigraphy. The extent of racemisation in enamel is therefore concordant with age, but the slower rate of racemisation means a lower resolution than for *Bithynia* opercula (Figure 4.11).

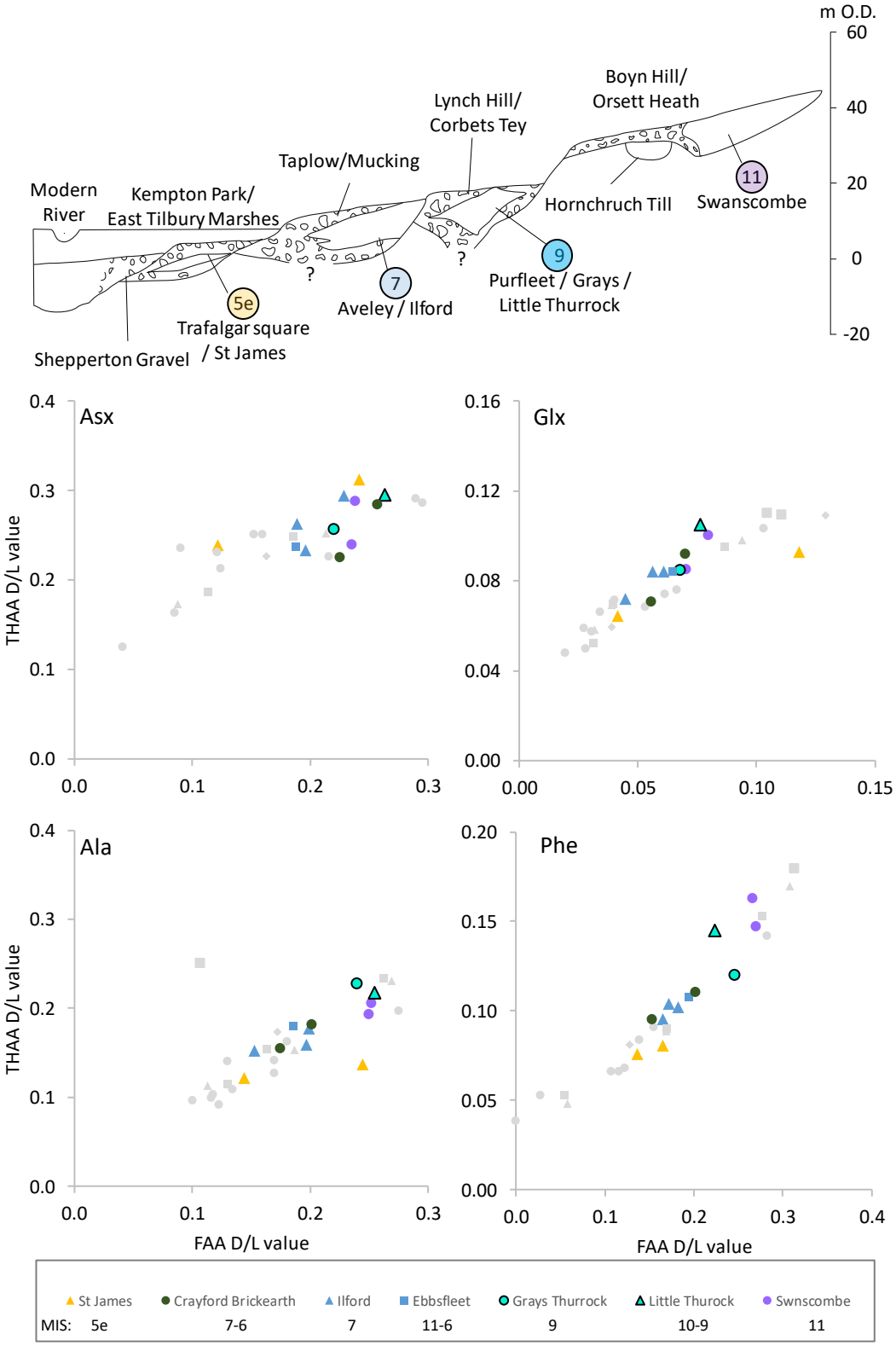

Figure 4.10. Idealised transverse section through the Lower Thames terrace (Bridgland et al., 2014) and FAA vs THAA D/L value plots for Asx, Glx, Ala and Phe, highlighting Lower Thames sites.

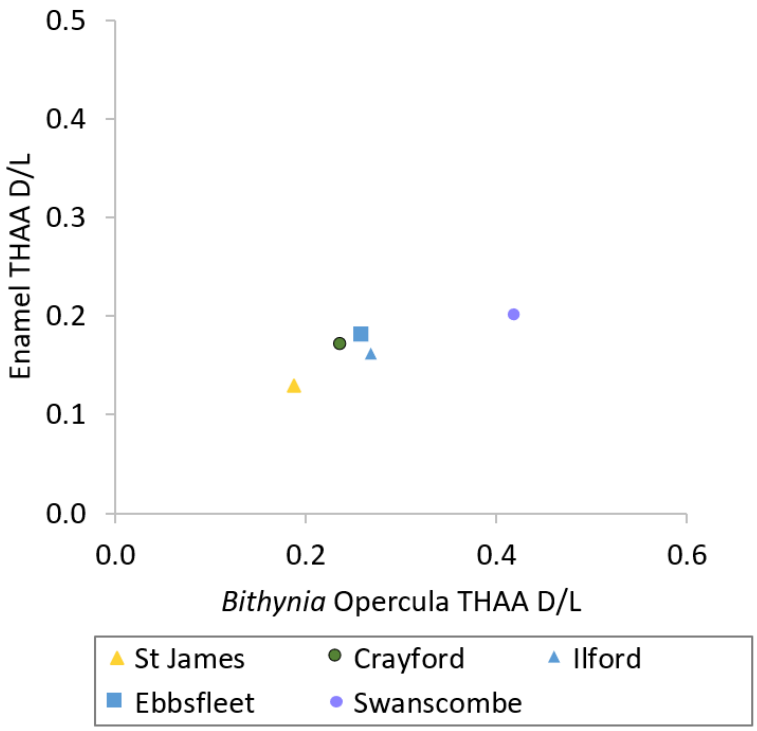

Figure 4.11. Extent of Ala racemisation in enamel vs Bithynia *opercula from contemporaneous deposits within the Lower Thames river terrace. Extent of racemisation increases in both biominerals with increasing independent evidence of age.* Bithynia *opercula D/L values are taken from Penkman* et al. (2013).

4.3.2. Overall trends in racemisation

Overall, the extent of racemisation increases with independent evidence of age for all four amino acids studied (Figure 4.12). In general, the extent of FAA and THAA racemisation is highly correlated for all four of the amino acids studied (Figure 4.8). This strongly indicates that enamel is sufficiently retaining the THAA and FAAs and therefore is acting as a closed system over Quaternary time scales. Each of the amino acids are racemising at different rates (Asx > Ala > Phe >> Glx) and this results in different temporal resolutions. Asx has the fastest rate of racemisation, which is facilitated by a relatively fast rate of racemisation when free, and also the formation of a cyclic succinimide which enables in-chain racemisation when bound (Smith & Reddy, 1989; Brennan & Clarke, 1993). Consequently, Asx is more likely to yield a higher resolution during the late to mid-Pleistocene. In contrast, Glx D/L values are < 0.4 after ~2.5 Ma and may therefore be used to temporally assign material spanning a longer time scale. This slow rate of racemisation is thought to be in part caused by the formation of pyroglutamic acid (Wilson & Cannan, 1937).

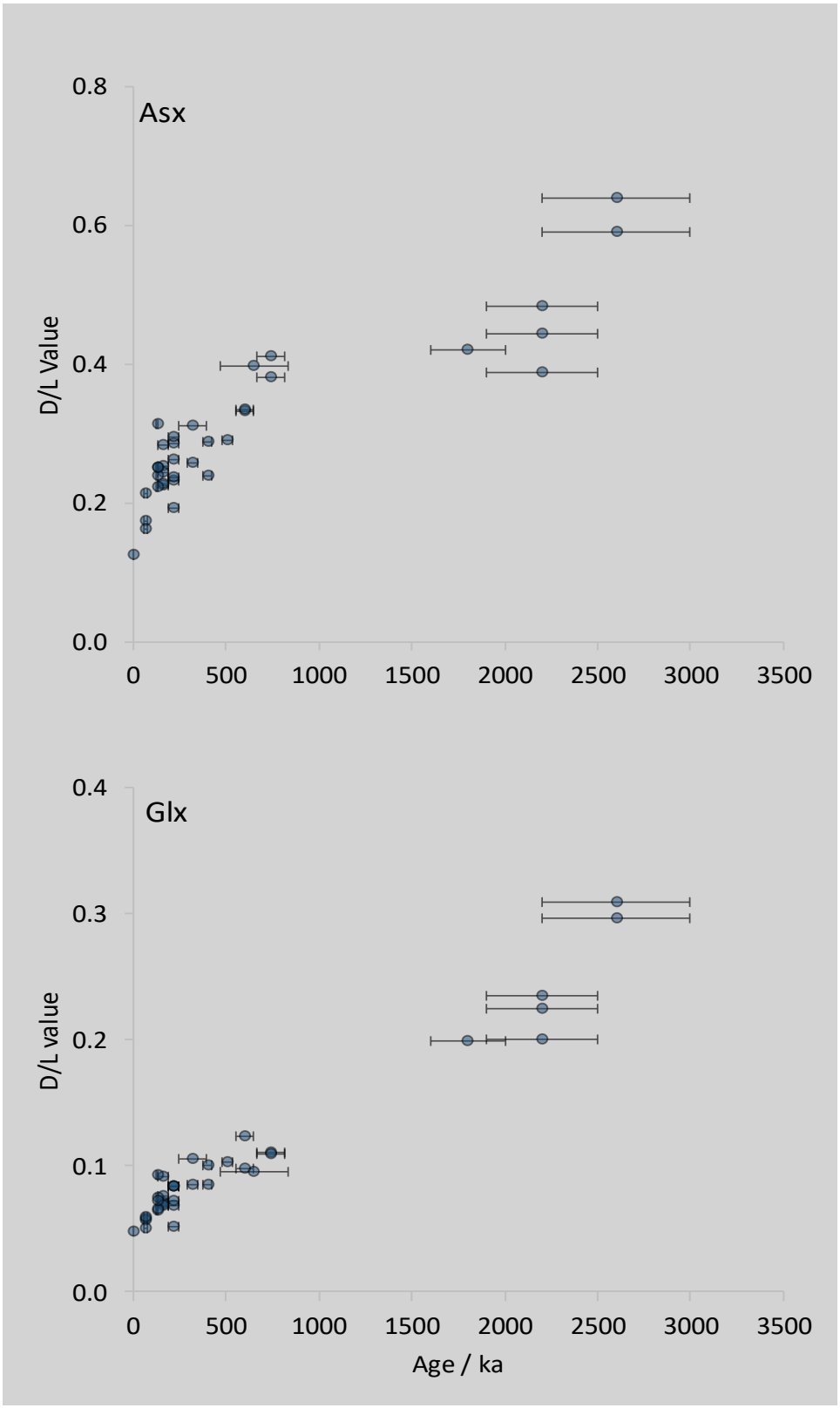

Figure 4.12. THAA D/L values of Asx, Glx, Ala and Phe of Proboscidean enamel from a range of temporally well constrained UK sites plotted against independent evidence of age. Error bars are estimates of the temporal constraints of each sample based on the provenance of the sample and length of the time period it has been correlated with.

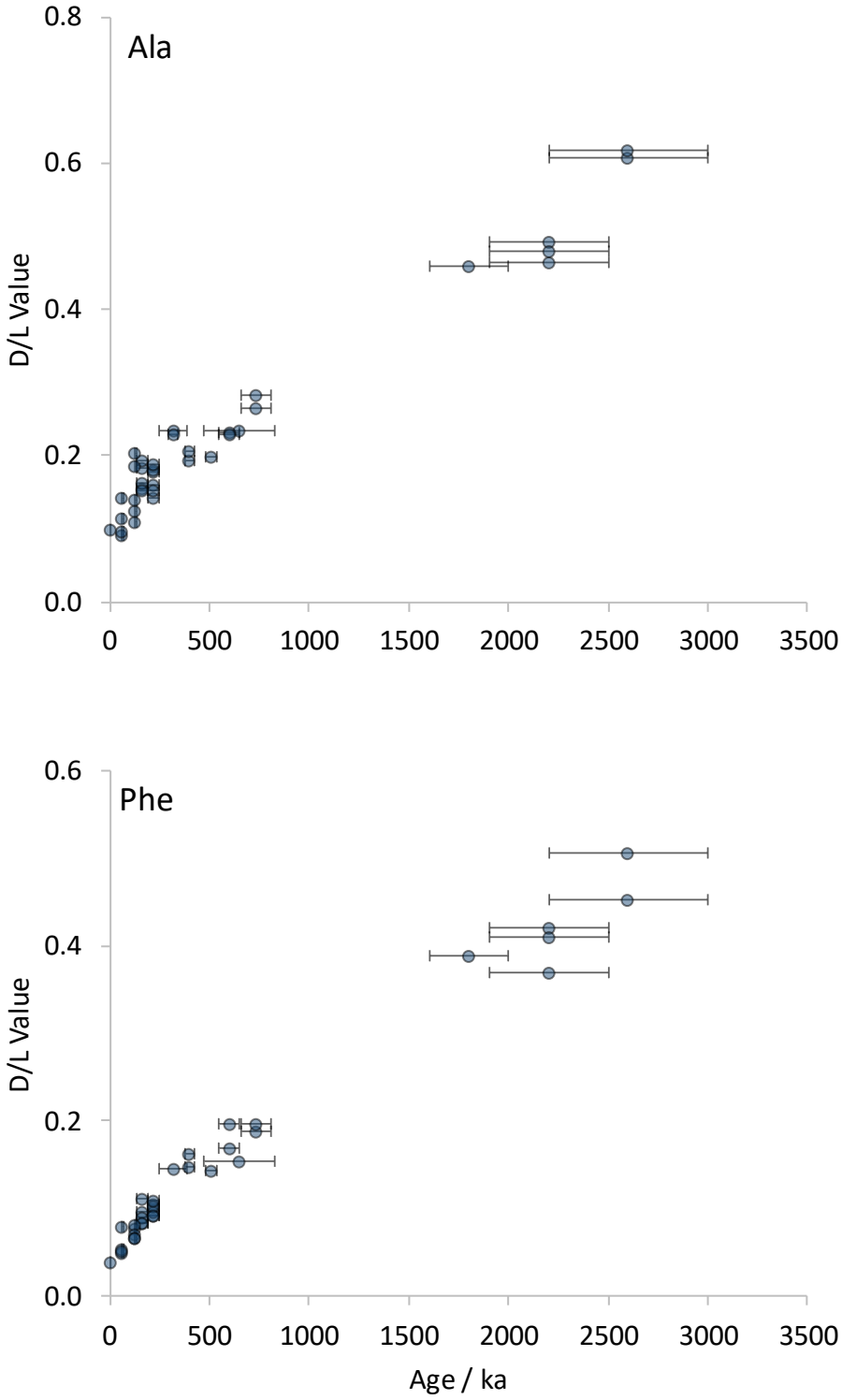

Figure 4.12 continued. THAA D/L values of Asx, Glx, Ala and Phe of Proboscidean enamel from a range of temporally well constrained UK sites plotted against independent evidence of age. Error bars are estimates of the temporal constraints of each sample based on the provenance of the sample and length of the time period it has been correlated with.

Sites have been colour-coded based on their independent evidence of age (Figure 4.8). In general, there is some overlap between MIS clusters, indicating enamel AAR cannot temporally resolve material to individual marine oxygen isotope stages. However, for dating pre-Anglian material, this technique can provide resolution between samples that are separated by a few MIS. The dataset is also able to place samples from the Cromerian Complex in the correct relative order, but due to the limited number of samples obtained from this time period, the exact resolution of the technique has not been fully established.

4.3.3. Hydrolysis: Increase in the percentage of FAAs

Hydrolysis of the proteinaceous portion of biominerals occurs progressively over time, resulting in a higher percentage of FAAs present in older samples (Miller *et al*., 2000). The evidence of this trend in fossil biominerals is thought to be a strong indicator FAAs are retained and not lost via leaching, thus suggesting a closed system is present (Penkman *et a*l., 2008). Labile peptide bonds (such as those containing serine and aspartic acid residues) hydrolyse the fastest, segmenting the protein chains into smaller peptides. These peptides are further hydrolysed via internal aminolysis, eventually resulting in free amino acids. This general trend of increasing FAA content with age is observed in the amino acids studied in these enamel samples (Figure 4.13).

The outlying sample from Kessingland (KeME2) that had a lower than expected D/L value (Circled in Figure 4.8) also has a lower than expected percentage of FAAs. This is consistent with FAAs leaching out of the enamel and affecting the observed FAA D/L value. This temporary period of open system behaviour may have been caused by crystal changes in the enamel matrix, but this was not explored in this study.

Free Asx is known to be comparatively unstable and therefore its relative concentration is expected to be reduced once the rate of breakdown of Asx is greater than its generation from the bound fraction. The oldest material analysed in this study is from the Red Crag deposits in Norfolk, thought to be Pliocene in age. The percentage of free Asx in these samples is much lower than in those from the younger Norwich Crag deposits. This trend is not as pronounced in Glx, Ala or Phe, supporting the evidence that Asx is less stable at this antiquity than the other studied amino acids (Miller *et al*., 2000).

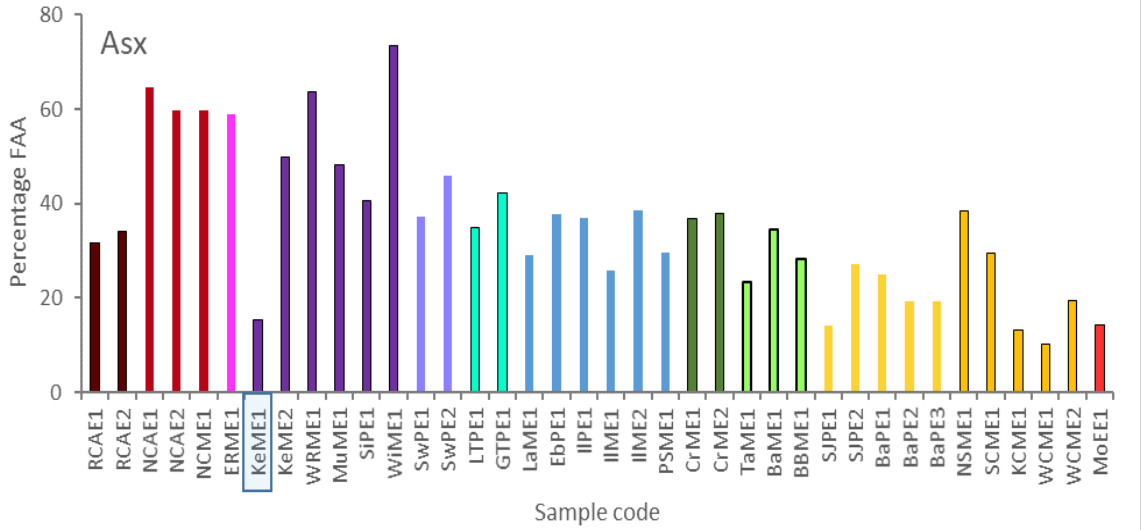
Asx
Percentage FAA
80
60
40
20
0
RCAE1
RCAE2
NCAE1
NCAE2
NCME1
ERME1
KeME1
KeME2
WRME1
MuME1
SiPE1
WiME1
SwPE1
SwPE2
LTPE1
GTPE1
LaME1
EbPE1
IIPE1
IIME1
IIME2
PSME1
CrME1
CrME2
TaME1
BaME1
BBME1
SJPE1
SJPE2
BaPE1
BaPE2
BaPE3
NSME1
SCME1
KCME1
WCME1
WCME2
MoEE1
Sample code

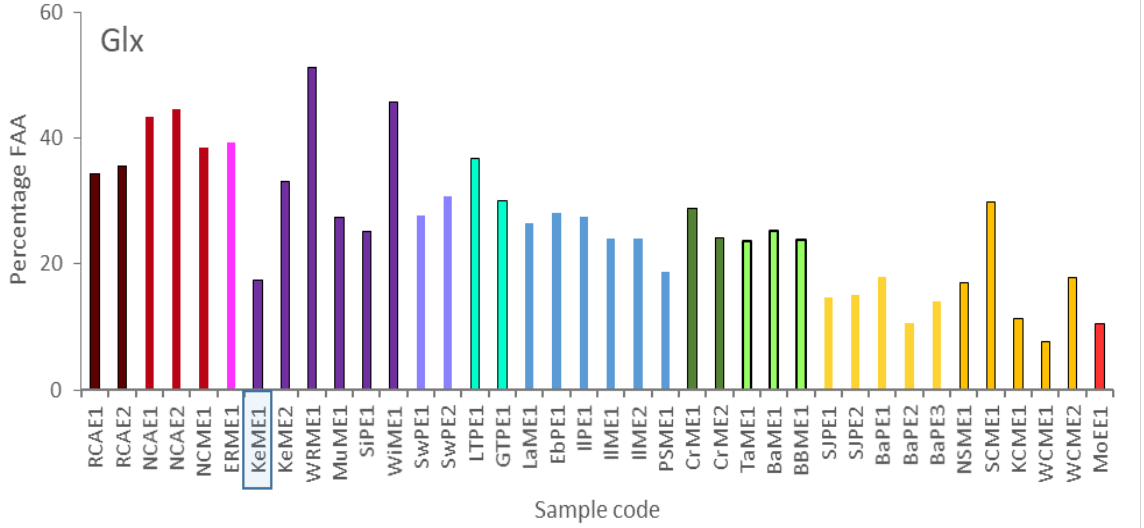
Glx
Percentage FAA
60
40
20
0
RCAE1
RCAE2
NCAE1
NCAE2
NCME1
ERME1
KeME1
KeME2
WRME1
MuME1
SiPE1
WiME1
SwPE1
SwPE2
LTPE1
GTPE1
LaME1
EbPE1
IIPE1
IIME1
IIME2
PSME1
CrME1
CrME2
TaME1
BaME1
BBME1
SJPE1
SJPE2
BaPE1
BaPE2
BaPE3
NSME1
SCME1
KCME1
WCME1
WCME2
MoEE1
Sample code

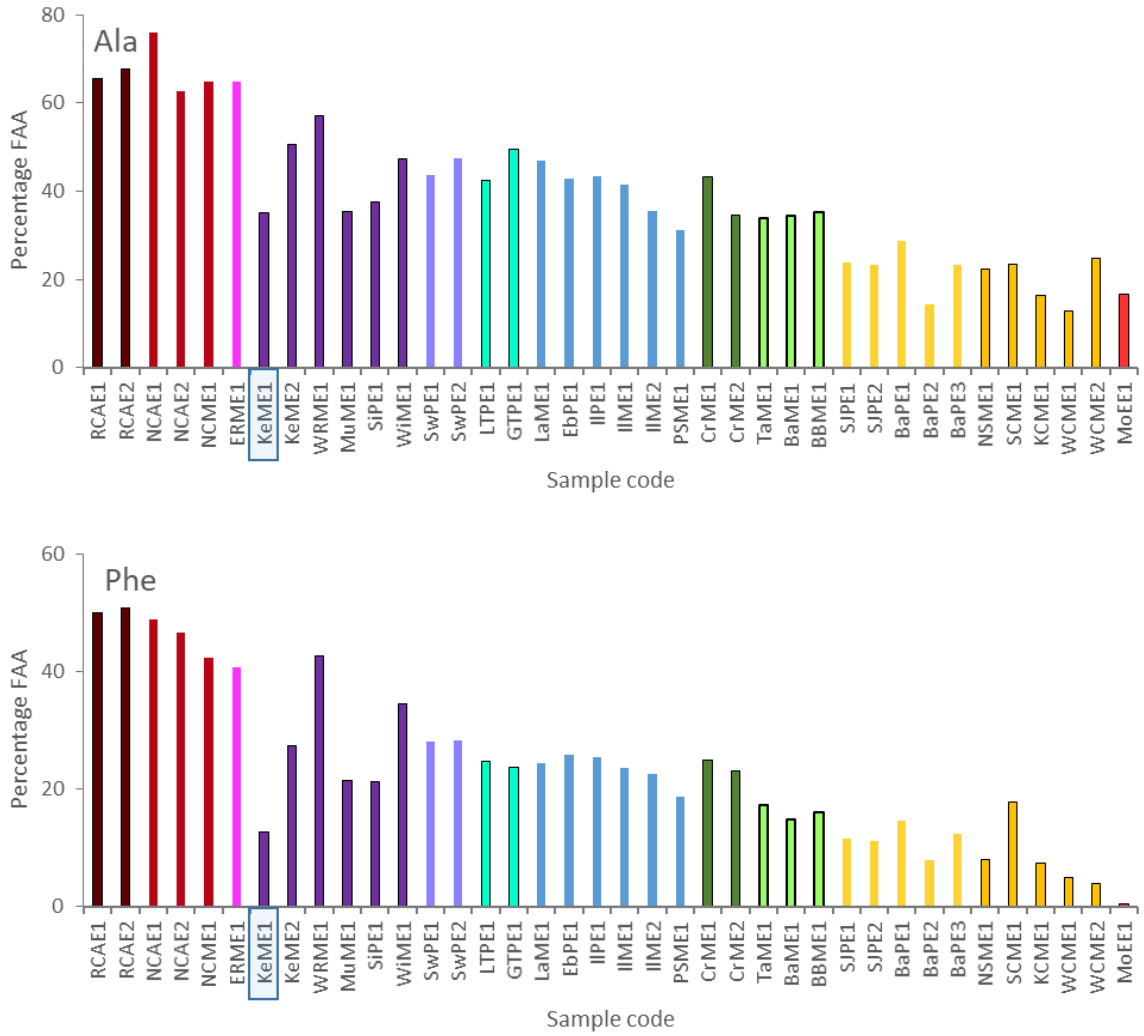

Figure 4.13. Percentage of FAAs Asx, Glx, Ala and Phe in the fossil enamel samples from the UK sites. Samples are arranged in decreasing age from left to right and are coloured using the same scheme used for the FAA vs THAA D/L plots. Trends show an increasing percentage of FAAs with increasing antiquity. KeME1 has been highlighted because it falls outside the expected trend.

4.3.4. Diagenetic breakdown of Ser

Even in a closed system, the concentration of amino acids in biominerals decreases gradually over time (Miller, 2000). The amino acid composition of biominerals changes over time, with Asx, Ser and Gly becoming less prevalent (Matter *et al*., 1969; Penkman *et al*., 2013) due to the selective preservation of proteins/peptides with certain amino acid compositions and the relative diagenetic stability of an amino acid side chain (Akiyama, 1980). For example, Ser is known to be a relatively unstable amino acid when free, and undergoes a dehydration degradation pathway via an aldol reaction whilst peptide bound (Bada & Mann, 1980). Ser has also been found to be thermally unstable, breaking down into Gly and Ala whilst both peptide bound (Akiyama, 1980) and as a free amino acid

(Vallentyne, 1964). The ratio of the concentration of Ser to one of its breakdown products (such as Ala) can therefore be used as an indicator of age, with a higher [Ser]/[Ala] value indicating less diagenetic breakdown and thus younger samples (Walton, 1998). However, the temporal resolution of this ratio is comparatively poor when compared to other diagenetic process, such as racemisation, and is therefore better used in tandem with other analyses or as an indicator of potential contamination.

The [Ser]/[Ala] values in the teeth decreases with increasing age (Figure 4.14), which is consistent with data from other biominerals (Penkman *et al*., 2010; Tomiak *et al*., 2013) and also consistent with closed-system behaviour of the intra-crystalline amino acids over these time scales. However, the temporal resolution of these data is not able to correlate specific samples with individual climate zones in the MIS record.

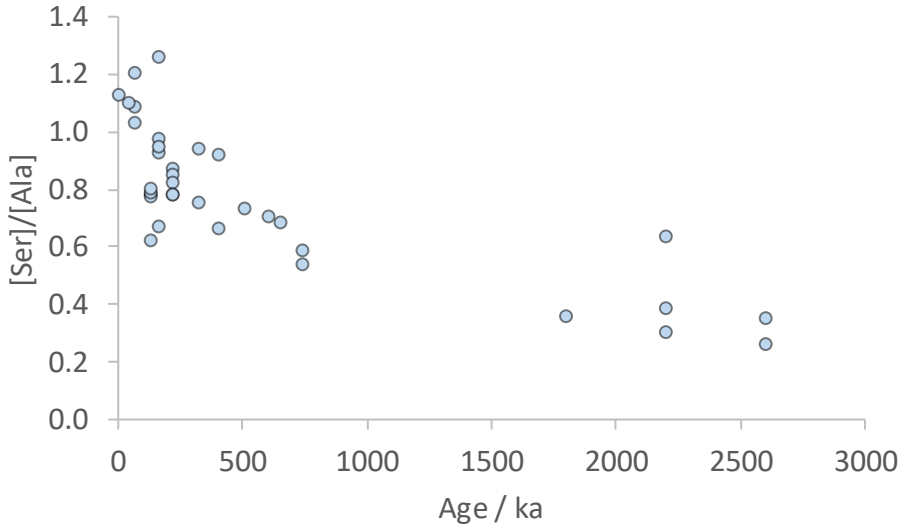

Figure 4.14. Ratio of Ser to Ala concentrations decreasing with independent evidence of age, which indicates enamel is acting as a closed system.

4.3.5. Taxonomic effect

Taxonomy has been shown to influence the rates of AAR within biominerals at both the family and genus levels (Wehmiller, 1980; Hill, 1965; Bright & Kaufman, 2011; Reichert *et al*., 2011). The protein composition and amino acid bond strengths are thought to cause differences in IcPD, which can vary between taxa (Hill, 1965; Patel & Borchardt, 1990; Collins *et al*., 1999). In particular, the relative proportion of Asx is thought to influence AAR rates between taxa, potentially due to bonding interactions with the inorganic matrix (Weiner & Hood 1975; Wehmiller, 1980; Demarchi *et al*., 2016).

The material used in this chronology is from the taxonomic order Proboscidea but contains four different genera; Elephas (*E. maximus*), Mammuthus (*M. meridionalis, M. trogontherii* and *M. primigenius*), Anancus (*A. arvernensis*) and Palaeoloxodon (*P. antiquus*). Each of these species is separated by thousands, or millions, of years of evolution (Lister, 2001) and thus, there has been time for significant evolutionary changes to the primary sequence of proteins or mineral formation of their teeth to have occurred.

The FAA vs THAA D/L values for the different species plot along the same trajectory. This does not signify that the rate of racemisation is the same between species, but it does indicate that the protein breakdown and closed system properties are similar (Figure 4.15).

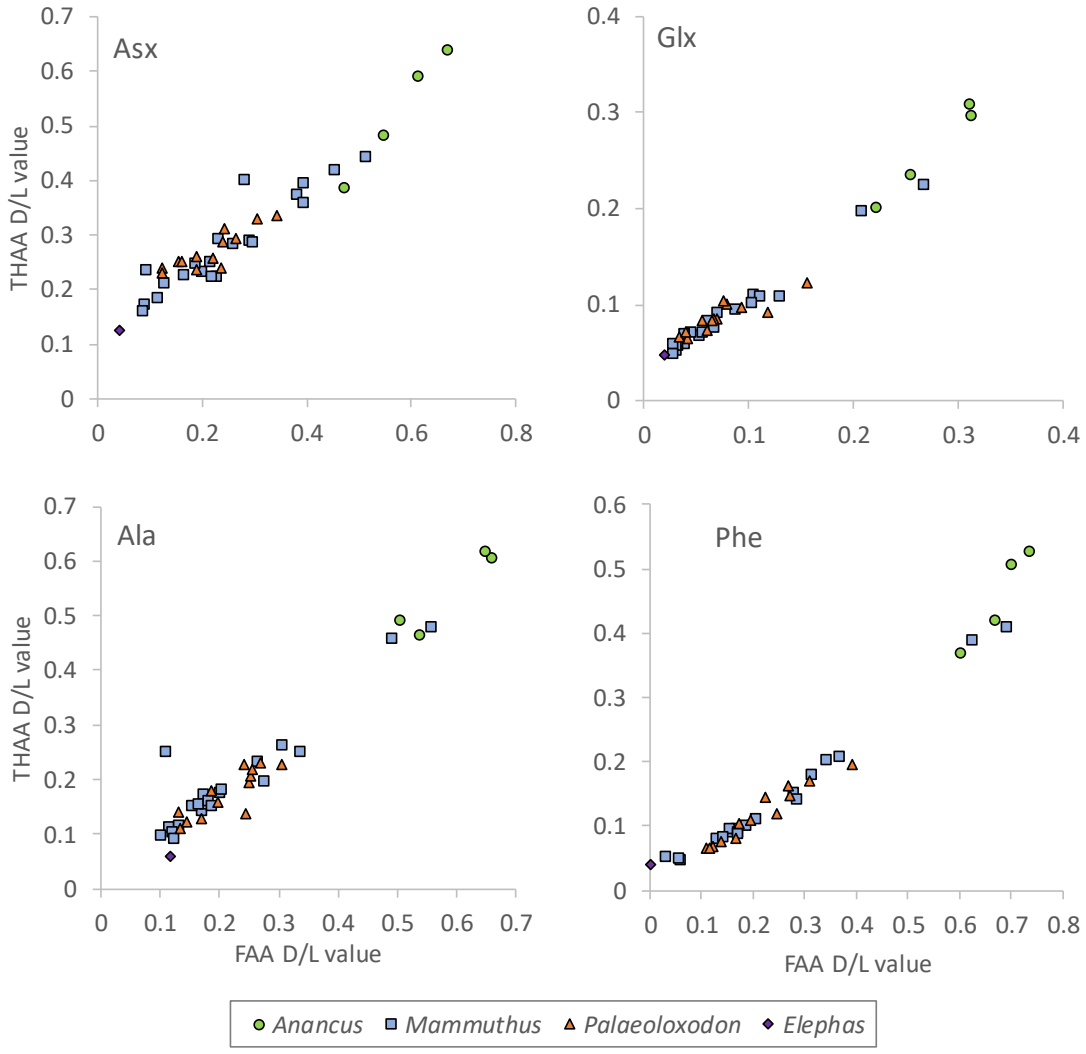

Figure 4.15. Extent of IcPD within bleached Anancus*,* Mammuthus, Palaeoloxodon *and* Elephas *enamel from a range of UK sites. The patterns of FAA vs THAA racemisation appear to be broadly analogous between the studied taxa.*

The relative variance in rates of racemisation can be evaluated at sites with more than one taxon; in this study Ilford and the Norwich Crag furnished relevant material. The deposits at Ilford contain both *Mammuthus* and *Palaeoloxodon* specimens from the same horizon. Analysis of the D/L values has yielded similar results, but due to the limited number of samples (n=3), statistical tests such as two-tailed t-tests were not conducted. The difference in mean THAA D/L values lies between 1 and 8 % and for FAA lies between 1 and 11 % of the average values, which is similar to the extent of variability expected between samples of the same taxon (1 - 10%). The mean THAA compositions of the two genera (*Mammuthus* and *Palaeoloxodon*) from Ilford are also very similar (Figure 4.16), indicating the protein breakdown is similar, and thus demonstrating they are likely to be suitable for direct comparison. Additionally, *Anancus* and *Mammuthus* samples from Norwich Crag deposits also yield similar D/L values, potentially indicating that taxonomic differences within the Proboscidae are not significant. However, these Crag specimens are not from the same deposits and two of the samples have poor provenance, and thus may differ in age slightly.

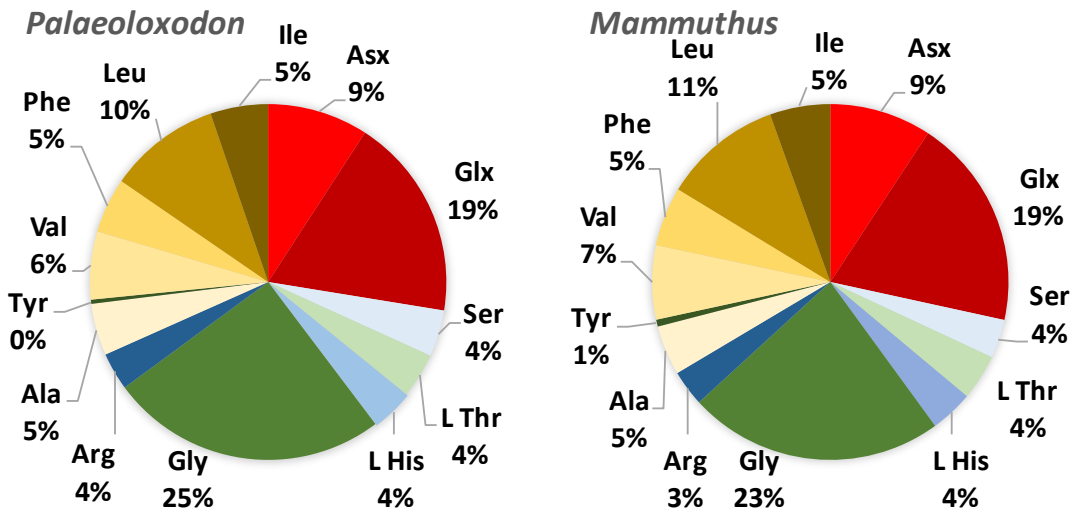

Figure 4.16. Mean THAA compositions of Palaeoloxodon and Mammuthus from the deposits at Ilford.

4.4. Conclusions

In summary:

1. Analysis of 37 teeth from a range of UK sites has consistently demonstrated a predictable breakdown in the intra-crystalline proteins isolated from Elephantidae tooth enamel, making enamel a suitable biomineral for use as a geochronological tool.
2. Minimal intra-tooth variability was observed in amino acid D/L values from comparison of six different sample locations from a tooth from the Thorpe sand and gravel deposits at Tattershall.
3. No detectable taxonomic affect was observed between the three genera of Proboscidea in this study. However, the number of samples from the sites with multiple taxa was very limited and therefore limits the robustness of these conclusions. Further investigations, using a larger number of specimens from the same sites are required to robustly investigate taxonomic affects within the taxonomic order Proboscidae.

Chapter 5: Mediterranean island dwarfing: a pilot Sicilian elephant geochronology

Island dwarfing of elephantids is a phenomenon that is evidenced across the globe (Roth, 1992). Biodiversity and endemism on islands is often higher than on the mainland, which is in part due to the low rate of immigration and emigration of terrestrial species (Myers *et al*., 2000) and higher rate of evolution (Millien, 2006). Evolutionary changes in body mass size on islands has been linked to resource limitation (Heaney, 1978), reduced inter-specific competition and reduced predation (Raia & Meiri, 2006). Larger fauna tend to become smaller after isolation on an island, with small species tending to become larger (van Valen, 1973), although some notable exceptions have been documented (Meiri *et al*., 2004; 2008).

Proboscideans are excellent swimmers and thus during the Pleistocene appear to have colonised and become isolated on islands when sea levels changed (Stock, 1935). Dwarf or small-size mammoths (*Mammuthus exilis*) have been unearthed from the Californian Channel Islands: which are descended from the larger, North American mammoth (*M. columbi*; Stack & Furlong, 1928). Wrangel Island in the Arctic Ocean has yielded *M. primigenius* remains that fall into two sizes; the larger specimens date to the late Pleistocene and the small specimens (teeth 20-25 % smaller) have been radiocarbon dated to as late as ~3700 years BP (Vartanyan *et al*., 1995). Alongside the dwarf elephants recovered from the Mediterranean islands are a range of insular taxa including dwarf hippopotamus, dwarf deer and giant rodents (Marra, 2005).

Recovered from the Isle of Sicily, at least three differently sized species of dwarf elephant have been identified from the Pleistocene: small-sized (<1 m tall) *E. falconeri*, medium-sized *E. mnaidriensis*, and 'large-sized' *Palaeoloxodon sp. nov* (Herridge, 2010). Chronologically constraining the arrival and extinction of these species of elephant on the island is paramount to understanding the process of their evolution and their demise. Several techniques have been employed to date the Mediterranean dwarf elephants (^{14}C, ESR, U-series), however, the application of these techniques has been shown to have a low reliability/precision in most instances due to limitations in the techniques used (Herridge, 2010). Enamel AAR has the potential to directly date and therefore establish a relative chronology for these species. This can therefore address some of the key questions that

remain regarding whether *E. mnaidriensis* could potentially be older, and thus ancestral to, *E. falconeri* and if specimens assigned to the large-sized species are contemporaneous (Herridge, 2010).

In this chapter, samples from six elephant teeth from strategic Sicilian sites have been analysed for their IcPD. The samples have been taken from teeth that are also being analysed by ESR. All six samples are from the elephant species *E. falconeri*. The main aim of this study was to determine if enamel AAR is capable of temporally resolving samples in this region. The limited number of samples from each site (1 or 2) restricts the strength of the relative chronology but will provide an initial framework on which to build a larger and more targeted study. It will also indicate the extent of protein degradation and thus the likely time range enamel AAR will be able to be applied, informing future studies.

5.1. Mediterranean island dwarfing: experimental

5.1.1. Spinagallo cave

Sample name: SpPE1 [272]

Spinagallo cave is a complex site located in the Hyblean Plateau, inland of Syracuse. The site contains three distinct fossiliferous layers: a low marine 'Panchina' (Layer 2) which primarily contains molluscan fauna, overlain by an upper bone breccia horizon (Layer 3) which contains the remains of *P. mnaidriensis* and by red calcareous sands (Layer 4) containing *E. falconeri* (Ambrosetti, 1968). *E. falconeri* has a smaller body mass than *E. mnaidriensis* and thus according to the theory of insular dwarfism, the initial interpretation of the depositional sequence was that despite overlying Layer 4, Layer 3 must be stratigraphically older (Ambrosetti, 1968). Whole-enamel AAR dating of elephant remains from Spinagallo (Belluomini & Bada, 1985; Bada *et al*., 1991) and biostratigraphical evidence from the Comiso-Chiaramonte Gulfi area revealed that there may have been several separate invasions of continental elephants to Sicily (Bonfigilo & Insacco, 1992). Subsequently, the stratigraphical order of Layers 3 and 4 has been re-evaluated, and it is now thought that Layer 4 is stratigraphically older than Layer 3 (Bada *et al*., 1991; Bonfiglio & Insacco, 1992). Belluomini and Bada (1985) proposed an age of 550 ±165 ka for the Spinagallo elephants (exact deposits were unspecified) based on isoleucine epimerisation, calibrated to the central Italian deposits at Isernia la Pineta. One *E. falconeri* tooth from Spinagallo cave (layer 4) was analysed in preparative duplicate.

5.1.2. Contrada Frategianni and Cozzo del Re

Sample name: Contrada frategianni – CoPE1 [CF02/2B], CoPE2 [CF572] Cozzo del Re – CoPE4 [CR1a1/654], CoPE5 [CR1e/652]

Cozzo del Re and Contrada Frategianni are hills to the south-west of Comiso and they form part of the Comiso-Chiaramonte Gulfi area (Lat: 37.03134, Long: 14.70128). Both the masculine and feminine morphotypes of *E. falconeri* have been found within the limnic deposits of the Comiso-Chiaramonte Gulfi area (Bonfiglio & Insacco, 1992). A reconstructed lithographic sequence of the succession at Cozzo del Re and Contrada is shown in Figure 5.1. The age of the sequence is largely based on the biostratigraphical evidence from the elephant remains (Bonfiglio and Insacco, 1992). *P. falconeri* bones were recovered from units b, e and h and thus were thought to be a roughly analogous in age to the *E. falconeri* from Spinagallo cave and Luparello, which are of Middle Pleistocene age (Belluomini & Bada, 1985). However, the Comiso-Chiaramonte Gulfi area has also yielded evidence of an *E. falconeri* endemic fauna with a greater antiquity, which based on biostratigraphy is thought to have originated during the Early to early Middle Pleistocene (Bonfiglio & Insacco, 1992). These findings support the assumption that Sicily experienced two elephant immigrations during the Pleistocene (Bonfiglio & Insacco, 1992). Two *Elephas* teeth from Cozzo del Re from red aeolian sand layer (Bonfiglio & Insacco's (1992) layer h) were analysed in preparative duplicate. Two *E. Falconeri* teeth from Contrada Fratigianni were analysed in preparative duplicate; CoPE1 was from Bonfiglio & Insacco's (1992) layer b and CoPE2 could be from layers a, b, or e.

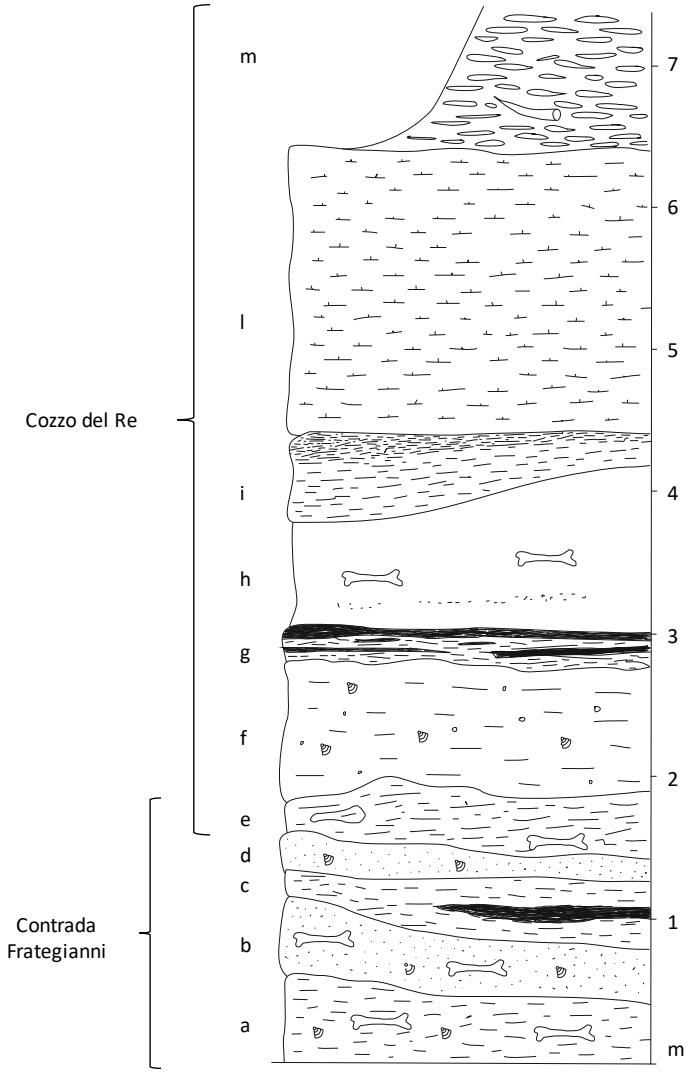

Figure 5.1. Reconstructed lithographic column at Contrada Frategianni and Cozzo del Re. Unit descriptions: a) greenish clay; b) whitish fine sands which contain remains of an elephant larger than Elephas falconeri *Busk; c) grey clays and interbedded lenses of red clays; d) whitish sands containing red sand levels and pulmonate molluscs; e) blue clays containing* Elephas falconeri*; f) earthy limestone with pulmonate molluscs becoming g) clayey upwards, grey and reddish-brown coloured; h) fine bright red aeolian sands containing remains of* Elephas falconeri*; i) towards the summit of h) sands display lenses of blackish clays containing carbonate nodules; l) earthy limestone; m) travertines. Figure and unit descriptions taken from Bonfiglio and Insacco (1992).*

5.1.3. Contrada Mazzaronello

Sample name: CoPE3 [CM1]

The deposits at Contrada Mazzaronello form part of the lumic deposits of the Comiso-Chiaramonte Gulfi area (Figure 5.1). This site has not been extensively studied, and as such little is known about the age of the deposits. One *E. falconeri* tooth from Contrada Mazzaronello was analysed in preparative duplicate.

5.1.4. Experimental protocols

All samples were prepared and analysed using the protocols outlined in Chapter 3, section 3.2. Each tooth was analysed in preparative duplicate alongside standards and blanks to check for contamination.

5.2. Extent of racemisation

Similar extents of racemisation were observed in the four teeth from Contrada Fratigianni and Cozzo del Re (Figure 5.2), indicating that these are likely to be similar in age, within the level of resolution of the method. Except for Asx (which is likely to not yield robust temporal resolution, given the results from Chapter 4), the extent of racemisation in the enamel from the deposits at Contrada Mazzaronello is greater than those from Contrada Fratigianni and Cozzo del Re, indicating the elephant remains at Contrada Mazzaronello are older. The extent of racemisation in the enamel sample from the deposits at Spinagallo cave is generally lower than in the other specimens, indicating that this may be younger in age. This is only clearly observed in the racemisation of Asx; however, Asx is unlikely to yield high temporal resolution in this region of D/L values. It is therefore difficult to state with certainty how instructive this single sample is in attributing a relative age for the elephant remains at Spinagallo cave. The extent of Phe FAA racemisation for all six samples is close to D/L values > 0.7. The temporal resolution of amino acid racemisation is reduced at higher D/L values due to the non-linear relationship between time and racemisation (Bada, 1973). Therefore, Phe may not be the most instructive amino acid for dating samples to this resolution in this region of this age and more weight should be placed on the interpretation of the less racemised amino acids (such as Glx) when estimating relative age.

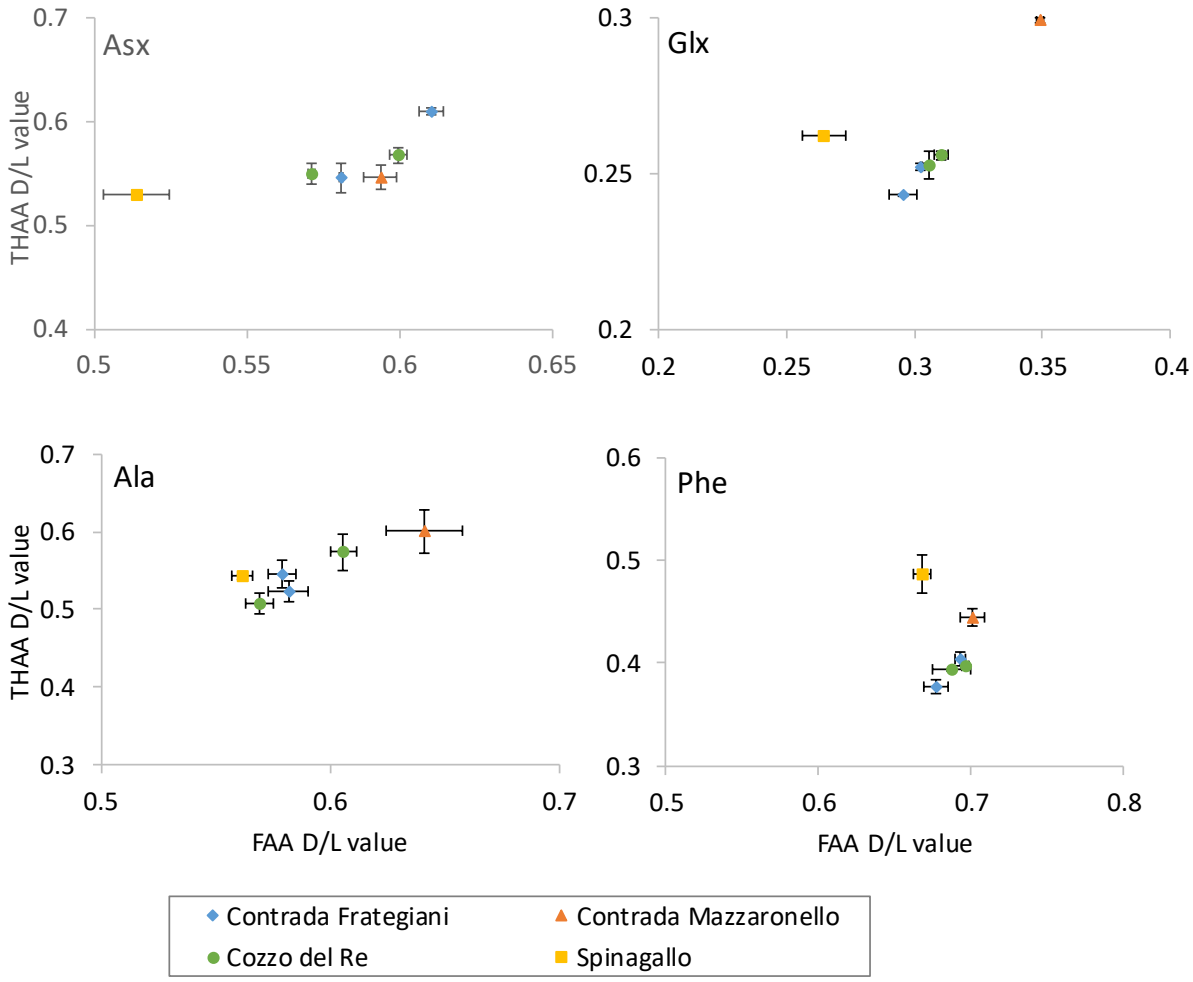

Figure 5.2. FAA vs THAA D/L plots of elephant enamel from four different Sicilian sites. Error bars depict one standard deviation about the mean (n=2).

The relationship between FAA and THAA D/L values in a closed system should remain the same irrespective of differences in depositional temperature; only the overall rate of racemisation should change (Preece & Penkman, 2005; Penkman *et al*. 2008; Crisp *et al*., 2013). This assumes that the processes/mechanisms governing the degradation of proteins and amino acids are comparable at different temperatures. To test this hypothesis the D/L values of the Sicilian Elephantidae material have been compared to Proboscidae data obtained from UK sites. The extent of IcPD observed in the samples from Sicily is comparable to those found in enamel from the Crag deposits in the UK which were laid down during the Early Pleistocene/Pliocene (Figure 5.3). However, due to the increased depositional temperatures in Sicily, this does not relate to a comparable antiquity (the Sicilian material is likely to be much younger). The relationship between the extent of FAA and THAA racemisation appears to be similar in both temperature regions, indicating that

analogous degradational process are occurring in the two different temperature regions. The increased rates of racemisation in the Sicilian enamel indicate that enamel AAR will not have the same temporal span as in the UK, but these faster rates of racemisation my result in greater temporal resolution.

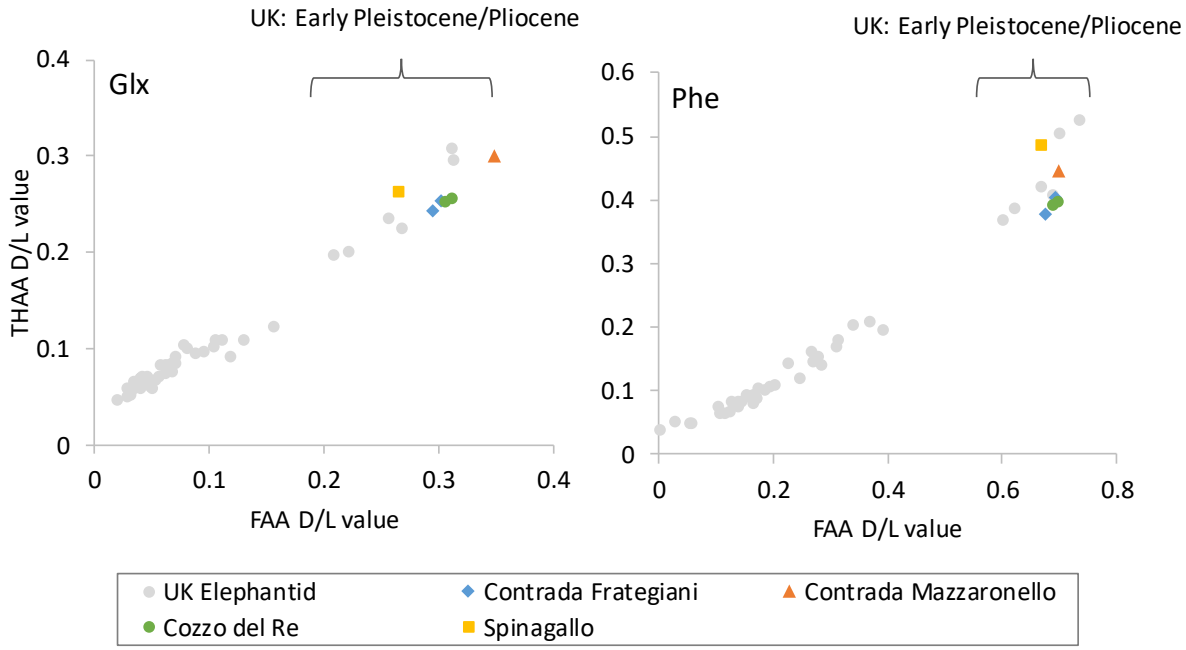

Figure 5.3. Comparison of the extents of racemisation in the Sicilian material to UK Elephantid samples.

5.3. Mediterranean island dwarfing: Conclusions

This pilot study indicates that enamel AAR is potentially capable of chronologically assigning the elephant material found in the Sicily deposits and therefore can be used to start to address some of the unanswered questions regarding the evolution and extinction of these taxa on the island. However, the limited number of samples analysed from Sicilian sites limit the robustness of the conclusions drawn from this study, and so additional samples are required for a stronger interpretation of the relative chronology of elephants in this area.

Chapter 6: Summary of conclusions and future work

At present, directly dating mammalian skeletal remains outside the limits of radiocarbon analysis is challenging. Techniques frequently rely on assumptions that are difficult to account for and thus often yield unreliable age estimates (Zhou *et al*., 1997; Grün *et al*., 2010; Duval & Grün, 2016). Previous attempts to target enamel as a suitable repository of amino acids for AAR geochronological assessment have not been consistently successful (Bada, 1981; Belluomini & Bada, 1985; Blackwell *et al*., 1990). The experiments outlined in this body of work develop a protocol suitable for the routine analysis of the intra-crystalline amino acids in enamel, which has subsequently been used to develop a UK Elephantidae geochronology capable of dating enamel material of unknown age from this region.

The use of HILIC SPE for the extraction of amino acids from inorganic phosphate species yielded mixed results (Chapter 2). A variety of different mobile phase conditions were adjusted, many of which impacted the separation of amino acids from phosphate ions. A mobile phase composition of 30 % MeOH to water adjusted to pH 8 was found to yield the most precise and accurate results. However, single use of HILIC SPE cartridges and limited scalability for multiple analyses meant the protocols using this method were relatively expensive and labour intensive and therefore are not recommended for application to the routine analysis of amino acids in enamel.

A biphasic separation method capable of separating inorganic phosphate species from the bulk amino acid content has also been developed (Chapter 3). This method utilises the pH-dependent formation of a gel, which becomes a biphasic solution upon centrifugation. This method has been shown to: have good amino acid recovery rates, be relatively inexpensive, have a high degree of reproducibility ($1\sigma < 5\%$ of total value) and be capable of scaling up for multiple analyses. Experiments evaluating the impact of different acid and base volumes on the efficiency of separation mean that 25 and 20 µL/mg of HCl (1 M) for the FAA and THAA fractions respectively is recommended for the demineralisation and re-dissolution of samples, and 28 µL/mg of KOH (1 M) is recommended for the formation of a monophasic gel-like solution.

The intra-crystalline fraction contained within several different biominerals has been shown to yield more accurate and precise D/L values and it is reasoned that this fraction is less prone to exogenous contamination and external factors that might otherwise influence the protein/amino acid breakdown (Sykes *et al*., 1995; Penkman *et al*., 2008). Oxidative pre-treatment of enamel, using 72 h exposure to 12 % (w/v) NaOCl has been shown to leave a stable fraction of amino acids (Chapter 3); this fraction is termed the intra-crystalline fraction. Elevated-temperature experiments (simulating long-term degradation) have shown that the intra-crystalline fraction in enamel exhibits minimal leaching, indicating closed system behaviour over geological timescales.

Elevated-temperature experiments have enabled the patterns of protein and amino acid breakdown in the intra-crystalline fraction of enamel to be described. Predictable breakdown of amino acids is observed, indicating that IcPD is an appropriate proxy for age estimation in fossil enamel. Mathematical models have also been applied to the dataset acquired from the elevated-temperature experiments on enamel. Apparent reversible first order rate (RFOK) kinetics have previously been shown to describe the racemisation of free amino acids in solution (Bada & Schroeder, 1972), but they have been less successful in describing racemisation in biominerals (Mitterer & Kriausakul, 1989; Penkman *et al*., 2008; Allen *et al*., 2013; Crisp *et al*., 2013; Tomiak *et al*., 2013). As such, a range of different mathematical models have been applied to datasets to attempt to better describe trends (Clarke & Murray-Wallace, 2006). In this study, RFOK and constrained power law kinetics (CPK) were used to describe the rates of racemisation in enamel. It was discovered that a reasonable conformity to RFOK ($R^2 > 0.97$) was observed for Asx, Glx, Ala, Phe and Val over limited D/L ranges, which was improved for Glx when CPK were applied.

Datasets from both elevated-temperature experiments and fossil enamel and *Bithynia* opercula were compared, which revealed that at elevated temperatures enamel and *Bithynia* opercula have similar rates of IcPD, but in the burial environment IcPD in enamel is much slower. This indicates that elevated-temperature experiments are potentially not suitable for accurately extrapolating ambient-temperature rates of racemisation in enamel.

Enamel samples from 37 Proboscidean teeth from UK sites with independent evidence of age were analysed for their intra-crystalline amino acid contents. The strength of the evidence of age varies between sites, especially when analysing samples of increasing antiquity, where fewer robust dating techniques are available. However, sites have been selected to provide a range of different aged samples from deposits with relatively well-

constrained temporal history. The extent of IcPD in these Proboscidean teeth was used to build a relative geochronology, which was in approximate agreement with the independent evidence of age. This provides robust evidence that enamel IcPD dating can be used as a tool for dating material spanning the Quaternary and has provided a framework on which to date unknown aged Proboscidean enamel in the UK . Two of the samples exhibited IcPD data that was inconsistent with independent evidence of age. However, these samples also did not follow the expected patterns of IcPD, falling outside the predicted FAA vs THAA relationship and thus could easily be identified and removed from further interpretations.

A pilot study building a relative geochronology for dwarf elephants from Sicily revealed that enamel AAR has the potential to provide insight into the mechanisms of island dwarfing in the Mediterranean. Many of the sites in the area are not temporally well constrained, and thus the lineage of the elephant fossils remains uncertain (Herridge, 2010). This pilot study indicates that enamel AAR has the temporal resolution to provide a relative chronology for the elephant species, and thus provide a foundation for further studies into the causes of insular dwarfing on the isle of Sicily.

6.1. Future work

The work described in this thesis has focused on the development and testing of a new method for the dating of mammalian remains by IcPD of enamel. As such there are two key areas of focus for future work: developing the understanding of the fundamental processes governing IcPD in enamel, and the application of the technique to building relative chronologies and directly dating unknown material. This thesis describes isolation of closed system amino acids based on assumptions and theories primarily developed and tested on other biominerals (e.g. Gries *et al.*, 2009). However, the formation and maturation processes that occur in enamel are fundamentally different to those of other biominerals, and as such their mechanism for preservation may be different. One area of future study stemming from the work in this thesis would be to investigate further the potential locations of amino acids and proteins in enamel and to examine the mechanisms for their preservation. Imaging techniques such as TEM could be used in conjunction with elemental analysis (such as energy-dispersive X-ray analysis and electron energy-loss spectroscopy) to locate intra- and inter-crystalline organic matter and thus provide evidence to support the mechanism for the preferential preservation of a fraction of closed system amino acids in enamel.

The work described in this thesis has primarily focused on the degradation of amino acids and proteins, but the hydroxyapatite mineral matrix of enamel will also degrade over geological time scales. Changes relating to remineralisation of opercula have been reported to impact D/L values (Preece & Penkman, 2005), and thus understanding enamel hydroxyapatite degradation may be important to the application of enamel IcPD. Techniques such as FT-IR and X-ray diffraction can be used to gain insight into crystal structure changes when comparing different enamel samples. These changes may help to identify samples that are likely to have experienced open system behaviour, and thus could potentially be unsuitable for enamel IcPD geochronological assessment. Studies such as these, may help identify the cause of the anomalous IcPD in samples such SJPE2, and thus provide a screening protocol to improve the precision of enamel AAR dating.

Two geochronologies have been presented in this thesis: one from UK and the other from Sicilian deposits; both studies have the potential to be expanded upon. The UK model has sufficient comparative material to begin to be used as a tool for dating UK Elephantidae enamel of unknown age. However, additional known age enamel material would greatly improve the estimations of temporal resolution, especially in time periods such as the Cromerian where few samples have yet been analysed. Analysis of Proboscidean remains from key sites in continental Europe could enable cross-correlation of deposits from the UK (once temperature effects have been evaluated); this could be especially useful for comparisons with Early Pleistocene deposits where the UK has a fractured occurrence of this taxon, and thus a lack of comparative material (Hamblin *et al*., 2005).The Sicilian geochronology could be expanded upon to include samples from *E. falconeri* , *E. mnaidriensis* and the elephant species that exhibit *Palaeoloxodon* characteristics. Sites such as Puntali, Luparello, Za Minica and San Teodoro could be included in a future framework which would cover a larger span (refs). This would enable key questions regarding the appearance and extinctions of the endemic elephant species to be placed in chronological context.

The rate of racemisation in enamel is much slower than that observed in the calcium carbonate biominerals analysed so far (Penkman *et al*., 2013). As such, the temporal range of enamel AAR may extend into the Pliocene and potentially further, which is especially significant as there is a much-diminished range of techniques for age estimation for these time periods (Grün *et al*., 2010). Therefore, expanding the geochronology to include older material may extend the use of this technique.

Taxonomic effects within the order of Proboscidae have briefly been investigated, using deposits where multiple taxa are present (Ilford and the Norwich Crag formation), with no detectable differences between taxa in this limited dataset (Chapter 4). However, this study could be built upon by using much larger sample sizes to enable statistical tests to be valid. For example, samples from deposits such as those at Stanton Harcourt, where there is an abundance of both *P. antiquus* and *M. trogontherii* (Scott, 2001) would be ideal. Larger studies would help to establish taxonomic tolerances of the geochronologies.

Finally, the geochronologies built in this thesis were constructed using a single taxonomic family, but enamel IcPD has the potential to be expanded to other taxa. Taxonomic affects are likely to restrict direct comparisons between taxa that are separated by significant evolutionary changes, due to differences in the primary sequence of amino acids and potential changes to the inorganic matrix (King & Neville, 1977; Lajoie *et al*., 1980). However, new chronologies for alternative taxon can be built to provide chronological frameworks for a great number of species; perhaps the most valuable of these would be its potential use to develop a geochronology for hominin evolution on human teeth.

Appendix

Appendix Table 1: Source, provenance and geochronological evidence of each of the samples analysed for the UK enamel ARR geochronology. Estimated numerical ages are based on the MIS boundaries outlined in Lisiecki & Raymo (2005). BGS = British geological survey

Sample name (species)	Source [Collection number]	Site	Grid ref	Stratigraphical unit	Independent age control	British terrestrial stage	MIS	Numerical age estimate
MoEE1 *(E. maximus)*	A. Lister collection	N/A	N/A	N/A	N/A	N/A	N/A	<0.1 ka
WCME1 (*M. primigenius*)	Twickenham Gravel Co Ltd 1932 [GSM50288] BGS	Waltham Cross Pit, Hertfordshire	TL366010	From the floodplain gravel 3 m down associated with the Arctic bed. Part of the low terrace gravels of the River Lea	Radiocarbon dating of organic matter ca. 28 ka (Allison *et al.,* 1954; Stuart, 1982); Key associated mammalian fauna: *M. primigenius, Coelodonta antiquitatis* (Lister, 2001a)	Devensian	MIS 2-3 (Stuart, 1982)	29 –71 ka
WCME2 (*M. primigenius*)	Twickenham Gravel Co Ltd 1932 [GSM50289] BGS							

Appendix Table 1 continued: Source, provenance and geochronological evidence of each of the samples analysed for the UK enamel ARR geochronology. Estimated numerical ages are based on the MIS boundaries outlined in Lisiecki & Raymo (2005). BGS = British geological survey

Sample name (species)	Source [Collection number]	Site	Grid ref	Stratigraphical unit	Independent age control	British terrestrial stage	MIS	Numerical age estimate
KCME1 (*M. primigenius*)	Rev J. MacEnery Collection. BGS	Kents Cavern, Torquay	SX935641 5	Unknown. Most likely from the A2 Loamy Cave Earth (Campbell & Sampson, 1971)	Biostratigraphy of the Cave Earth deposits lower limit of MIS 4 (Current & Jacobi, 1997); Radiocarbon of hominin material 41-39 ka cal BP (Higham *et al.,* 2011)	Devensian	MIS 2-3 assuming the sample is from the A2 Loamy Cave Earth	29-71 ka
SCME1 (*M. primigenius*)	Katharine Scott Coll. [SC1240]	Sutton Courtenay, Oxfordshire	SU 511947	Flood-plain Terrace, Upper Thames valley (Briggs & Gilbertson, 1980)	Radiocarbon dating ca. 35-12 ka (Briggs and Gilbertson, 1980); Biostratigraphy MIS 3 (Scott & Eeles, in prep)	Devensian	MIS 3, based on biostratigraphy (Scott & Eeles, in prep)	64-71 ka

Appendix Table 1 continued: Source, provenance and geochronological evidence of each of the samples analysed for the UK enamel ARR geochronology. Estimated numerical ages are based on the MIS boundaries outlined in Lisiecki & Raymo (2005). BGS = British geological survey.

Sample name (species)	Source [Collection number]	Site	Grid ref	Stratigraphical unit	Independent age control	British terrestrial stage	MIS	Numerical age estimate
NSME1 (*M. primigenius*)	A. Lister Coll.	North Sea	Unknown	Brown Bank	Radiocarbon ca. 34-49 (Mol *et al*., 2006)	Devensian	MIS 4-3	34-49 ka
BtPE1 (*P. antiquus*)	H. Keeping Coll. 1885 [GSM919-20] BGS	Barrington, Cambridgeshire	TL381491 - TL406498	Unknown,	Mammalian biostratigraphy MIS 5e, strongly indicated by the presence of *H. amphibius* and absence of *E. ferus* (Turner, 1973; Schreve, 2001). Pollen analysis, Ipswichian zone IIb (Gibbard & Stuart, 1975).	Ipswichian	MIS 5e	123-130 ka
BtPE2 (*P. antiquus*)	H. Keeping Coll. 1885 [GSM925]. BGS							
BtPE3 (*P. antiquus*)	Unknown. BGS							

Appendix Table 1 continued: Source, provenance and geochronological evidence of each of the samples analysed for the UK enamel ARR geochronology. Estimated numerical ages are based on the MIS boundaries outlined in Lisiecki & Raymo (2005). BGS = British geological survey.

Sample name (species)	Source [Collection number]	Site	Grid ref	Stratigraphical unit	Independent age control	British terrestrial stage	MIS	Numerical age estimate
SJPE1 (*P. antiquus*)	History Unknown [GSM60236] BGS	St James, Sewer excavations	TQ300804 (Trafalgar square)	Kempton Park Formation, interglacial deposits	Mammalian biostratigraphy MIS 5e based on presence of *Hippopotamus amphibius* and absence of *Equus ferus* (Stuart, 1976; Schreve, 1999)	Ipswician	MIS 5e	123-130 ka
SJPE2 (*P. antiquus*)	Presented by J. W. Read 1898 [GSM6399] BGS	St James, Pleistocene gravel; No. 19 Cleveland house						

Appendix Table 1 continued: Source, provenance and geochronological evidence of each of the samples analysed for the UK enamel ARR geochronology. Estimated numerical ages are based on the MIS boundaries outlined in Lisiecki & Raymo (2005). BGS = British geological survey.

Sample name (species)	Source [Collection number]	Site	Grid ref	Stratigraphical unit	Independent age control	British terrestrial stage	MIS	Numerical age estimate
BBME1 (*M. primigenius*)	G. Mantell 1911 [GSM654] BGS	Brighton, exact location unknown	Unknown	Black Rock	Mammalian biostratigraphy (Parfitt, 1998; Westaway *et al*., 2006), AAR from whole shell Macoma/Arctica MIS 7 (Bates *et al*., 2000). OSL dates indicate MIS 6-7 (Bates *et al.,* 2010)	Pre-Ipswician Late Middle Pleistocene	MIS 6	130 ±31 ka
BaME1 (*M. primigenius*)	Unknown	Balderton, Lincolnshire	SK 837561	Cold stage sands & gravels (Lister & Brandon, 1991)	Terrace Stratigraphy: MIS 6 (Brandon & Sumbler, 1991; Bridgland *et al.,* 2015) ESR: 130-190 ka (Grun, 1991)	Pre-Ipswician Late Middle Pleistocene	MIS 6	130 ±31 ka

Appendix Table 1 continued: Source, provenance and geochronological evidence of each of the samples analysed for the UK enamel ARR geochronology. Estimated numerical ages are based on the MIS boundaries outlined in Lisiecki & Raymo (2005). BGS = British geological survey.

Sample name (species)	Source [Collection number]	Site	Grid ref	Stratigraphical unit	Independent age control	British terrestrial stage	MIS	Numerical age Estimate
TaME1 *(M. primigenius*)	J. Rackham Collection [6A/36]	Tattershall Thorpe, Lincolnshire	TF228605	Cold stage sands & gravels (Girling, 1974; Rackham, 1978; Holyoak & Preece, 1985)	Mollusc fauna (Meijer & Preece, 2000); terrace stratigraphy (Bridgland *et al.,* 2015): MIS 6	Pre-Ipswician Late Middle Pleistocene	MIS 6	130 ±31 ka
CrME1 (*M. primigenius/ trogontherii*)	F. C. J. Spurrell Coll. 1893/4 [GSM5123]	Crayford, Kent	TQ517758	Unknown. Likely form the Brickearth	Mammalian fauna of the Brickearth (Schreve, 2001), terrace stratigraphy (Bridgland, 2014): late MIS 7	Pre-Ipswician Late Middle Pleistocene	Late MIS 7	191 ±26 ka
CrME2 (*M. primigenius/ trogontherii*)	W. H. Penning Coll. [GSM117009] BGS	Crayford, Kent	TQ517758	Lower Crayford Brickearth (Chandler, 1914)				

Appendix Table 1 continued: Source, provenance and geochronological evidence of each of the samples analysed for the UK enamel ARR geochronology. Estimated numerical ages are based on the MIS boundaries outlined in Lisiecki & Raymo (2005). BGS = British geological survey.

Sample name (species)	Source [Collection number]	Site	Grid ref	Stratigraphical unit	Independent age control	British terrestrial stage	MIS	Numerical age Estimate
HRME1 (*M. trogontherii*)	Surrey 1939 [SEH424] BGS	Histon Road, Pumping station	TL445663	Histon Road Member	IcPD AAR of *Bithynia* opercula (Penkman *et al.,* 2013): biostratigraphy (Coope, 2001; Boreham *et al.,* 2010), presence of *C. fluminalis;* MIS 7	Pre-Ipswician Late Middle Pleistocene (Wolstonian)	MIS 7	191 ±26 ka
IlPE1 (*P. antiquus*)	Cotton Coll. [GSM114881] BGS	Ilford, Essex	TQ 437860	Brickearths within Taplow/Muckin g Formation (Sutcliffe, 1975; Schreve, 2001)	Terrace stratigraphy (Bridgland, 1994), fauna (Preece, 1999; Coope, 2001; Schreve, 2001): MIS 7	Pre-Ipswician Late Middle Pleistocene (Wolstonian)	MIS 7	191 ±26 ka
IlME1 (*M. trogontherii*)	Cotton Coll. [GSM114884] BGS							
IlME2	Museum (BGS) Coll. [GSM114892]							

Appendix Table 1 continued: Source, provenance and geochronological evidence of each of the samples analysed for the UK enamel ARR geochronology. Estimated numerical ages are based on the MIS boundaries outlined in Lisiecki & Raymo (2005). BGS = British geological survey.

Sample name (species)	Source [Collection number]	Site	Grid ref	Stratigraphical unit	Independent age control	British terrestrial stage	MIS	Numerical age estimate
EbPE1 (*P. antiquus*)	F. C. J. Spurrell collection 1893/4 [GSM5031] BGS	Lower Ebbsfleet. Most likely equivalent to Wenban-Smith's (2013) trench D, Southfleet Road.	TQ611735	Unknown. *Palaeoloxodon antiquus* represented in Wenban-Smith (2013) phases 6 and 5	OSL dating of the fluvial gravel (phase 9 and 8) of the deposits in Wenban-Smith's (2013) trench D (Schwenninger & Wenban-Smith, 2013): MIS 8. IcPD AAR dating of *Bithynia* opercula from phases 6-3 of Wenban-Smith's (2013) trench D (Penkman & Wenban-Smith, 2013): MIS 11	Pre-Ipswician Late Middle Pleistocene	MIS 11-6	

Appendix Table 1 continued: Source, provenance and geochronological evidence of each of the samples analysed for the UK enamel ARR geochronology. Estimated numerical ages are based on the MIS boundaries outlined in Lisiecki & Raymo (2005). BGS = British geological survey.

Sample name (species)	Source [Collection number]	Site	Grid ref	Stratigraphical unit	Independent age control	British terrestrial stratigraphical stage	MIS	Numerical age estimate
LaME1 (*M. primigenius*)	Katharine Scott Coll. [LQ95]	Latton, Wiltshire	SU081965	Northmoor Member, Association A (Lewis *et al.,* 2006)	*Presence of Equus ferus and Mammuthus primigenius in Association A,* biostratigraphy (Schreve, 2001; Scott, 2001): MIS 7. U-series dating of *Equus ferus* bone indicates a minimum age of 147 ±20 ka. IcPD AAR dating of *Valvata piscinalis* (Penkman *et al.,* 2007): MIS 7	Pre-Ipswician Late Middle Pleistocene	MIS 7	191 ±26 ka

Appendix Table 1 continued: Source, provenance and geochronological evidence of each of the samples analysed for the UK enamel ARR geochronology. Estimated numerical ages are based on the MIS boundaries outlined in Lisiecki & Raymo (2005). BGS = British geological survey.

Sample name (species)	Source [Collection number]	Site	Grid ref	Stratigraphical unit	Independent age control	British terrestrial stage	MIS	Numerical age Estimate
GTPE1 (*P. antiquus*)	R. Cotton 1878 [GSM115520] BGS	Grays Thurrock	Unknown	Grays Thurrock member	IcPD AAR dating of *Bithynia* opercula (Penkman *et al.,* 2013): MIS 9. Terrace stratigraphy (Bridgland, 2006): MIS 9. Presence of *U. arctos,* biostratigraphy (Schreve, 1997): MIS 9.	Pre-Ipswician Late Middle Pleistocene	MIS 9	319 ±19 ka
LTPE1 (*P. antiquus*)	Presented by Peasson Sq. BGS	Little Thurrock	TQ625783	Little Thurrock Gravel Member	Lies stratigraphically below the Greys Thurrock member, Terrace stratigraphy and biostratigraphy (Bridgland *et al.,* 2014): MIS 10-9	Pre-Ipswician Late Middle Pleistocene	MIS 10-9	337 ±37

Appendix Table 1 continued: Source, provenance and geochronological evidence of each of the samples analysed for the UK enamel ARR geochronology. Estimated numerical ages are based on the MIS boundaries outlined in Lisiecki & Raymo (2005). BGS = British geological survey.

Sample name (species)	Source [Collection number]	Site	Grid ref	Stratigraphical unit	Independent age control	British terrestrial stage	MIS	Numerical age Estimate
SwPE1 (*P. antiquus*)	Presented by Stone Court Ballast Co 1932 [53040] BGS	Barnfield Pit, Swanscombe, Kent	TQ 595745	Silts, sands & gravels of Boyn Hill Terrace	Boyn Hill Gravel above Anglian boulder clay at Hornchurch; terrace stratigraphy & U-series (Bridgland, 1994); thermoluminescence (Bridgland *et al*., 1985), fauna (Schreve, 2001): MIS 11.	Hoxnian	MIS 11	399 ±25
SwPE2 (*P. antiquus*)	Presented by Stone Court Ballast Co 1932 [53041] BGS	Barnfield Pit, Swanscombe, Kent	TQ 595745	Silts, sands & gravels of Boyn Hill Terrace Lower Gravel		Hoxnian	MIS 11c (Ashton *et al* 2018).	399 ±25
WiME1 (*M. trogontherii*)	J. Rose collection	Witham	TF 030177	Witham Member	Unknown	Cromerian to Anglian (Early Middle Pleistocene)	MIS 13-12	475 ±25 ka (Rose, *pers comm*)

Appendix Table 1 continued: Source, provenance and geochronological evidence of each of the samples analysed for the UK enamel ARR geochronology. Estimated numerical ages are based on the MIS boundaries outlined in Lisiecki & Raymo (2005). BGS = British geological survey.

Sample name (species)	Source [Collection number]	Site	Grid ref	Stratigraphical unit	Independent age control	British terrestrial stage	MIS	Numerical age Estimate
SiPE1 (*P. antiquus*)	G. W. Lamplugh 1899 [GSM6574] BGS	Sidestrand	TG 262401	Cromerian Forest Bed	*Ex situ* mammal fauna encompasses Early & early Middle Pleistocene but *P. antiquus* limited to mid-late part of early Middle Pleistocene (Lister, 1993; 1996).	Cromerian (Early Middle Pleistocene)	MIS 15-13	550 ±72 ka
MuME1 (*M. trogontherii*)	A. King 1868 [GSM7333] BGS	Mundersley	TG 319363	Cromerian Forest- bed Formation or the overlying Anglian deposits (blue clay)	Mammalian biostratigraphic (Lister, 1993): Cromerian. Anglian age deposits overlying the Cromerian Forest-bed formation at Mundesley (West, 1980)	Cromerian to Anglian (Early Middle Pleistocene)	MIS 18-12	593 ±169 ka

Appendix Table 1 continued: Source, provenance and geochronological evidence of each of the samples analysed for the UK enamel ARR geochronology. Estimated numerical ages are based on the MIS boundaries outlined in Lisiecki & Raymo (2005). BGS = British geological survey.

Sample name (species)	Source [Collection number]	Site	Grid ref	Stratigraphical unit	Independent age control	British terrestrial stage	MIS	Numerical age estimate
WRME1 (*M. trogontherii*)	Norwich Museum Service [JAS M1]	West Runton, Norfolk	TG 189441	Cromer Forest-bed Formation	Mammalian fauna from the West Runton freshwater bed includes: *M. savini, E. altidens and M. savini.* Biostratigraphic correlation based on mammals from the Cromer Forest-bed Formation (Lister, 1993): Cromerian. ESR dating of enamel (Rink *et al.,* 1996): 460 ±80 ka. IcPD AAR dating of *Bithynia* opercula (Penkman et al., 2010): pre-MIS 13.	Cromerian (Early Middle Pleistocene)	MIS 18-14	647 ±114 ka

Appendix Table 1 continued: Source, provenance and geochronological evidence of each of the samples analysed for the UK enamel ARR geochronology. Estimated numerical ages are based on the MIS boundaries outlined in Lisiecki & Raymo (2005). BGS = British geological survey

Sample name (species)	Source [Collection number]	Site	Grid ref	Stratigraphical unit	Independent age control	British terrestrial stage	MIS	Numerical age Estimate
KeME1 (*M. trogontherii*)	Unknown [GSM118478] BGS	Kessingland, Suffolk	TM 536862	Unknown, sample taken from tooth fragments	Biostratigraphy: *H. amphibius, M. dawkinsi, M. savini.* (Lister & Stuart, 2010; Preece & Parfitt, 2012) temperate stage in the Early Cromerian.	Early Cromerian (Early Middle Pleistocene)	MIS 15 or 17	638 ±75 ka
KeME2 (*M. trogontherii*)	Unknown [GSM118477] BGS	Kessingland, Suffolk	TM 536862	Unknown				
ERME1 (*M. meridionalis*)	Surrey (Clement Reid) [GSM116503] BGS	East Runton, Norfolk	TG 194430-205427	Wroxham Crag deposits	Biostratigraphy: *M. meridionalis, Eucladoceros spp., E. stenonis, M. balthica*. Palaeomagnetic data (Lister, 1998): Pre-pastonian	Pre-Pastonian (Early Pleistocene)	~MIS 65-68	~1.9-1.8 Ma

Appendix Table 1 continued: Source, provenance and geochronological evidence of each of the samples analysed for the UK enamel ARR geochronology. Estimated numerical ages are based on the MIS boundaries outlined in Lisiecki & Raymo (2005). BGS = British geological survey

Sample name (species)	Source [Collection number]	Site	Grid ref	Stratigraphical unit	Independent age control	British terrestrial stage	MIS	Numerical age Estimate
NCME1 (*M. meridionalis*)	H. E. P. Spenser 1949 [1385] BGS	Holton Gravel Pits	Approx. TM 405773	Norwich Crag Formation, Westleton beds	Biostratigraphic correlation based on mammals, molluscs, foraminifera and dinoflagellates (Stuart, 1982; Zalasiewicz *et al*., 1991; Hamblin *et al*., 1997; Lister, 1998): ca. 2.0-1.8 Ma	Antian/Bramertionian to Baventian/Pre-Pastonian;	~MIS 77-65	~2.0-1.8 Ma
NCAE1 (*A. arvernensis*)	Geological Society Coll. 1911 [GSD5988] BGS	Easton Bavents, Suffolk	TM 518787	Norwich Crag Formation				
NCAE2 (*A. arvernensis*)	H. A. Allen Coll. 1902 [GSM7971] BGS	Whittingham, Suffolk	Approx. TL 720989	Norwich Crag Formation				

Appendix Table 1 continued: Source, provenance and geochronological evidence of each of the samples analysed for the UK enamel ARR geochronology. Estimated numerical ages are based on the MIS boundaries outlined in Lisiecki & Raymo (2005). BGS = British geological survey

Sample name (species)	Source [Collection number]	Site	Grid ref	Stratigraphical unit	Independent age control	British terrestrial stage	MIS	Numerical age Estimate
RCAE1 (*A. arvernensis*)	Museum Coll. [GSM116468] BGS	Felixstowe	Approx. TM 302346	Red Crag Formation	Biostratigraphic of dinoflagellates and foraminifera (Head, 1998; Funnell, 1998): ca. 2.6-2.4 Ma	Pre-Ludhamian	~MIS 94-104	~2.6-2.4
RCAE2 (*A. arvernensis*)	Museum Coll. [GSM2204] BGS							

References

Abelson, P. H., 1954. Amino acids in fossils. Science 119, 576

Akiyama, M., 1980. Diagenetic decomposition of Peptide-linked serine residues in the fossil scallop shells. In: Biogeochemistry of amino acids. Hare, P. E., Hoering, T. C., King, K., 115-120. John Wiley & Sons

Allen, A. P., Kosnik, M. A., Kaufman, D. S., 2013. Characterizing the dynamics of amino acid racemization using time-dependent reaction kinetics: A Bayesian approach to fitting age-calibration models. Quaternary Geochronology 18, 63-77

Allison, J., Godwin, H., Warren, S. H., 1952. Late-glacial deposits at Nazeing in the Lea Valley, North London. Philosophical Transactions of the Royal Society B 236, 169-230

Alpert, A. J., 1990. Hydrophilic-interaction chromatography for the separation of peptides, nucleic acids and other polar compounds. Journal of Chromatography 499, 177-196

Ambrosetti, P., 1968. The Pleistocene dwarf elephants of Spinagallo (Siracusa, South-Eastern Sicily). Geologica Romana VII, 277-398

Amend, J. P., Helgeson, H. C., 1997. Solubilities of the common L-a-amino acids as a function of temperature and solution pH. Pure and applied chemistry 69, 935-942

Anderson, J. B., Shipp, S. S., Lowe, A. L., Wellner, J. S., Mosola, A. B., 2002. The Antarctic Ice Sheet during the Last Glacial Maximum and its subsequent retreat history: A review. Quaternary Science Reviews 21, 49-70

Andrews, T., Gregory, J. M., Webb, M. J., Taylor, K. E., 2012. Forcing, feedbacks and climate sensitivity in CMIP5 coupled atmosphere-ocean climate models. Geophysical Research Letters 39, 1-7

Anon, (2018). In: 1st ed. [online] Available at: http://www.oxforddictionaries.com/definition/fossil [Accessed 22 Jan. 2018]

Antoine, P., Limondin Lozouet, N., Chausse, C., Lautridou, J. -P., Pastre, J. -F., Auguste, P., Bahain, J. -J., Falgueres, C., Galehb, B., 2007. Pleistocene fluvial terraces from northern France (Seine, Yonne, Somme): synthesis, and new results from interglacial deposits. Quaternary Science Review 26, 2701-2723

Ashton, N. M., McNabb, J., Bridgland, D. R., 1995. Barnfield Pit, Swanscombe. In: The Quaternary of the lower reaches of the Thames, Field guide. Quaternary Research Association.

Ashton, N. 2018. Landscapes of habit and persistent places during MIS 11 in Europe. In (Pope, M., McNabb, J. & Gamble, C., eds) Crossing the Human Threshold: Dynamic Transformation and Persistent Places during the Middle Pleistocene), pp. 142-164. London: Routledge

Aitken, M.J., 1998. An Introduction to Optical Dating. Oxford University Press, Oxford

Bada J. L., 1972a. Kinetics of Racemization of Amino Acids as a Function of pH. Journal of the American Chemical Society 94, 1371-1373

Bada, J. L., 1972b. The dating of fossil bones using the racemization of isoleucine. Earth and Planetary Science Letters 15, 223-231

Bada, J. L., 1981. Racemization of amino acids in fossil bones and teeth from the Olduvai Gorge region, Tanzania, East Africa. Earth Planetary Science Letters 55, 292-298

Bada, J. L., 1984. *In Vivo* racemisation in Mammalian proteins. Methods in Enzymology 106, 98-115

Bada J. L. 1985. Amino acids racemization dating of fossil bones. Annual Review Earth Planetary Science 13, 241-268

Bada, J. L., 1987. Paleoanthropological applications of amino acid racemization dating of fossil bones and teeth. Anthropological Anzeiger 45, 1-8

Bada, J. L. & Mann E. H., 1980. Amino acid analysis in Deep Sea drilling cores: kinetic and mechanisms of some reactions and their application in geochronology and in palaeotemperature and heat flow determinations. Earth Science Reviews 16, 21-55

Bada, J. L. & Shou, M. Y., 1980. Kinetics and mechanism of amino acid racemisation in aqueous solution and in bones. In: Hare, P. E., Hoering, T. C., King, Jr K., Eds. Biogeochemistry of Amino Acids. 35-40. New York: Wiley

Bada, J. L. & Schroeder, R. A., 1975. Amino acid racemization reactions and their geochemical implications. Die Naturwissenschaften 62, 71-79.

Bada, J. L., Kvenvolden, K. A., Peterson, E., 1973. Racemization of amino acids in bones. Nature 245, 308-310

Bada, J. L., Belluomini, G., Bonfiglio, L., Branca, M., Burgio, E., Dellitala, L., 1991. lsoleucine epimerization ages of Quaternary Mammals of Sicily. Quaternario 4, 49-54

BGS Report, 2011. Geo Reports. BGS Repot No: GR_000000/1

Bateman, R. M. & Rose, J., 1994. Fine sands and mineralogy of the early and middle Pleistocene Bytham Sands and Gravels of the midland England and East Anglia. Proceeding of the Geologists' Assosiation 105, 33-39

Bates, M. R., Parfitt, S. A., Roberts, M. B. 1997. The chronology, palaeogeography and archaeological significance of the marine Quaternary record of the West Sussex Coastal Plain, Southern England. Quaternary Science Reviews, 16, 1227–1252

Bates, M. R., Briant, R. M., Rhodes, E. J., Schwenninger, J. -L., Whittaker, J. E., 2010. A new chronological framework for Middle and Upper Pleistocene landscape evolution in the Sussex/Hampshire Coastal Corridor, UK. Proceedings of the Geologists' Association 121, 369–392Belluomini G., 1985. Direct aspartic acid racemisation dating of human bones from archaeological site of Central Southern Italy. Archeometria 69, 135-171

Belluomini, G., & Bada, J. L., 1985. Isoleucine epimerisation age of the dwarf elephants of Sicily. Geology 13, 451-452

Bennett, K. D., 1987. Holocene pollen stratigraphy of central East Anglia, England, and comparison of pollen zones across the British Isles. New Phytol 109 237-253

Berger, R., Horney, A. G., Libby, W. F., 1964. Radiocarbon Dating of Bone and Shell from Their Organic Components. American Association for the Advancement of Science 144, 999-1001

Bern, M., Phinney, B. S., Goldberg, D., 2009. Reanalysis of Tyrannosaurus rex Mass Spectra research articles. Journal of Proteome research 8, 4328-4332

Bischoff, J. L., Rosenbauer, R. J., Uranium series dating of human skeletal remains from the del Mar and Sunnyvale sites, California. Science 1981, 213, 1003–1005

Blaauw, M., 2012. Out of tune: the dangers of aligning proxy archives. Quaternary Science Reviews 36, 38-49

Blackwell, B., Rutter, N. W., Debénath, A. 1990. Amino acid racemization in mammalian bones and teeth from La Chaise-de-Vouthon (Charente), France. Geoarchaeology 5, 121-147

Blake, J. H., 1877. On the age of the mammalian Rootlet Bed at Kessingland. Geological Magazine 4, 298–300

Blake, J. H., 1890. The geology of the country near Yarmouth and Lowestoft. Memoirs of the Geological Survey, England and Wales

Bol'shakov, V. A., 2014. A Link between Global Climate Variability in the Pleistocene and Variations in the Earth's Orbital Parameters. Stratigraphy and Geological Correlation 22 (5), 538-551

Bonfiglio, L. & Insacco, G., 1992. Palaeoenvironmental, paleontologic and stratigraphic significance of vertebrate remains in pleistocene limnic and alluvial deposits from southeastern Sicily. Palaeogeography, Palaeoclimatology, Palaeoecology 95, 195-208

Bony, S., Colman, R., Kattsov, V., M., Allan, R. P., Bretherton, C. S., Dufresne, J., Hall, A., Hallegatte, S., Holland, M. M., Ingram, W., Randall, D. A., Soden, B. J., Tselioudis, G., Webb, M. J., 2006. How Well Do We Understand and Evaluate Climate Change Feedback Processes? Journal of Climate 19, 3445-3482

Boreham, S., White, T. S., Bridgland, D. R., Howard, A. J., White, M. J., 2010. The Quaternary history of the walsh fluvial network, UK. Proceedings of the Geologists' Association 121, 393-409

Bouchet, V. M. P., Sauriau, p., Debenay, J., Mermillod-Blondin, F., Schmidt, S., Amiard, J., Dupas, B., 2009. Influence of the mode of macrofauna-mediated bioturbation on the vertical distribution of living benthic foraminifera: First insight from axial tomodensitometry. Journal of Experimental Marine Biology and Ecology 371, 20-33

Bowen, 1999. A revised correlation of Quaternary deposits in the British Isles. Eds. The Geological society special report No. 23. Henry Ling Ltd, Dorset.

Bowen, D.Q., Sykes, G.A., Reeves, A., Miller, G.H., Andrews, J.T., Brew, J.S., Hare, P.E., 1985. Amino acid geochronology of raised beaches in Southwest England. Quaternary Science Reviews 4,279-318

Bowen, D. Q., Sykes, G. A., Maddy, D., Bridgland, D. R., Lewis, S. G., 1995. Aminostratigraphy and amino acid geochronology of English lowland valleys the Lower Thames in context In: Bridgland, D. R., Allen, P., Haggart, B. A. (eds) The Quaternary of the lower reaches of the Thames Quaternary Research Association Field Guide, Durham, 61-63

Boyde A. & Martin L. B., 1984. The microstructure of promate dental enamel. New York: Plenum Press.

Brandon, A. & Sumbler, M. G., 1991. The Balderton Sand and Gravel: Pre-Ipswichian cold stage fluvial deposits near Lincoln, England. Journal of Quaternary Science 6, 117-138

Bravenec, A. D., Ward, K. D., Ward, T. J., 2018. Amino acid racemization and its relation to geochronology and archaeometry. Separation Science 41, 1489–1506

Brennan, T. V., Clarke, S., 1993. Spontaneous degradation of polypeptides at aspartyl and asparaginyl residues effects of the solvent dielectric. Protein Science 2, 331-338

Briant, R. M., Brock, F., Demarchi, B., Langford, H. E., Penkman, K. E. H., Schreve, D. C., Schwenninger, J. Taylor, S., 2018. Quaternary Geochronology Improving chronological control for environmental sequences from the last glacial period. Quaternary Geochronology 43, 40-49

Bridgland, D. R., 1985. Pleistocene sites in the Thames-Avon system. Earth science Conservation 22, 36-39

Bridgland, D. R., 1994. Quaternary of the Thames, Geological Conservation Review Series No. 7

Bridgland, D. R., 2000. River terrace systems in north-west Europe: an archive of environmental change, uplift and early human occupation. Quaternary Science Reviews 19, 1293-1303

Bridgland, D. R., 2006. The Middle and Upper Pleistocene sequence in the Lower Thames: A record of Milankovitch climatic fluctuation and early human occupation of southern Britain. Proceedings of the Geologists' Association 117, 281-305

Bridgland, D. R., 2014. Lower Thames terrace stratigraphy: latest views. In: Bridgland, D. R., Allen, P., White, T. S. The Quaternary of the Lower Thames & Eastern Essex. Field Guide. Quaternary research association Cambridge, 1-10

Bridgland, D. R., & Harding, P. 1994. Globe Pit, Little Thurrock. In: Bridgland, D. R. 1994. Quaternary of the Thames. Geological review series, 7. Chapman and Hall, London, 228-237.

Bridgland, D. R. & Gibbard, P. L., 1997. Quaternary river diversions in the London Basin and the eastern English Channel. Geographic Physique et Quaternaire 51, 337-346

Bridgland, D. R. & Schreve, D., 2004. Quaternary lithostratigraphy and mammalian biostratigraphy of the Lower Thames terrace system, South-East England. Quaternaire 15, 29-40

Bridgland, D.R., Gibbard, P. L., Harding, P., Kemp, R. A., Southgate, G., 1985. New information and results from recent excavations at Barnfield pit, Swanscombe. Quaternary Newslatter 46, 25-39

Bridgland, D. R., Field, M. H., Holmes, J. A., McNabb, J., Preece, R. C., Selby, I., Wymer, J. J., Boreham, S., Irving, B. G., Parfitt, S. A., Stuart, A. J., 1999. Middle Pleistocene interglacial Thames—Medway deposits at Clacton-on-Sea, England: Reconsideration of the biostratigraphical and environmental context of the type Clactonian Palaeolithic industry. Quaternary Science Reviews 18 109-146

Bridgland, D. R., Schreve, D. C., Allen, P., Keen, D. H., 2003. Key Middle Pleistocene localities of the Lower Thames: Site conservation issues, recent research and report of a Geologists' Association excursion, 8 July, 2000. Proceedings of the Geologists' Association 144, 211-225

Bridgland, D.R., Howard, A.J., White, M.J., White, T.S., 2014. The Quaternary of the Trent. Oxbow Books, Oxford

Bridgland, D. R., Howard, A. J., White, M. J., White, T. S., Westaway, R., 2015. New insight into the Quaternary evolution of the River Trent, UK. Proceedings of the Geologists' Association 126, 466-479

Briggs, D. J. & Gilbertson, D. D., 1980. Quaternary Processes and Environments in the upper Thames Valley. Transactions of the Institute of British Geographers 5, 53-65

Bright, J., Kaufman, D. S., 2011a. Amino acids in lacustrine ostracodes, part III: Effects of pH and taxonomy on racemization and leaching. Quaternary Geochronology 6, 574-597

Bright, J., Kaufman, D. S., 2011b. Amino acid racemization in lacustrine ostracodes, part I: effect of oxidizing pre-treatments on amino acid composition. Quaternary Geochronology 6, 154-173

Brooks, A.S., Hare, P.E., Kokis, J.E., Miller, G.H., Ernst, R.D., Wendorf, F., 1990. Dating Pleistocene archaeological sites by protein diagenesis in ostrich eggshell. Science 248, 60-64

Buckley, M., Larkin, N., Collins, M., 2011. Mammoth and Mastodon collagen sequences; survival and utility. Geochimica et Cosmochimica Acta 75, 2007-2016

Bruckner, H., Wittner, R., Godel, H., 1991. Fully automated high-performance liquid chromatographic separation of DL-amino acids derivatized with o-phthaldialdehyde together with N-isobutyryl-cysteine. Application to food samples. Chromatographia 32, 383-388

Campbell, J. B. & Sampson, C. G., 1971. A New analysis of Kent's Cavern. Devonshire, England. University of Oregon Anthropological Papers 3, 1-40

Candy, I., White, T. S., Elias, S., 2016. How warm was Britain during the Last Interglacial? A critical review of Ipswichian (MIS 5e) palaeotemperature reconstructions. Journal of Quaternary Science 31 (8), e2910-868

Canoira, L., García-Martínez, M. J., Llamas, J. F., Ortíz, J. E., Torres, T., 2003. Kinetics of Amino Acid Racemization (Epimerization) in the Dentine of Fossil and Modern Bear Teeth. International Journal of Chemical Kinetics 35, 576-591

Carneiro, K. M. M., Zhai, H., Zhu, L., Horst, J. A., Sitlin, M., Nguyen, M., Wagner, M., Simpliciano, C., Milder, M., Chen, C. L., Ashby, P., Bonde, J., Li, W., Habelitz, S., 2016. Amyloid-like ribbons of amelogenins in enamel mineralization. Scientific Reports 6:23105

Carstrom D., Angmar, B., Glas, J. -E., 1963. Studies on the ultrastructure of dental enamel. IV. The mineralization of normal human enamel. Journal of Ultrastructure Research 8 (1), 12-23

Chandler, R. H., 1914. The Pleistocene Deposits of Crayford. Proceeding of the Geological Association 25, 61 - 71

Clarke, S. J., Murray-Wallace, C. V., 2006. Mathematical expressions used in amino acid racemization geochronology: a review. Quaternary Geochronology 1, 261-278

Clark, C. D., Evans, D. J. A., Khatwa, A., Bradwell, T., Jordan, C. J., Marsh, S. H., Mitchell, W. A., Bateman, M. D., 2004. Map and GIS database of landforms and features related to the last British Ice Sheet. Boreas 33 (4), 359-375Coles, B. J. 2000 Doggerland: the cultural dynamics of a shifting coastline. In: K. Pye and S. R. L. Allen (eds) Coastal and Estuarine Environments: Sedimentology, Geomorphology and Geoarchaeology, 393-401. Geological Society Special Publication 175. The Geological Society, London

Collins, M. J. & Riley, M. S., 2000. Amino acid racemization in biominerals, the impact of protein degradation and loss. In: Goodfriend, G. A., Collins, M. J., Fogel, M. L., Macko, S. A.,

Wehmiller, J. F. (Eds.), Perspectives in Amino Acid and Protein Geochemistry. Oxford University Press, 120–142

Collins, M. J., Waite E. R., van Duin, A. C. T., 1999. Predicting protein decomposition: the case of aspartic-acid racemization kinetics. Philosophical Transcript Royal Society London Series B-Biological Sciences 354, 51– 64

Collins, M. J., Penkman, K. E. H., Rohland, N., Shapiro, B., Dobberstein, R. C., Ritz-Timme, S., Hofreiter, M., 2009. Is amino acid racemization a useful tool for screening for ancient DNA in bone? Proceedings of the Royal Society B. 1-7

Coope, G. R., 2001. Biostratigraphical distinction of interglacial coleopteran assemblages from southern Britain attributed to Oxygen Isotope Stages 5e and 7. Quaternary Science Reviews 20, 1717-1722

Corrigan, J. J., 1969. D-amino acids in animals. Science 164, 142-149

Coughlan, M., Fleischer, M., Wheeler, A. J., Hepp, D. A., Hebbeln, D., Morz, T. 2018. A revised stratigraphical framework for the Quaternary deposits of the German North Sea sector: a geological-geotechnical approach. Boreas 47, 80–105

Crenshaw, M. A., 1972. The soluble matrix from Mercenaria mercenaria shell. Biomineralisation 6, 6-11

Crisp, M., Demarchi, B., Collins, M., Morgan-Williams, M., Pilgrim, E., Penkman, K., 2013. Isolation of the intra-crystalline proteins and kinetic studies in Struthio camelus (ostrich) eggshell for amino acid geochronology. Quaternary Geochronology 16, 110-128.

Csapó, J., Csapó-Kiss, Z., Wágner, L., Tálos, T., Martin, T. G., Folestad, S., Tivesten, A., Némethy, S., 1997. Hydrolysis of proteins performed at high temperatures and for short times with reduced racemization, in order to determine the enantiomers of D- and L-amino acids. Analytica Chimica Acta 339, 99-107

Current, A. & Jacobi, R., 1997. Vertebrate Faunas of the British Late Pleistocene and the Chronology of Human Settlement. Quaternary Newsletter 82, 1-8

Demarchi, B., Collins, M., Bergström, E., Dowle, A., Penkman, K., Thomas-Oates, J., Wilson, J., 2013a. New experimental evidence for in-chain amino acid racemization of serine in a model peptide. Analytical Chemistry 85, 5835-5842

Demarchi, B., Rogers, K. Fa, D. A., Finlayson, C. J., Milner, N., Penkman, K. E. H., 2013b. Intra-crystalline protein diagenesis (IcPD) in Patella vulgata. Part I: Isolation and testing of the closed system. Quaternary Geochronology 16, 144-157.

Demarchi, B., Collins, M. J., Tomiak, P. J., Davies, B. J., Penkman, K. E. H., 2013c. Intra-crystalline protein diagenesis (IcPD) in Patella vulgata. Part II: breakdown and temperature sensitivity. Quaternary Geochronology 16, 158-172

Demarchi, B., Hall, S., Roncal-Herrero, T., Freeman, C. L., Woolley, J., Crisp, M. K., Wilson, J., Fotakis, A., Fischer, R., Kessler, B. M., Jersie-Christensen, R. R., Olsen, J. V., Haile, J., Thomas, J., Marean, C. W., Parkington, J., Presslee, S., Lee-Thorp, J., Ditchfield, P., Hamilton, J. F., Ward, M. W., Wang, C. M., Shaw, M. D., Harrison, T., Dominguez-Rodrigo, M., Macphee, R. D. E., Kwekason, A., Ecker, M., Horwitz, L. K., Chazan, M., Kroger, R., Thomas-Oates, J., Harding, J. H., Cappellini, E., Penkman, K., Collins, M. J., 2016. Protein sequences bound to mineral surfaces persist into deep time. eLife 5, 1-50

Denton, G. H. & Hughes T. J., 1981. The last great ice sheets Eds, Wiley-interscience, New York

Dirks, P. H. G. M., Roberts, Eric M., Hilbert-Wolf, H., Kramers, J. D., Hawks, J., Dosseto, A., Duval, M., Elliott, M., Evans, M., Grün, R., Hellstrom, J., Herries, A. I. R., Joannes-Boyau, R., Makhubela, T. V., Placzek, C. J., Robbins, J., Spandler, C., Wiersma, J., Woodhead, J., Berger, L. R., 2017. The age of homo naledi and associated sediments in the rising star cave, South Africa. eLife e24231

Dobberstein, R. C., Collins, M. J., Craig, O. E., Taylor, G., Penkman, K. E. H., Ritz-Timme, S., 2009. Archaeological collagen: Why worry about collagen diagenesis? Archaeological and Anthropological Science 1:31, 31-42

Dong, L. & Huang, J., 2007. Effect of Temperature on the Chromatographic Behaviour of Epirubicin and its Analogues on High Purity Silica Using Reversed-Phase Solvents. Chromatographia 65, 519-526

Du, C., Cui, F. Z., Zhang, W., Feng, Q. L., Zhu, X. D., Groot, K, d., 2000. Formation of calcium phosphate / collagen composites through mineralization of collagen matrix. Journal of Biomedical Materials Research 50, 518-527

Dunseth, Z. C., Junge, A., Lomax, J., Boaretto, E., Finkelstein, I., Fuchs, M., Shahack-gross, R., 2017. Dating archaeological sites in an arid environment: A multi-method case study in the Negev Highlands, Israel. Journal of Arid Environments 144, 156-169

Duval, M., 2015. Evaluating the accuracy of ESR dose determination of pseudo-Early Pleistocene fossil tooth enamel samples using dose recovery tests. Radiation Measurements 79, 24-32

Duval, M. & Grün, R., 2016. Are published ESR dose assessments on fossil tooth enamel reliable? Quaternary Geochronology 31, 19-27

Emiliani, C., 1954. Depth habitats of some species of pelagic foraminifera as indicated by oxygen

isotopes ratios. American Journal of Science, 252, 149–158

Emiliani, C., 1955. Pleistocene Temperatures. The Journal of Geology 63, 538-578

Emiliani, C., & Geiss, J., 1959. On glaciations and their causes. International Journal of Earth Sciences 46, 576–601

Engels, S., Bohncke, S., Bos, J. A. A., Heiri, O., Vandenberghe, J., Wallinga, J., 2008. Environmental inferences and chironomid-based temperature reconstructions from fragmentary records of the Weichselian Early Glacial and Pleniglacial periods in the Niederlausitz area (eastern Germany). Palaeogeography Palaeoclimatology Palaeoecology 260, 405-416

EPICA Community members, 2004. Eight glacial cycles from an Antarctic ice core. Nature 429, 623-628

Erez, J., 1978. Vital effect on stable-isotope composition seen in foraminifera and coral skeletons. Nature 273. 199-202

Erez J., Luz, B., 1983. Experimental paleotemperature equation for planktonic foraminifera. Geochimica et Cosmochimica Acta 47, 1025-1031

Fairbanks, R. G. & Matthews, R. K., 1978. The marine isotope record in Pleistocene coral, Barbados, West Indies. Quaternary Research 10, 181-196

Faure, G., 1986. Principals of isotope geology Eds. Wiley

Feduccia, A., 1995. Explosive evolution in Tertiary Birds and Mammals. Science 267, 637

Frouin, M., Lahaye, C., Valladas, H., Higham, T., Debénath, A., Delagnes, A., 2017. Dating the Middle Paleolithic deposits of La Quina Amont (Charente, France) using luminescence methods. Journal of Human Evolution 109, 30-45

Fuchs, S. A., Berger, R., Klomp, L. W. J., De Koning, T. J., 2005. D-Amino acids in the central nervous system in health and disease. Molecular Genetics and Metabolism 85, 168-180

Fujii, N., 2005. D-Amino acid in elderly tissues. Biological & Pharmaceutical Bulletin, 28, 1585-1589

Funnell, B. M., 1998. Climatic evolution of the North Sea and North Atlantic during the Pliocene-Pleistocene (2.7 to 1.7 Ma). Mededelingen Nederlands Instituut voor Toegepaste Geowetenschappen 60, 227-238

Funnell, B. M. & West, R. G., 1962. The Early Pleistocene of Easton Bavents, Suffolk. Quarterly Journal of the Geological Society of London 118, 125-141

Funnell, B. M. & West, R. G., 1977. Preglacial Pleistocene deposits of East Anglia. In: Shotton, F. W., (Eds.) British Quaternary Studies: recent advances. Clarendon, Oxford, 247-256

Furukawa, A., Tanaka, H., 2010. Key role of hydrodynamic interactions in colloidal gelation. Physical Review Letters 104, 1-4

Gama, M. R., da Costa S., R. G., Collins, Carol H., Bottoli, C. B. G., 2012. Hydrophilic interaction chromatography. Trends in Analytical Chemistry 37, 48-60

Garot, E., Couture-Veschambre, C., Manton, D., Rodriguez, V., Lefrais, Y., Rouas, P., 2007. Diagnostic guide enabling distinction between taphonomic stains and enamel hypomineralisation in an archaeological context. Archives of Oral Biology 74, 28-36

Gash, A. E., Tillotson, T. M., Satcher, J. H., Hrubesh, L W., Simpson, R. L., 2001. New sol-gel synthetic route to transition and main-group metal oxide aerogels using inorganic salt precursors. Journal of Non-Crystalline Solids 285, 22-28

Genchi, G., 2017. An overview on D-amino acids. Amino acids 49, 1521-1533

Gibbard, P. L., 1979. Middle Pleistocene drainage of the Thames Valley, Geological Magazine 116, 35-44

Gibbard, P. L. 1985. The Pleistocene History of the Middle Thames Valley. Cambridge University Press, Cambridge

Gibbard, P. L., 1994. Pleistocene History of the Lower Thames Valley. Cambridge University press

Gibbard, P. L. & Stuart, A. J., 1975. Flora and vertebrate fauna of the Barrington Beds. Geological Magazine 112, 493 - 501

Gibbard, P. L., Zalasiewicz, J. A., Mathers, S. J., 1998. Stratigraphy of the marine Plio-Pleistocene Crag deposits of East Anglia. Mededelingen Nederlands Instituut voor Toegepaste Geowetenschappen 60, 239-262

Gibbard, P. L., Head, M. J., Walker, M. J. C., 2010. Formal ratification of the Quaternary System/Period and the Pleistocene Series/Epoch with a base at 2.58 Ma. Journal of Quaternary Science 25, 96-102

Gillard, R. D. & Phipps, 1970. The selective activation of amin oacids and peptides. Chemical communications 800- 801

Girling, M. A., 1974. Evidence from Lincolnshire of the age and intensity of the Mid-Devensian temperate episode. Nature 250, 270

Girling, M. A., 1980. Late Pleistocene insect faunas from two sites. Unpublish PhD thesis, University of Birmingham

Graham, R. W., Belmecheri, S., Choy, K., Culleton, B. J., Davies, L. J., Froese, D., Heintzman, P. D., Hritz, C., Kapp, J. D., Newsom, L. A., Rawcliffe, R., Saulnier-Talbot, E., Shapiro, B., Wang, Y., Williams, J. W., Wooller, M. J., 2016. Timing and causes of mid-Holocene mammoth extinction on St. Paul Island, Alaska. PNAS 133, 9310-9314

Gregor, H. P., Collins, F. C., Pope, M., 1951. Studies on ion-exchange resins. III. Diffusion of Neutral molecules in a sulfonic acid cation-exchange resin. Journal of Colloid Science 6, 304-322

Gries, K., Kröger, R., Kübel, C., Fritz, M., Rosenauer, A., 2009. Investigations of voids in the aragonite platelets of nacre. Acta Biomaterialia 5, 3038-3044

Griffin, R. C., 2006. Application of amino acid racemization in enamel to the estimation of age at death of archaeological remains. Unpublish PhD thesis

Griffin, R. C., Moody, H., Penkman, K. E. H., Collins, M. J., 2008. The application of amino acid racemization in the acid soluble fraction of enamel to the estimation of the age of human teeth. Forensic Science International 175, 11-16

Griffin, R. C., Chamberlain, A. T., Hotz, G., Penkman, K. E. H., Collins, M. J., 2009. Age estimation of archaeological remains using amino acid racemization in dental enamel: A comparison of morphological, biochemical, and known ages-at-death. American Journal of Physical Anthropology 140, 244-252

Grellet-Tinner, G., Corsetti, F., Buscalioni, A. D., 2010. The importance of microscopic examinations of eggshells: discrimination of bioalteration and diagenetic overprints from biological features. Journal of Iberian Geology 36, 181-192

Grumbach, E. S., Foutain, K. J., Comprehensive Guide to HILIC: Hydrophilic Interaction Chromatography, Waters, Corporation, Milford, 2010

Grün, R., 1991. Appendix 5. Electron spin resonance age estimates on elephant teeth from the Balderton Sand and Gravel. In: Brandon, A. & Sumbler, M. G. The Balderton Sand and Gravel: Pre-Ipswichian cold stage fluvial deposits near Lincoln, England. Journal of Quaternary Science 6, 135-136

Grün, R., 2006. A simple method for the rapid assessment of the qualitative ESR response of fossil samples to laboratory irradiation. Radiation Measurements 41, 682-689

Grün, R., Aubert, M., Hellstrom, J., Duval, M., 2010. The challenge of direct dating old human fossils. Quaternary International 223-224, 87-93

Guo, Y., 2015. Recent progress in the fundamental understanding of hydrophilic interaction chromatography (HILIC). Analyst 140, 6452-6466

Guo, Y. & Gaiki, S., 2011. Retention and selectivity of stationary phases for hydrophilic interaction chromatography. Journal of Chromatography A 1218, 5920-5938

Hamblin, R. J. O., Moorlock, B. S. P., Booth, S. J., Jeffery, D. H., Morigi, A. N., 1997. The Red Crag and Norwich Crag formations in eastern Suffolk. Proceedings of the Geologists' Association 108, 11-23

Hao, Z., Lu, C. Y. Xiao, B., Weng, N., Parker, B., Knapp, M., Ho, C. T., 2007. Separation of amino acids, peptides and corresponding Amadori compounds on a silica column at elevated temperature. Journal of Chromatography A 1147, 165-171

Hao, Z., Xiao, B., Weng, N., 2008. Impact of column temperature and mobile phase components on selectivity of hydrophilic interaction chromatography (HILIC). Journal of Separation Science 31, 1449-1464

Hare, P. E., 1974. Amino acid dating of one – the influence on water. Carnegie Institution of Washington 73, 576-581

Hare, P. E., 1975. Amino acid composition by column chromatography. In S.B. Needleman (Ed.), Molecular Biology, Biochemistry, and Biophysics 8, 205-231

Hare, P. E., 1988. Organic geochemistry of bone and its relation to the survival of bone in the natural environment. In: Behrensmeyer, A. K. & Hill, A. P., Fossils in the making: Vertebrate Taphonomy and paleoecology. The University of Chicago Press

Hare, P.E. & Mitterer, R.M., 1967. Non-protein amino acids in fossil shells. Carnegie Institution of Washington 65, 362—364.

Hare, P. E. & Abelson, P. H., 1968. Racemization of amino acids in fossil shells, Carnegie Institute Washington. Year book 66, 526-528

Harriman, S., 2012. Investigation into phosphate extraction methods for use in AAR analysis. Unpublished MChem dissertation

Harris, D. C., 2007. Quantitative chemical analysis (Eds. 7th). W. H. Freeman and Company

Haynes, V., 1968. Radiocarbon: Analysis of Inorganic Carbon of Fossil Bone and Enamel. American Association for the Advancement of Science 161, 687-688.

Hays, J. D. Imbrie, J., Shackleton, N. J., 1976. Variations in the Earth's Orbit: Pacemaker of the Ice Ages. Science 194, 1121-1132

He, L. H., Swain, M. V., 2007. Contact induced deformation of enamel. Applied Physics Letters 90, 171916

He, L. H. & Swain, M. V., 2008. Understanding the mechanical behaviour of human enamel from its structural and compositional characteristics. Journal of the Mechanical Behavior of Biomedical Materials I, 18-29

He, L. H., Fujisawa, N., Swain, M. V., 2006. Elastic modulus and stress-strain response of human enamel by nano-indentation. Biomaterials 27, 4388-4398

Hu, C.-C., Fukae, M., Uchida, T., 1997. Sheathalin: Cloning, cDNA polypeptide sequences, and immunolocalization of porcine enamel sheath proteins. Journal of Dentistry Research 76, 648–657

Head, M., 1998. Marine environmental change in the Pliocene and early Pleistocene of eastern England: the dinoflagellate evidence reviewed. Mededelingen Nederlands Instituut voor Toegepaste Geowetenschappen 60, 199-226

Heaney, L.R. 1978. Island area and body size of insular mammals: evidence from the tri-colored squirrel (*Callosciurus prevosti*) of Southeast Asia. Evolution 32, 29-44

Herridge, V. L., 2010. Dwarf elephants on Mediterranean islands: A natural experiment in parallel evolution (Ph.D. thesis). University College London. Published online at. http://discovery.ucl.ac.uk/133456/

Hedges, R. E. M., Wallace, C. J. A., 1980. The survival of protein in bone, In: Hare, P. E., Hoering, T. C., King, Jr K., Eds. Biogeochemistry of Amino Acids. 35-40. New York: Wiley

Hedges, R. E. M., Housley, R.A., Law, I. A., Bronk, C. R., 1989. Radiocarbon dates from the Oxford AMS system: Archaeometry datelist 9. Archaeometry 31, 207–234

Heier-Nielsen, S., Conradsen, K., Heinemeier, J., Knudsen, K.L., Nielsen, H. L., Rud, N., Sveinbjornsdottir A. E., 1995. Radiocarbon Dating of Shells and Foraminifera from the Skagen core, Denmark: Evidence of Reworking. Radiocarbon 37 (2), 119-130.

Helfman, P. M. & Bada, J. L., 1975. Aspartic acid racemization in tooth enamel from living humans. Proceedings of the National Academy of Sciences of the United States of America 72, 2891-2894

Helfman, P. M. & Bada, J. L., 1976. Aspartic acid racemization in dentine as a measure of aging. Nature 262, 279–281

Hendy, E. J., Tomiak, P. J., Collins, M. J., Hellstrom, J., Tudhope, A. W., Lough, J. M., Penkman, K. E. H., 2012. Assessing amino acid racemization variability in coral intra-crystalline protein for geochronological applications. Geochimica et Cosmochimica Acta 86, 338-353

Herridge, V. L., 2010. Dwarf elephants on Mediterranean islands: A natural experiment in parallel evolution. Publish PhD thesis.

Herridge, V. L**.** et al., New, robust dates for *Palaeoloxodon falconeri* at Spinagallo Cave, Sicily. *In prep*

Hershkovitz, I., Weber, G. W., Quam, R., Duval, M., Grün, R., Kinsley, L., Ayalon, A., Bar-Mattews, M., Valladas, H., Mercier, N., Arsuaga, J. L., Martinon-Torres, M., Bermudez de Castro, J. M., Fornai, C., Martin-Frances, L., Sarig, R., May, H., Krenn, V. A., Slon, V.,

Rodriguez, L., Garcia, R., Lorenzo, C., Carretero, J. M., Frumkin, A., Shahack-Gross, R., Mayer, D. E. B., Cui, Y., Wu, X., Peled, N., Groman-Yaroslavski, I., Weissbrod, L., Yeshurun, R., Tsatskin, A., Zaidner, Y., Weinstein-Evron, M., 2018. The earliest modern humans outside Africa. Science 359, 456-459

Hey, R. W., 1991. Pleistocene gravels in the lower Wye Valley. Geological Journal 26, 123-136

Higham, T. F. G., Jacobi, R. M., Bronk R. C., 2006. AMS radiocarbon dating of ancient bone using ultrafiltration. Radiocarbon 48, 179-195

Higham, T., Compton, T., Stringer, C., Jacobi, R., Shapiro, B., Trinkaus, E., Chandler, B., Groning, F., Collins, C., Hillson, S., O'Higgins, P., FitzGerald, C., Fagan, M., 2011. The earliest evidence for anatomically modern humans in northwestern Europe. Nature letters, 1-4

Hill, R. L., 1965. Hydrolysis of proteins. In: Anfinsen Jr., C. B., Anson, M. L., Edsall, J. T., Richards, F. M. (Eds.), Advances in Protein Chemistry 20. Academic Press, New York, NY, 37-107

Hillson, s., 2005. Teeth, Manuals in Archaeology, 2nd Ed. Cambridge University Press, UK, Cambridge

Hodgson, J. M., 1964. The low-level Pleistocene marine sands and gravels of the West Sussex coastal plain. Proceedings of the Geologists' Association, 75, 547–562

Hoering, T. C., 1980. The organic constituents of fossil mollusc shells. , In: Hare, P. E., Hoering, T. C., King Jr, K., Eds., Biogeochemistry of Amino Acids, 193-201, New York: Wiley

Holyoak, D. T. & Preece R. C., 1985. Late Pleistocene Interglacial deposits at Tattershall, Lincolnshire. Philosophical Transactions of the Royal Society of London. Series B, Biological Sciences 311, 1149, 193-236

Hoffmann, A. A., Sgro, C. M., 2011. Climate change and evolutionary adaptation. Nature 470, 479-485

Hofreiter, M., Collins, M., Stewart, J. R., 2012. Ancient biomolecules in Quaternary palaeoecology. Quaternary Science Reviews 33, 1-13

Hu, C. C., Fukae, M., Uchida, T., 1997. Sheathalin: Cloning, cDNA polypeptide sequences, and immunologicalization of porcine enamel sheath proteins. Journal of Dental Research 76, 648-657

Ikeya, M., 1975. Dating a stalactite by electron paramagnetic resonance. Nature 255, 48-50

Ikeya, M., 1982. A model of linear uranium accumulation for ESR age of Heidelberg (Mauer) and Tautavel bones. Japanese Journal of applied Physics 22, 763-765

Ikeya M., 1993 - New applications of electron spin resonance - dating, dosimetry and spectroscopy, World scientific, 500

Imbrie, J., Hays, J., Martinson, D., et al., 1984. The orbital theory of Pleistocene climate: support from a revised chronology of the marine $\delta^{18}O$ record. In: Milankovitch and Climate, Berger, A. L. et al., Eds., Dordrecht: Reidel, 269–305

Ingalls, A. E., Lee, C., Druffel, E. R. M., 2003. Preservation of organic matter in mound-forming coral skeletons. Geochimica et Cosmochimica Acta 67, 2827-2841

Inglis, A. S., 1950. Cleavage at Aspartic acid. Methods in enzymology 91, 255-263

Ivanova, T. I., Frank-Kamenetskaya, O.V. Kol'tsov, A. B., Ugolkov, V. L., 2001. Crystal Structure of Calcium-Deficient Carbonated Hydroxyapatite. Thermal Decomposition. Journal of Solid State Chemistry 160, 340-349

Jacobi, R. M., Higham, T. F. G., Bronk R. C., 2006. AMS radiocarbon dating of Middle and Upper Palaeolithic bone in the British Isles: Improved reliability using ultrafiltration. Journal of Quaternary Science 21, 557-573

Jackson, S. T., Webb, R. S., Anderson, K. H., Overpeck, J. T., Webb, T., Williams, J. W., Hansen, B. C. S., 2000. Vegetation and environment in Eastern North America during the Last Glacial Maximum. Quaternary Science Reviews 19, 489-508

Jones, J., 1992. Amino Acid and Peptide Synthesis, Oxford Chemistry Primer. Oxford University Press

Kaczynski, P., 2017. Clean-up and matrix effect in LC-MS/MS analysis of food of plant origin for high polar herbicides. Food chemistry 230, 524-531

Kato, M., Kato, H., Eyama, S., Takatsu, A., 2009. Application of amino acid analysis using hydrophilic interaction liquid chromatography coupled with isotope dilution mass spectrometry for peptide and protein quantification. Journal of Chromatography B 877, 3059-3064

Kaufman, D. S., 2000. Amino acid racemization in ostracodes. In: Goodfriend, G. A., Collins, M. J., Fogel, M. L., Macko, S. A., Wehmiller, J. F. (Eds.), Perspectives in Amino Acid and Protein Geochemistry. Oxford University Press, New York, 145-160

Kaufman, D. S. & Manley, W. F., 1998. A new procedure for determining DL amino acid ratios in fossils using reverse phase liquid chromatography. Quaternary Science Reviews 17, 987-1000

Keen, D. H., 2001. Towards a late Middle Pleistocene non-marine molluscan biostratigraphy for the British Isles. Quaternary Science Reviews 20, 1657-1665

Kendall, C., & Caldwell, E. A., 1998. Fundamentals of Isotope Geochemistry, In: C. Kendall & J.J. McDonnell (Eds.), Isotope Tracers in Catchment Hydrology. Elsevier Science, Amsterdam, 51-86

Kessels, H. J. & Dungworth, G., 1980. Necessity of Reporting Amino Acid Compositions of Fossil Bones Where Racemization Analyses are Used for Geochronological Applications: inhomogeneities of D/L Amino Acids in Fossil Bones, In: P.E. Hare, T.C. Hoering, and K. King Jr., Eds., Biogeochemistry of Amino Acids, 527-541, New York: Wiley

Kim, Y., Carloni, J. D., Demarchi, B., Sparks, D., Reid, D. G., Kunitake, M. E., Tang, C. C., Duer, M. J., Freeman, C. L., Pokroy, B., Penkman, K., Harding, J. H., Estroff, L. A., Baker, S. P., Meldrum, F., 2016. Hardness in calcite by incorporation of amino acids. Nature Materials 15, 903-910

King, W. B.R. & Oakley, K. P., 1936. The Pleistocene Succession in the Lower parts of the Thames Valley. Proceedings of the Prehistoric Society 2, 52-76

King, K. Jr, & Neville, C., 1977. Isoleucine epimerisation for dating marine sediments: importance of analysing monospecific foraminiferal samples. Science 195, 1333-1335

Kojo, S., 2010. Origin of Homochirality of Amino Acids in the Biosphere. Symmetry 2, 1022-1032

Kostadinov, T. S. & Gilb, R., 2014. Earth Orbit v2.1: a 3-D visualization and analysis model of Earth's orbit, Milankovitch cycles and insolation. Geoscientific Model Development 7, 1051-1068

Kriausakul, N. & Mitterer, R. M., 1978. Isoleucine epimerization in peptides and proteins: kinetic factors and application to fossil proteins. Science 201, 1011-1014

Kriausakul, N. & Mitterer, R. M., 1980. Some factors affecting the Epimerization of Isoleucine in peptides and proteins., Hare, P.E., Hoering, T. C., and King Jr. K., Eds., Biogeochemistry of Amino Acids, 283-297, New York: Wiley

Kromer B. & Münnich K. O. 1992. Co_2 Gas Proportional Counting in Radiocarbon Dating — Review and Perspective. In: Taylor R. E., Long A., Kra R.S. (eds) Radiocarbon After Four Decades. Springer, New York, NY

Kopaciewicz, W., Rounds, M. A. Fausnaugh, J., Regnier, F. E., 1983. Retention model for high-performance ion-exchange chromatography. Journal of Chromatography A 266, 3-21

Krumpochova, P., Bruyneel, B., Molenaar, D., Koukou, A., Wuhrer, M., Niessen, W. M. A., Giera, M., 2015. Amino acid analysis using chromatography–mass spectrometry: An inter platform comparison study. Journal of Pharmaceutical and Biomedical Analysis 114, 398-407

Lajoie, K. R., Wehmiller, J. F., Kennedy, G. L., 1980. Inter- and intra-generic trends in apparent racemization kinetics of amino acids in Quaternary Molluscs. . In: Biogeochemistry of amino acids. Hare, P. E., Hoering, T. C., King, K., 115-120. John Wiley & Sons

Lam, H., Oh, D., Cava, F., Takacs, C. N., Jon, C., de Pedro, M. a., Waldor, M. K., 2009. D-Amino Acids Govern Stationary Phase. Science 325, 1552-1555

Laws, R. M., 1966. Age criteria for the African elephant, *Loxodonta a. africana*. East African Wildlife Journal 4, 1 – 37

Lee, J. R., Candy, I., Haslam, R., 2017. The Neogene and Quaternary of England: landscape evolution, tectonics, climate change and their expression in the geological record, Proceedings of the Geological Association 129, 452-481

Lendaro, E., Ippoliti, R., Bellelli, Maurizio, B., Zito, R., Citro, G., Ascenzi, A., 1991. On the problem of immunological detection of antigens in skeletal remains. American Journal of Physical Anthropology 86

Lewis, S. G., 1999. Eastern England. In: Bowen D. Q., A revised correlation of Quaternary deposits in the British Isles. The Geological Society, 10-27

Lewis, S. G., Maddy, D., Buckingham, C., Coope, G. R., Field, M. H., Keen, D. H., Pike, A. W. G., Roe, D. A., Scaife, R. G., Scott, K., 2006. Pleistocene fluvial sediments, palaeontology and

archaeology of the upper River Thames at Latton, Wiltshire, England. Journal of Quaternary Science 21, 181-205

Linden J. C. & Lawhead, C. L., 1975. Liquid Chromatography of Saccharides. Journal of Chromatography 105, 125-133

Lister, M. A., 1986. New Results on Deer from Swanscombe, and the Stratigraphical Significance of Deer in the Middle and Upper Pleistocene of Europe. Journal of Acheological Science 13, 319-338

Lister, A. M., 1993. The stratigraphical significance of deer species in the cromer forest-bed formation. Journal of Quaternary Science 8, 95-108

Lister A. M., 1994. The stratigraphical interpretation of deer species in the Cromer Forest-bed Formation. Journal of Quaternary Science 8: 95– 108

Lister, A. M., 1996. The stratigraphical interpretation of large mammal remains from the Cromer Forest-bed Formation. In: The Early Middle Pleistocene in Europe ed. 25-44. Rotterdam

Lister, A. M., 1998. The age of Early Plistocene mammal faunas from the 'Weybourne Crag' and Cromer Forest-bed Formation (Norfolk, England). Mededelingen Nederlands Instituut voor Toegepaste Geowetenschappen 60, 271-280

Lister, A. M., 2001a. The origins and evolution of the woolly mammoth. Science 294, 1094-1097

Lister, A. M., 2001b. Age profile of mammoths in a Late Pleistocene hyena den at Kent's Cavern, Devon, England. In: D.L. West (Ed.), Proceedings of the International Conference on Mammoth Site Studies, Anthropological Papers University of Kansas 22, 35-43

Lister, A. M., 2009. Late-glacial mammoth skeletons (*Mammuthus primigenius*) from Condover (Shropshire, UK): anatomy, pathology, taphonomy and chronology significance. Geological Journal 44, 447-479.

Lister, A. M. & Brandon, A., 1991. A pre-Ipswichian cold stage mammalian fauna from the Balderton Sand and Gravel, Lincolnshire, England. Journal of Quaternary Science 6, 139-157

Lister, A. M. & Scott, K., *in prep*

Lister, A, M. & Sher, A. V., 2001. The origin and evolution of the woolly mammoth. Science 294, 1094-1097

Lister, A. M. & Van Essen, H., 2003. *Mammuthus rumanus* (Stefanescu), the earliest mammoth in Europe. Advances in Vertebrate Paleontology “Hen to Panta”, 47-52

Lister, A. M., Sher, A. V., van Essen, H., Wei, G., 2005. The pattern and process of mammoth evolution in Eurasia. Quaternary International 126-128., 49-64

Lisiecki, L. E., Raymo, M. E., 2005. A Pliocene-Pleistocene stack of 57 globally distributed benthic $\delta^{18}O$ records. Paleoceanography 20. PA1003

Lord, N. S., Crucifix, M., Lunt, D. J., Thorne, M. C., Bounceur, N., Dowsett, H., O'Brien, C. L., Ridgwell, A., 2017. Emulation of long-term changes in global climate: Application to the late Pliocene and future. Climate of the Past Discussions 13, 1539-1571

Lowe, D., 1989. Problems associated with the use of coal as a source of ^{14}C free background material. Radiocarbon 31, 117-120.

Lowe, J. J., and Walker, M. J. C., 2014. Reconstructing Quaternary environments. 3rd Ed. Routledge, London.

Macherey-Nagel, 2012. Chromabond HILIC flyer, KATEN200105. Germany

MacPhee, R. D. E., Tikhonov, A. N., Mol, D., de Marliave, C., van der Plicht, H., Greenwood, A. D., 2002. Radiocarbon Chronologies and Extinction Dynamics of the Late Quaternary Mammalian Megafauna of the Taimyr Peninsula, Russian Federation. Journal of Archaeological Science 29, 1017-1042

Maddy, D., 1997. Uplift-driven valley incision and river terrace formation in southern England. Journal of Quaternary Science 12, 339-345

Manley, W. F., Miller, G. H., Czywczynski, J., 2000. Kinetics of aspartic acid racemization in Mya and Hiatella: modelling age and palaeotemperature of high- latitude Quaternary molluscs. In: Goodfriend, G. A., Collins, M. J., Fogel, M. L., Macko, S. A., Wehmiller, J. F. (Eds.), Perspectives in Amino Acid and Protein Geochemistry. Oxford University Press, New York, 120-141

Margolis, H. C., Beniash, E., Fowler, C. E., 2006. Role of macromolecular assembly of enamel matrix proteins in enamel formation. Journal of Dentistry Research 85, 775-793

Marin, F., Luquet, G., Marie, B., Medakovic, D., 2008. Molluscan Shell Proteins: Primary Structure, Origin, and Evolution. Current Topics in Developmental Biology 80, 209-276

Marra, A. C., 2005. Pleistocene mammals of Mediterranean islands. Quaternary International 129, 5-14

Marshall, E., 1990. Racemization dating: great expectations. Science 247, 799

Mason, S. F., 1984. Origins of bimolecular handedness. Nature 311, 19-23

Mathers, S. J. & Zalasiewicz, J. A. 1988. The Red Crg and Norwich Crag formations of southern East Anglia. Proceedings of the Geologists Association 99, 261-278

Mathers, S. J. & Hamblin, R. J. O., 2015. Late Pliocene and Pleistocene marine deposits, In: Lee, J. R., Woods, M. A., Moorlock, B. S. P. (5th Eds.), British Regional Geology: East Anglia. British Geological Survey, Keyworth, Nottingham, 110-129

Matter, P. III, Davidson, F. D., Wyckoff, R. W. G., 1969. The composition of fossil oyster shell proteins, Proceedings of the National Academy of Science U.S.A. 69, 790-792

Maul, L. C. & Parfitt, S. A., 2010. Micromammals from the 1995 Mammoth Excavation at West Runton, Norfolk, UK: Morphometric data, biostratigraphy and taxonomic reappraisal. Quaternary International 228, 91-115

Mayhew, D. F. & Stuart, A. J., 1986. Stratigraphic and taxonomic revision of the fossil vole remains (Rodentia, Microtinae) from the Lower Pleistocene Deposits of Eastern England. Philosophical transactions 312, 431-485

McCally, D. V., 2010. Study of the selectivity, retention mechanisms and performance of alternative silica-based stationary phases for separation of ionised solutes in hydrophilic interaction chromatography. Journal of Chromatography A 1217, 3408-3417

McCudden, C. R., Kraus, V. B., 2006. Biochemistry of amino acid racemization and clinical application to musculoskeletal disease. Clinical Biochemistry 39, 1112-1130

Meijer, T. & Preece, R. C., 2000. A review of the occurrence of *Corbicula* in the Pleistocene of North-West Europe. Geologie en Mijnbouw/Netherlands Journal of Geosciences 79**,** 241-255

Meiri, S., Dayan, T. and Simberloff, D. 2004. Body size of insular carnivores: little support for the island rule. *American Naturalist* 163, 469-479

Meiri, S., Cooper, N. and Purvis, A. 2008. The island rule: made to be broken. Proceedings of the Royal Society B 275, 141-148

Metcalfe, J. Z., Longstaffe, F. J., Zazula, G. D., 2010. Nursing, weaning, and tooth development in woolly mammoths from Old Crow, Yukon, Canada: Implications for Pleistocene extinctions. Palaeogeography, Palaeoclimatology, Palaeoecology 298, 257-270

Miller, G. H., Hollin, J. T., Andrews, J. T., 1979. Aminostratigraphy of UK Pleistocene Deposits. Nature 281, 538-543

Miller, G. H., Sejrup, H. P., Mangerud, J., Andersen, B. G., 1983. Amino acid ratios in Quaternary molluscs and foraminifera from western Norway: correlation, geochronology and paleotemperature estimates. Boreas 12, 107-124

Miller, G. H., Hart, C. P., Roark, E. B., Johnson, B. J., 2000. Isoleucine epimerization in eggshells of the flightless Australian birds Genyornis and Dromaius. In: Goodfriend, G. A., Collins, M. J., Fogel, M. L., Macko, S. A., Wehmiller, J. F. (Eds.), Perspectives in Amino Acid and Protein Geochemistry. Oxford University Press, Oxford, 161–181

Millien, V. 2006. Morphological evolution is accelerated among island mammals. PLoS Biology 4, e.321

Mitchell, G. F., Penny, L. F., Shotton, F. W., West, R. G., 1973. A Correlation of Quaternary deposits in the British Isles. Geological Society, London special reports, 4.

Mitterer, R. M., Kriausakul, N., 1984. Comparison of the rates and degrees of isoleucine epimerization in dipeptides and tripeptides. Organic Geochemistry 7, 91-98

Mol, D., Post, K., Reumer, J. W. F., van der Plicht, J., de Vos, J., van Geel, van Reenen, G., Pals, J. P., Glimmerveen, J., 2006. The Eurogeul - First report of the palaeontological, palynological and archaeological investigations of this part of the North Sea. Quaternary International 142-143, 178-185

Mook, W. G., 1986. Business meeting – recommendations resolutions adopted by the 12th international radiocarbon conference. Radiocarbon 28 799-799

Moradian-Oldak, J., Tan, J., Fincham, A. G., 1998. Interaction of amelogenin with hydroxyapatite crystals: An adherence effect through amelogenin molecular self-association. Biopolymers 46, 225-238

Morris, V., 2011. Enamel phosphate method development. Unpublished MChem dissertation

Murray-Wallace, C. V. & Bourman, R. P., 1990. Direct radiocarbon calibration for amino acid racemization dating. Australian Journal of Earth Sciences 37, 365-367

Myers, H. M., 1965. Trapped water of dental enamel. Nature 206, 713-714

Myers, N., Mittermeier, R. A., Mittermeier, C. G., da Fonseca, G. A. B., Kent, J. 2000. Biodiversity hotspots for conservation priorities. Nature 403, 853-858

Naidong, W., 2003. Bioanalytical liquid chromatography tandem mass spectrometry methods on underivatized silica columns with aqueous/organic mobile phases. Journal of Chromatography B 796, 209-224

NEEM community members, 2013. Eemian interglacial reconstructed from a Greenland folded ice core. Nature 493, 489-494

Neuberger, A. 1948. Stereochemistry of amino acids. Advances in protein chemistry 4, 297-383

Norton, P. E. P., 2000. Shells in sugar bags or, the Crag Mollusca revisited. The Geological Society of Norfolk, 50th Anniversary Jubilee Volume, 55-58

Oakley, K. P., 1952. Swanscombe man. Proceeding of the Geological Association 63, 271-300

Oches, E. A., McCoy, W. D., Clark, P. U., 1996. Amino acid estimates of latitudinal temperature gradients and geochronology of loess deposition during the last glacial maximum, Mississippi Valley, United States. Geological Society of America Bulletin 108, 892–903

Ogino, T, Ogino, H., Nagy, B., 1985. Application of aspartic-acid racemization to forensic Odontology – Postmortem designation of age at death. Forensic science international 29, 259-267

Ohtani, S., Kato, S., Sugeno, H., Sugimoto, H., Marumo, T., Yamazaki, M.,Yamamoto, K., 1988. A study on the use of the amino acid racemization method to estimate the ages of unidentified cadavers from their teeth, Bulletin Kanagawa Dental College 16, 11–21

Orem, C. A., Kaufman, D. S., 2011. Effects of basic pH on Amino acid racemisation and leaching in freshwater mollusk shell. Quaternary Geochronology 6, 233-245

Ortiz, J. E., Torres, T., Pérez-González, A., 2013. Amino acid racemization in four species of ostracodes: Taxonomic, environmental, and microstructural controls. Quaternary Geochronology 16, 129-143

Ortiz, J. E., Sánchez-Palencia, Y., Gutiérrez-Zugasti, I., Torres, T., González-Morales, M., 2018. Protein diagenesis in archaeological gastropod shells and the suitability of this material for amino acid racemisation dating: Phorcus lineatus (da Costa, 1778). Quaternary Geochronology 46, 16-27

Ouladdiaf, B., Rodriguez-Carvajal, J., Goutaudier, C., Ouladdiaf, S., Grosgogeat, B., Pradelle, N., Colon, P., 2015. Crystal structure of human tooth enamel studied by neutron diffraction. Materials Research Express 2, 025401

Owen-Smith, N., 1989. Megafaunal Extinctions: The Conservation Message from 11,000 Years B.P. Conservation Biology 3, 405-412

Pan, B., Ricci, M. S., Trout, B. L., 2011. A Molecular Mechanism of Hydrolysis of Peptide Bonds at Neutral pH Using a Model Compound. The Journal of Physical Chemistry B 115, 5958-5970

Parfitt, S. A., 1998. Pleistocene vertebrate faunas of the West Sussex Coastal Plain: their stratigraphic and palaeoenvironmental significance. In: Murton, J. B., Whiteman, C. A., Bates, M. R., Bridgland, D. R., Long, A. J., Roberts, M. B. and Waller, M. P. (eds), The Quaternary of Kent and Sussex. Field Guide, 121–134. Quaternary Research Association, London

Parfitt, S. A., 2003. Mammalian biostratigraphy. In: Wenban-Smith, The Ebbsfleet Elephant, Excavations to Southfleet Road, Swanscombe in advance of High Speed I, 2003-4. 233-262 Oxford Archaeology Monograph No. 20

Passey B. H. & Cerling T. E., 2002. Tooth enamel mineralization in ungulates: implications for recovering a primary isotopic time-series. Geochim. Cosmochim. Acta 66, 3225–3234

Patel, K. & Borchardt, R. T., 1990. Chemical Pathways of Peptide Degradation. III. Effect of Primary Sequence on the Pathways of Deamidation of Asparaginyl Residues in Hexapeptides. Pharmaceutical Research 7, 787-793

Paz, A., Guadarrama, D., López, M., González, J. E., Brizuela, N., Aragón, J., 2012. A Comparative Study of Hydroxyapatite Nanoparticles Synthesized by Different Routes. Química Nova 35, 1724-1727

Peglar, S. M., Fritz, S. C., Birks, H. J. B., 1989. Vegetation and Land-Use History at Diss, Norfolk, UK. Journal of Ecology 77, 203-222

Penkman, K. E. H., 2010. Amino acid geochronology: Its impact on our understanding of the Quaternary stratigraphy of the British Isles. Journal of Quaternary Science 25 (4), 501-514

Penkman, K. E H., Preece, R. C., Keen, D. H., Maddy, D., Schreve, D. C., Collins, M. J., 2007. Testing the aminostratigraphy of fluvial archives: the evidence from intra-crystalline proteins within freshwater shells. Quaternary Science Reviews 26, 2958-2969

Penkman, K. E. H., Kaufman, D. S., Maddy, D., Collins, M. J., 2008. Closed-system behaviour of the intra-crystalline fraction of amino acids in mollusc shells. Quaternary Geochronology 3, 2-25

Penkman, K. E. H., Preece, R. C., Keen, D. H., Collins, M. J., 2010. Amino acid geochronology of the type Cromerian of West Runton, Norfolk, UK. Quaternary International 228, 25-37

Penkman, K. E. H., Preece, R. C., Bridgland, D. R., Keen, D. H., Meijer, T., Parfitt, S. A., White, T. S., Collins, M. J., 2011. A chronological framework for the British Quaternary based on Bithynia opercula. Nature 476, 446-449

Penkman, K. E. H., Preece, R. C., Bridgland, D. R., Keen, D. H., Meijer, T., Parfitt, S. A., White, T. S., Collins, M. J., 2013. An aminostratigraphy for the British Quaternary based on Bithynia opercula. Quaternary Science Reviews 61, 111-134

Perelra, A. D. S, David, F., Vanhoenacker, G., Sandra, P., 2009. The acetonitrile shortage: Is reversed HILIC with water an alternative for the analysis of highly polar ionizable solutes?. Journal of separation science 32, 2001-2007

Periat, A., Krull, I. S., Guillarme, D., 2015. Applications of hydrophilic interaction chromatography to amino acids, peptides, and proteins. Journal of Separation Science 38, 357–367

Petit, J. R., Jouzel, J., Raynaud, D., Barkov, N. I., Barnola, J. M., Basile, I., Bender, M., Chappellaz, J., Davis, M., Delaygue, G., Delmotte, M., Kotiyakov, V. M., Legrand, M., Lipenkov, V. Y., Lorius, C., Pépin, L., Ritz, C., Saltzman, E., Stievenard, M., 1999. Climate and atmospheric history of the past 420,000 years from the Vostok ice core, Antarctica. Nature 399, 429-436

Pigati, J. S., Quade, J., Wilson, J., Jull, T. A. J., Lifton, N. A., 2007. Development of low-background vacuum extraction and graphitization systems for ^{14}C dating of old (40–60 ka) samples. Quaternary International 166, 4-14

Poinar, H. N., Stankiewicz, B. A., 1999. Protein preservation and DNA retrieval from ancient tissues. Proceedings of the National Academy of Sciences of the United States of America 96, 8426-8431

Powell, J., Collins, M. J., Cussens, J., Macleod, N., Penkman, K. E. H., 2013. Quaternary Geochronology Results from an amino acid racemization inter-laboratory proficiency study; design and performance evaluation. Quaternary Geochronology 16, 183-197

Pettitt, P. & White, M., 2012. The British Palaeolithic: Human Societies at the Edge of the Pleistocene World. Routledge

Preece, R. C., 1999. Mollusca from Last Interglacial fluvial deposits of the River Thames at Trafalgar Square, London. Journal of Quaternary Science 14, 77-89

Preece, R. C. & Penkman, K. E. H., 2005. New faunal analyses and amino acid dating of the Lower Palaeolithic site at East Farm, Barnham, Suffolk. Proceedings of the Geologists' Association 116, 363-377

Preece, R. C., Parfitt, S. A., Coope, G. R., Penkman, K. E. H., Ponel, P., Whittaker, J. E., 2009. Biostratigraphic and aminostratigraphic constraints on the age of the Middle Pleistocene glacial succession in north Norfolk, UK. Journal of Quaternary Science 24, 557-580

Procopio, N., Chamberlain, A. T., Buckley, M., 2018. Exploring Biological and Geological Age-related Changes through Variations in Intra- and Intertooth Proteomes of Ancient Dentine. Journal of Proteome Research 17, 1000-1013

Proctor, C. J., 1996. Kent's Cavern. In: Charman, D. J., Newman, R. M., Croot, D. G., (eds), The Quaternary of Devon and East Cornwall, Field guide, Quaternary Research Association, London, 163-167

Rackman, D. J., 1978. Evidence for the changing vertebrate communities in the Middle Devensian. Quaternary Newsletter 25, 1-3

Radkiewicz, J. L., Zipse, H., Clarke, S., Houk, K. N., 1996. Accelerated racemization of aspartic acid and asparagine residues via succinimide intermediates: An ab initio theoretical exploration of mechanism. Journal of the American Chemical Society 118, 9148-9155

Radzicka, A. & Wolfenden, R. 1996. Rates of uncatalyzed peptide bond hydrolysis in neutral solution and the transition state affinities of proteases. Journal of the American Chemical Society 118, 6105-6109

Raia, P. & Meiri, S. 2006. The island rule in large mammals: paleontology meets ecology. Evolution 60, 1731-1742

Ravelo, A. C. & Hillaire-Marcel, C., The use of oxygen and carbon isotopes of foraminifera in paleoceanography. In: Developments in marine geology Volume 1 Eds. Elsevier

Reichert, K. L., Licciardi, J. M., Kaufman, D. S., 2011. Amino acid racemization in lacustrine ostracodes, part II: Paleothermometry in Pleistocene sediments at Summer Lake, Oregon. Quaternary Geochronology 6, 174-185

Reid, C. 1890. The Pliocene deposits of Britain. Memoirs of the Geological Survey U.K.

Reid, E. M., 1949. The Late-Glacial Flora of the Lea Valley. The New Phytologist 48, 245-252

Riley, M. S., Collins, M. J., 1994. The polymer model of collagen degradation. Polymer degradation and stability 46, 93-97

Refsnider, K. A., Miller, G. H., Frechette, B., Rood, D. H., 2013. A chronological framework for the Clyde Foreland Formation, Eastern Canadian Arctic, derived from amino acid racemization and cosmogonic radionuclides. Quaternary Geochronology 16, 21-34

Reimer, P., Bard, E., Bayliss, A., Beck, J., Blackwell, P., Ramsey, C., Buck, C. E., Cheng, H., Edwards, R. L., Friedrich, M., Grootes, P. M., Guilderson, P. T., Haflidason, H., Hajdas, I., Hatté, C., Heaton, T. J., Hoffmann, D. L., Hogg, A. G., Hughen, K. A., Kaiser, K. F., Kromer, B., Manning, S. W., Niu, M., Reimer, R. W., Richards, D. A., Scott, E. M., Southon, J. R., Staff, R. A., Turney, C. S. M., Van der Plicht, J., 2013. IntCal13 and Marine13 Radiocarbon Age Calibration Curves 0–50,000 Years cal BP. *Radiocarbon, 55*(4), 1869-1887.

Rees-Jones, J. & Tite, M. S., 1997. Optical dating results for British Archaeological sediments. Archaeometry 39, 177-187

Rivals, F., Mol, D., Lacombat, F., Lister, A. M., Semprebon, G. M., 2015. Resource partitioning and niche separation between mammoths (Mammuthus rumanus and Mammuthus meridionalis) and gomphotheres (Anancus arvernensis) in the Early Pleistocene of Europe. Quaternary International 379, 164-170

Rink, W. J., 1997. Electron Spin Resonance (ESR) dating and ESR application in Quaternary science and archaeometry. Radiation measurements 27, 975-1025

Rink, W. J., Schwarcz, H.P., Stuart, A.J., Lister, A.M., Marseglias, E., Brennan, B.J., 1996. ESR dating of the type Cromerian Freshwater Bed at West Runton, U.K. Quaternary Science Reviews Quaternary Geochronology 15, 727-738

Ritz-Timme, S. & Collins, M. J., 2002 Racemization of aspartic acid in human proteins. Ageing Research Reviews, 1, 43-59

Rixon, G., Briant, R. M., Cordier, S., Duval, M., Jones, A., Scholz, D., 2017. Revealing the pace of river landscape evolution during the Quaternary: recent developments in numerical dating methods. Quaternary Science Reviews 166, 91-113

Robinson, C., Fuchs P., Weatherall J. A., 1977. The fate of matrix proteins during the development of dental enamel. Calcified Tissue Research 22:185-190

Robinson C., Briggs H., Atkinson P., Weatherell, J., 1979. Matrix and mineral changes in developing enamel. Journal of dentist research 58, 871-882

Robinson, C., Kirkham, J., Brookes, S. J., Bonass, W. A., Shore, R. C., 1995. The chemistry of enamel development. International Journal of Developmental Biology 39, 145-152

Robinson, C. Brookes, S. J., Shore, R. C., Kirkham, J., 1998. The developing enamel matrix: nature and function. Oral sciences 106, 282-291

Roth, L., 1992. Inferences from allometry and fossils: dwarfing of elephants on islands. In: Futuyma, D., Antonovics, J., Oxford surveys in evolutionary biology vol 8. Oxford university press.

Ruddiman, W. F., Raymo, M., McIntyre, A., 1986. Matuyama 41000 year cycles: north Atlantic ocean and Northern Hemisphere ice sheets, Earth Planetary Science Letters 80, 117–129.

Ruta, J., Rudaz, S., McCalley, D. V., Veuthey J., Guillarme, D., 2010. A systematic investigation of the effect of sample diluent on peak shape in hydrophilic interaction liquid chromatography. Journal of Chromatography A 1217, 8230–8240

Sabel, N., Robertson, A., Nietzsche, S., Norén, J. G., 2011. Demineralization of Enamel in Primary Second Molars Related to Properties of the Enamel. The Scientific World Journal 2012, 587254

Skeie, R. B., Berntsen, T., Aldrin, M., Holden, M., Myhre, G., 2018. Climate sensitivity estimates – sensitivity to radiative forcing time series and observational data. Earth System Dynamics 9, 879–894

Sambridge, M., Grün, R., Eggins, S., 2012. Quaternary Geochronology U-series dating of bone in an open system: The diffusion-adsorption-decay model. Quaternary Geochronology 9, 42-53

Schreve, D. C., 2001. Differentiation of the British late Middle Pleistocene interglacials: the evidence from mammalian biostratigraphy. Quaternary Science Reviews 20, 1693-1705

Schreve, D. C. & Candy, I., 2010. Interglacial climates: Advances in our understanding of warm climate episodes. Progress in Physical Geography 34 (6), 845-856

Schreve, D. C., Bridgland, D. R., Allen, P., Blackford, J. J., Gleed-Owen, C. P., Griffiths, H. I., 2002. Sedimentology, palaeontology and archaeology of late Middle Pleistocene river Thames terrace deposits at Purfleet, Essex, UK. Quaternary Science Reviews 21, 12-13

Schroeder R. A. & Bada, J. L., 1973. Glacial-Postglacial Temperature Difference Deduced from Aspartic Acid Racemisation in Fossil Bones. Science 182, 479-182

Schroeder R. A. & Bada, J. L., 1976. A review of the geochemical application of the amino acid racemisation reaction. Earth-Science Reviews 12, 347-391

Schwarcz, H. P., 1989. Uranium series dating of Quaternary deposits. Quaternary International 1, 7-17

Schweitzer, M. H., Chiappe, L., Garrido, A. C., Lowenstein, J. M., Pincus, S. H., 2005. Molecular preservation in Late Cretaceous sauropod dinosaur eggshells. Proceedings of the Royal Society B 272, 775-784

Schweitzer, M. H., Zheng, W., Cleland, T. P., Bern, M., 2013. Molecular analyses of dinosaur osteocytes support the presence of endogenous molecules. Bone 52, 414-423

Scott, K., 2001. Late Middle Pleistocene Mammoths and Elephants of the Thames Valley, Oxfordshire. 1st International Congress: La terra degli elefanti, 247-254

Scott, K. & Eeles, R. M. E., in preparation. The large vertebrate fauna from Upper Pleistocene (MIS 5-3) gravels at Sutton Courtenay, Oxfordshire, UK

Serdyuk, N. V., 2006. Paleoreconstruction of Pleistocene Environments of Human Habitats in the Late Pleistocene and Holocene near the Charyshskii Naves Cave, Central Altai, Russia. Paleontological Journal 40, 501-507

Shoshani, J., 1996. Skeletal and other basic anatomical features of elephants. In: Shoshani, J., Tassy, P. (Eds.), The Proboscidea: Evolution and Palaeoecology of Elephants and their Relatives. Oxford University Press, Oxford, 9-20

Shou, P. M., Bada, J. L. 1980. The pK ' s of Amino Acids at Elevated Temperatures Estimated from Racemization Data. Naturwissenschaften 67, 37-38

Simpson, N. J. K., 2000. Solid-phase extraction, Principals, Techniques, and Application. Marcel Dekker Inc. New York

Smith, G. G. & De Sol, S. B., 1980. Racemization of amino acids in dipeptides shows COOH > NH_2 for non-sterically hindered residues. Science 207, 765-767

Smith, G. G. & Evans, R. C., 1980. The effect of structure and conditions on the rate of racemisation of free and bound amino acids. In P.E. Hare, T.C. Hoering, and K. King Jr., Eds., Biogeochemistry of Amino Acids, 257-282, New York: Wiley

Smith, G. G. & Reddy, G. V., 1989. Effect of the side-chain on the racemization of amino-acids in aqueous solution. Journal of Organic Chemistry 54, 4529-4535

Smith, G. G., Williams, K. M., Wonnacott, D. M. 1978. Factors Affecting the Rate of Racemization of Amino Acids and Their Significance to Geochronology. Journal of Organic Chemistry 43, 1-5

Smyth, J. R. & Ahrens, T. J., 1997. The crystal structure of calcite III. Geophysical Research Letters 24, 1595-1598

Sparks, B. W. & West, R. G., 1959. The palaeoecology of the interglacial deposits at Histon Road, Cambridge. Eiszeitalter und Gegenwart 10, 123-143

Steinberg, S. M. & Bada, J. L., 1981. Diketopiperazine formation during investigations of amino acid racemization in dipeptides. Science 213, 544–545

Steinberg, S. M. & Bada, J. L., 1983. Peptide decomposition in the neutral pH range via formation of diketopiperazines. Journal of Organic Chemistry 48, 2295-2298

Steinberg, S. M., Masters, P. M., Bada, J. L., 1984. The racemisation of free and peptide-bound serine and aspartic acid at 100 °C as a function of pH: implications for *in vivo* racemisation. Bioorganic chemistry 12, 349-355

Stephenson, R. C. & Clarke, S., 1989. Succinimide formation from aspartyl and asparaginyl peptides as a model for the spontaneous degradation of proteins. Journal of Biological Chemistry 264, 6164-6170

Stock, C., 1935. Exiled Elephants of the Channel Islands, California. American Association for the Advancement of Science 41, 205-214

Stock, C., & Furlong, E. L., 1928. The Pleistocene Elephants of Santa Rosa Island, California. Science 68, 140-141

Stokes, S., Ingram, S., Aitken, M.J., Sirocko, F., Anderson, R., Leuschner, D., 2003. Alternative chronologies for Late Quaternary (Last Interglacial–Holocene) deep sea sediments via optical dating of silt-size quartz. Quaternary Science Reviews 22, 925–941

Stuart, A. J., 1975. The History of the Mammal Fauna during the Ipswichian/Last Interglacial in England. Philosophical Transactions of the Royal Society B: Biological Sciences 276, 221-250

Stuart, A. J. 1982. Pleistocene Vertebrates in the British Isles. London: Longman

Stuart, A. J., Kosintsev, P. A., Higham, T. F. G., Lister, A. M., 2004. Pleistocene to Holocene extinction dynamics in giant deer and woolly mammoth. Nature 431, 684-689

Sutcliffe, A. J., 1975. A hazard in the interpretation of glacial - interglacial sequences. Quaternary Newsletter 17, 1-3

Sykes, G. A., Collins, M. J., Walton, D. I., 1995. The significance of a geochemically isolated intracrystalline organic fraction within biominerals. Organic Geochemistry 23, 1059-1065

Takahashi, O., 2013. Two-water-assisted racemization of the succinimide intermediate formed in proteins. A computational model study. Health 12, 2018-2021

Takahashi, O., Kobayashi, K., Oda, A., 2010. Computational insight into the mechanism of serine residue racemization. Chemistry and Biodiversity 7, 1625-1629

Tandon, L., Iyengar, G. V., Parr, R.M., 1998. A review of radiologically important trace

elements in human bones. Applied Radiation and Isotopes 49, 903-910

Taylor, R. E., 1983. Non-concordance of Radiocarbon and Amino Acid Racemisation Deduced Age Estimates on Human Bone. Radiocarbon 25 (2), 647-654

Taylor, W. R., 1986. The classification of amino acid conservation. Journal of theoretical biology 119, 205-218

Taylor, R. E., 1987. Radiocarbon dating. London: Academic Press.

Timme, M., Timme, W. H., Olze, A., Ottow, C., Ribbecke, S., Pfeiffer, H., Dettmeyer, R., Schmeling, A., 2017. Dental age estimation in the living after completion of third molar mineralization: new data for Gustafson's criteria. International Journal of Legal Medicine 131, 567-577

Tinner, W. & Lotter, A. F., 2001. Central European vegetation response to abrupt climate change at 8.2 ka. Geology 29 (6), 551-554

Tolstikov, V. V. & Fiehn, O., 2002. Analysis of Highly Polar Compounds of Plant Origin: Combination of Hydrophilic Interaction Chromatography and Electrospray Ion Trap Mass Spectrometry. Analytical Biochemistry 301, 298-307

Tomiak, P. J., Penkman, K. E H., Hendy, E. J., Demarchi, B., Murrells, S., Davis, S., McCullagh, P., Collins, M. J. 2013. Testing the limitations of artificial protein degradation kinetics using known-age massive Porites coral skeletons. Quaternary Geochronology 16, 87-109

Torres, T., Llamas, J. F., Canoira, L., García-Alonso, P., García-Cortés, A., Mansilla, H., 1997. Amino acid chronology of the lower pleistocene deposits of Venta Micena (Orce, Granada, Andalusia, Spain). Organic Geochemistry 26, 85-97

Towe, K. M., 1980. Preserved organic ultrastructure: An unreliable indicator for Paleozoic amino acid biogeochemistry. Hare, P. E., Hoering, T. C., King, K. (Eds.), Biogeochemistry of Amino Acids. Wiley, New York, pp. 65-74

Towe, K. M. & Thompson, G. R., 1972. The structure of some bivalve shell carbonates prepared by ion-beam thinning - A Comparison Study. Calcified Tissue Research 10, 38-48

Trayler, R. B., Kohn, M. J., 2017. Tooth enamel maturation re-equilibrates oxygen isotope compositions and supports simple sampling methods. Geochimica et Cosmochimica Acta 198, 32-47

Turner, C. 1973. Eastern England. In: Mitchell, G. F. et al. (Eds): A correlation of Quaternary deposits in the British Isles. Geological Society London, Special Report 4

Turner-Walker, G., 2007. The chemical and microbial degradation of bones and teeth. Advances in human palaeopathology. John Wiley & Sons, Ltd. 11-15

Tzedakis, P. C., Andrieu, V., de Beaulieu, J. -L., Crowhurst, S., Follieri, M., Hooghiemstra, H., Magri, D., Reille, M., Sadori, L., Shackleton, N. J., Wijmstra, T. A., 1997. Comparison of terrestrial and marine records of changing climate of the last 500,000 years. Earth and Planetary Science Letters 150, 171-176

Vartanyan, S. L., Garutt, V. E., Sher, A. V., 1993. Holocene dwarf mammoths from Wrangel Island in the Siberian Arctic. Nature 362, 337-340

van Asperen, E. N., 2011. Distinguishing between the late Middle Pleistocene interglacials of the British Isles: A multivariate approach to horse biostratigraphy. Quaternary International 231, 110-115

Van Valen, L. M., 1973. Pattern and the balance of nature. Evolutionary Theory 1, 31-49

Vanderlaan, T. A. & Ebach, M. C., 2014. Systematic biostratigraphy: A solution to problematic classification systems in biostratigraphy. Palaeoworld 23, 105-111

Vartanyan, S. L., Arslanov, K. H. A., Tertychnaya, T. V., Chernov, S. B., 1995. Radiocarbon dating evidence for mammoths on Wrangel Island, Artic Ocean, until 2000 BC[1]. Radiocarbon 37, 1-6

Vasenko, L. & Qu, H., 2018. Calcium phosphates recovery from digester supernatant by fast precipitation and recrystallization. Journal of Crystal Growth 481, 1-6

Vincent, E., & Berger W. H., 1981. Planktonic foraminifera and their use in Paleoceanography.

In: C. Emiliani (Ed.), The oceanic lithosphere. The sea vol:7, 1025–1119. Hoboken, N. J.:

Wiley-Interscience

von Endt, D. W., 1980 Protein Hydrolysis and amino acid racemisation in sized bone. In: Biogeochemistry of amino acids., Hare, P.E., Hoering, T. C., and King Jr. K., Eds., Biogeochemistry of Amino Acids, 297-304, New York: Wiley

Walker, M., 2005. Quaternary dating methods Eds. John Wiley & sons, Ltd. West Sussex

Walton, D., 1998. Degradation of intracrystalline proteins and amino acids in fossil brachiopods. Organic Geochemistry 28, 389-410

Weber, E., Bloch, L., Guth, C., Fitch, A. N., Weiss, I. M., Pokroy, B., 2014. Incorporation of a Recombinant Biomineralization Fusion Protein into the Crystalline Lattice of Calcite. Chemisty of Materials 26, 4925-4932

Wehmiller, J. F., 1980. Intergeneric differences in apparent racemization kinetics in mollusks and foraminifera: implications for models of diagenetic racemization. In: Hare, P. E., Hoering, T. C., King, K. (Eds.), Biogeochemistry of Amino Acids. Wiley, New York, pp. 341-355

Wehmiller, J. F., 1982. A review of amino acid racemization studies in Quaternary mollusks: Stratigraphic and chronologic applications in coastal and interglacial sites, pacific and Atlantic coasts, United States, United Kingdom, baffin Island, and tropical islands. Quaternary Science Reviews 1, 83-120

Wehmiller, J.F., 1984a. Interlaboratory comparison of amino acid enantiomeric ratios in fossil Pleistocene mollusks. Quaternary Research, 22, 109-120

Wehmiller, J. F., 1984b. Relative and Absolute Dating of Quaternary Mollusks (sic) with Amino Acid Racemization: Evaluation, Applications, and Questions, in: W.C. Mahaney, Ed., Quaternary Dating Methods. 431 Amsterdam: Elsevier

Wehmiller, J. F., 2013. Interlaboratory comparison of amino acid enantiomeric ratios in Pleistocene fossils. Quaternary Geochronology 16, 173-182

Wehmiller, J. F. & Hare, P. E., 1971. Racemisation of amino acids in marine sediments. Science 173, 907-911

Wehmiller, J. F., Harris, W. B., Boutin, B. S., Farrell, K. M., 2012. Calibration of amino acid racemization (AAR) kinetics in United States mid-Atlantic Coastal Plain Quaternary mollusks using 87Sr/86Sr analyses: Evaluation of kinetic models and estimation of regional Late Pleistocene temperature history. Quaternary Geochronology 7, 21-36

Weiner, S. & Hood, L., 1975. Soluble protein of the organic matrix of mollusk shells: a potential template for shell formation. Science 190, 987-989

Weiner, S. & Addadi, L., 1997. Design strategies in mineralized biological materials. Journal of Materials Chemistry 7, 689-702

Wenban-Smith, 2003. The Ebbsfleet Elephant, Excavations to Southfleet Road, Swanscombe in. advance of High Speed I, 2003-4. Oxford Archaeology Monograph No. 20

West, R. G., 1980. The pre-glacial Pleistocene of the Norfolk and Suffolk Coasts. Cambridge University Press

Westaway, R., Bridgland, D., White, M., 2006. The Quaternary uplift history of central southern England: evidence from the terraces of the Solent River system and nearby raised beaches. Quaternary Science Reviews 25, 2212-2250

Westaway, R., 2011. A re-evaluation of the timing of the earliest reported human occupation of Britain: The age of the sediments at Happisburgh, eastern England. Proceedings of the Geologists' Association 122, 383-396

White, M., Scott, B., Ashton, N., 2006. The early Middle Palaeolithic in Britain: archaeology, settlement history and human behaviour. Journal of Quaternary Science 21 (5), 525-541

White, T. S., Bridgland, D. R., Westaway, R., Howard, A. J., White, M. J. 2010. Evidence from the Trent terrace archive, Lincolnshire, UK, for lowland glaciation of Britain during the Middle and Late Pleistocene. Proceedings of the Geologists' Association 121, 141-153

White, T. S., Bridgland, D. R., Limondin-lozouet, N., Schreve, D. C., 2017. Fossils from Quaternary fluvial archives: Sources of biostratigraphical, biogeographical and palaeoclimatic evidence. Quaternary Science Reviews 166, 150-176

Wiedemann-Bidlack, F. B., Beniash, E., Yamakoshi, Y., Simmer, J. P., Margolis, H. C., 2007. pH triggered self-assembly of native and recombinant amelogenins under physiological pH and temperature in vitro. Journal of Structural Biology 160, 57-69

Wilson, H., Cannan, R. K., 1937. The Glutamic acid-pyrrolidonecarboxylic acid system. Journal of Biological Chemistry 119, 309-331

Yanagida, A., Murao, H., Ohnishi-kameyama, M., Yamakawa, Y., Shoji, A., Tagashira, M., Kanda, T., Shindo, H. Shibusawa, Y., 2007. Retention behavior of oligomeric proanthocyanidins in hydrophilic interaction chromatography. Journal of Chromatography A, 153-161

Zalasiewicz, J. A., Mathers, S. J., Gibbard, P. L., Peglar, S. M., Funnell, B. M., Catt, J. A., Harland, R., Long, P. E., Austin, T. J. F., 1991. Age and Relationships of the Chillesford Clay (Early Pleistocene: Suffolk, England). Philosophical Transactions of the Royal Society B: Biological Sciences 333, 81-100

Zazzo, A. & Saliege, J. -F., 2011. Radiocarbon dating of biological apatites: A review. Palaoegeography, Palaoeclimatology, Palaeoecology 310, 52-61

Zeichner-David, M., 2001. Is there more to enamel matrix proteins than biomineralization? Matrix Biology 20, 307-316

Zhou, L. P., McDermott, F., Rhodes, E. J., Marseglia. E. A., Mellars. P. A., 1997. Esr and Mass-Spectrometric Uranium-series Dating Studies of a Mammoth Tooth from Stanton Harcourt, Oxfordshire, England. Quaternary Science Reviews (Quaternary Geochronology) 16, 445-454